Biological Markers in Pediatric Brain Tumors

The Pediatric Oncology Foundation Rotterdam (KOCR), Sakura Finetek Europe B.V. and Innogenetics N.V kindly provided financial support for the print and reproduction of this thesis.

ISBN 978-90-8559-411-6
Layout: Optima Grafische Communicatie, Rotterdam
Cover: Optima Grafische Communicatie, Rotterdam
Illustratie kaft: "The headache", George Cruikshank 1792-1878.
Printed by Optima Grafische Communicatie, Rotterdam

Biological Markers in Pediatric Brain Tumors

Biologische markers in hersentumoren bij kinderen

Proefschrift

ter verkrijging van de graad van doctor aan de
Erasmus Universiteit Rotterdam
op gezag van de
rector magnificus
Prof.dr. S.W.J. Lamberts
en volgens besluit van het College voor Promoties.

De openbare verdediging zal plaatsvinden op vrijdag 19 september 2008 om 11.00 uur

door

Judith Maria de Bont
geboren te Leiden

ERASMUS UNIVERSITEIT ROTTERDAM

PROMOTIECOMMISSIE

Promotor:	Prof.dr. R. Pieters
Overige leden:	Prof.dr. P.A.E. Sillevis Smitt Prof.dr. J.M. Kros Prof.dr. W.F.M. Arts
Copromotor:	Dr. M.L. den Boer

CONTENTS

Chapter 1

General Introduction

The most common solid tumors in children are brain tumors[1]. Yearly, approximately 2-2.5 per 100,000 children of <15 years of age are diagnosed with a brain tumor[1]. Despite improved survival rates, brain tumors in children are still the second leading cause of death due to cancer in children. Moreover, serious long-term side effects due to the localization of the tumor and due to treatment result in a considerable decrease in the quality of life in surviving patients.

Pediatric brain tumors differ from those arising in adults in localization, histology and responsiveness to therapy[2, 3]. Approximately 50% of the brain tumors in childhood are found infratentorial, whereas most of the tumors in adults arise in and around the cerebral hemispheres[3]. Regarding histology, embryonal central nervous system (CNS) tumors are almost solely found in children, whereas meningeomas and metastases to the brain predominantly arise in adults and are rare in children (Table 1).

Astrocytic tumors are the most frequent brain tumors in children (~25%). This group of tumors comprises a wide range of clinically, histologically and biologically distinct subtypes[4]. In children, the most common subtype is the grade I pilocytic astrocytoma, whereas grade III anaplastic astrocytoma and grade IV glioblastoma predominate in adults. Unlike adults, children frequently develop malignant glioma within the brainstem, which is associated with a very poor prognosis due to the limited treatment options[5].

The second most common pediatric brain tumors are the embryonal tumors (~20%), which are subdivided into 3 large subgroups[4, 6]: medulloblastoma, primitive neuroectodermal tumors (PNETs) and atypical teratoid/rhabdoid tumors (AT/RTs). Medulloblastoma, first reported in 1925 by Bailey and Cushing, is a grade IV embryonal tumor localized in the posterior fossa and has a tendency to metastasize within the CNS. The classification of medulloblastomas has been discussed frequently over the years. Classic medulloblastoma is the most frequently observed medulloblastoma subtype and is characterized by densely packed cells with round nuclei and scant cytoplasm, generally arranged in sheets and neuroblastic (Homer Wright) rosettes. A second subtype, the desmoplastic/nodular medulloblastoma, consists of 2 components: reticulin-free nodules, the so-called pale islands and highly proliferative reticulin-rich desmoplastic areas[6]. This subtype tends to occur more often in the lateral cerebellar hemisphere than does the classic medulloblastoma, which usually arises in the cerebellar vermis. Desmoplastic medulloblastoma are predominantly observed in adolescents and adults[7-9]. Medulloblastoma with extensive nodularity, a third variant, was previously called cerebellar neuroblastoma. These tumors usually occur in children under the age of 3 and are characterized by extreme lobularity, resulting from large reticulin free zones, which contain small cells resembling those of a central neurocytoma. Both desmoplastic medulloblastoma and medulloblastoma with extensive nodularity are associated with a more favorable outcome[10-13]. The more aggressive and poorly prognostic large cell and anaplastic medulloblastomas show considerable similarities. The large cell subtype displays large round nuclei and prominent nucleoli and the anaplastic variant is characterized by nuclear

Table 1. Overview of pediatric tumors according to histologic subtype and localization[45, 46]

localization and histopathological type	Percentage of all brain tumors
Infratentorial	
Primitive neuroectodermal tumor	5
Medulloblastoma	20
Low-grade astrocytoma, cerebellum	12-18
Ependymoma	4-8
Malignant glioma, brain stem	3-9
Low-grade astrocytomas, brain stem	3-6
Other	2-5
Supratentorial	
Low-grade astrocytoma	8-20
Malignant glioma	6-12
Ependymoma	2-5
Mixed glioma	1-5
Ganglioglioma	1-5
Oligodendroglioma	1-2
Plexus Choreoid tumor	1-2
Primitive neuroectodermal tumor	1-2
Meningeoma	0.5-2
Other	1-3
Midline	
Suprasellar craniopharyngeoma	6-9
Chiasmatic/hypothalamic glioma	4-8
Germinoma	1-2
Pituitary adenoma	0.5-2.5
Pineal region	
Glioma	1-2
Germinoma	0.5-2
Pinealoma	0.5-2

pleomorphism and nuclear moulding[14]. Both types show a high mitotic activity and high apoptotic rate with large areas of necrosis.

The prognosis of medulloblastoma patients is still mainly predicted by clinical characteristics at diagnosis. Young age, metastatic disease and residual disease after surgery are found to be indicative of poor prognosis[15, 16]. With current treatment regimens including surgery, radiotherapy and chemotherapy 5-year survival rates of up to 60-80% are achieved in good risk patients, but only ~25% of the poor risk patients can be cured[17, 18]. In addition to maximal surgical resection, additional craniospinal radiotherapy has been shown to be mandatory due to the tendency of the tumor to disseminate. Because of the high risk of late effects, radiotherapy is often avoided in young children, which may contribute to the decreased survival rates in these patients[19-22]. Therefore, much effort is being put in studying possible dose reduction of craniospinal irradiation[17]. The importance of chemotherapy,

including CCNU, cisplatinum and vincristine, in medulloblastoma treatment has been shown in various trials[18, 23-25].

The two other variants of embryonal CNS tumors, the PNETs and the AT/RTs are uncommon. The term PNET refers to a heterogeneous group of embryonal tumors. PNETs may morphologically appear similar to medulloblastoma, but they arise in the supratentorial region, brain stem and spinal cord, are generally more aggressive and have a different genetic signature[26]. Since the 1993 WHO classification, AT/RTs are regarded as a separate entity[27]. This tumor is mainly found in the posterior fossa of young children and is associated with a very poor prognosis, often being refractory to therapy[27, 28]. Some of the histological features are similar to those of rhabdoid kidney tumors and some patients present with both. Tumors consist of rhabdoid cells and because of the combination with other tumor elements, such as primitive neuroepithelial, epithelial and mesenchymal components, they are often misdiagnosed as medulloblastomas or PNETs.

The third most common brain tumors of childhood are the ependymomas, accounting for approximately 10% of cases. They may develop in all age groups, but there is an age peak at ~6 years of age and between 30-40 years of age. Ependymomas can arise anywhere within or adjacent to the ependymal lining of the ventricular system, but the majority of ependymomas in children are found intracranial, predominantly in the posterior fossa, whereas spinal tumors are predominantly observed in adults[29, 30]. Subependymoma and the myxopapillary ependymoma are rarely seen in children[4]. The most common variants of ependymomas show perivascular pseudorosettes and ependymal rosettes and they can be further classified into the most common cellular and the rare papillary, clear cell and tanycytic ependymoma. All variants can progress to anaplastic tumors with increased cellularity and mitotic activity, vascular proliferation, necrosis and nuclear polymorphism. Unfortunately, correlations between histological features and clinical outcome have not been conclusive[31, 32]. In contrast to other pediatric malignancies, such as leukemia, prognosis of ependymoma has not significantly improved during the last 3 decades[33]. In general, outcome of ependymomas in children is significantly worse than in adults. This is partly caused by the tumor localization, but probably also by different biological characteristics. It has been difficult to define independent prognostic factors for ependymoma as the tumor is rare and there are many age, site and histological subgroups. The most important prognostic factor in ependymomas is the extent of tumor resection[31, 34, 35]. In patients with completely resected tumors survival rates are ~50-70%, whereas incomplete resection results in only 0-30% survival. Only a small proportion of patients (<10%) develops metastases and recurrences are usually local. Additional radiotherapy is beneficial for achieving local control, but in contrast to medulloblastomas, the results of chemotherapy in ependymomas have been disappointing[36-40].

Other brain tumor subtypes, such as choroid plexus tumors, germ cell tumors and craniopharyngeomas are relatively rare in children.

OUTLINE OF THIS THESIS

Biological and genetic factors leading to the development of a brain tumor are largely unknown. Only a very small proportion of brain tumors is caused by hereditary gene defects, previous irradiation or immune suppression[41, 42]. Understanding the genetic and biological mechanisms involved in the pathogenesis of these tumors is necessary to further improve the outcome of these patients. The aim of this thesis was to identify new markers that may improve the classification and risk stratification of patients or may be used as new therapeutic targets in medulloblastomas and ependymomas.

Chapter 2 provides an overview of the currently known genetic and biological features of pediatric medulloblastomas and ependymomas. It describes the deregulation of signaling pathways involved in the development of the brain, the potential cells of origin, chromosomal abnormalities and abnormalities at (epi)genetic and proteomic level.

In **chapter 3** we used gene expression profiling to identify genes that are differentially expressed in medulloblastoma and ependymoma compared to normal cerebellum and that are predictive for outcome of these tumors. The differential expression of the identified markers was validated at the protein level by immunohistochemistry.

In addition to gene expression profiling, protein expression profiling may also be a useful tool to identify brain tumor markers. In **chapter 4** we used 2-dimensional difference gel electrophoresis to analyze protein expression profiles of pediatric medulloblastomas, PNETs and ependymomas. Differentially expressed proteins were characterized by tandem mass spectrometry and validation was performed by immunohistochemistry at the protein level and at mRNA level by using the gene expression data from chapter 3.

As brain tumor cells might be capable of inducing the secretion of proteins into the cerebrospinal fluid (CSF), either by the tumor cells itself or by surrounding tissue, we extended our protein expression studies from the tumor cells to the CSF. In **chapter 5** SELDI protein chip technology was used to detect protein markers being differentially expressed in the CSF of brain tumor patients compared to normal controls. These markers were subsequently purified and identified by tandem mass spectrometry. Immunohistochemistry was used to confirm protein expression of the identified CSF markers in tumor cells.

It is known that brain tumor patients suffer from long-term neurological and neuropsychological side effects. In **chapter 6** we evaluated the influence of the presence of a brain tumor and hydrocephalus on the CSF levels of the neurodegenerative markers total tau (t-Tau), hyperphosphorylated Tau (p-$Tau_{(181P)}$) and ß-$amyloid_{(1-42)}$.

In **chapter 7** we combined the gene expression profiles of tumor cells from chapter 3 and CSF protein expression profiles after tumor resection, in order to identify tumor-related markers that may be used in the follow-up to screen for residual disease or early detection of relapse. In this study, we focused on members of the IGF signaling pathway, which is known to be important in brain tumor pathogenesis[43, 44].

Another important signaling pathway known to be involved in the development of cancer, the p53 signaling pathway was studied in **chapter 8**. Here we screened for p53 mutations and analyzed gene expression levels of the genes affecting the activity of p53.

Finally, the work presented in this thesis is summarized and discussed in **chapter 9**. In **chapter 10** these data are presented in Dutch.

REFERENCES

1. Bleyer WA. Epidemiologic impact of children with brain tumors. Childs Nerv Syst 1999;15(11-12):758-763.
2. Packer RJ. Childhood medulloblastoma: progress and future challenges. Brain Dev 1999;21(2):75-81.
3. Pollack IF. Pediatric brain tumors. Semin Surg Oncol 1999;16(2):73-90.
4. Louis DN, Ohgaki H, Wiestler OD, et al. The 2007 WHO Classification of Tumours of the Central Nervous System. Acta Neuropathol (Berl) 2007;114(2):97-109.
5. Hargrave DR, Zacharoulis S. Pediatric CNS tumors: current treatment and future directions. Expert Rev Neurother 2007;7(8):1029-1042.
6. Kleihues P, Louis DN, Scheithauer BW, et al. The WHO classification of tumors of the nervous system. J Neuropathol Exp Neurol 2002;61(3):215-225; discussion 226-219.
7. Hubbard JL, Scheithauer BW, Kispert DB, et al. Adult cerebellar medulloblastomas: the pathological, radiographic, and clinical disease spectrum. J Neurosurg 1989;70(4):536-544.
8. Bloom HJ, Bessell EM. Medulloblastoma in adults: a review of 47 patients treated between 1952 and 1981. Int J Radiat Oncol Biol Phys 1990;18(4):763-772.
9. Carrie C, Lasset C, Blay JY, et al. Medulloblastoma in adults: survival and prognostic factors. Radiother Oncol 1993;29(3):301-307.
10. Bailey CC, Gnekow A, Wellek S, et al. Prospective randomised trial of chemotherapy given before radiotherapy in childhood medulloblastoma. International Society of Paediatric Oncology (SIOP) and the (German) Society of Paediatric Oncology (GPO): SIOP II. Med Pediatr Oncol 1995;25(3):166-178.
11. Sure U, Berghorn WJ, Bertalanffy H, et al. Staging, scoring and grading of medulloblastoma. A postoperative prognosis predicting system based on the cases of a single institute. Acta Neurochir (Wien) 1995;132(1-3):59-65.
12. Jenkin D, Shabanah MA, Shail EA, et al. Prognostic factors for medulloblastoma. Int J Radiat Oncol Biol Phys 2000;47(3):573-584.
13. Rutkowski S, von Bueren A, von Hoff K, et al. Prognostic relevance of clinical and biological risk factors in childhood medulloblastoma: results of patients treated in the prospective multicenter trial HIT'91. Clin Cancer Res 2007;13(9):2651-2657.
14. Brown HG, Kepner JL, Perlman EJ, et al. "Large cell/anaplastic" medulloblastomas: a Pediatric Oncology Group Study. J Neuropathol Exp Neurol 2000;59(10):857-865.
15. Zeltzer PM, Boyett JM, Finlay JL, et al. Metastasis stage, adjuvant treatment, and residual tumor are prognostic factors for medulloblastoma in children: conclusions from the Children's Cancer Group 921 randomized phase III study. J Clin Oncol 1999;17(3):832-845.
16. Kortmann RD, Kuhl J, Timmermann B, et al. Postoperative neoadjuvant chemotherapy before radiotherapy as compared to immediate radiotherapy followed by maintenance chemotherapy in the treatment of medulloblastoma in childhood: results of the German prospective randomized trial HIT '91. Int J Radiat Oncol Biol Phys 2000;46(2):269-279.
17. Packer RJ, Goldwein J, Nicholson HS, et al. Treatment of children with medulloblastomas with reduced-dose craniospinal radiation therapy and adjuvant chemotherapy: A Children's Cancer Group Study. J Clin Oncol 1999;17(7):2127-2136.
18. Packer RJ, Siegel KR, Sutton LN, et al. Efficacy of adjuvant chemotherapy for patients with poor-risk medulloblastoma: a preliminary report. Ann Neurol 1988;24(4):503-508.
19. Deutsch M. The impact of myelography on the treatment results for medulloblastoma. Int J Radiat Oncol Biol Phys 1984;10(7):999-1003.
20. Deutsch M. Medulloblastoma: staging and treatment outcome. Int J Radiat Oncol Biol Phys 1988;14(6):1103-1107.

21. Saran FH, Driever PH, Thilmann C, et al. Survival of very young children with medulloblastoma (primitive neuroectodermal tumor of the posterior fossa) treated with craniospinal irradiation. Int J Radiat Oncol Biol Phys 1998;42(5):959-967.
22. Heideman RL. Overview of the treatment of infant central nervous system tumors: medulloblastoma as a model. J Pediatr Hematol Oncol 2001;23(5):268-271.
23. Tait DM, Thornton-Jones H, Bloom HJ, et al. Adjuvant chemotherapy for medulloblastoma: the first multi-centre control trial of the International Society of Paediatric Oncology (SIOP I). Eur J Cancer 1990;26(4):464-469.
24. Taylor RE, Bailey CC, Robinson K, et al. Results of a randomized study of preradiation chemotherapy versus radiotherapy alone for nonmetastatic medulloblastoma: The International Society of Paediatric Oncology/United Kingdom Children's Cancer Study Group PNET-3 Study. J Clin Oncol 2003;21(8):1581-1591.
25. Evans AE, Jenkin RD, Sposto R, et al. The treatment of medulloblastoma. Results of a prospective randomized trial of radiation therapy with and without CCNU, vincristine, and prednisone. J Neurosurg 1990;72(4):572-582.
26. MacDonald TJ, Rood BR, Santi MR, et al. Advances in the diagnosis, molecular genetics, and treatment of pediatric embryonal CNS tumors. Oncologist 2003;8(2):174-186.
27. Rorke LB, Packer RJ, Biegel JA. Central nervous system atypical teratoid/rhabdoid tumors of infancy and childhood: definition of an entity. J Neurosurg 1996;85(1):56-65.
28. Burger PC, Yu IT, Tihan T, et al. Atypical teratoid/rhabdoid tumor of the central nervous system: a highly malignant tumor of infancy and childhood frequently mistaken for medulloblastoma: a Pediatric Oncology Group study. Am J Surg Pathol 1998;22(9):1083-1092.
29. Hamilton RL, Pollack IF. The molecular biology of ependymomas. Brain Pathol 1997;7(2):807-822.
30. Teo C, Nakaji P, Symons P, et al. Ependymoma. Childs Nerv Syst 2003;19(5-6):270-285.
31. Pollack IF, Gerszten PC, Martinez AJ, et al. Intracranial ependymomas of childhood: long-term outcome and prognostic factors. Neurosurgery 1995;37(4):655-666; discussion 666-657.
32. Sutton LN, Goldwein J, Perilongo G, et al. Prognostic factors in childhood ependymomas. Pediatr Neurosurg 1990;16(2):57-65.
33. Grill J, Pascal C, Chantal K. Childhood ependymoma: a systematic review of treatment options and strategies. Paediatr Drugs 2003;5(8):533-543.
34. Robertson PL, Zeltzer PM, Boyett JM, et al. Survival and prognostic factors following radiation therapy and chemotherapy for ependymomas in children: a report of the Children's Cancer Group. J Neurosurg 1998;88(4):695-703.
35. Perilongo G, Massimino M, Sotti G, et al. Analyses of prognostic factors in a retrospective review of 92 children with ependymoma: Italian Pediatric Neuro-oncology Group. Med Pediatr Oncol 1997;29(2):79-85.
36. Bouffet E, Foreman N. Chemotherapy for intracranial ependymomas. Childs Nerv Syst 1999;15(10):563-570.
37. Zacharoulis S, Levy A, Chi SN, et al. Outcome for young children newly diagnosed with ependymoma, treated with intensive induction chemotherapy followed by myeloablative chemotherapy and autologous stem cell rescue. Pediatr Blood Cancer 2007;49(1):34-40.
38. Evans AE, Anderson JR, Lefkowitz-Boudreaux IB, et al. Adjuvant chemotherapy of childhood posterior fossa ependymoma: cranio-spinal irradiation with or without adjuvant CCNU, vincristine, and prednisone: a Childrens Cancer Group study. Med Pediatr Oncol 1996;27(1):8-14.
39. Goldwein JW, Corn BW, Finlay JL, et al. Is craniospinal irradiation required to cure children with malignant (anaplastic) intracranial ependymomas? Cancer 1991;67(11):2766-2771.
40. Merchant TE, Mulhern RK, Krasin MJ, et al. Preliminary results from a phase II trial of conformal radiation therapy and evaluation of radiation-related CNS effects for pediatric patients with localized ependymoma. J Clin Oncol 2004;22(15):3156-3162.

41. Wrensch M, Minn Y, Chew T, et al. Epidemiology of primary brain tumors: current concepts and review of the literature. Neuro Oncol 2002;4(4):278-299.
42. Bondy M, Wiencke J, Wrensch M, et al. Genetics of primary brain tumors: a review. J Neurooncol 1994;18(1):69-81.
43. Wang JY, Del Valle L, Gordon J, et al. Activation of the IGF-IR system contributes to malignant growth of human and mouse medulloblastomas. Oncogene 2001;20(29):3857-3868.
44. Ogino S, Kubo S, Abdul-Karim FW, et al. Comparative immunohistochemical study of insulin-like growth factor II and insulin-like growth factor receptor type 1 in pediatric brain tumors. Pediatr Dev Pathol 2001;4(1):23-31.
45. CBTRUS. Statistical report: Primary brain tumors in the United States, 1997-2001. Published by the Central Brain Tumor Registry of the United States, 2004.
46. Hoogenhout J, Lippens RJ, Valk J. Hersentumoren. In: Schadé E, ed. Kinderoncologie. Houten: Bohn Stafleu van Loghum, 1997: 257-280.

Chapter 2

Biological Background of Pediatric Medulloblastoma and Ependymoma

A review from a translational research perspective

Judith M. de Bont[1], Roger J. Packer[2], Erna M. Michiels[1], Monique L. den Boer[1], Rob Pieters[1]

[1]Erasmus MC – Sophia Children's Hospital - University Medical Center Rotterdam – Department of Pediatric Oncology and Hematology, The Netherlands;
[2]Children's National Medical Center - The Brain Tumor Center- Washington, USA

Neuro-Oncology 2008; in press

ABSTRACT

Survival rates of pediatric brain tumor patients have significantly improved over the years due to developments in diagnostic techniques, neurosurgery, chemotherapy, radiotherapy and supportive care. However, brain tumors are still an important cause of cancer-related deaths in children. Prognosis is still highly dependent on clinical characteristics, such as the age of the patient, tumor type, stage and localization, but increased knowledge about the genetic and biological features of these tumors is being obtained and might be useful to further improve the outcome of these patients. It has become clear that the deregulation of signaling pathways essential in brain development, e.g. SHH, Wnt and Notch, plays an important role in the pathogenesis and biological behavior of especially medulloblastomas. More recently, data have become available about the cells of origin of brain tumors and about the possible existence of brain tumor stem cells. Newly developed array-based techniques for studying gene expression, protein expression, copy number aberrations and epigenetic events have led to the identification of other potentially important biological abnormalities in pediatric medulloblastomas and ependymomas.

INTRODUCTION

The causes of pediatric brain tumors are largely unknown. Environmental factors, such as smoking, diet and other exposures do not predispose to the development of a brain tumor[1]. Only a very small proportion of brain tumors is caused by hereditary gene defects (Table 1), irradiation or immune suppression. Additional knowledge about the biological characteristics of pediatric brain tumors may provide new information about the pathogenesis, facilitate the diagnosis, contribute to a better risk group stratification for therapy or may be used as new therapeutic targets. To identify these biological factors, many techniques have been developed over the years. This review provides an overview of newly identified aberrantly expressed genes and proteins, chromosomal changes, DNA copy number abnormalities and other genetic changes that may be important in the pathogenesis and biological behavior of 2 frequent pediatric brain tumor subtypes, medulloblastomas and ependymomas.

Table 1. Hereditary syndromes predisposing to the development of a brain tumor.
Several hereditary syndromes are associated with an increased risk to develop a brain tumor. This table displays these syndromes, including the responsible gene, involved chromosomal region and the type of sporadic brain tumors in which these genes have also been shown to be affected.

Disease	Gene (chromosomal location)	CNS tumor associated with disease	Involvement in sporadic CNS tumor
Li-Fraumeni syndrome	p53 (17p13.1)	Astrocytoma Medulloblastoma	Astrocytoma Choroid plexus tumor
Neurofibromatosis type I	NF1 (17q11.2)	Astrocytoma Vestibular and spinal schwannoma	?
Neurofibromatosis type II	NF2 (22q12.2)	Ependymoma Meningeoma	Meningeoma Schwannoma
Nevoid basal cell carcinoma syndrome (Gorlin syndrome)	PTCH (9q22.3)	Medulloblastoma	Medulloblastoma
Tuberous sclerosis	TSC1 (9q34) TSC2 (16p13)	Subependymal giant cell tumor	?
Turcot's syndrome A	APC (5q21-q22) MLH1 (3p21.3) MSH2 (2p22-p21) MLH3 (14q24)	Medulloblastoma	Medulloblastoma
Turcot's syndrome B	PMS1 (2q31-q33) PMS2 (7p22)	Glioblastoma Ependymoma	(Astrocytic tumor)
Von Hippel Lindau disease	VHL (3p25)	Hemangioblastoma	?
Cowden disease	PTEN (10q22-q23)	Astrocytoma	Glioblastoma
Melanoma-astrocytoma syndrome	CDKN2A (9p21)	Astrocytoma	Astrocytoma
Rubenstein-Taybi syndrome	CBP (16p13.3)	Medulloblastoma Meningeoma Oligodendroglioma	?
MEN1 syndrome	MEN1 (11q13)	Ependymoma	Ependymoma Pituitary tumor

MEDULLOBLASTOMA

Clinical aspects

Medulloblastoma is the most common embryonal central nervous system (CNS) tumor of childhood and is comprised of biologically different subsets of tumors arising from stem and/or progenitor cells of the cerebellum. The World Health Organization recognizes at least 5 different histological types of medulloblastoma and there is increasing evidence that prognosis and possibly response to therapy is dependent on the cell of origin of the tumor and the cellular pathways active in tumor development and growth.

Medulloblastomas, which by definition arise in the posterior fossa, are conventionally stratified on the basis of clinical parameters, such as extent of tumor at the time of diagnosis and the completeness of surgical resection, into average or high-risk (poor) disease[2]. For both children greater than 3 years of age with non-disseminated and/or partially resected "high-risk" disease, standard therapy includes both treatment with radiotherapy and adjuvant chemotherapy[3]. Five-year disease-free survival rates of 80% or greater are now being reported by multiple groups for patients with average-risk medulloblastoma and a major focus of new treatment approaches is the development of innovative ways to reduce long-term toxicity of therapy[3]. Approaches which have been used and are under study include reduction of the total dose of craniospinal radiation therapy, reduction of the volume of local boost radiotherapy, or utilization of less neurotoxic chemotherapeutic agents[3]. Even in patients with high-risk disease, with current means of treatment, 5-year survival rates of 60% or higher are now being reported[4]. Most therapeutic approaches for "high-risk" patients have continued to utilize relatively high doses of craniospinal radiation therapy and aggressive chemotherapeutic approaches[4].

The treatment for infants with medulloblastoma remains highly problematic. The volumes and doses of radiotherapy required for disease control cause significant brain injury in patients at all ages, predominantly manifest by long-term neurocognitive sequelae, but are especially damaging in the very young child[5]. For this reason, most therapeutic approaches have focused on either delaying or eliminating radiotherapy by the use of increasingly aggressive chemotherapeutic approaches which have incorporated potentially neurotoxic drugs, such as methotrexate, or high-dose chemotherapy supported by autologous peripheral stem cell rescue[6]. There is some suggestion that such approaches are more effective, but some of these apparent improvements in survival may also be related to separation of more aggressive tumors, such as atypical teratoid/rhabdoid tumors from the cohort of these patients treated or the inclusion of better-risk patients, such as those with desmoplastic tumors, on treatment protocols[7]. A major hope for the future is that the incorporation of biologic agents targeting specific signaling pathways will not only make treatment more effective, but will also allow a reduction in neurotoxic therapy.

Developmental signaling pathways

Several hereditary syndromes predispose to the development of a brain tumor (Table 1) and the underlying gene defects were thought to provide information about the critical genes in the pathogenesis of brain tumors. The genes mutated in syndromes predisposing to medulloblastoma development are frequently involved in cellular signaling pathways (Table 2), which are important regulators of brain development, such as sonic hedgehog (SHH), Wnt and Notch (Figure 1).

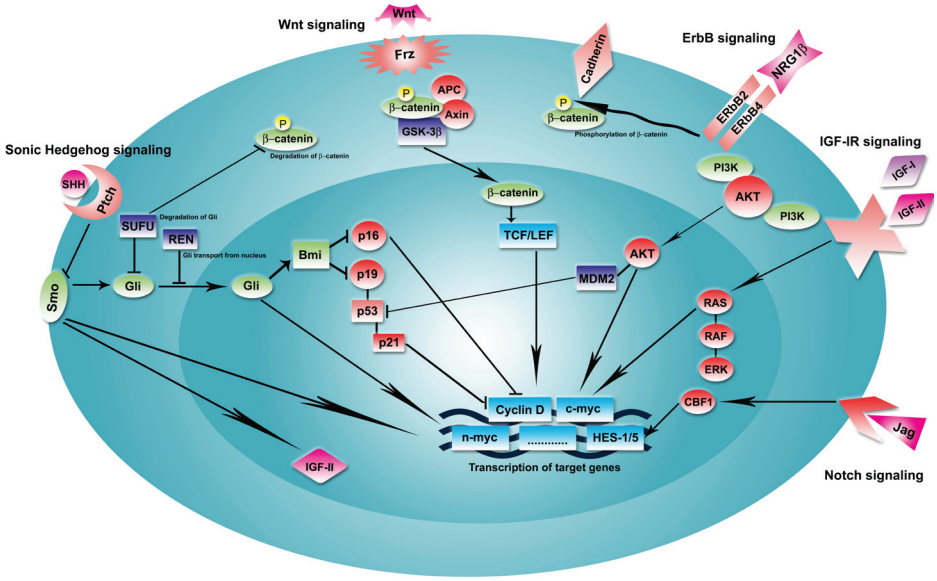

Figure 1. Signaling pathways involved in the development of the brain and pathogenesis of medulloblastoma and ependymoma.
This figure shows the important signaling pathways involved in brain development. Deregulation of these pathways is important in the pathogenesis of medulloblastoma and ependymoma. Interactions between these pathways are multiple and complex.

Sonic Hedgehog (SHH) signaling

Gorlin's syndrome is an autosomal dominant disorder that is characterized by multiple developmental defects and a predisposition for basal cell carcinoma, rhabdomyosarcoma and medulloblastoma[8]. The tumor suppressor gene Patched 1 (PTCH1) on chromosome 9q22.3, encoding a transmembrane surface receptor for Hedgehog proteins, is mutated in this syndrome. The Hedgehog-patched signaling pathway controls normal development of the external granular layer of the cerebellum[9]. SHH, produced by Purkinje cells, binds to the PTCH1 receptor and induces proliferation of cerebellar granule cell precursors by relieving the inhibition of Smo and inducing the activation of the Gli family of transcription factors[9].

Mutations in various components of the SHH pathway, such as PTCH1 and Smo occur in ~30% of sporadic medulloblastoma, predominantly desmoplastic medulloblastoma (Table 2). These tumors show up-regulation of important SHH target genes, such as Gli1 and BMI1, indicating active SHH signaling. BMI1 is overexpressed in medulloblastomas, which might result in the abnormal regulation of both the Rb and the p53 pathway[10]. The importance of the SHH pathway in medulloblastoma is underlined by the observed growth inhibition after treatment with inhibitors of the SHH pathway[11]. As only a small subset of PTCH1 +/- mice develops medulloblastoma, other genetic events are thought to influence the susceptibility of developing medulloblastoma. For example, concomitant loss of p53 or Ink4C have been shown to facilitate the development of medulloblastoma[12].

Wnt signaling

The Wnt signaling pathway is a second pathway that may be involved in regulating the embryonal development of the brain. One of the genes involved in this pathway, APC, is mutated in patients with Turcot's syndrome who have a predisposition to develop colon cancers, glioblastomas and medulloblastomas (Table 2). APC forms a protein complex together with β-catenin, GSK3-β and axin[13]. Activation of the Wnt pathway results in decreased β-catenin degradation followed by the interaction with TCF/LEF transcription factors and activation of Wnt targets, such as c-Myc, Cyclin D1 and AXIN2[14]. Activating mutations in the Wnt pathway occur in a substantial number of medulloblastomas (Table 2)[15, 16]. Most mutations have been found in the β-catenin gene, but mutations in the APC and AXIN2 gene and deletions of the AXIN1 gene are also described (Table 2). However, deletions of AXIN1 are also identified in normal brain tissue, suggesting at least a part of the AXIN1 deletions found in medulloblastoma to represent polymorphisms or PCR artefacts[17]. Increased expression of survivin, an apoptosis inhibitor, is also associated with activation of the Wnt signaling pathway (Table 2). Survivin expression is related to an unfavorable outcome, independent of clinical staging or tumor histology[18, 19]. SOX gene family members can also regulate the Wnt signaling pathway[20]. Interestingly, SOX4 and SOX11 are overexpressed in predominantly classic medulloblastoma[21-23].

The SHH and Wnt signaling pathways interact with each other, but also with other signaling pathways, including Notch, ErbB and IGF (Figure 1). Cyclin D1, an important mediator of the proliferation of cerebellar granule cell precursors, is for example an important downstream target of both SHH, Wnt and Notch signaling. Moreover, medulloblastoma of PTCH1 +/- mice show increased expression of genes involved in activation of both SHH and Wnt signaling[24].

Notch signaling

In the cerebellum, Notch2 is predominantly expressed in proliferating cerebellar granule cell precursors, whereas Notch1 is found in differentiated internal granule layer neurons[25].

Notch2 is overexpressed in a subset of medulloblastoma, whereas Notch1 expression is scarce. Activation of the Notch signaling pathway results in the transcriptional activation of HES1 and HES5[26]. HES1 expression is associated with decreased survival rates of medulloblastoma patients (Table 2). It is recently hypothesized that HES1 forms transcriptional repressor complexes with FOXG1 to negatively regulate the differentiation of neural progenitor cells. Interestingly, the function of the FOXG1 gene is deregulated in the majority of medulloblastoma (Table 2). Treatment of medulloblastoma xenografts with inhibitors of the Notch signaling pathway results in decreased proliferation and increased apoptosis[27].

Table 2. Differentially expressed genetic and proteomic markers identified in medulloblastomas (A.) and ependymomas (B.).
This table displays the currently known differentially expressed biological markers in subgroups of medulloblastomas and ependymomas that have been identified by e.g. mutational analysis, gene expression profiling, protein expression profiling, immunohistochemistry and epigenetic profiling.

A. Medulloblastoma				
Gene	**Change**	**%**	**Reference**	**Correlating with**
SHH signaling				
PTCH1	mutation	4.8-13.5%	132-136	desmoplastic subtype
PTCH2	overexpression	unknown	16	_
SUFU	mutation	0-9%	137, 138	desmoplastic subtype
Smo	mutation	0-10%	139, 140	desmoplastic subtype
Gli	overexpression	~30%	16, 24, 27	desmoplastic subtype
BMI1	overexpression	~67%	10	_
REN^{KCTD11}	deletion	~39%	141	_
Wnt signaling				
Axin 1	mutation	1.2-5.6%	17, 142, 143	_
	deletion	12-41.7%	17, 142	_
Axin 2	mutation	~3%	144	_
APC	mutation	1.3-4.3%	145, 146	_
β-catenin	mutation	0.5-63.8%	15, 143, 145-148	favorable outcome
Survivin	overexpression	0.5-50%	18, 19, 149, 150	unfavorable outcome
SOX4	overexpression	unknown	21, 22, 151	_
SOX11	overexpression	unknown	21, 22	_
Cyclin D1	overexpression	unknown	23, 24	_
Cyclin D2	overexpression	unknown	24, 151	_
Lef1	overexpression	unknown	16, 24, 152	_
Notch signaling				
HES1	overexpression	up to 46%	24, 25, 27	unfavorable outcome
HES5	overexpression	up to 71%	24, 27	_
JAG1	overexpression	unknown	24	_
Notch 1	overexpression	~75%	27	_
Notch 2	overexpression	12.5-15%	24, 25, 27	_
Notch 3	overexpression	unknown	24	_
FOXG1	overexpression	>90%	111	_
Mushashi	overexpression	unknown	151	_

A. Medulloblastoma				
Gene	**Change**	**%**	**Reference**	**Correlating with**
ErbB signaling				
ErbB4	overexpression	~66%	28, 30, 31, 153	unfavorable outcome
ErbB2	overexpression	70-86%	153, 154	unfavorable outcome
CIC	overexpression	unknown	155	_
NRG-1β	overexpression	~87%	28	_
c-myc	amplification	5-10%	39, 156-160	anaplasia and unfavorable outcome
	overexpression	~42%		
MnT	underexpression	~43%	161, 162	_
n-myc	amplification	~5%	24, 38, 39, 120, 157, 163, 164	unfavorable outcome
JPO2	overexpression	unknown	165	metastases
BCAT1	overexpression	unknown	22	metastases
IGF signaling				
IGF-IR	expression/ phosphorylation	~80%	166	_
IRS-1	overexpression	unknown	166	_
IGF-II	overexpression	unknown	37, 44	desmoplastic subtype
AKT/PKB	phosphorylation	unknown	166	_
Erk-1	phosphorylation	unknown	166	_
Erk-2	phosphorylation	unknown	166	_
IGFBP-2	overexpression	unknown	47	_
IGFBP-3	overexpression	unknown	47	_
Other				
CXCR4	overexpression	~51%	16, 167	desmoplastic and extensive nodularity subtype
PDGFRB	overexpression	unknown	168	metastatic medulloblastoma
OTX2	overexpression	>70%	52, 53, 151, 169, 170	classic subtype and anaplastic features
	amplification	~33%		_
ATOH1	expression	unknown	16	desmoplastic subtype
$p75^{NTR}$	expression	unknown	48, 171	desmoplastic subtype and unfavorable outcome?
TrkA	overexpression	~67%	172	apoptotic index
TrkC	overexpression	29-73%	39, 172-176	favorable outcome
Heparanase	expression	62-88%	176, 177	_
NeuroG1	expression	~55%	178, 179	non-desmoplastic metastatic medulloblastoma and unfavorable outcome
Calbindin	expression	~41%	180	non-desmoplastic medulloblastoma and tumor recurrence
p53	mutation	0-11%	181-184	unfavorable outcome
PAX5	overexpression	~70%	185	_

A. Medulloblastoma

Gene	Change	%	Reference	Correlating with
MDM2	overexpression	0-20%	181, 186	unfavorable outcome in adults
CDK6	overexpression	~30%	62	unfavorable outcome
HIC1	hypermethylation	~70%	187, 188	unfavorable outcome
EEF1D	overexpression	unknown	118	unfavorable outcome
RPL30	overexpression	unknown	118	unfavorable outcome
RPS20	overexpression	unknown	118	unfavorable outcome
STMN1	overexpression	unknown	23, 189	unfavorable outcome
hTERT	overexpression	~42%	108, 190	tumor progression
SGNE1/7B2	hypermethylation	~70%	37, 191	classic medulloblastoma
RASSF1A	hypermethylation	80-90%	71, 187	_
CASP8	hypermethylation	~90%	73, 187, 192-195	classic and anaplastic subtype and unfavorable outcome
ZIC2	hypermethylation	unknown	74	_
$p14^{ARF}$	hypermethylation	4-50%	187	_
$p16^{INK4A}$	hypermethylation	2-14%	187, 192, 196, 197	_
TIMP3	hypermethylation	0-11%	187, 192, 196	_
CDH1	hypermethylation	~8%	192	_
$p18^{INK4C}$	hypermethylation	~20%	198	_
S100A6	hypermethylation	~12%	199	large cell anaplastic subtype
S100A10	hypermethylation	~12%	199	_
S100A4	hypomethylation	~17%	199	metastatic medulloblastoma
MCJ	hypermethylation	~33%	200	
RB1	hypermethylation	~18%	201	
DKK1	histone acetylation	unknown	202	

B. Ependymoma

Gene	Change	%	Reference	Correlating with
SHH signaling				
Gli1	overexpression	unknown	87	_
Gli2	overexpression	unknown	87	_
Cyclin D1	overexpression	unknown	82, 87	supratentorial ependymoma
Wnt signaling				
EB1	underexpression	unknown	86	_
Notch signaling				
HES1	overexpression	unknown	87	_
JAG1	overexpression	unknown	82	supratentorial ependymoma
JAG2	overexpression	unknown	82	supratentorial ependymoma
Notch 1	overexpression	unknown	87	_
Notch 2	overexpression	unknown	87	_
FZD1	overexpression	unknown	87	_

B. Ependymoma				
Gene	**Change**	**%**	**Reference**	**Correlating with**
HEY2	overexpression	unknown	[87]	_
EPHB-EPHRIN signaling				
EPHRIN A3	overexpression	unknown	[82]	Supratentorial ependymoma
EPHB3	overexpression	unknown	[82]	Supratentorial ependymoma
EPHB2	overexpression	unknown	[82]	Supratentorial ependymoma
ErbB signaling				
ErbB4	overexpression	>75%	[203]	Proliferation activity and unfavorable outcome
ErbB2	overexpression	>75%	[203]	Proliferation activity and unfavorable outcome
IGF signaling				
IGF-1R	expression	29-80%	[204]	anaplastic ependymoma?
IGF-2	overexpression	unknown	[47, 205]	_
IGFBP-2	overexpression	unknown	[47]	_
IGFBP-3	overexpression	unknown	[47]	_
IGFBP-5	overexpression	unknown	[47]	_
Other				
NF2	mutation hypermethylation	10-71% 0-7%	[206-208] [209, 210]	spinal ependymoma _
SCHIP1	underexpression	unknown	[86]	_
MEN1	mutation	~2%	[81, 211]	recurrent ependymoma
SULT4A1	underexpression	unknown	[87]	_
SOX9	overexpression	unknown	[189]	favorable outcome
Calcyphosine	expression	~59%	[189]	epithelial differentiation
hTERT	amplification	~24%	[97, 212]	proliferation activity and unfavorable outcome
CBX7	underexpression	~55%	[86]	_
p53	mutation	0-6%	[184, 213-216]	_
MDM2	amplification	4-35%	[213, 217]	_
p73	overexpression hypermethylation	unknown 5-33%	[218, 219] [210, 220, 221]	grade II ependymoma _
$p14^{ARF}$	deletion hypermethylation	1-7% 0-28%	[82, 97] [220-222]	supratentorial ependymoma adults
$p15^{INK4B}$	hypermethylation	0-21%	[220, 222]	adults
$p16^{INK4A}$	deletion hypermethylation	1-7% 0-32%	[82, 97] [87, 210, 220, 222]	supratentorial ependymoma adults
RASSF1A	hypermethylation	56-86%	[209, 220]	_
CASP8	hypermethylation	4-50%	[209, 210, 220]	myxopapillary ependymoma
DAPK	hypermethylation	0-57%	[87, 209, 210, 221]	_

B. Ependymoma				
Gene	**Change**	**%**	**Reference**	**Correlating with**
MGMT	hypermethylation	0-20%	87, 209, 210, 220, 221	_
FHIT	hypermethylation	22%	209	_
TFRSF10C	hypermethylation	9-50%	209	_
TFRSF10D	hypermethylation	36%	209	_
BLU	hypermethylation	14%	209	_
RARB	hypermethylation	0-15%	87, 209	_
THBS1	hypermethylation	0-30%	210, 220	_
TIMP3	hypermethylation	0-40%	210, 220, 221	_
RB1	hypermethylation	0-14%	201, 209, 221	_
MCJ	hypermethylation	10%	199	_
GSTP1	hypermethylation	28%	221	_
HIC1	hypermethylation	83%	87, 223	_

ErbB signaling

ErbB belongs to the receptor tyrosine kinase family I, which consists of four receptor tyrosine kinases (ErbB1-4) and a variety of ligands, including several neuregulins being important in regulating the development of neuronal tissue[28]. ErbB4 expression, especially the CYT1 isoform, is overexpressed in tumors with low Gli1 levels, which suggests that ErbB signaling is regulated by SHH signaling[29]. CYT1 is the only isoform of ErbB4 that is able to activate anti-apoptotic PI3K/AKT signaling[30], which is important in medulloblastoma development. Overexpression of the CYT1 ErbB4 isoform is correlated to the anaplastic medulloblastoma subtype and ErbB2 expression levels. As the ErbB2 gene is located on chromosome 17q11.--q12, a region that is frequently gained in medulloblastomas, ErbB2 was regarded as a potential medulloblastoma oncogene. ErbB2 expression, especially in combination with high ErbB4 expression has poor prognostic impact in medulloblastoma, and is associated with the presence of metastases and a high mitotic index[28, 31]. Overexpression of ErbB2 increases the migration of medulloblastoma cells in vitro and pro-metastatic genes, e.g. involved in cell adhesion and invasion, are up-regulated by ErbB2[32]. Approximately one third of the medulloblastomas co-expressing ErbB2 and ErbB4 also express the ErbB ligand NRG1-β, suggesting an autocrine loop resulting in disease progression. Interestingly, one of the targets of NRG1-β is c-myc[33].

c-myc signaling

c-myc belongs to the myc transcription factor family which is important in cell cycle regulation, proliferation and differentiation and is involved in many human malignancies[34]. c-myc overexpression in medulloblastoma is associated with the large cell/anaplastic subtype and poor survival (Table 2). c-myc activation can be caused by the activation of the SHH and Wnt pathways[35], translocations, activating mutations, viral insertion and genomic amplification. In mouse models, c-myc alone is not sufficient to induce medulloblastomas, but it is

suggested that c-myc cooperates with SHH in the pathogenesis of medulloblastoma[36]. The c-myc binding protein JPO2 can potentiate c-myc transforming activity and is associated with metastatic medulloblastoma (Table 2). We observed up-regulation of mRNA levels of BCAT1, a myc-target, in metastatic medulloblastoma and also detected the BCAT1 protein in the cerebrospinal fluid of medulloblastoma patients[22]. Another member of the myc-family, n-myc, is amplified in ~5% of medulloblastoma and is an important and direct target of the SHH signaling pathway promoting cell cycle progression in the developing cerebellum (Table 2). In concordance, n-myc up-regulation is observed in medulloblastoma associated with activated SHH signaling[37, 38]. N-myc amplification correlates with unfavorable survival, but this correlation is less clear than for c-myc[39]. Prevention of n-myc degradation by PI3K[40], may provide an explanation for the enhancing effect of IGF/PI3K signaling pathway on the SHH-related development of medulloblastoma[38].

IGF/PI3K signaling

The insulin-like growth factor (IGF) system also plays an important role in neuronal development and is involved in the development of brain tumors[41]. The majority of medulloblastoma overexpress the IGF-1R protein and more than half of medulloblastomas express the activated phosphorylated form of the IGF-1R (Table 2). Moreover, activated forms of downstream signaling molecules of IGF-1R, such as IRS-1, PI3K, AKT/PKB, Erk-1 and Erk-2, are detected in the majority of medulloblastoma. Inhibition of IGF-1R signaling reduces medulloblastoma tumor growth[42]. This inhibition is augmented by constitutive GSK3β phosphorylation[43], suggesting that the combined inhibition of the IGF-1R and dephosphorylation of GSK3β might be an effective treatment for medulloblastoma. The IGF-1R ligands, IGF-1 and IGF-2, are important mitogens in cerebellar granule precursors and medulloblastoma[44, 45]. Patti et al.[45] show the presence of an autocrine loop causing IGF-1R activation and leading to proliferation in a medulloblastoma cell line. IGF-2 is a downstream target of SHH signaling[46] and in concordance, IGF-2 overexpression is predominantly observed in desmoplastic medulloblastomas. The IGF-binding proteins (IGFBPs) modulate IGF action and are differentially expressed in brain tumors. We observe increased IGFBP-2 and IGFBP-3 mRNA expression levels in medulloblastoma, which is accompanied by increased IGFBP-3 levels and IGFBP-3 proteolysis in the cerebrospinal fluid of brain tumor patients[47]. The IGF-1R signaling pathway may result in activation of AKT and PI3K, and also RAS/MAPK signaling. Downstream targets of the RAS/MAPK pathway and PDGFRB are up-regulated in metastatic medulloblastoma (Table 2).

Cells of origin – lateral cerebellar hemispheres

Activation of different signaling pathways in different medulloblastoma subtypes suggests that medulloblastoma has different origins. Potential cells of origin are the stem and/or progenitor cells in the external granular layer that have persisted after the first years of life and the pluripotent stem cells of the ventricular subependymal matrix, which are capable of

differentiating into neuronal or glial cells. Several findings support this hypothesis of double origin. Desmoplastic medulloblastoma are usually found in the cerebellar hemispheres and are thought to arise from neural precursor cells in the external granule layer[48]. In concordance, they are characterized by activated SHH signaling and IGF-2 overexpression, which affects the proliferation of cerebellar granule precursors. CXCR4, ATOH1 and the p75 neurotrophin receptor ($p75^{NTR}$) are markers of the stem and/or progenitor cells in the external granular layer and are predominantly found in desmoplastic medulloblastoma (Table 2). CXCR4 is important for migration and cell cycle control of granular precursors and is a target of SHH. Aberrant activation of the CXCR4 receptor might contribute to an increased malignant potential, but mutations in CXCR4 are only rarely observed in medulloblastoma. ATOH1 is a basic helix-loop-helix transcription factor that influences the development of granular cerebellar precursors via the Notch pathway[49]. $p75^{NTR}$ belongs to the family of neurotrophins and neurotrophin receptors, which are important in the normal development of the cerebellum[50]. Expression of $p75^{NTR}$ is suggested to be a marker of tumor progression (Table 2). Another neurotrophin receptor, TrkC, is one of the first biological markers in medulloblastoma and is found to be a strong predictor of favorable outcome (Table 2). This is probably caused by the fact that binding of the TrkC ligand to the receptor induces apoptosis[50].

Cells of origin – cerebellar vermis

In contrast to the desmoplastic medulloblastoma arising in the lateral cerebellar hemispheres, medulloblastoma subtypes arising in the cerebellar vermis are suggested to originate from cells in the ventricular matrix and Purkinje neurons. Calbindin and NeuroG1 expression are specific for stem and/or progenitor cells in the cerebellar ventricular zone. Calbindin is expressed in the majority of classic medulloblastoma and its expression is suggested to be a marker for recurrence in medulloblastoma (Table 2). NeuroG1 (NeuroD3), belongs to the NeuroD family of basic helix-loop-helix transcription factors, regulating the transcription of genes involved in neuronal differentiation[51]. NeuroG1 expression is correlated to the overexpression of myc and is indicative of a poor prognosis in medulloblastoma (Table 2).

OTX2 overexpression, observed in more than two thirds of medulloblastomas, is also characteristic for the classic medulloblastomas arising in the cerebellar vermis (Table 2). However, as cells of the fetal external granular cerebellar layer are also shown to express OTX2, it is suggested that a subset of classic medulloblastoma negative for calbindin, may also arise from the external granular layer[52]. OTX2 expression is correlated to the presence of proliferating, poorly differentiated cells to anaplastic features, but no correlation with outcome was observed. Amplification of OTX2 occurs in up to one third of primary medulloblastomas, but mutations have not been identified. OTX2 knockdown, either by siRNAs or by treatment with all-trans-retinoic acid, induced apoptosis in vitro, which suggests that OTX2 might be an interesting therapeutic target[53].

Table 3. Balanced chromosomal translocations identified in medulloblastomas and ependymomas.

Medulloblastoma	Reference	Ependymoma	Reference
t(1;3)(p13;p13)	224	t(1;2)(p33;q21)	225
t(1;3)(q32;q27)	104	t(1;2)(q21;q35)	226
t(1;4)(q31;q35)	227	t(1;3)(p34;q21)	226
t(1;6)(p21;q11-13)	228	t(1;7)(q25;q35)	229
t(1;8)(q1?;q2?)	230	t(1;8)	225
t(1;8)(q25;q22)	231	t(1;9)(p36;q13)	232
t(1;11)(q32;p15)	233	t(1;14)(q?;p?)	233
t(1;14)(p22;q31)	234	t(1;20)(q21;q13)	225
t(1;15)(p36;q11)	233	t(1;22)(q11;q13)	235
t(2;12)(q21;q23)	233	t(2;4)(q34;q35)	236
t(2;15)(q37;q15)	237	t(2;10)(p25;q12)	236
t(3;6)(p21;q12)	237	t(2;17)(p11;p11)	225
t(3;9)(q27;q22)	233	t(2;22)(p12;q13)	234
t(3;12)(p21;q13)	233	t(2;22)(p13;q13)	238
t(3;17)(p13;p13)	233	?t(3;3)(q29;q25)	239
t(5;6)(q13;q21)	237	t(3;4)(q?;q?)	233
t(5;8;10)(q34;q24;q24)	233	t(3;6)(q11;q11)	238
t(6;13)(q25;q14)	104	t(3;11)(q29;q25)	240
t(6;14)(q27;q11)	104	t(3;15)(q?;q?)	233
t(6;19)(q21;q13)	227	t(4;22)(p16;p13)	240
t(7;13)(q11;q34)	241	t(6;11)(p?;q?)	233
t(7;19)(p11;p11)	233	t(6;11)(q27;q25)	240
t(9;11)(q34;q13)	224	t(6;16)	242
t(9;19)(q22;q13)	225	t(9;11)(q34;q25)	240
t(10;16)	230	t(9;16)(q?;q??	233
t(11;13)(p13;q14)	104	t(9;17)(q34;q25)	240
t(11;13)(q15;q11)	227	t(10;11;15)(p12;q13;p12)	243
t(12;13)(p13;p11)	225	t(11;12)(q13;q24)	211
t(12;21)	241	t(11;17)(q13;q21)	241
t(13;14)(q11;p11)	225	t(11;17)(q25;q25)	240
t(13;15)(q32;q22)	233	t(11;18)(q13;q21)	225
t(?15;16)(q13;p13)	164	t(11;19)(q25;q13)	240
t(16;17)(q?;q?)	244	t(12;18)(p11;q11)	225
t(16;20)(q13-22;q13)	54		
t(17;17)(p?;p?)	241		
t(17;18)(p11;q11)	104		
t(18;22)(q23;q11)	104		
t(18;20)(q23;p13)	245		
t(X;15)(p22;q25)	233		
t(X;18)(p11;q11)	225		
t(X;22)(p22;q11)	246		

Cytogenetics

Much knowledge about cytogenetic abnormalities of brain tumors has been obtained by conventional cytogenetic, loss of heterozygosity and molecular genetic analyses, e.g.

comparative genomic hybridization (CGH). Karyotyping reveals that balanced translocations are relatively infrequent in medulloblastomas compared to chromosomal gains and losses (Table 3). No recurrent translocations have thus far been identified in medulloblastoma. Figure 2 provides a summary of the chromosomal gains and losses in medulloblastomas identified by CGH. Conventional CGH can detect regions of copy number change, and the recent development of array-based CGH has resulted in higher-resolution analyses allowing to define more precisely which regions are involved. In addition, correlation of these data with gene expression levels may identify genes that are the potential important driver genes in these copy abnormalities.

Chromosome 17

The most commonly reported cytogenetic change in medulloblastoma is loss of 17p in up to ~50% of medulloblastoma, often associated with a gain of 17q leading to the formation of an isochromosome 17q (i(17q))[54]. As i(17q) can be found as single structural abnormality, it is suggested as primary event in medulloblastoma development. In some studies loss of 17p is associated with a poor prognosis, while others fail to find this association[55, 56]. The incidence of i(17q) is low in desmoplastic medulloblastoma compared to classic and large cell anaplastic medulloblastoma. Despite the identification of several common chromosomal breakpoint regions at 17p11.2, 17p11.2-17q11.2 and 17q21.31 and various commonly deleted regions on 17p, e.g. 17p13.1 and 17p13.3[57, 58], the affected tumor suppressor gene involved in the pathogenesis of medulloblastoma has not been identified thus far.

p53, one of the most important tumor suppressor genes, was initially suggested to be of importance in medulloblastoma, as it is localized on chromosome 17p13. However, despite the fact that patients with germline p53 mutations have a predisposition to develop medulloblastomas (Table 1), that loss of p53 facilitates medulloblastoma development in mouse models[12] and that up to 40% of medulloblastoma show p53 protein expression indicating a dysfunctional p53 protein, we and others showed that the incidence of p53 mutations in sporadic medulloblastoma is low (Table 2). MDM2 overexpression, known to cause inactivation of p53, is also very rare in medulloblastomas (Table 2). p53 inhibition by PAX5 is suggested to play a role in medulloblastomas as the expression of PAX5 is deregulated in ~70% of cases (Table 2).

Besides p53, several other candidate tumor suppressor genes on 17p are suggested. Interestingly, 17p carries several genes suggested to be involved in the regulation of SHH signaling. HIC1, located on 17p13.3 is aberrantly methylated in medulloblastoma and the subsequent transcriptional silencing is associated with poor outcome (Table 2). Recently it was found that loss of HIC1 together with loss of PTCH1 results in a higher incidence of medulloblastomas[59]. This is probably related to the cooperation of HIC1 and PTCH1 in the silencing of ATOH1 expression, which is required for medulloblastoma growth. REN^{KCTD11}, a putative tumor suppressor gene located on chromosome 17p13.2 is deleted in 39% of medulloblastoma (Table

2). REN^{KCTD11} inhibits medulloblastoma cell proliferation by antagonizing the activation of SHH target genes. Deletion of this gene might thus result in enhanced SHH signaling and increased proliferation of granule cell precursors. The myc inhibitor MnT, mapped to 17p13.3 is also deleted or underexpressed in medulloblastoma. As myc and n-myc are both targets of SHH signaling, loss of the Mnt gene on 17p might again link this chromosomal abnormality to SHH signaling.

Gain of 17q can also occur in the absence of a 17p deletion, suggesting that duplication of genes on 17q influence medulloblastoma development. An amplicon on 17q23.2 contains the APPBP2 and PPM1D genes[58]. PPM1D overexpression can for example inhibit p53 tumor suppressor activity[60]. As the regions of loss of 17p and gain of 17q are large, it is also suggested that a gene dosage effect of genes on 17p and 17q, rather than one tumor suppressor gene, is tumorigenic in medulloblastoma[58].

Chromosome 7

A cytogenetic abnormality that is often seen in combination with a gain of 17q is gain of chromosome 7. As for chromosome 17, the gene of interest is not yet identified. Hui et al.[61] indicate an amplification core at 7q34-q35, containing several oncogenes. A novel amplicon at 7q21.2 only contained the CDK6 gene. CDK6 can phosphorylate RB1, being an important regulator of proliferation and differentiation. CDK6 is overexpressed and indicative of a poor prognosis in medulloblastomas (Table 2).

Other copy number abnormalities

Other recurrent abnormalities in medulloblastomas are losses on 6q, 8p, 9q, 10q, 11, 16q, 20, X and Y and gains on 1q, 2p, 4q, 6q, 9p, 13q, 14q and 18 (Figure 2). Several regions with consistent copy number gain have been identified on 1q, e.g. 1q21.3-23.1[61], 1q32.1[61, 62] and 1q32.3-qter[62, 63]. HLX1 is suggested to be involved in the gain on 1q, as its expression was markedly increased in medulloblastomas[64]. Concerning losses on 6q, a small region of deletion is identified at 6q23.1[61]. The commonly deleted region on 8p is localized between 8p21.3-8p23.2, adjacent to the tumor suppressor gene DLC1[63, 65]. The minimal region of overlap of losses on chromosome 16q is at the distal end of 16q, at 16q22.2-qter[66]. Regarding losses of chromosome 10, several minimal regions of overlap are observed, one involving the 10q23 region containing the PTEN gene, another involving a hemizygous deletion in 10q25.1 and a third involving the 10q26.3 region[66-68]. The SUFU gene, mutated in a small subset of medulloblastomas, maps to 10q24.3 and is therefore suggested to have a role as tumor suppressor gene (Table 2). Loss of 11p is identified in 10-20% of medulloblastoma (Figure 2). However, LOH analyses show allelic loss of 11p in >50% of tumors[68]. Minimal overlapping regions of loss on chromosome 11 are 11pter-11p11.2 and 11q13.2-11qter. The region of gain on 14q is mapped to 14q12 and contains the FOXG1 gene, which is aberrantly expressed in the majority of medulloblastoma (described above). Loss of chromosome

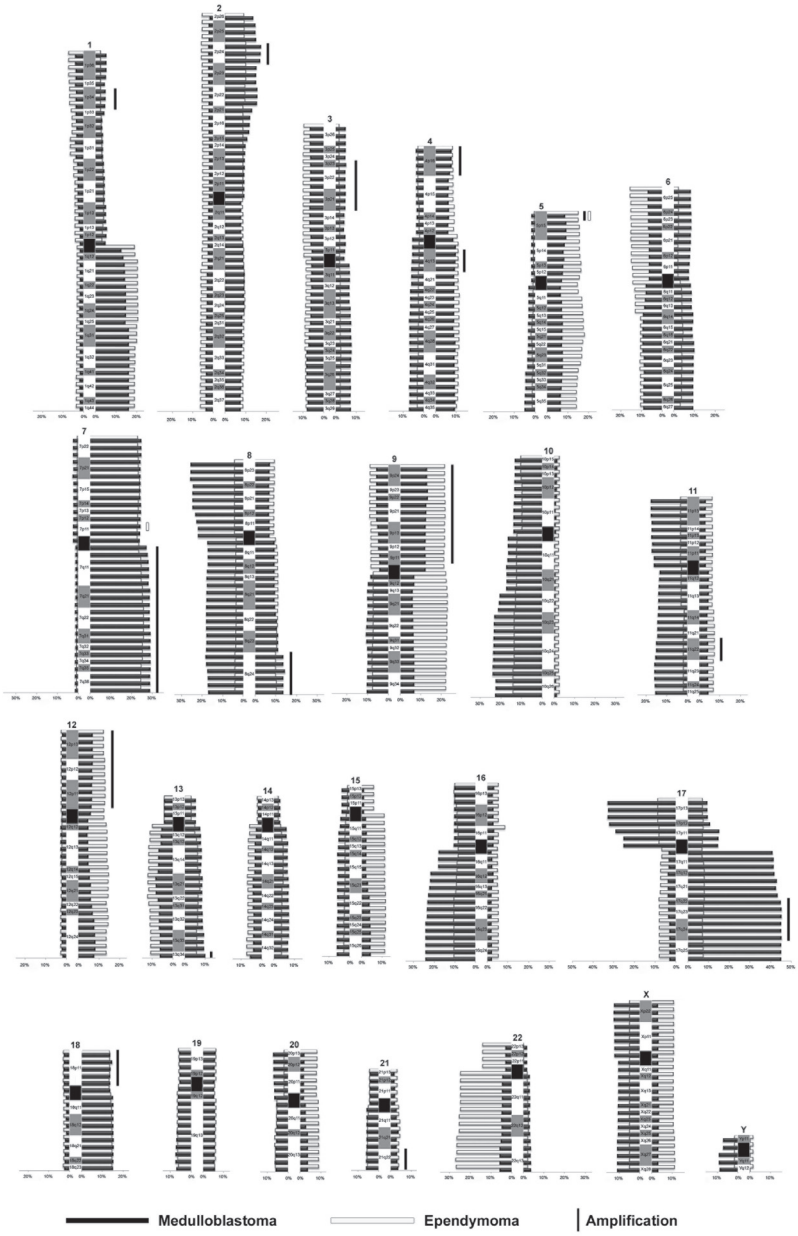

Figure 2. Copy number aberrations and amplifications in medulloblastomas and ependymomas by (a)CGH.

This figure displays the frequency of copy number abnormalities and amplifications described in medulloblastomas (n=455)[55, 64, 66, 67, 69, 104-121] and ependymomas (n=354)[96, 98, 99, 113, 122-130]. Some studies only provided a summary of their data[61-63, 87, 97] or did not separate between medulloblastomas and PNETs[131] and these results are therefore not included in this figure. Important findings from these studies are described in the text.

20 frequently involves the whole chromosome. However, the commonly deleted region on chromosome 20 is recently identified at 20q13.2-q13.3[61, 63], but no target genes have been identified yet.

Amplifications

Gene amplifications are relatively rare in medulloblastomas. The identified amplification sites are displayed in figure 2. Several potential oncogenes are involved in these amplifications. MYCL1 is an important candidate gene in the amplification region on chromosome 1p34[63]. The c-myc and n-myc gene on respectively chromosome 8q24 and 2p24 are amplified in a small proportion of tumors, mainly large cell anaplastic medulloblastoma (Table 2). However, gain of 8q, including the 3 ribosomal genes EEF1D, RPL30 and RPS20, is also predictive of poor outcome independent of myc (Table 2). The amplicon on 5p15 involves the hTERT gene, a gene amplified and overexpressed in medulloblastoma (Table 2). hTERT is able to compensate for progressive telomere shortening, leading to immortalization. Amplification of hTERT is associated with tumor progression in medulloblastoma. Further analysis of the 9p amplification suggested the importance of the 9p23-p24 region, including the JMJD2C gene. The 11q22.3 region maps the cyclin D1 locus, which is amplified in a variety of tumors. A possible candidate gene for the 13q34 amplification is IRS2[69]. This gene is amplified and overexpressed in a small subset of glioblastoma.

Epigenetics

Recently, also epigenetic changes have shown to be important in tumorigenesis. Both histone modifications (acetylation, methylation and phosphorylation) and hypermethylation of CpG motifs in promoter regions may induce transcriptional silencing of tumor suppressor genes[70]. Several putative tumor suppressor genes are aberrantly methylated in subgroups of medulloblastoma (Table 2). RASSF1A regulates cyclin D1 expression, being important in controlling the cell cycle. In contrast to other malignancies, hypermethylation of RASSF1A in medulloblastoma is not accompanied by allelic loss of 3p21.3 or mutation, indicating that bi-allelic loss is the primary mechanism of inactivation of RASSF1A[71]. CASP8 is a cystein protease involved in death receptor-mediated apoptosis[72]. We and others showed that promoter hypermethylation of CASP8 leading to loss of CASP8 mRNA expression induces resistance to TRAIL induced apoptosis in embryonal tumors of childhood, such as medulloblastoma and neuroblastoma[73]. In primary tumors, aberrant promoter methylation of CASP8 was seen most frequently in classic and anaplastic medulloblastoma, being an independent unfavorable prognostic factor. Transcriptional silencing of SGNE1/7B2, a gene located on 15q11-15, occurs predominantly in classic medulloblastoma. SGNE1 is a calcium-dependent serine protease, which inhibits tumor cell proliferation. ZIC2 is a zinc-finger transcription factor essential for the developing central nervous system and its expression is down-regulated in medulloblastomas[74]. $P18^{INK4C}$ is a CDK inhibitor and loss of expression of this gene can

induce medulloblastoma in mouse models in collaboration with loss of PTCH1 or p53[75]. Three members of the S100 gene family are aberrantly methylated in 10-20% of medulloblastoma (Table 2). Hypermethylation and silencing of S100A6 is associated with the large cell anaplastic subtype of medulloblastoma. In contrast, S100A4 is hypomethylated, which results in increased expression. The pro-metastatic gene S100A4 is a direct target of ErbB2 signaling, associated with a poor prognosis in medulloblastoma. MCJ, a member of the DNAJ protein family that influences chemotherapy resistance can be inactivated by bi-allelic hypermethylation, but hypermethylation of 1 allele also occurs in combination with genetic loss of the second allele (Table 2). Dickkopf-1 (DKK1) is epigenetically silenced in medulloblastoma by histone acetylation in the promoter region (Table 2). DKK1, a Wnt signaling antagonist, is an important suppressor of cell growth and inducer of apoptosis.

Proteomics

Despite enormous progress in applications and sensitivity, proteomic techniques are not frequently used to screen for aberrantly expressed proteins in brain tumors. The proteome of two representative medulloblastoma cell lines, DAOY and D283MED was studied by 2-dimensional (2D) gel electrophoresis with subsequent matrix-assisted laser desorption/ionization identification[76]. Several proteins, described previously in other malignancies, such as SIP or HSP27 and other new candidate tumor-related proteins were identified. We studied protein expression profiles of primary medulloblastoma using two-dimensional difference gel electrophoresis (2D-DIGE) followed by mass spectrometry and found STMN1 to be overexpressed in medulloblastoma (Table 2).

EPENDYMOMA

Clinical aspects

Ependymomas, predominantly occurring in the posterior fossa in childhood, may also arise supratentorially, and account for approximately 10% of all intracranial tumors in childhood and a higher proportion, up to 30% in some series, in children younger than 3 years of age[77]. A variety of different subtypes of ependymomas have been identified and the anaplastic variant seems to carry a worse prognosis[77, 78]. Surgery remains a major component of the management of ependymomas and patients with posterior fossa ependymomas who have tumors amenable to gross total resections and are subsequently treated with radiotherapy, have a 70% or higher likelihood of long-term disease control and possibly cure.

Recent studies have focused on the utility of chemotherapy followed by second-look surgery prior to radiotherapy in those patients whose tumors are not totally, or near-totally resected[79]. There is increasing evidence to suggest that ependymomas are chemosensitive, but in older children chemotherapy has been primarily reserved for those patients with

subtotally resected tumors or those with anaplastic lesions. Conformal radiation therapy techniques are primarily utilized in children with ependymomas and radiotherapy has now been utilized in cooperative group studies in children as young as one year of age. In very young children, especially those less than one year of age, treatment with chemotherapy is often utilized in attempts to delay and, in select cases obviate, the need for radiotherapy, but high-dose chemotherapeutic regimens supported by autologous peripheral stem cell rescue have not been effective[79]. The incidence of leptomeningeal dissemination at the time of diagnosis varies significantly between series, but in general less than 10% of children will have disseminated disease at the time of diagnosis and craniospinal radiotherapy is reserved for those with documented disseminated disease. There is increasing evidence that suggests that supratentorial ependymomas differ biologically from those arising in the posterior fossa. Although standard treatment of partially resected supratentorial ependymomas is the same as for partially resected posterior fossa tumors, there are studies evaluating the efficacy of surgery alone for totally resected supratentorial tumors.

Unfortunately, biological characteristics of ependymomas are largely unknown. This is mainly caused by the fact that ependymoma is a heterogeneous disease and can be subdivided into a wide range of subgroups based on histology and localization, which results in relatively small series of patients.

Developmental signaling pathways

NF2

As in medulloblastomas, genetic syndromes associated with a predisposition to develop ependymomas, such as neurofibromatosis type 2 (NF2) (Table 1), were initially thought to provide clues about the genetic abnormalities involved in the pathogenesis of ependymomas. The NF2 gene is located on 22q12 and as allelic loss of chromosome 22 is frequently observed in ependymomas, NF2 was suggested to be a tumor suppressor gene involved in the development of ependymomas. However, mutations of the NF2 gene are rarely observed in sporadic ependymomas, except for the spinal ependymomas (Table 2). Inactivation of NF2 by hypermethylation is also rare (Table 2). Interestingly, although NF2 does not play an important role in sporadic non-spinal ependymomas, the expression of SCHIP-1, an NF2 interacting gene is significantly down-regulated in pediatric ependymomas (Table 2).

MEN1

Also, other hereditary forms of ependymoma are uncommon. Ependymomas have been described in patients with MEN1 syndrome, which is characterized by the development of multiple endocrine tumors[80]. The MEN1 gene is located on chromosome 11q13, a chromosomal region that is involved in allelic loss and rearrangements in ependymomas[81]. However,

mutations in the MEN1 gene are only described in a small number of recurrent ependymomas (Table 2).

An important recent finding is the fact that gene expression signatures of ependymomas from different locations of the central nervous system correlated with those of the corresponding region of the normal developing CNS[82]. The differentially expressed genes are predominantly involved in the regulation of neural precursor cell proliferation and differentiation. In addition, ependymomas contain rare populations of cancer stem cells resembling radial glia cells, which are sufficient to give rise to tumor development in mice[82]. Therefore, it is hypothesized that these radial glial cells in different parts of the CNS are predisposed to acquire distinct genetic abnormalities that transform these cells into cancer stem cells of supratentorial, infratentorial and spinal ependymomas. These data imply that signaling pathways involved in the development of the brain and neural stem cells, such as Notch, Wnt, SHH and p53 are important in the pathogenesis of ependymomas (Figure 1).

EPHB-EPHRIN and Notch signaling

Active EPHB-EPHRIN and Notch signaling is indeed observed in ependymomas, especially in those located in the supratentorial region (Table 2). Both signaling pathways are important for the maintenance of neural stem cells in the cerebral sub-ventricular zone[83, 84]. The overexpression of the Notch target ErbB2 in the majority of ependymomas and its correlation with proliferation and poor outcome also points to the importance of Notch signaling in ependymomas.

Wnt signaling

Ependymomas have been described in patients with APC mutations associated with Turcot's syndrome[85]. However, in contrast to medulloblastomas, mutations in APC and β-catenin are not found in sporadic ependymomas (Table 2). Despite the absence of these mutations, gene expression profiling identifies aberrantly expressed genes involved in the Wnt signaling pathway, suggesting alternative mechanisms for disruption of this pathway[86].

SHH signaling

Involvement of SHH signaling in ependymomas is suggested by the overexpression GLI2, GLI and STK36 and underexpression of PRKAR1B[87]. In addition, overexpression of the SHH target IGF-2, is frequently observed in these tumors (Table 2). Besides the overexpression of IGF-2, we find overexpression of IGFBP-2, -3 and -5 in ependymomas, also suggesting the involvement of the IGF-system in the pathogenesis of ependymomas[47].

p53 signaling

Only one patient with a germline p53 mutation has been reported with an ependymoma[88]. Despite the fact that p53 immunostaining is suggested to be associated with an unfavorable

prognosis[89], p53 mutations are extremely rare in sporadic ependymomas (Table 2). Other ways of p53 inactivation have been observed in subgroups of ependymomas, but are also relatively uncommon. Some report a high incidence of mdm2 expression and amplification in ependymomas, whereas others conclude that mdm2 plays a role in only a very small number of patients (Table 2). p73, a gene that shares structural and functional homologies with p53 and is able to induce mdm2, is overexpressed in grade II ependymoma (Table 2). Inhibition of p53 expression by PAX5 is not of importance in ependymomas. The negative regulation of p53 by $p14^{ARF}$ is recently suggested to be of importance in subgroups of ependymomas. $p14^{ARF}$ is located on chromosome 9p21 together with two other tumor suppressor genes, $p15^{INK4B}$ and $p16^{INK4A}$, which are all cell cycle regulators[90]. Expression of these genes is decreased by homozygous deletion, promoter hypermethylation or point mutations in several malignancies. In ependymomas, decreased protein levels of $p14^{ARF}$ are found to correlate with increased tumor grade and p53 protein accumulation[91]. Deletion of the $p16^{INK4A}$/$p14^{ARF}$ locus is recently associated with supratentorial ependymomas (Table 2). The observed frequency of inactivation by hypermethylation of the 3 tumor suppressor genes in ependymomas is variable (Table 2), and is observed more frequently in adults than in children.

Gene expression and clinical characteristics

Although recent gene expression profiling studies from our and other laboratories have correlated sets of genes to patient characteristics, tumor location and tumor grade, the significance of these genes in the pathogenesis of ependymomas still needs to be determined. Genes that are overexpressed in ependymomas compared to normal control tissue were for example GLU, RAF1, SOX9, calcyphosine, annexin A1 and YAP1. We showed that SOX9 expression is associated with a favorable outcome in pediatric ependymomas (Table 2). Several genes are characteristic for tumor location. Intracranial ependymomas are characterized by the overexpression of EMX2, MSI2, ABCG1, FLT1, TOP2A, CRIM1, CAMK2D, TFPI2, EBI2, ACTR3, NRCAM, PAX3, NET1 and MSX1, in which the first 3 were specifically up-regulated in supratentorial ependymomas and the last 3 in infratentorial ependymomas. ADAM9, TFAM, EDN1 and GAS2L1 were down-regulated in intracranial ependymomas. HOX genes might play a role in the maintenance of the cancer stem cell phenotype in spinal ependymomas, as HOX family members, such as HOXB5 and HOXA9 are predominantly overexpressed in spinal ependymomas[82].

Underexpression of pro-apoptotic NFκ-β2 and pleckstrin and the overexpression of a PTEN homologue are associated with tumor recurrence[92]. Several genes, such as NRCAM, COL4A2, CDK4 and survivin are overexpressed in ependymomas with high proliferation indices[93, 94]. Tumor proliferation, reflected by Ki-67 positivity, is an important factor in the discrimination between low- and high grade ependymoma and is a more reliable unfavorable prognostic factor than histological grading[95].

Cytogenetics

As is described for medulloblastomas, advanced cytogenetic techniques now allow more precise determination of chromosomal breakpoint regions and the identification of the genes involved. Table 2 and figure 2 respectively provide the identified balanced translocations and a summary of observed copy number aberrations in ependymomas.

Recurrent copy number abnormalities

Frequently observed copy number abnormalities in ependymomas are losses of 6, 9p, 10, 11, 13, 17 and 22 and gains of 1q, 5, 7, 9 and 12. Gain of 1q e.g. occurs more frequently in children compared to adults, correlating with an intracranial tumor localization and grade III ependymomas[96, 97]. More specified regions on chromosome 1q, 1q21.1-32.1 and 1q25 are associated with unfavorable outcome[97, 98]. As in medulloblastoma, the 5p15.3 region, containing the hTERT gene is frequently gained in ependymomas and high hTERT expression is associated with proliferation and unfavorable outcome (Table 2). Loss of 6q is associated with intracranial, predominantly infratentorial tumors[99]. Gain of chromosome 7 is predominantly found in spinal cord tumors[96, 99], and gain or high-level amplification of EGFR at 7p11.2 also predicts prognosis in intracranial tumors[97]. Another region of gain on 7p21 contains the candidate proto-oncogenes TWIST1 and HDAC9[87] and a small region on 7q34 contains the ARHGEF5 gene[97]. Gain of chromosome 12q and loss of chromosome 13 are predominantly observed in intracranial ependymomas[96, 97]. HOXC4 and CDK4 on 12q13 are mentioned as genes being important in the 12q gain[97, 99]. Loss of 17p13.3 is associated with intracranial infratentorial ependymomas[87]. HIC1 on 17p13.3 is suggested as the potentially involved oncogene. In addition to chromosomal loss, HIC1 hypermethylation and consequent transcriptional repression is observed in a substantial percentage of ependymomas (Table 2), suggesting an important role in ependymoma development.

Chromosome 22

Monosomy 22 is found more frequently in adults than in children, which probably results from the higher incidence of spinal tumors in adults compared to children. The existence of ependymomas with loss of 22q lacking NF2 mutations, suggests that other tumor suppressor genes are located on this chromosome. Multiple regions have been suggested, such as 22pter~22q11.2[100, 101] distally to the hSNF5/INI1 locus or 22q13.3, including the SULT4A1 gene (Table 2). Mutations in hSNF5/INI are rare/absent in ependymomas[102]. Gene expression profiling of ependymomas revealed several underexpressed genes on 22q12.3-q13.3, e.g FBX, c22orf2, CBX7 and SBF1[86]. Interestingly, CBX7 is involved in gene silencing of e.g. the $p16^{INK4A}$/$p14^{ARF}$ locus (Table 2).

Epigenetics

Epigenetic studies have also resulted in the identification of genes potentially being important in ependymoma pathogenesis (Table 2). Independent of clinical and histological subtype, RASSF1A is transcriptionally silenced by methylation in the majority of ependymomas, suggesting a function as a tumor suppressor gene. The fact that methylation is almost 100% at every CpG site, suggests that RASSF1A inactivation is an early event in tumorigenesis. CASP8, TFRSF10C and TFRSF10D are genes involved in the TRAIL apoptosis pathway and methylation of CASP8 is suggested to be characteristic of low-grade myxopapillary ependymomas. MGMT is involved in DNA repair and silencing of the gene is associated with increased sensitivity to alkylating agents in gliomas[103].

CONCLUSION AND FUTURE DIRECTIONS

Much progress has been made in the identification of biological factors involved in the pathogenesis of pediatric medulloblastomas and ependymomas in the past years, but still much has to be discovered. Deregulation of signaling pathways involved in brain development seems to play a more important role in the pathogenesis of these tumors than abnormalities in well-known tumor oncogenes and tumor suppressors, such as p53 or EGFR. Large collaborative studies are needed to provide insights into the importance of the genes discovered so far, in order to evaluate their possible use for improved risk stratification of patients and their use as therapeutic target. In addition, data from newly developed techniques such as microRNA profiling and the use of SNP or exon arrays may provide new insights into the regulation of post-transcriptional gene expression and alternative splicing.

REFERENCES

1. Wrensch M, Minn Y, Chew T, et al. Epidemiology of primary brain tumors: current concepts and review of the literature. Neuro Oncol 2002;4(4):278-299.
2. Ray A, Ho M, Ma J, et al. A clinicobiological model predicting survival in medulloblastoma. Clin Cancer Res 2004;10(22):7613-7620.
3. Packer RJ, Gajjar A, Vezina G, et al. Phase III study of craniospinal radiation therapy followed by adjuvant chemotherapy for newly diagnosed average-risk medulloblastoma. J Clin Oncol 2006;24(25):4202-4208.
4. Taylor RE, Bailey CC, Robinson K, et al. Results of a randomized study of preradiation chemotherapy versus radiotherapy alone for nonmetastatic medulloblastoma: The International Society of Paediatric Oncology/United Kingdom Children's Cancer Study Group PNET-3 Study. J Clin Oncol 2003;21(8):1581-1591.
5. Ris MD, Packer R, Goldwein J, et al. Intellectual outcome after reduced-dose radiation therapy plus adjuvant chemotherapy for medulloblastoma: a Children's Cancer Group study. J Clin Oncol 2001;19(15):3470-3476.
6. Rutkowski S, Bode U, Deinlein F, et al. Treatment of early childhood medulloblastoma by postoperative chemotherapy alone. N Engl J Med 2005;352(10):978-986.
7. Packer RJ, Biegel JA, Blaney S, et al. Atypical teratoid/rhabdoid tumor of the central nervous system: report on workshop. J Pediatr Hematol Oncol 2002;24(5):337-342.
8. Cowan R, Hoban P, Kelsey A, et al. The gene for the naevoid basal cell carcinoma syndrome acts as a tumour-suppressor gene in medulloblastoma. Br J Cancer 1997;76(2):141-145.
9. Wechsler-Reya RJ, Scott MP. Control of neuronal precursor proliferation in the cerebellum by Sonic Hedgehog. Neuron 1999;22(1):103-114.
10. Leung C, Lingbeek M, Shakhova O, et al. Bmi1 is essential for cerebellar development and is overexpressed in human medulloblastomas. Nature 2004;428(6980):337-341.
11. Romer JT, Kimura H, Magdaleno S, et al. Suppression of the Shh pathway using a small molecule inhibitor eliminates medulloblastoma in Ptc1(+/-)p53(-/-) mice. Cancer Cell 2004;6(3):229-240.
12. Wetmore C, Eberhart DE, Curran T. Loss of p53 but not ARF accelerates medulloblastoma in mice heterozygous for patched. Cancer Res 2001;61(2):513-516.
13. Polakis P. Wnt signaling and cancer. Genes Dev 2000;14(15):1837-1851.
14. Novak A, Dedhar S. Signaling through beta-catenin and Lef/Tcf. Cell Mol Life Sci 1999;56(5-6):523-537.
15. Clifford SC, Lusher ME, Lindsey JC, et al. Wnt/Wingless pathway activation and chromosome 6 loss characterize a distinct molecular sub-group of medulloblastomas associated with a favorable prognosis. Cell Cycle 2006;5(22):2666-2670.
16. Thompson MC, Fuller C, Hogg TL, et al. Genomics identifies medulloblastoma subgroups that are enriched for specific genetic alterations. J Clin Oncol 2006;24(12):1924-1931.
17. Baeza N, Masuoka J, Kleihues P, et al. AXIN1 mutations but not deletions in cerebellar medulloblastomas. Oncogene 2003;22(4):632-636.
18. Pizem J, Cort A, Zadravec-Zaletel L, et al. Survivin is a negative prognostic marker in medulloblastoma. Neuropathol Appl Neurobiol 2005;31(4):422-428.
19. Fangusaro JR, Jiang Y, Holloway MP, et al. Survivin, Survivin-2B, and Survivin-deltaEx3 expression in medulloblastoma: biologic markers of tumour morphology and clinical outcome. Br J Cancer 2005;92(2):359-365.
20. Zorn AM, Barish GD, Williams BO, et al. Regulation of Wnt signaling by Sox proteins: XSox17 alpha/beta and XSox3 physically interact with beta-catenin. Mol Cell 1999;4(4):487-498.
21. Lee CJ, Appleby VJ, Orme AT, et al. Differential expression of SOX4 and SOX11 in medulloblastoma. J Neurooncol 2002;57(3):201-214.

22. de Bont JM, Kros JM, Passier MMCJ, et al. Differential expression and prognostic significance of SOX genes in pediatric medulloblastoma and ependymoma identified by microarray analysis Neuro-oncology 2007;in press.
23. Neben K, Korshunov A, Benner A, et al. Microarray-based screening for molecular markers in medulloblastoma revealed STK15 as independent predictor for survival. Cancer Res 2004;64(9):3103-3111.
24. Dakubo GD, Mazerolle CJ, Wallace VA. Expression of Notch and Wnt pathway components and activation of Notch signaling in medulloblastomas from heterozygous patched mice. J Neurooncol 2006;79(3):221-227.
25. Fan X, Mikolaenko I, Elhassan I, et al. Notch1 and notch2 have opposite effects on embryonal brain tumor growth. Cancer Res 2004;64(21):7787-7793.
26. Baron M. An overview of the Notch signalling pathway. Semin Cell Dev Biol 2003;14(2):113-119.
27. Hallahan AR, Pritchard JI, Hansen S, et al. The SmoA1 mouse model reveals that notch signaling is critical for the growth and survival of sonic hedgehog-induced medulloblastomas. Cancer Res 2004;64(21):7794-7800.
28. Gilbertson RJ, Clifford SC, MacMeekin W, et al. Expression of the ErbB-neuregulin signaling network during human cerebellar development: implications for the biology of medulloblastoma. Cancer Res 1998;58(17):3932-3941.
29. Ferretti E, Di Marcotullio L, Gessi M, et al. Alternative splicing of the ErbB-4 cytoplasmic domain and its regulation by hedgehog signaling identify distinct medulloblastoma subsets. Oncogene 2006;25(55):7267-7273.
30. Elenius K, Choi CJ, Paul S, et al. Characterization of a naturally occurring ErbB4 isoform that does not bind or activate phosphatidyl inositol 3-kinase. Oncogene 1999;18(16):2607-2615.
31. Bal MM, Das Radotra B, Srinivasan R, et al. Expression of c-erbB-4 in medulloblastoma and its correlation with prognosis. Histopathology 2006;49(1):92-93.
32. Hernan R, Fasheh R, Calabrese C, et al. ERBB2 up-regulates S100A4 and several other prometastatic genes in medulloblastoma. Cancer Res 2003;63(1):140-148.
33. Amin DN, Tuck D, Stern DF. Neuregulin-regulated gene expression in mammary carcinoma cells. Exp Cell Res 2005;309(1):12-23.
34. Henriksson M, Luscher B. Proteins of the Myc network: essential regulators of cell growth and differentiation. Adv Cancer Res 1996;68:109-182.
35. He TC, Sparks AB, Rago C, et al. Identification of c-MYC as a target of the APC pathway. Science 1998;281(5382):1509-1512.
36. Rao G, Pedone CA, Coffin CM, et al. c-Myc enhances sonic hedgehog-induced medulloblastoma formation from nestin-expressing neural progenitors in mice. Neoplasia 2003;5(3):198-204.
37. Pomeroy SL, Tamayo P, Gaasenbeek M, et al. Prediction of central nervous system embryonal tumour outcome based on gene expression. Nature 2002;415(6870):436-442.
38. Browd SR, Kenney AM, Gottfried ON, et al. N-myc can substitute for insulin-like growth factor signaling in a mouse model of sonic hedgehog-induced medulloblastoma. Cancer Res 2006;66(5):2666-2672.
39. Eberhart CG, Kratz J, Wang Y, et al. Histopathological and molecular prognostic markers in medulloblastoma: c-myc, N-myc, TrkC, and anaplasia. J Neuropathol Exp Neurol 2004;63(5):441-449.
40. Kenney AM, Widlund HR, Rowitch DH. Hedgehog and PI-3 kinase signaling converge on Nmyc1 to promote cell cycle progression in cerebellar neuronal precursors. Development 2004;131(1):217-228.
41. Zumkeller W, Westphal M. The IGF/IGFBP system in CNS malignancy. Mol Pathol 2001;54(4):227-229.
42. Wang JY, Del Valle L, Gordon J, et al. Activation of the IGF-1R system contributes to malignant growth of human and mouse medulloblastomas. Oncogene 2001;20(29):3857-3868.

43. Urbanska K, Trojanek J, Del Valle L, et al. Inhibition of IGF-1 receptor in anchorage-independence attenuates GSK-3beta constitutive phosphorylation and compromises growth and survival of medulloblastoma cell lines. Oncogene 2007;26(16):2308-2317.
44. Hartmann W, Koch A, Brune H, et al. Insulin-like growth factor II is involved in the proliferation control of medulloblastoma and its cerebellar precursor cells. Am J Pathol 2005;166(4):1153-1162.
45. Patti R, Reddy CD, Geoerger B, et al. Autocrine secreted insulin-like growth factor-I stimulates MAP kinase-dependent mitogenic effects in human primitive neuroectodermal tumor/medulloblastoma. Int J Oncol 2000;16(3):577-584.
46. Hahn H, Wojnowski L, Specht K, et al. Patched target Igf2 is indispensable for the formation of medulloblastoma and rhabdomyosarcoma. J Biol Chem 2000;275(37):28341-28344.
47. De Bont JM, Van Doorn J, Reddingius RE, et al. Various components of the insulin-like growth factor system in tumor tissue, cerebrospinal fluid and peripheral blood of pediatric medulloblastoma and ependymoma patients. Accepted Int J Cancer 2008.
48. Buhren J, Christoph AH, Buslei R, et al. Expression of the neurotrophin receptor p75NTR in medulloblastomas is correlated with distinct histological and clinical features: evidence for a medulloblastoma subtype derived from the external granule cell layer. J Neuropathol Exp Neurol 2000;59(3):229-240.
49. Gazit R, Krizhanovsky V, Ben-Arie N. Math1 controls cerebellar granule cell differentiation by regulating multiple components of the Notch signaling pathway. Development 2004;131(4):903-913.
50. Kruttgen A, Schneider I, Weis J. The dark side of the NGF family: neurotrophins in neoplasias. Brain Pathol 2006;16(4):304-310.
51. Lee JE. NeuroD and neurogenesis. Dev Neurosci 1997;19(1):27-32.
52. de Haas T, Oussoren E, Grajkowska W, et al. OTX1 and OTX2 expression correlates with the clinicopathologic classification of medulloblastomas. J Neuropathol Exp Neurol 2006;65(2):176-186.
53. Di C, Liao S, Adamson DC, et al. Identification of OTX2 as a medulloblastoma oncogene whose product can be targeted by all-trans retinoic acid. Cancer Res 2005;65(3):919-924.
54. Biegel JA, Rorke LB, Packer RJ, et al. Isochromosome 17q in primitive neuroectodermal tumors of the central nervous system. Genes Chromosomes Cancer 1989;1(2):139-147.
55. Pan E, Pellarin M, Holmes E, et al. Isochromosome 17q is a negative prognostic factor in poor-risk childhood medulloblastoma patients. Clin Cancer Res 2005;11(13):4733-4740.
56. Biegel JA, Janss AJ, Raffel C, et al. Prognostic significance of chromosome 17p deletions in childhood primitive neuroectodermal tumors (medulloblastomas) of the central nervous system. Clin Cancer Res 1997;3(3):473-478.
57. Burnett ME, White EC, Sih S, et al. Chromosome arm 17p deletion analysis reveals molecular genetic heterogeneity in supratentorial and infratentorial primitive neuroectodermal tumors of the central nervous system. Cancer Genet Cytogenet 1997;97(1):25-31.
58. Mendrzyk F, Korshunov A, Toedt G, et al. Isochromosome breakpoints on 17p in medulloblastoma are flanked by different classes of DNA sequence repeats. Genes Chromosomes Cancer 2006;45(4):401-410.
59. Briggs KJ, Corcoran-Schwartz IM, Zhang W, et al. Cooperation between the Hic1 and Ptch1 tumor suppressors in medulloblastoma. Genes Dev 2008;22(6):770-785.
60. Bulavin DV, Demidov ON, Saito S, et al. Amplification of PPM1D in human tumors abrogates p53 tumor-suppressor activity. Nat Genet 2002;31(2):210-215.
61. Hui AB, Takano H, Lo KW, et al. Identification of a novel homozygous deletion region at 6q23.1 in medulloblastomas using high-resolution array comparative genomic hybridization analysis. Clin Cancer Res 2005;11(13):4707-4716.
62. Mendrzyk F, Radlwimmer B, Joos S, et al. Genomic and protein expression profiling identifies CDK6 as novel independent prognostic marker in medulloblastoma. J Clin Oncol 2005;23(34):8853-8862.

63. McCabe MG, Ichimura K, Liu L, et al. High-resolution array-based comparative genomic hybridization of medulloblastomas and supratentorial primitive neuroectodermal tumors. J Neuropathol Exp Neurol 2006;65(6):549-561.
64. Lo KC, Rossi MR, Burkhardt T, et al. Overlay analysis of the oligonucleotide array gene expression profiles and copy number abnormalities as determined by array comparative genomic hybridization in medulloblastomas. Genes Chromosomes Cancer 2007;46(1):53-66.
65. Yin XL, Pang JC, Ng HK. Identification of a region of homozygous deletion on 8p22-23.1 in medulloblastoma. Oncogene 2002;21(9):1461-1468.
66. Lo KC, Rossi MR, Eberhart CG, et al. Genome wide copy number abnormalities in pediatric medulloblastomas as assessed by array comparative genome hybridization. Brain Pathol 2007;17(3):282-296.
67. Rossi MR, Conroy J, McQuaid D, et al. Array CGH analysis of pediatric medulloblastomas. Genes Chromosomes Cancer 2006;45(3):290-303.
68. Yin XL, Pang JC, Liu YH, et al. Analysis of loss of heterozygosity on chromosomes 10q, 11, and 16 in medulloblastomas. J Neurosurg 2001;94(5):799-805.
69. Ehrbrecht A, Muller U, Wolter M, et al. Comprehensive genomic analysis of desmoplastic medulloblastomas: identification of novel amplified genes and separate evaluation of the different histological components. J Pathol 2006;208(4):554-563.
70. Jones PA, Baylin SB. The fundamental role of epigenetic events in cancer. Nat Rev Genet 2002;3(6):415-428.
71. Lusher ME, Lindsey JC, Latif F, et al. Biallelic epigenetic inactivation of the RASSF1A tumor suppressor gene in medulloblastoma development. Cancer Res 2002;62(20):5906-5911.
72. Debatin KM, Krammer PH. Death receptors in chemotherapy and cancer. Oncogene 2004;23(16):2950-2966.
73. Grotzer MA, Eggert A, Zuzak TJ, et al. Resistance to TRAIL-induced apoptosis in primitive neuroectodermal brain tumor cells correlates with a loss of caspase-8 expression. Oncogene 2000;19(40):4604-4610.
74. Pfister S, Schlaeger C, Mendrzyk F, et al. Array-based profiling of reference-independent methylation status (aPRIMES) identifies frequent promoter methylation and consecutive downregulation of ZIC2 in pediatric medulloblastoma. Nucleic Acids Res 2007;35(7):e51.
75. Uziel T, Zindy F, Xie S, et al. The tumor suppressors Ink4c and p53 collaborate independently with Patched to suppress medulloblastoma formation. Genes Dev 2005;19(22):2656-2667.
76. Peyrl A, Krapfenbauer K, Slavc I, et al. Protein profiles of medulloblastoma cell lines DAOY and D283: identification of tumor-related proteins and principles. Proteomics 2003;3(9):1781-1800.
77. Horn B, Heideman R, Geyer R, et al. A multi-institutional retrospective study of intracranial ependymoma in children: identification of risk factors. J Pediatr Hematol Oncol 1999;21(3):203-211.
78. Merchant TE, Jenkins JJ, Burger PC, et al. Influence of tumor grade on time to progression after irradiation for localized ependymoma in children. Int J Radiat Oncol Biol Phys 2002;53(1):52-57.
79. Grundy RG, Wilne SA, Weston CL, et al. Primary postoperative chemotherapy without radiotherapy for intracranial ependymoma in children: the UKCCSG/SIOP prospective study. Lancet Oncol 2007;8(8):696-705.
80. Kato H, Uchimura I, Morohoshi M, et al. Multiple endocrine neoplasia type 1 associated with spinal ependymoma. Intern Med 1996;35(4):285-289.
81. Lamszus K, Lachenmayer L, Heinemann U, et al. Molecular genetic alterations on chromosomes 11 and 22 in ependymomas. Int J Cancer 2001;91(6):803-808.
82. Taylor MD, Poppleton H, Fuller C, et al. Radial glia cells are candidate stem cells of ependymoma. Cancer Cell 2005;8(4):323-335.
83. Conover JC, Doetsch F, Garcia-Verdugo JM, et al. Disruption of Eph/ephrin signaling affects migration and proliferation in the adult subventricular zone. Nat Neurosci 2000;3(11):1091-1097.

84. Hitoshi S, Alexson T, Tropepe V, et al. Notch pathway molecules are essential for the maintenance, but not the generation, of mammalian neural stem cells. Genes Dev 2002;16(7):846-858.
85. Mullins KJ, Rubio A, Myers SP, et al. Malignant ependymomas in a patient with Turcot's syndrome: case report and management guidelines. Surg Neurol 1998;49(3):290-294.
86. Suarez-Merino B, Hubank M, Revesz T, et al. Microarray analysis of pediatric ependymoma identifies a cluster of 112 candidate genes including four transcripts at 22q12.1-q13.3. Neuro Oncol 2005;7(1):20-31.
87. Modena P, Lualdi E, Facchinetti F, et al. Identification of tumor-specific molecular signatures in intracranial ependymoma and association with clinical characteristics. J Clin Oncol 2006;24(33):5223-5233.
88. Metzger AK, Sheffield VC, Duyk G, et al. Identification of a germ-line mutation in the p53 gene in a patient with an intracranial ependymoma. Proc Natl Acad Sci U S A 1991;88(17):7825-7829.
89. Zamecnik J, Snuderl M, Eckschlager T, et al. Pediatric intracranial ependymomas: prognostic relevance of histological, immunohistochemical, and flow cytometric factors. Mod Pathol 2003;16(10):980-991.
90. Michalides RJ. Cell cycle regulators: mechanisms and their role in aetiology, prognosis, and treatment of cancer. J Clin Pathol 1999;52(8):555-568.
91. Korshunov A, Golanov A, Timirgaz V. p14ARF protein (FL-132) immunoreactivity in intracranial ependymomas and its prognostic significance: an analysis of 103 cases. Acta Neuropathol (Berl) 2001;102(3):271-277.
92. Sowar K, Straessle J, Donson AM, et al. Predicting which children are at risk for ependymoma relapse. J Neurooncol 2006;78(1):41-46.
93. Lukashova-v Zangen I, Kneitz S, Monoranu CM, et al. Ependymoma gene expression profiles associated with histological subtype, proliferation, and patient survival. Acta Neuropathol 2007;113(3):325-337.
94. Preusser M, Wolfsberger S, Czech T, et al. Survivin expression in intracranial ependymomas and its correlation with tumor cell proliferation and patient outcome. Am J Clin Pathol 2005;124(4):543-549.
95. Wolfsberger S, Fischer I, Hoftberger R, et al. Ki-67 immunolabeling index is an accurate predictor of outcome in patients with intracranial ependymoma. Am J Surg Pathol 2004;28(7):914-920.
96. Hirose Y, Aldape K, Bollen A, et al. Chromosomal abnormalities subdivide ependymal tumors into clinically relevant groups. Am J Pathol 2001;158(3):1137-1143.
97. Mendrzyk F, Korshunov A, Benner A, et al. Identification of gains on 1q and epidermal growth factor receptor overexpression as independent prognostic markers in intracranial ependymoma. Clin Cancer Res 2006;12(7 Pt 1):2070-2079.
98. Dyer S, Prebble E, Davison V, et al. Genomic imbalances in pediatric intracranial ependymomas define clinically relevant groups. Am J Pathol 2002;161(6):2133-2141.
99. Jeuken JW, Sprenger SH, Gilhuis J, et al. Correlation between localization, age, and chromosomal imbalances in ependymal tumours as detected by CGH. J Pathol 2002;197(2):238-244.
100. Hulsebos TJ, Oskam NT, Bijleveld EH, et al. Evidence for an ependymoma tumour suppressor gene in chromosome region 22pter-22q11.2. Br J Cancer 1999;81(7):1150-1154.
101. Rousseau-Merck M, Versteege I, Zattara-Cannoni H, et al. Fluorescence in situ hybridization determination of 22q12-q13 deletion in two intracerebral ependymomas. Cancer Genet Cytogenet 2000;121(2):223-227.
102. Sevenet N, Sheridan E, Amram D, et al. Constitutional mutations of the hSNF5/INI1 gene predispose to a variety of cancers. Am J Hum Genet 1999;65(5):1342-1348.
103. Esteller M, Garcia-Foncillas J, Andion E, et al. Inactivation of the DNA-repair gene MGMT and the clinical response of gliomas to alkylating agents. N Engl J Med 2000;343(19):1350-1354.

104. Bayani J, Zielenska M, Marrano P, et al. Molecular cytogenetic analysis of medulloblastomas and supratentorial primitive neuroectodermal tumors by using conventional banding, comparative genomic hybridization, and spectral karyotyping. J Neurosurg 2000;93(3):437-448.
105. Avet-Loiseau H, Venuat AM, Terrier-Lacombe MJ, et al. Comparative genomic hybridization detects many recurrent imbalances in central nervous system primitive neuroectodermal tumours in children. Br J Cancer 1999;79(11-12):1843-1847.
106. Eberhart CG, Kratz JE, Schuster A, et al. Comparative genomic hybridization detects an increased number of chromosomal alterations in large cell/anaplastic medulloblastomas. Brain Pathol 2002;12(1):36-44.
107. Nishizaki T, Harada K, Kubota H, et al. Genetic alterations in pediatric medulloblastomas detected by comparative genomic hybridization. Pediatr Neurosurg 1999;31(1):27-32.
108. Yoshimoto M, Bayani J, Nuin PA, et al. Metaphase and array comparative genomic hybridization: unique copy number changes and gene amplification of medulloblastomas in South America. Cancer Genet Cytogenet 2006;170(1):40-47.
109. Gilhuis HJ, Anderl KL, Boerman RH, et al. Comparative genomic hybridization of medulloblastomas and clinical relevance: eleven new cases and a review of the literature. Clin Neurol Neurosurg 2000;102(4):203-209.
110. Inda MM, Perot C, Guillaud-Bataille M, et al. Genetic heterogeneity in supratentorial and infratentorial primitive neuroectodermal tumours of the central nervous system. Histopathology 2005;47(6):631-637.
111. Adesina AM, Nguyen Y, Mehta V, et al. FOXG1 dysregulation is a frequent event in medulloblastoma. J Neurooncol 2007;85(2):111-122.
112. Reardon DA, Michalkiewicz E, Boyett JM, et al. Extensive genomic abnormalities in childhood medulloblastoma by comparative genomic hybridization. Cancer Res 1997;57(18):4042-4047.
113. Shlomit R, Ayala AG, Michal D, et al. Gains and losses of DNA sequences in childhood brain tumors analyzed by comparative genomic hybridization. Cancer Genet Cytogenet 2000;121(1):67-72.
114. Michiels EM, Weiss MM, Hoovers JM, et al. Genetic alterations in childhood medulloblastoma analyzed by comparative genomic hybridization. J Pediatr Hematol Oncol 2002;24(3):205-210.
115. Russo C, Pellarin M, Tingby O, et al. Comparative genomic hybridization in patients with supratentorial and infratentorial primitive neuroectodermal tumors. Cancer 1999;86(2):331-339.
116. Brown HG, Kepner JL, Perlman EJ, et al. "Large cell/anaplastic" medulloblastomas: a Pediatric Oncology Group Study. J Neuropathol Exp Neurol 2000;59(10):857-865.
117. Jay V, Squire J, Bayani J, et al. Oncogene amplification in medulloblastoma: analysis of a case by comparative genomic hybridization and fluorescence in situ hybridization. Pathology 1999;31(4):337-344.
118. De Bortoli M, Castellino RC, Lu XY, et al. Medulloblastoma outcome is adversely associated with overexpression of EEF1D, RPL30, and RPS20 on the long arm of chromosome 8. BMC Cancer 2006;6:223.
119. Tong CY, Hui AB, Yin XL, et al. Detection of oncogene amplifications in medulloblastomas by comparative genomic hybridization and array-based comparative genomic hybridization. J Neurosurg 2004;100(2 Suppl Pediatrics):187-193.
120. Fruhwald MC, O'Dorisio MS, Rush LJ, et al. Gene amplification in PNETs/medulloblastomas: mapping of a novel amplified gene within the MYCN amplicon. J Med Genet 2000;37(7):501-509.
121. Nicholson J, Wickramasinghe C, Ross F, et al. Imbalances of chromosome 17 in medulloblastomas determined by comparative genomic hybridisation and fluorescence in situ hybridisation. Mol Pathol 2000;53(6):313-319.
122. Gilhuis HJ, van der Laak J, Wesseling P, et al. Inverse correlation between genetic aberrations and malignancy grade in ependymal tumors: a paradox? J Neurooncol 2004;66(1-2):111-116.

123. Reardon DA, Entrekin RE, Sublett J, et al. Chromosome arm 6q loss is the most common recurrent autosomal alteration detected in primary pediatric ependymoma. Genes Chromosomes Cancer 1999;24(3):230-237.
124. Ward S, Harding B, Wilkins P, et al. Gain of 1q and loss of 22 are the most common changes detected by comparative genomic hybridisation in paediatric ependymoma. Genes Chromosomes Cancer 2001;32(1):59-66.
125. Grill J, Avet-Loiseau H, Lellouch-Tubiana A, et al. Comparative genomic hybridization detects specific cytogenetic abnormalities in pediatric ependymomas and choroid plexus papillomas. Cancer Genet Cytogenet 2002;136(2):121-125.
126. Carter M, Nicholson J, Ross F, et al. Genetic abnormalities detected in ependymomas by comparative genomic hybridisation. Br J Cancer 2002;86(6):929-939.
127. Scheil S, Bruderlein S, Eicker M, et al. Low frequency of chromosomal imbalances in anaplastic ependymomas as detected by comparative genomic hybridization. Brain Pathol 2001;11(2):133-143.
128. Zheng PP, Pang JC, Hui AB, et al. Comparative genomic hybridization detects losses of chromosomes 22 and 16 as the most common recurrent genetic alterations in primary ependymomas. Cancer Genet Cytogenet 2000;122(1):18-25.
129. Rickert CH, Korshunov A, Paulus W. Chromosomal imbalances in clear cell ependymomas. Mod Pathol 2006;19(7):958-962.
130. Granzow M, Popp S, Weber S, et al. Isochromosome 1q as an early genetic event in a child with intracranial ependymoma characterized by molecular cytogenetics. Cancer Genet Cytogenet 2001;130(1):79-83.
131. Schutz BR, Scheurlen W, Krauss J, et al. Mapping of chromosomal gains and losses in primitive neuroectodermal tumors by comparative genomic hybridization. Genes Chromosomes Cancer 1996;16(3):196-203.
132. Vorechovsky I, Tingby O, Hartman M, et al. Somatic mutations in the human homologue of Drosophila patched in primitive neuroectodermal tumours. Oncogene 1997;15(3):361-366.
133. Wolter M, Reifenberger J, Sommer C, et al. Mutations in the human homologue of the Drosophila segment polarity gene patched (PTCH) in sporadic basal cell carcinomas of the skin and primitive neuroectodermal tumors of the central nervous system. Cancer Res 1997;57(13):2581-2585.
134. Pietsch T, Waha A, Koch A, et al. Medulloblastomas of the desmoplastic variant carry mutations of the human homologue of Drosophila patched. Cancer Res 1997;57(11):2085-2088.
135. Raffel C, Jenkins RB, Frederick L, et al. Sporadic medulloblastomas contain PTCH mutations. Cancer Res 1997;57(5):842-845.
136. Zurawel RH, Allen C, Wechsler-Reya R, et al. Evidence that haploinsufficiency of Ptch leads to medulloblastoma in mice. Genes Chromosomes Cancer 2000;28(1):77-81.
137. Taylor MD, Liu L, Raffel C, et al. Mutations in SUFU predispose to medulloblastoma. Nat Genet 2002;31(3):306-310.
138. Koch A, Waha A, Hartmann W, et al. No evidence for mutations or altered expression of the Suppressor of Fused gene (SUFU) in primitive neuroectodermal tumours. Neuropathol Appl Neurobiol 2004;30(5):532-539.
139. Reifenberger J, Wolter M, Weber RG, et al. Missense mutations in SMOH in sporadic basal cell carcinomas of the skin and primitive neuroectodermal tumors of the central nervous system. Cancer Res 1998;58(9):1798-1803.
140. Zurawel RH, Allen C, Chiappa S, et al. Analysis of PTCH/SMO/SHH pathway genes in medulloblastoma. Genes Chromosomes Cancer 2000;27(1):44-51.
141. Di Marcotullio L, Ferretti E, De Smaele E, et al. REN(KCTD11) is a suppressor of Hedgehog signaling and is deleted in human medulloblastoma. Proc Natl Acad Sci U S A 2004;101(29):10833-10838.
142. Dahmen RP, Koch A, Denkhaus D, et al. Deletions of AXIN1, a component of the WNT/wingless pathway, in sporadic medulloblastomas. Cancer Res 2001;61(19):7039-7043.

143. Yokota N, Nishizawa S, Ohta S, et al. Role of Wnt pathway in medulloblastoma oncogenesis. Int J Cancer 2002;101(2):198-201.
144. Koch A, Hrychyk A, Hartmann W, et al. Mutations of the Wnt antagonist AXIN2 (Conductin) result in TCF-dependent transcription in medulloblastomas. Int J Cancer 2007;121(2):284-291.
145. Koch A, Waha A, Tonn JC, et al. Somatic mutations of WNT/wingless signaling pathway components in primitive neuroectodermal tumors. Int J Cancer 2001;93(3):445-449.
146. Huang H, Mahler-Araujo BM, Sankila A, et al. APC mutations in sporadic medulloblastomas. Am J Pathol 2000;156(2):433-437.
147. Zurawel RH, Chiappa SA, Allen C, et al. Sporadic medulloblastomas contain oncogenic beta-catenin mutations. Cancer Res 1998;58(5):896-899.
148. Ellison DW, Onilude OE, Lindsey JC, et al. beta-Catenin status predicts a favorable outcome in childhood medulloblastoma: the United Kingdom Children's Cancer Study Group Brain Tumour Committee. J Clin Oncol 2005;23(31):7951-7957.
149. Bodey B, Bodey V, Siegel SE, et al. Survivin expression in childhood medulloblastomas: a possible diagnostic and prognostic marker. In Vivo 2004;18(6):713-718.
150. Haberler C, Slavc I, Czech T, et al. Histopathological prognostic factors in medulloblastoma: high expression of survivin is related to unfavourable outcome. Eur J Cancer 2006;42(17):2996-3003.
151. Yokota N, Mainprize TG, Taylor MD, et al. Identification of differentially expressed and developmentally regulated genes in medulloblastoma using suppression subtraction hybridization. Oncogene 2004;23(19):3444-3453.
152. Thomson SA, Kennerly E, Olby N, et al. Microarray analysis of differentially expressed genes of primary tumors in the canine central nervous system. Vet Pathol 2005;42(5):550-558.
153. Gilbertson RJ, Perry RH, Kelly PJ, et al. Prognostic significance of HER2 and HER4 coexpression in childhood medulloblastoma. Cancer Res 1997;57(15):3272-3280.
154. Bal MM, Das Radotra B, Srinivasan R, et al. Does c-erbB-2 expression have a role in medulloblastoma prognosis? Indian J Pathol Microbiol 2006;49(4):535-539.
155. Lee CJ, Chan WI, Scotting PJ. CIC, a gene involved in cerebellar development and ErbB signaling, is significantly expressed in medulloblastomas. J Neurooncol 2005;73(2):101-108.
156. Stearns D, Chaudhry A, Abel TW, et al. c-myc overexpression causes anaplasia in medulloblastoma. Cancer Res 2006;66(2):673-681.
157. Aldosari N, Bigner SH, Burger PC, et al. MYCC and MYCN oncogene amplification in medulloblastoma. A fluorescence in situ hybridization study on paraffin sections from the Children's Oncology Group. Arch Pathol Lab Med 2002;126(5):540-544.
158. Bruggers CS, Tai KF, Murdock T, et al. Expression of the c-Myc protein in childhood medulloblastoma. J Pediatr Hematol Oncol 1998;20(1):18-25.
159. Grotzer MA, Hogarty MD, Janss AJ, et al. MYC messenger RNA expression predicts survival outcome in childhood primitive neuroectodermal tumor/medulloblastoma. Clin Cancer Res 2001;7(8):2425-2433.
160. Herms J, Neidt I, Luscher B, et al. C-MYC expression in medulloblastoma and its prognostic value. Int J Cancer 2000;89(5):395-402.
161. Sommer A, Waha A, Tonn J, et al. Analysis of the Max-binding protein MNT in human medulloblastomas. Int J Cancer 1999;82(6):810-816.
162. Cvekl A, Jr., Zavadil J, Birshtein BK, et al. Analysis of transcripts from 17p13.3 in medulloblastoma suggests ROX/MNT as a potential tumour suppressor gene. Eur J Cancer 2004;40(16):2525-2532.
163. Pession A, Tonelli R. The MYCN oncogene as a specific and selective drug target for peripheral and central nervous system tumors. Curr Cancer Drug Targets 2005;5(4):273-283.
164. Tomlinson FH, Jenkins RB, Scheithauer BW, et al. Aggressive medulloblastoma with high-level N-myc amplification. Mayo Clin Proc 1994;69(4):359-365.
165. Huang A, Ho CS, Ponzielli R, et al. Identification of a novel c-Myc protein interactor, JPO2, with transforming activity in medulloblastoma cells. Cancer Res 2005;65(13):5607-5619.

166. Del Valle L, Enam S, Lassak A, et al. Insulin-like growth factor I receptor activity in human medulloblastomas. Clin Cancer Res 2002;8(6):1822-1830.
167. Schuller U, Koch A, Hartmann W, et al. Subtype-specific expression and genetic alterations of the chemokinereceptor gene CXCR4 in medulloblastomas. Int J Cancer 2005;117(1):82-89.
168. Gilbertson RJ, Clifford SC. PDGFRB is overexpressed in metastatic medulloblastoma. Nat Genet 2003;35(3):197-198.
169. Boon K, Eberhart CG, Riggins GJ. Genomic amplification of orthodenticle homologue 2 in medulloblastomas. Cancer Res 2005;65(3):703-707.
170. Michiels EM, Oussoren E, Van Groenigen M, et al. Genes differentially expressed in medulloblastoma and fetal brain. Physiol Genomics 1999;1(2):83-91.
171. Salsano E, Pollo B, Eoli M, et al. Expression of MATH1, a marker of cerebellar granule cell progenitors, identifies different medulloblastoma sub-types. Neurosci Lett 2004;370(2-3):180-185.
172. Ohta T, Watanabe T, Katayama Y, et al. TrkA expression is associated with an elevated level of apoptosis in classic medulloblastomas. Neuropathology 2006;26(3):170-177.
173. Grotzer MA, Janss AJ, Fung K, et al. TrkC expression predicts good clinical outcome in primitive neuroectodermal brain tumors. J Clin Oncol 2000;18(5):1027-1035.
174. Segal RA, Goumnerova LC, Kwon YK, et al. Expression of the neurotrophin receptor TrkC is linked to a favorable outcome in medulloblastoma. Proc Natl Acad Sci U S A 1994;91(26):12867-12871.
175. Korshunov A, Golanov A, Timirgaz V. Immunohistochemical markers for prognosis of ependymal neoplasms. J Neurooncol 2002;58(3):255-270.
176. Sinnappah-Kang ND, Mrak RE, Paulsen DB, et al. Heparanase expression and TrkC/p75NTR ratios in human medulloblastoma. Clin Exp Metastasis 2006;23(1):55-63.
177. Sinnappah-Kang ND, Kaiser AJ, Blust BE, et al. Heparanase, TrkC and p75NTR: their functional involvement in human medulloblastoma cell invasion. Int J Oncol 2005;27(3):617-626.
178. Salsano E, Croci L, Maderna E, et al. Expression of the neurogenic basic helix-loop-helix transcription factor NEUROG1 identifies a subgroup of medulloblastomas not expressing ATOH1. Neuro Oncol 2007;9(3):298-307.
179. Rostomily RC, Bermingham-McDonogh O, Berger MS, et al. Expression of neurogenic basic helix-loop-helix genes in primitive neuroectodermal tumors. Cancer Res 1997;57(16):3526-3531.
180. Katsetos CD, Herman MM, Krishna L, et al. Calbindin-D28k in subsets of medulloblastomas and in the human medulloblastoma cell line D283 Med. Arch Pathol Lab Med 1995;119(8):734-743.
181. Adesina AM, Nalbantoglu J, Cavenee WK. p53 gene mutation and mdm2 gene amplification are uncommon in medulloblastoma. Cancer Res 1994;54(21):5649-5651.
182. Saylors RL, 3rd, Sidransky D, Friedman HS, et al. Infrequent p53 gene mutations in medulloblastomas. Cancer Res 1991;51(17):4721-4723.
183. Raffel C, Thomas GA, Tishler DM, et al. Absence of p53 mutations in childhood central nervous system primitive neuroectodermal tumors. Neurosurgery 1993;33(2):301-305; discussion 305-306.
184. Nozaki M, Tada M, Matsumoto R, et al. Rare occurrence of inactivating p53 gene mutations in primary non-astrocytic tumors of the central nervous system: reappraisal by yeast functional assay. Acta Neuropathol 1998;95(3):291-296.
185. Kozmik Z, Sure U, Ruedi D, et al. Deregulated expression of PAX5 in medulloblastoma. Proc Natl Acad Sci U S A 1995;92(12):5709-5713.
186. Giordana MT, Duo D, Gasverde S, et al. MDM2 overexpression is associated with short survival in adults with medulloblastoma. Neuro-oncol 2002;4(2):115-122.
187. Lindsey JC, Lusher ME, Anderton JA, et al. Identification of tumour-specific epigenetic events in medulloblastoma development by hypermethylation profiling. Carcinogenesis 2004;25(5):661-668.
188. Rood BR, Zhang H, Weitman DM, et al. Hypermethylation of HIC-1 and 17p allelic loss in medulloblastoma. Cancer Res 2002;62(13):3794-3797.

189. de Bont JM, den Boer ML, Kros JM, et al. Identification of novel biomarkers in pediatric primitive neuroectodermal tumors and ependymomas by proteome-wide analysis. J Neuropathol Exp Neurol 2007;66(6):505-516.
190. Fan X, Wang Y, Kratz J, et al. hTERT gene amplification and increased mRNA expression in central nervous system embryonal tumors. Am J Pathol 2003;162(6):1763-1769.
191. Waha A, Koch A, Hartmann W, et al. SGNE1/7B2 is epigenetically altered and transcriptionally downregulated in human medulloblastomas. Oncogene 2007;26(38):5662-5668.
192. Ebinger M, Senf L, Wachowski O, et al. Promoter methylation pattern of caspase-8, P16INK4A, MGMT, TIMP-3, and E-cadherin in medulloblastoma. Pathol Oncol Res 2004;10(1):17-21.
193. Zuzak TJ, Steinhoff DF, Sutton LN, et al. Loss of caspase-8 mRNA expression is common in childhood primitive neuroectodermal brain tumour/medulloblastoma. Eur J Cancer 2002;38(1):83-91.
194. Pingoud-Meier C, Lang D, Janss AJ, et al. Loss of caspase-8 protein expression correlates with unfavorable survival outcome in childhood medulloblastoma. Clin Cancer Res 2003;9(17):6401-6409.
195. Gonzalez-Gomez P, Bello MJ, Inda MM, et al. Deletion and aberrant CpG island methylation of Caspase 8 gene in medulloblastoma. Oncol Rep 2004;12(3):663-666.
196. Muhlisch J, Bajanowski T, Rickert CH, et al. Frequent but borderline methylation of p16 (INK4a) and TIMP3 in medulloblastoma and sPNET revealed by quantitative analyses. J Neurooncol 2007.
197. Fruhwald MC, O'Dorisio MS, Dai Z, et al. Aberrant promoter methylation of previously unidentified target genes is a common abnormality in medulloblastomas--implications for tumor biology and potential clinical utility. Oncogene 2001;20(36):5033-5042.
198. Uziel T, Zindy F, Sherr CJ, et al. The CDK inhibitor p18Ink4c is a tumor suppressor in medulloblastoma. Cell Cycle 2006;5(4):363-365.
199. Lindsey JC, Lusher ME, Anderton JA, et al. Epigenetic deregulation of multiple S100 gene family members by differential hypomethylation and hypermethylation events in medulloblastoma. Br J Cancer 2007;97(2):267-274.
200. Lindsey JC, Lusher ME, Strathdee G, et al. Epigenetic inactivation of MCJ (DNAJD1) in malignant paediatric brain tumours. Int J Cancer 2006;118(2):346-352.
201. Gonzalez-Gomez P, Bello MJ, Alonso ME, et al. CpG island methylation status and mutation analysis of the RB1 gene essential promoter region and protein-binding pocket domain in nervous system tumours. Br J Cancer 2003;88(1):109-114.
202. Vibhakar R, Foltz G, Yoon JG, et al. Dickkopf-1 is an epigenetically silenced candidate tumor suppressor gene in medulloblastoma. Neuro-oncol 2007;9(2):135-144.
203. Gilbertson RJ, Bentley L, Hernan R, et al. ERBB receptor signaling promotes ependymoma cell proliferation and represents a potential novel therapeutic target for this disease. Clin Cancer Res 2002;8(10):3054-3064.
204. Ogino S, Kubo S, Abdul-Karim FW, et al. Comparative immunohistochemical study of insulin-like growth factor II and insulin-like growth factor receptor type 1 in pediatric brain tumors. Pediatr Dev Pathol 2001;4(1):23-31.
205. Korshunov A, Neben K, Wrobel G, et al. Gene expression patterns in ependymomas correlate with tumor location, grade, and patient age. Am J Pathol 2003;163(5):1721-1727.
206. Rubio MP, Correa KM, Ramesh V, et al. Analysis of the neurofibromatosis 2 gene in human ependymomas and astrocytomas. Cancer Res 1994;54(1):45-47.
207. Birch BD, Johnson JP, Parsa A, et al. Frequent type 2 neurofibromatosis gene transcript mutations in sporadic intramedullary spinal cord ependymomas. Neurosurgery 1996;39(1):135-140.
208. Ebert C, von Haken M, Meyer-Puttlitz B, et al. Molecular genetic analysis of ependymal tumors. NF2 mutations and chromosome 22q loss occur preferentially in intramedullary spinal ependymomas. Am J Pathol 1999;155(2):627-632.
209. Michalowski MB, de Fraipont F, Michelland S, et al. Methylation of RASSF1A and TRAIL pathway-related genes is frequent in childhood intracranial ependymomas and benign choroid plexus papilloma. Cancer Genet Cytogenet 2006;166(1):74-81.

210. Alonso ME, Bello MJ, Gonzalez-Gomez P, et al. Aberrant CpG island methylation of multiple genes in ependymal tumors. J Neurooncol 2004;67(1-2):159-165.
211. Urioste M, Martinez-Ramirez A, Cigudosa JC, et al. Complex cytogenetic abnormalities including telomeric associations and MEN1 mutation in a pediatric ependymoma. Cancer Genet Cytogenet 2002;138(2):107-110.
212. Rushing EJ, Yashima K, Brown DF, et al. Expression of telomerase RNA component correlates with the MIB-1 proliferation index in ependymomas. J Neuropathol Exp Neurol 1997;56(10):1142-1146.
213. Tong CY, Ng HK, Pang JC, et al. Molecular genetic analysis of non-astrocytic gliomas. Histopathology 1999;34(4):331-341.
214. Gaspar N, Grill J, Geoerger B, et al. p53 Pathway dysfunction in primary childhood ependymomas. Pediatr Blood Cancer 2006;46(5):604-613.
215. von Haken MS, White EC, Daneshvar-Shyesther L, et al. Molecular genetic analysis of chromosome arm 17p and chromosome arm 22q DNA sequences in sporadic pediatric ependymomas. Genes Chromosomes Cancer 1996;17(1):37-44.
216. Fink KL, Rushing EJ, Schold SC, Jr., et al. Infrequency of p53 gene mutations in ependymomas. J Neurooncol 1996;27(2):111-115.
217. Suzuki SO, Iwaki T. Amplification and overexpression of mdm2 gene in ependymomas. Mod Pathol 2000;13(5):548-553.
218. Loiseau H, Arsaut J, Demotes-Mainard J. p73 gene transcripts in human brain tumors: overexpression and altered splicing in ependymomas. Neurosci Lett 1999;263(2-3):173-176.
219. Kamiya M, Nakazato Y. The expression of p73, p21 and MDM2 proteins in gliomas. J Neurooncol 2002;59(2):143-149.
220. Hamilton DW, Lusher ME, Lindsey JC, et al. Epigenetic inactivation of the RASSF1A tumour suppressor gene in ependymoma. Cancer Lett 2005;227(1):75-81.
221. Alonso ME, Bello MJ, Gonzalez-Gomez P, et al. Aberrant promoter methylation of multiple genes in oligodendrogliomas and ependymomas. Cancer Genet Cytogenet 2003;144(2):134-142.
222. Rousseau E, Ruchoux MM, Scaravilli F, et al. CDKN2A, CDKN2B and p14ARF are frequently and differentially methylated in ependymal tumours. Neuropathol Appl Neurobiol 2003;29(6):574-583.
223. Waha A, Koch A, Hartmann W, et al. Analysis of HIC-1 methylation and transcription in human ependymomas. Int J Cancer 2004;110(4):542-549.
224. Bhattacharjee MB, Armstrong DD, Vogel H, et al. Cytogenetic analysis of 120 primary pediatric brain tumors and literature review. Cancer Genet Cytogenet 1997;97(1):39-53.
225. Neumann E, Kalousek DK, Norman MG, et al. Cytogenetic analysis of 109 pediatric central nervous system tumors. Cancer Genet Cytogenet 1993;71(1):40-49.
226. Stratton MR, Darling J, Lantos PL, et al. Cytogenetic abnormalities in human ependymomas. Int J Cancer 1989;44(4):579-581.
227. Bigner SH, McLendon RE, Fuchs H, et al. Chromosomal characteristics of childhood brain tumors. Cancer Genet Cytogenet 1997;97(2):125-134.
228. Biegel JA, Rorke LB, Janss AJ, et al. Isochromosome 17q demonstrated by interphase fluorescence in situ hybridization in primitive neuroectodermal tumors of the central nervous system. Genes Chromosomes Cancer 1995;14(2):85-96.
229. Vagner-Capodano AM, Zattara-Cannoni H, Gambarelli D, et al. Cytogenetic study of 33 ependymomas. Cancer Genet Cytogenet 1999;115(2):96-99.
230. Cohen N, Betts DR, Tavori U, et al. Karyotypic evolution pathways in medulloblastoma/primitive neuroectodermal tumor determined with a combination of spectral karyotyping, G-banding, and fluorescence in situ hybridization. Cancer Genet Cytogenet 2004;149(1):44-52.
231. Vagner-Capodano AM, Zattara-Cannoni H, Gambarelli D, et al. Detection of i(17q) chromosome by fluorescent in situ hybridization (FISH) with interphase nuclei in medulloblastoma. Cancer Genet Cytogenet 1994;78(1):1-6.

232. Ransom DT, Ritland SR, Kimmel DW, et al. Cytogenetic and loss of heterozygosity studies in ependymomas, pilocytic astrocytomas, and oligodendrogliomas. Genes Chromosomes Cancer 1992;5(4):348-356.
233. Chadduck WM, Boop FA, Sawyer JR. Cytogenetic studies of pediatric brain and spinal cord tumors. Pediatr Neurosurg 1991;17(2):57-65.
234. Vagner-Capodano AM, Gentet JC, Gambarelli D, et al. Cytogenetic studies in 45 pediatric brain tumors. Pediatr Hematol Oncol 1992;9(3):223-235.
235. Weremowicz S, Kupsky WJ, Morton CC, et al. Cytogenetic evidence for a chromosome 22 tumor suppressor gene in ependymoma. Cancer Genet Cytogenet 1992;61(2):193-196.
236. Rogatto SR, Casartelli C, Rainho CA, et al. Chromosomes in the genesis and progression of ependymomas. Cancer Genet Cytogenet 1993;69(2):146-152.
237. Agamanolis DP, Malone JM. Chromosomal abnormalities in 47 pediatric brain tumors. Cancer Genet Cytogenet 1995;81(2):125-134.
238. Yamada K, Kasama M, Kondo T, et al. Chromosome studies in 70 brain tumors with special attention to sex chromosome loss and single autosomal trisomy. Cancer Genet Cytogenet 1994;73(1):46-52.
239. Mazewski C, Soukup S, Ballard E, et al. Karyotype studies in 18 ependymomas with literature review of 107 cases. Cancer Genet Cytogenet 1999;113(1):1-8.
240. Sawyer JR, Miller JP, Ellison DA. Clonal telomeric fusions and chromosome instability in a subcutaneous sacrococcygeal myxopapillary ependymoma. Cancer Genet Cytogenet 1998;100(2):169-175.
241. Sainati L, Bolcato S, Montaldi A, et al. Cytogenetics of pediatric central nervous system tumors. Cancer Genet Cytogenet 1996;91(1):13-27.
242. Pearson AD, Reid MM, Davison EV, et al. Cytogenetic investigations of solid tumours of children. Arch Dis Child 1988;63(9):1012-1015.
243. Dal Cin P, Sandberg AA. Cytogenetic findings in a supratentorial ependymoma. Cancer Genet Cytogenet 1988;30(2):289-293.
244. Karnes PS, Tran TN, Cui MY, et al. Cytogenetic analysis of 39 pediatric central nervous system tumors. Cancer Genet Cytogenet 1992;59(1):12-19.
245. Thiel G, Losanowa T, Kintzel D, et al. Karyotypes in 90 human gliomas. Cancer Genet Cytogenet 1992;58(2):109-120.
246. Roberts P, Chumas PD, Picton S, et al. A review of the cytogenetics of 58 pediatric brain tumors. Cancer Genet Cytogenet 2001;131(1):1-12.

Chapter 3

Differential Expression and Prognostic Significance of SOX Genes in Pediatric Medulloblastoma and Ependymoma Identified by Microarray Analysis

Judith M. de Bont[1], Johan M. Kros[2], Monique M.C.J. Passier[1], Roel E. Reddingius[1], Peter A.E. Sillevis Smitt[3], Theo M. Luider[3], Monique L. den Boer[1], Rob Pieters[1]

[1]Erasmus MC – Sophia Children's Hospital - University Medical Center Rotterdam – Department of Pediatric Oncology and Hematology, The Netherlands;
[2]Erasmus MC – University Medical Center Rotterdam – Department of Pathology, The Netherlands;
[3]Erasmus MC – University Medical Center Rotterdam – Department of Neuro-oncology, The Netherlands

Neuro-Oncology 2008; Jun 24 [Epub ahead of print]

ABSTRACT

The objective of this study was to identify differentially expressed and prognostically important genes in pediatric medulloblastoma and pediatric ependymoma by Affymetrix microarray analysis. Amongst the most discriminative genes, 3 different members of the SOX transcription factor family were differentially expressed. Both SOX4 and SOX11 were significantly overexpressed, respectively median 11-fold and 5-fold, in medulloblastoma compared to ependymoma and normal cerebellum. SOX9 was median 16-fold higher expressed in ependymoma compared to normal cerebellum and medulloblastoma ($p<0.001$ for all comparisons). The differential expression of the SOX genes was confirmed at protein level by immunohistochemistry.

Survival analysis of the most discriminative probe sets for each subgroup showed that respectively 35 and 13 probe sets were predictive of survival in medulloblastoma and ependymoma. There was a trend towards better survival with increasing SOX4 expression in medulloblastoma. SOX9 expression was predictive for favorable outcome in ependymoma. mRNA levels of BCAT1, a mediator of amino acid breakdown, were median 15-fold higher in medulloblastoma patients with metastases compared to those without metastasized disease ($p<0.01$). However, the correlation between BCAT1 expression and metastatic medulloblastoma could not be confirmed at protein level. In ongoing studies the potential prognostic impact of the genes associated with outcome should be evaluated in larger groups of patients. Furthermore, our data warrant further analysis of the functional properties of the selected genes, especially SOX4 and BCAT1 for medulloblastoma and SOX9 for ependymoma to evaluate the use of these genes as potential tumor markers, prognostic markers and drug target in pediatric brain tumors.

INTRODUCTION

Tumors of the central nervous system (CNS) are the second most common malignancy of childhood and generally associated with a worse prognosis than many other pediatric malignancies[1]. Medulloblastoma and ependymoma are frequently observed malignant brain tumors in children[2]. Medulloblastoma arise in the infratentorial posterior fossa and have the tendency to metastasize within the CNS[3, 4]. Ependymoma most frequently occur in the posterior fossa or spinal cord[3, 5].

Most prognostic factors currently known in pediatric brain tumors are based on clinical and histological criteria, such as age, extent of tumor resection and histological grading. However, insight into molecular abnormalities (genetic and/or post-transcriptional) underlying these tumors is limited. Hence, information on markers that can be used to characterize these tumors better, and potentially serve as new targets for therapy is lacking. Studies based on molecular analyses and gene expression profiling are now evolving and may provide possible clues about the pathogenesis and prognostic factors in pediatric brain tumors[6-8].

This study was aimed at identifying aberrantly expressed and prognostically important genes in pediatric medulloblastoma and ependymoma. By analyzing microarray data, we identified genes that may provide new insights into the biologic behavior of these brain tumors. The aberrant expression of these genes was validated at protein level by immunohistochemistry in a larger group of pediatric brain tumor samples. Further characterization of these genes may clarify whether these genes can serve as new tumor marker, prognostic factor or therapeutic target in pediatric brain tumors.

MATERIALS AND METHODS

Study population and samples

A total of 40 fresh frozen tumor samples from 25 newly diagnosed medulloblastoma (19 without and 6 with radiological visible leptomeningeal metastases), 2 medulloblastoma at relapse (1 without and 1 with radiological visible leptomeningeal metastases), 11 newly diagnosed ependymomas (4 cellular ependymoma and 7 anaplastic ependymoma) and 2 ependymomas at relapse (1 cellular ependymoma and 1 anaplastic ependymoma) were analyzed in this study. Most of these tumor samples were also analyzed by 2-dimensional difference in gel analysis, which resulted in the identification of stathmin, annexin A1 and calcyphosine as differentially expressed proteins in medulloblastoma and ependymoma[9]. Mean age at the time of tumor sample collection was 7.0 years (range 0.98-14.87 years) for the medulloblastoma patients and 5.6 years (range 0.66-15.57 years) for the ependymoma patients ($p>0.05$). All samples were collected at the Erasmus MC – University Medical Center – Sophia Children's Hospital, Rotterdam, the Netherlands between 1990 and 2004. After surgery, tumor samples

were immediately placed in liquid nitrogen and stored at -80°C until processing. Control cerebellar tissue was obtained post-mortem from 5 adult patients without a history of a brain tumor. Before RNA extraction, 4 µm cryosections were prepared of the same tissue blocks as used for RNA extraction and hematoxiline-eosine (HE) stained to confirm tumor histology.

Paraffin-embedded tissue for immunohistochemical validation of the differentially expressed genes was available for 23 (19 non-metastatic and 4 metastatic) of the 27 medulloblastoma and 10 (3 cellular ependymoma and 7 anaplastic ependymoma) of the 13 ependymoma studied by microarray. To enlarge the number of patients for these immunohistochemistry validation experiments, we also included paraffin embedded material from newly diagnosed medulloblastoma and ependymoma patients from whom no fresh frozen tissue was available for microarray analysis (see table with immunohistochemistry results). Additionally, paraffin embedded tissue from normal cerebellum, normal cortex, normal ependyma and normal plexus choroideus were included as normal control.

Microarray

RNA extraction, labeling and hybridization

Total RNA was isolated by homogenizing tissue samples in TRizol reagent (Invitrogen, Breda, the Netherlands) using a tissue homogenizer (B. Braun, Spangenberg, Germany). RNA was isolated according to the manufacturer's protocol with minor modifications[10]**.** RNA integrity was checked using the Agilent 2100 Bioanalyzer (Agilent, Santa Clara, USA). Production of biotinylated antisense cRNA and hybridization of the labeled cRNA to Human Genome U133 plus 2.0 GeneChip oligonucleotide microarrays (Affymetrix, Santa Clara, USA) was performed according to manufacturer's protocols. All arrays had a 3' to 5' GAPDH ratio < 3.0.

Statistical analysis of micro-array data

Expression data were analyzed using R version 2.4.0. Raw data were normalized using the variance stabilization procedure (vsn)[11]. Expression profiles of medulloblastoma, ependymoma and cerebellum were statistically compared using the Wilcoxon test and corrected for multiple testing errors by applying the false discovery rate (FDR) described by Benjamini and Hochberg[12] (MULTTEST package). A FDR <1% was considered statistically significant, meaning that less than 1% of the significant genes are false positives. The fold up- or down-regulation was calculated using the formula: $e^{(\text{vsn value A} - \text{vsn value B})}$, in which A and B are the groups to be compared.

Survival probabilities were estimated by the Kaplan Meier method using SPSS 11.0. Overall survival was defined as time from diagnosis until death or last contact. Event-free survival was defined as time from diagnosis until disease progression, relapse, second malignancy, death or last contact. A cox regression analysis using SPSS 11.0 was performed to identify genes whose expression was predictive for survival. For each gene, a hazard ratio and its

95% confidence interval was calculated. An effect was considered statistically significant if p was ≤ 0.05. A hazard ratio <1 indicates a favorable influence on survival and a hazard ratio >1 indicates an unfavorable influence on survival.

Functional properties of the differentially expressed genes were analyzed by Ontologizer, an XML-based Java application (www.charite.de/ch/medgen/ontologizer)[13], using annotations from the Gene Ontology database (http://www.geneontology.org). Probe sets with the same gene symbol were counted as one. Over-represented genes in brain tumor samples were identified by comparing the percentage of genes in each annotation from the total number of genes on the Human Genome U133 plus 2.0 array to the percentage of genes in each annotation from the selected subsets of genes using the parent-child method implemented in Ontologizer[13]. The parent-child method was preferred above the term-to-term method, as it takes the dependencies between different GO annotations into account. Over-representation of a GO annotation was thus measured with respect to the presence of its parental terms in the selected set of genes, instead of measuring individual GO terms. To correct for multiple testing errors the Westfall-Young correction[14] was used. A FDR of <1% was considered statistically significant.

Immunohistochemistry

For the selected discriminative genes, data were validated at the protein level by immunohistochemistry. For this purpose, formalin-fixed paraffin embedded tissue was collected for the medulloblastoma, ependymoma, control cerebella, cortex, normal ependyma and plexus choroideus. Four µm tissue sections were deparaffinized and rehydrated through a graded series of xylene-ethanol and incubated for 30 minutes in 3% hydrogen peroxide in PBS to inhibit endogenous peroxidases. Antigen retrieval was performed by boiling the slides for 15 minutes in 0.01 mol/L citric acid (pH 6.0). Six percent goat serum (Vector Laboratories, USA) in PBS was used as a protein block for 1 hour at room temperature. Tissue sections were incubated with antibodies against SOX4 (Sigma Aldrich, Zwijndrecht, the Netherlands, 1:500 in 1% goat serum), SOX9 (US Biological, Swampscott, USA, 1:2000 in 1% goat serum), SOX11 (Sigma Aldrich, Zwijndrecht, the Netherlands, 1:50 in 1% goat serum) and BCAT1 (BD Biosciences, Alphen aan den Rijn, the Netherlands, 1:200 in 1% goat serum) at 4ºC overnight. The sections were then incubated with biotinylated goat anti-rabbit IgG (Vector Laboratories, Burlingame, USA) at a dilution of 1:1000 in PBS for 1 hour at room temperature. This was followed by 1-hour incubation with avidin-biotin peroxidase complex (dilution 1:400; Vectastain ABC kit, Vector Laboratories, Burlingame, USA). Staining was performed using 0.5 mg/ml 3,3' diaminobenzidine (DAB), 0.03% (v/v) hydrogen peroxide in 30 mM imidazole/1 mM EDTA (pH 7.0). Tissue sections were slightly counterstained with hematoxylin, dehydrated and mounted. As negative control, the primary antibodies were omitted.

Immunohistochemistry was scored according to the percentage of cells that were positively stained in each slide: slides were scored weak when 0-25% of the cells stained positive, slides were scored moderate when 25-50% of the cells stained positive, strong was used for slides that showed positivity in 50-75% of the cells and very strong for positivity in 75-100% of the tumor cells. Differences in immunohistochemistry results for the analyzed subgroups were tested for significance using the Chi-square test in SPSS 11.0.

RESULTS

Micro-array gene expression analysis

Gene expression profiles were generated of 27 medulloblastoma, 13 ependymoma and 5 control cerebellum samples. A comparison between medulloblastoma and normal cerebellum samples revealed that 3447 probe sets were differentially expressed with a FDR <1%. Between ependymoma and normal cerebellum samples 3708 differentially expressed probe sets were found and between medulloblastoma and ependymoma 4720 probe sets were differentially expressed with a FDR <1% (Figure 1).

394 probe sets were most discriminative for medulloblastoma since these were significantly differentially expressed between both medulloblastoma and cerebellum and between medulloblastoma and ependymoma (Figure 1). Functional analysis (GO) revealed that the GO annotations involved in the regulation of the cell cycle, DNA replication and response to stimuli are over-represented in this set of 394 differentially expressed probe sets (corresponding to 253 genes with annotations in the GO database)(Figure 2). The number of most discriminative probe sets for ependymoma was 582 (Figure 1). Functional GO analysis did not reveal any significant over-representation of GO annotations in the 582 probe sets specific for ependymoma. 1541 probe sets were aberrantly expressed in both medulloblastoma and ependymoma compared to normal cerebellum, but these were not significantly different between medulloblastoma and ependymoma (Figure 1). Thus, these probe sets are likely to be related to the presence of a tumor, but not specifically discriminative for either medulloblastoma or ependymoma. Out of all probe sets, 133 probe sets were statistically differentially expressed between all subgroups (medulloblastoma, ependymoma and cerebellum) (Figure 1).

As previously found by others as well, OTX2 was found to be differentially expressed in medulloblastoma with the highest fold-change ratio (median 158) compared to cerebellum. Several members of the SOX gene family were differentially expressed between medulloblastoma, ependymoma and control cerebellum. SOX4 was median 16-fold higher expressed in medulloblastoma compared to normal cerebellum and median 8-fold higher in medulloblastoma compared to ependymoma (Figure 3A). SOX11 was highly overexpressed in both brain tumor types, but especially in medulloblastoma, being median 84-fold higher in medulloblastoma and median 21-fold higher in ependymoma compared to normal cerebellum (Figure

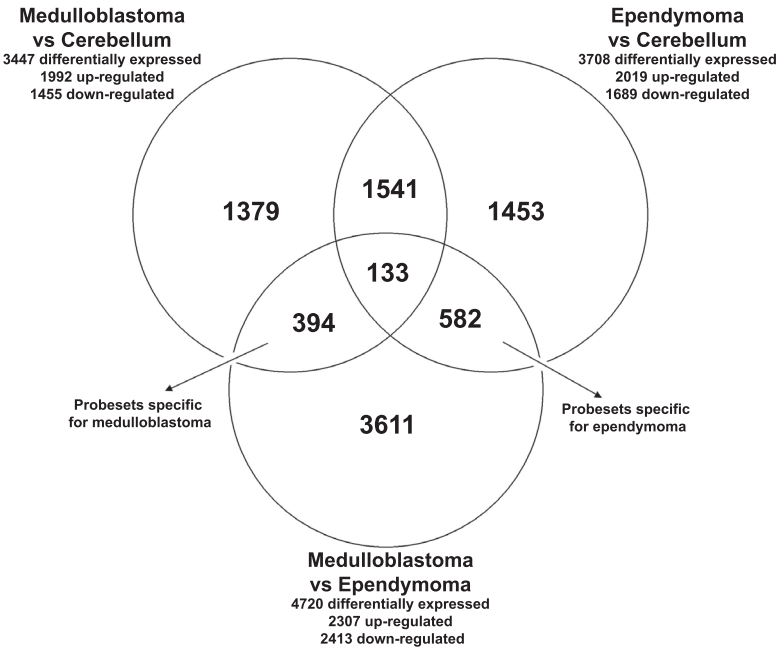

Figure 1. Venn diagram indicating the number of differentially expressed probesets of the comparisons between medulloblastoma, ependymoma and normal cerebellum.
All probesets that were differentially expressed with a FDR<1% between medulloblastoma, ependymoma and control cerebellum were used to create a Venn diagram. 394 probesets were most discriminant for medulloblastoma being differentially expressed between both medulloblastoma and cerebellum and between medulloblastoma and ependymoma. 582 probesets were found to be most discriminant for ependymoma, being significantly different between ependymoma and cerebellum and between ependymoma and medulloblastoma. 1541 were differentially expressed in both medulloblastoma and ependymoma when compared to cerebellum. However, they were not found to discriminate between medulloblastoma and ependymoma. 133 probesets were differentially expressed between all subgroups.

3B). SOX9 was significantly overexpressed in ependymoma, being median 10-fold higher expressed in ependymoma compared to normal cerebellum and median 17-fold higher in ependymoma compared to medulloblastoma (Figure 3C) ($p<0.001$ for all comparisons).

No significant probe sets were found that could explain differences between low- and high-grade ependymoma or between medulloblastoma with and without radiological metastases at diagnosis. The lack of significant probe sets after multiple testing may be due to the limited sample size. To get an impression of potentially metastasis-related probe sets in medulloblastoma, we also analyzed which probe sets were significantly differentially expressed at $p<0.01$ without correction for multiple testing and a fold-change ratio higher than 5. Remarkably, 3 out of 241 probe sets with $p<0.01$ encoded the BCAT1 gene. This gene was median 15-fold higher expressed in medulloblastoma patients with compared to

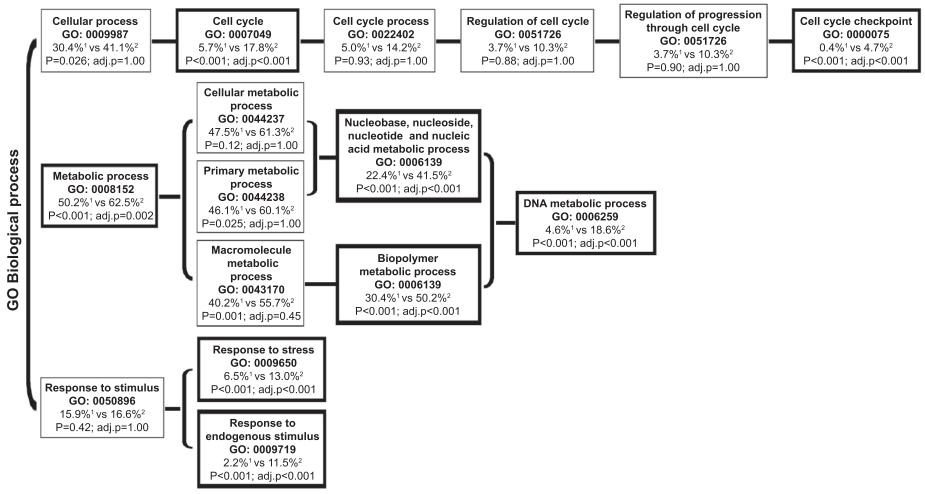

Figure 2. Functional GO analysis.

Figure 2 displays the GO annotations that were over-represented with a FDR<1% within the 394 probesets that were discriminant for medulloblastoma. The 394 probesets corresponded to 253 genes for which a biological GO annotation was available. Functional categories that are proportionally over-represented in the sets of selected probe sets as compared to all probe sets present on the array are shown in bold-printed boxes.

¹ percentage of genes from the total number of genes present on the HGU 133 plus 2.0 arrays per GO annotation

² percentage of genes from the selected differentially expressed genes in medulloblastoma per GO annotation

vs versus

adj.p p-value after correction for multiple testing

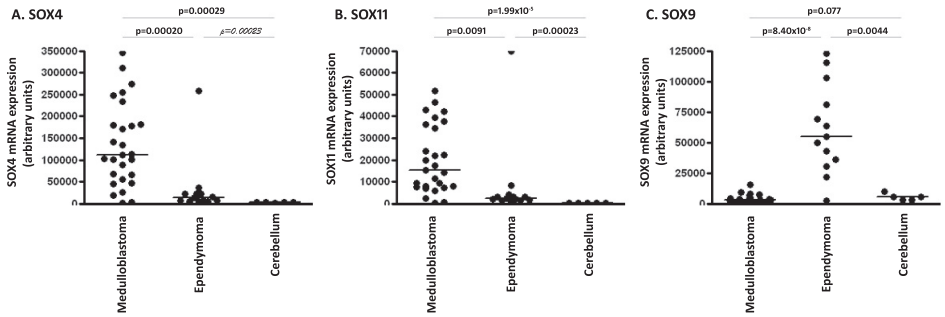

Figure 3. Differential expression of SOX4, SOX11 and SOX9 in medulloblastoma, ependymoma and control cerebellum.

Vsn normalized mRNA expression levels of SOX4 (A.), SOX11 (B.) and SOX9 (C.) in medulloblastoma, ependymoma and cerebellum obtained by Affymetrix HGU 133 plus 2.0 microarray analysis. SOX4 and SOX11 were significantly overexpressed in medulloblastoma, whereas SOX9 was significantly overexpressed in ependymoma.

medulloblastoma patients without radiological metastases (Figure 4). Between low- and high-grade ependymoma no probe sets were differentially expressed ($p<0.01$) with a fold-change ratio higher than 5.

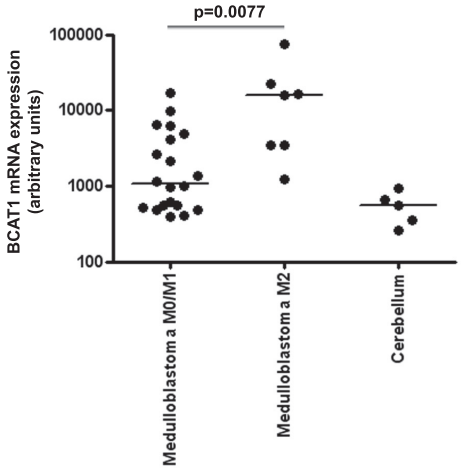

Figure 4. Differential BCAT1 expresion in metastatic medulloblastoma.
Vsn normalized mRNA expression levels of BCAT1 in medulloblastoma without (M0/M1) and with (M2) radiological leptomeningeal metastases at diagnosis obtained by Affymetrix HGU 133 plus 2.0 microarray analysis.

Survival analysis

Overall survival and event-free survival for medulloblastoma patients was respectively 31.7 ± 9.0% and 29.6 ± 9.0%. For ependymoma, overall survival was 9.7 ± 9.2% and event-free survival was 8.3 ± 8.0%. In medulloblastoma, increasing age was significantly associated with unfavorable survival (p=0.0040, hazard ratio 0.82). Metastatic disease was only predictive for unfavorable event-free survival and not for overall survival. For ependymoma, increasing age was not associated with unfavorable outcome.

Using the most discriminative probe sets for either medulloblastoma or ependymoma (respectively 394 and 582, as described above), a cox regression analysis was performed to identify the probe sets whose expression was predictive for outcome. In medulloblastoma, 14 probe sets were significantly correlated with a favorable overall survival and 21 probe sets were predictive of unfavorable overall survival (Table 1). In ependymoma, 6 probe sets were associated with favorable overall survival and 7 probe sets were indicative for unfavorable outcome (Table 2).

Additionally, the aberrantly expressed genes chosen for further analysis, SOX4, SOX9, SOX11 and BCAT1, were also evaluated for their predictive impact on survival. There was a trend towards favorable prognosis with increasing SOX4 expression levels in medulloblastoma

Table 1. Probesets predictive of overall survival of medulloblastoma.
A cox regression analysis was performed using the 394 probesets most discriminative for medulloblastoma. This table displays the probe sets that significantly contributed to the overall survival of medulloblastoma. 14 probe sets significantly correlated with a favorable overall survival (hazard ratio <1.0) and 21 probesets were indicative of poor outcome (hazard ratio >1.0).
95% CI 95% confidence interval

Probe id	Gene title	Gene symbol	Chromosomal location	p-value	Hazard ratio (95% CI)
236852_at	F-box protein 43	FBXO43	8q22.2	0.030	0.096 (0.012-0.80)
209884_s_at	solute carrier family 4, sodium bicarbonate cotransporter, member 7	SLC4A7	3p22	0.045	0.33 (0.11-0.97)
206142_at	zinc finger protein 135	ZNF135	19q13.4	0.022	0.36 (0.15-0.87)
1554101_a_at	transmembrane and tetratricopeptide repeat containing 4	TMTC4	13q32.3	0.022	0.38 (0.16-0.87)
225982_at	upstream binding transcription factor, RNA polymerase I	UBTF	17q21.3	0.024	0.39 (0.18-0.89)
235422_at	Full-length cDNA clone CS0DB008YK14 of Neuroblastoma Cot 10-normalized of Homo sapiens	---	---	0.036	0.41 (0.17-0.94)
242736_at	---	---	---	0.048	0.43 (0.19-0.99)
244387_at	Transcribed locus	---	---	0.0020	0.46 (0.28-0.75)
204061_at	protein kinase, X-linked	PRKX	Xp22.3	0.028	0.52 (0.29-0.93)
223627_at	ring finger and KH domain containing 3	RKHD3	15q25.2	0.045	0.54 (0.30-0.99)
219740_at	vasohibin 2	VASH2	1q32.3	0.045	0.57 (0.33-0.99)
230596_at	CDNA FLJ39261 fis, clone OCBBF2009391	---	---	0.0060	0.60 (0.42-0.87)
208497_x_at	neurogenin 1	NEUROG1	5q23-q31	0.0050	0.64 (0.47-0.88)
237007_at	---	---	---	0.028	0.66 (0.46-0.96)
227911_at	Rho GTPase activating protein 28	ARHGAP28	18p11.31	0.052	1.62 (1.00-2.63)
228109_at	Ras protein-specific guanine nucleotide-releasing factor 2	RASGRF2	5q13	0.015	1.63 (1.10-2.41)
213056_at	FERM domain containing 4B	FRMD4B	3p14.1	0.0010	1.81 (1.29-2.54)
204023_at	replication factor C (activator 1) 4, 37kDa	RFC4	3q27	0.036	2.24 (1.06-4.77)
205393_s_at	CHK1 checkpoint homolog (S. pombe)	CHEK1	11q24-q24	0.051	2.36 (1.00-5.56)
205394_at	CHK1 checkpoint homolog (S. pombe)	CHEK1	11q24-q24	0.043	2.36 (1.028-5.42)

Probe id	Gene title	Gene symbol	Chromosomal location	p-value	Hazard ratio (95% CI)
204407_at	transcription termination factor, RNA polymerase II	TTF2	1p22	0.029	2.80 (1.11-7.05)
201833_at	histone deacetylase 2	HDAC2	6q21	0.036	2.89 (1.07-7.79)
234863_x_at	F-box protein 5	FBXO5	6q25-q26	0.017	3.39 (1.24-9.23)
211450_s_at	mutS homolog 6 (E. coli)	MSH6	2p16	0.011	3.66 (1.34-10.01)
203207_s_at	mitochondrial fission regulator 1	MTFR1	8q13.1	0.0050	3.69 (1.48-9.17)
230503_at	Transcribed locus	---	---	0.011	3.89 (1.36-11.17)
234992_x_at	epithelial cell transforming sequence 2 oncogene	ECT2	3q26.1-q26.2	0.030	3.92 (1.15-13.44)
235295_at	Transcribed locus	---	---	0.023	3.92 (1.20-12.79)
227928_at	chromosome 12 open reading frame 48	C12orf48	12q23.2	0.027	4.33 (1.18-15.86)
216559_x_at	heterogeneous nuclear ribonucleoprotein A1	HNRPA1	10q11.22	0.010	4.72 (1.44-15.41)
223225_s_at	SEH1-like (S. cerevisiae)	SEH1L	18p11.21	0.021	6.49 (1.33-31.68)
218433_at	pantothenate kinase 3	PANK3	5q34	0.024	12.48 (1.40-111.51)
236030_at	REST corepressor 2	RCOR2	11q13.1	0.0010	12.73 (2.78-58.20)
231380_at	chromosome 8 open reading frame 34	C8orf34	8q13	0.018	14.1 (1.58-125-87)
205953_at	leucine-rich repeats and immunoglobulin-like domains 2	LRIG2	1p13.1	0.033	35.0 (1.32-927.42)

(p=0.065; hazard ratio 0.78). The expression of SOX9, SOX11 and BCAT1 was not significantly associated with the outcome of medulloblastoma. SOX9 expression was significantly associated with favorable overall survival in ependymoma (p=0.027; hazard ratio 0.44).

Validation of potential tumor markers by immunohistochemistry

The striking difference in mRNA expression of 3 SOX genes between medulloblastoma, ependymoma and cerebellum and the potential prognostic impact of SOX4 and SOX9 expression, prompted us to validate these genes with a different technique in an extended set of patient samples.

Immunohistochemistry confirmed the differential expression of SOX4 and SOX11, showing stronger SOX4 and SOX11 staining in medulloblastoma compared to ependymoma (Table 3, $p<0.001$ and $p<0.001$, respectively for SOX4 and SOX11). We observed strong to very strong SOX4 and SOX11 nuclear positivity in almost 75% of the medulloblastoma. Representative images of intense SOX4 and SOX11 staining in medulloblastoma are shown in figure 5A and

Table 2. Probesets predictive of overall survival of ependymoma.
A cox regression analysis was performed using the 582 probe sets most discriminative for ependymoma. This table displays the probe sets that significantly contributed to the overall survival of ependymoma. Six probe sets significantly correlated with a favorable overall survival (hazard ratio <1.0) and 7 probe sets were indicative of poor outcome (hazard ratio >1.0).
95% CI 95% confidence interval

Probe id	Gene title	Gene symbol	Chromosomal location	p-value	Hazard ratio (95% CI)
243929_at	---	---	---	0.022	0.0010 (0.00010-0.29)
238479_at	Full length insert cDNA clone ZC34E11	---	---	0.024	0.0040 (0.00010-0.47)
227313_at	Protein Associated with Tlr4	MGC40499	7q22.1	0.040	0.024 (0.0010-0.85)
233223_at	CDNA FLJ20843 fis, clone ADKA01954	---	---	0.025	0.052 (0.0040-0.69)
201324_at	epithelial membrane protein 1	EMP1	12p12.3	0.047	0.26 (0.068-0.98)
201426_s_at	vimentin	VIM	10p13	0.040	0.42 (0.18-0.96)
215321_at	Rap2-binding protein 9	RPIB9	7q21.12	0.027	2.26 (1.10-4.67)
217478_s_at	major histocompatibility complex, class II, DM alpha	HLA-DMA	6p21.3	0.048	3.53 (1.01-12.39)
229823_at	Transcribed locus	---	---	0.046	10.81 (1.04-112.08)
225792_at	hook homolog 1 (Drosophila)	HOOK1	1p32.1	0.039	11.72 (1.14-121.01)
211742_s_at	ecotropic viral integration site 2B	EVI2B	17q11.2	0.030	37.41 (1.43-979.18)
203998_s_at	synaptotagmin I	SYT1	12cen-q21	0.032	550.73 (1.743-174045.00)
206137_at	regulating synaptic membrane exocytosis 2	RIMS2	8q22.3	0.0080	1508.40 (6.73-338057.40)

5C, respectively. SOX4 staining was weak to moderate in all, but one, ependymoma cases. SOX11 expression was limited (<50% of the cells) in more than 75% of the ependymomas. Representative images of SOX4 and SOX11 staining in ependymomas are shown in figure 5B and 5D, respectively. SOX4 and SOX11 positivity was not observed in normal cerebellum, cortex, normal ependyma and plexus choroideus.

The high expression of SOX9 in ependymomas was also confirmed by immunohistochemistry. SOX9 staining was nuclear. SOX9 nuclear positivity was strong to very strong in approximately 75% of the ependymomas (Table 3; Figure 5F) and weak to moderate in more than 90% of the medulloblastoma (Table 3; p<0.001; Figure 5E). Cerebellum, cortex, normal ependyma and plexus choroideus were negative for SOX9.

Table 3. Immunohistochemistry results for SOX4, SOX9, SOX11 and BCAT1 immunoreactivity in medulloblastoma, ependymoma and control tissues.

Slides were scored "weak" when 0-25% of the cells stained positive. "moderate" was used for the slides with positivity in 25-50% of the cells and "strong" and "very strong" were used for respectively strong and very strong immunoreactivity. Immunohistochemistry confirmed the differential mRNA expression of SOX4, SOX11 and SOX9 at protein level. The differential mRNA expression of BCAT1 in metastatic medulloblastoma did not correlate with the protein expression levels observed with immunohistochemistry.

	n	0-25% weak	25-50% moderate	50-75% strong	75-100% very strong
SOX4					
Medulloblastoma	**29**	**7%**	**21%**	**31%**	**41%**
non-metastatic	25	8%	24%	28%	36%
metastatic	4	0%	0%	50%	50%
Ependymoma	**15**	**87%**	**13%**	**0%**	**0%**
cellulare	7	86%	14%	0%	0%
anaplastic	8	88%	13%	0%	0%
Cerebellum	5	100%	0%	0%	0%
Cortex	5	100%	0%	0%	0%
Normal ependyma	5	100%	0%	0%	0%
Plexus choroideus	5	100%	0%	0%	0%
SOX11					
Medulloblastoma	**30**	**7%**	**10%**	**30%**	**53%**
non-metastatic	24	8%	8%	29%	54%
metastatic	6	0%	17%	33%	50%
Ependymoma	**16**	**56%**	**19%**	**19%**	**6%**
cellulare	7	57%	29%	0%	14%
anaplastic	9	56%	11%	33%	0%
Cerebellum	5	100%	0%	0%	0%
Cortex	5	100%	0%	0%	0%
Normal ependyma	5	100%	0%	0%	0%
Plexus choroideus	5	100%	0%	0%	0%
SOX9					
Medulloblastoma	**30**	**63%**	**30%**	**7%**	**0%**
non-metastatic	25	60%	32%	8%	0%
metastatic	5	80%	20%	0%	0%
Ependymoma	**16**	**13%**	**13%**	**31%**	**44%**
cellulare	7	0%	14%	14%	71%
anaplastic	9	22%	11%	44%	22%
Cerebellum	5	100%	0%	0%	0%
Cortex	5	100%	0%	0%	0%
Normal ependyma	5	100%	0%	0%	0%
Plexus choroideus	5	100%	0%	0%	0%
BCAT1					
Medulloblastoma	**34**	**62%**	**12%**	**18%**	**9%**

	n	0-25% weak	25-50% moderate	50-75% strong	75-100% very strong
non-metastatic	28	64%	11%	21%	4%
metastatic	6	50%	17%	0%	33%
Ependymoma	5	100%	0%	0%	0%
Cerebellum	5	100%	0%	0%	0%
Cortex	5	100%	0%	0%	0%
Normal ependyma	5	100%	0%	0%	0%
Plexus choroideus	5	100%	0%	0%	0%

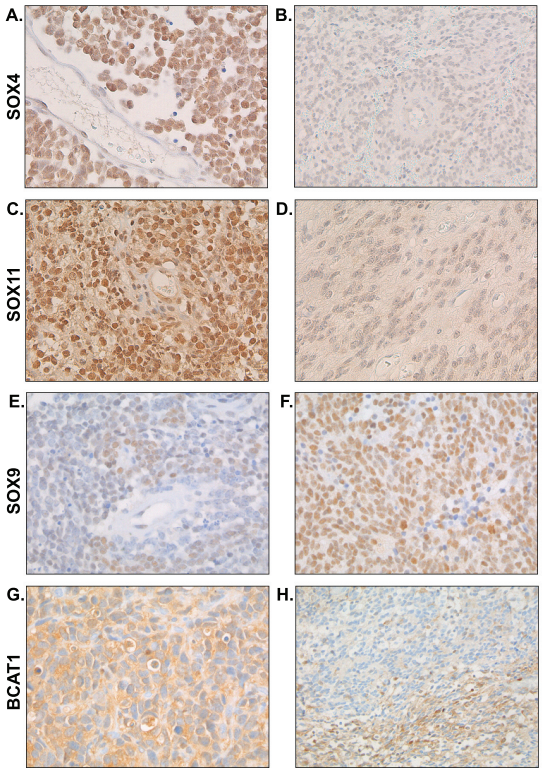

Figure 5. Immunohistochemistry for SOX4, SOX11, SOX9 and BCAT1 in medulloblastoma and ependymoma.

Immunohistochemistry confirmed the overexpression of SOX4 in medulloblastoma (A.) compared to ependymoma (B.). SOX11 protein expression was also shown to be higher in medulloblastoma (C.) compared to ependymoma (D.). In contrast, SOX9 expression was confirmed to be higher in ependymoma (F.) compared to medulloblastoma (E.). Figure G. and H. respectively show representative pictures of strong homogeneous cytoplasmic staining of BCAT1 and focal BCAT1 staining in predominantly metastasized medulloblastoma.

Expression of BCAT1, which was differentially expressed at the mRNA level between medulloblastoma with and without radiological metastases at diagnosis, was also studied by immunohistochemistry (Table 3). At protein level, the difference in BCAT1 expression between metastatic and non-metastatic medulloblastoma was not evident (Table 3). Three medulloblastomas showed very strong homogenous cytoplasmic BCAT1 staining (Figure 5G). Two of these had radiological metastases at diagnosis and 1 patient did not have radiological metastases, although tumor cells were found in the diagnostic cerebrospinal fluid of this case. Six medulloblastomas also showed very strong staining, but only within distinct areas of the tumor (50-75% of the cells) (Figure 5H). None of these patients had radiological visible metastases at diagnosis and only one of these patients had tumor cells in the diagnostic cerebrospinal fluid. Four medulloblastoma (1 of these had radiological visible metastases at diagnosis and in 1 tumor cells were found in the diagnostic cerebrospinal fluid) showed intense BCAT1 staining in less than 50% of the cells. In the other medulloblastomas, ependymomas, cerebellum, cortex, normal ependyma and plexus choroideus BCAT1 positivity was absent.

DISCUSSION

In this study we compared gene expression profiles of 27 pediatric medulloblastoma, 13 pediatric ependymoma and 5 normal cerebella. As at least part of all medulloblastoma is thought to arise from the external granular layer of the cerebellum, cerebellum was used as normal control. For each tumor subgroup we identified a set of probe sets that were most discriminative and that could be used for functional (GO) and survival analysis. Functional analysis (GO) of the most discriminative probe sets for medulloblastoma mainly showed over-representation of genes involved in regulation of the cell cycle, replication and response to stimuli, but amongst them there were also many transcription factors. OTX2 was for example found to be 140-fold higher expressed in medulloblastoma compared to normal cerebellum, which validates earlier findings using different techniques, i.e. SAGE[15].

Besides OTX2, several members of the SOX gene transcription factor family were differentially expressed in either medulloblastoma or ependymoma. SOX4 and SOX11 were highly overexpressed in medulloblastoma, whereas SOX9 was highly overexpressed in ependymoma. The differential mRNA expression of SOX4, SOX11 and SOX9 was confirmed at the protein level by immunohistochemistry. In addition, survival analysis showed that both SOX4 and SOX9 were predictive of outcome in respectively medulloblastoma and ependymoma. The SOX proteins comprise a family of more than 20 transcription factors characterized by the presence of a high mobility group DNA binding domain[16]. SOX4 and 11 belong to subgroup C of the SOX gene family. SOX4 is known to play a role in normal embryonic development of e.g. the heart, CNS, lungs and thymus[17-19]. SOX4 has shown to be overexpressed in various malignancies[20-22], including medulloblastoma[23, 24]. Interestingly, SOX4 is one of the

most frequently targeted genes by retroviral insertional mutagenesis[25, 26]. Down-regulation of SOX4 expression in prostate cancer[22] cell lines resulted in a strong decrease in cell viability and a corresponding increase in apoptosis. However, SOX4 induction has also been shown to impair cell viability and induce apoptosis[27]. The contradictory effect of SOX4 expression on apoptosis in different cell types suggests that SOX4, like c-Myc, has both anti- and pro-apoptotic activities. The balance between anti- and pro-apoptotic signals induced by SOX4 expression might thus be tissue-specific and dependent on external signals. Therefore, and as the biological role of high SOX4 expression in medulloblastoma is unknown, further research should focus on the functional characteristics of SOX4, e.g. by modulating SOX4 expression by RNAi. In our study SOX4 expression was associated with more favorable outcome in medulloblastoma. As these findings are in contrast with those of Neben et al[28], who found SOX4 to be a poor prognostic factor, prospective studies including large number of patients should be conducted to determine the exact influence of SOX4 on outcome in medulloblastoma.

SOX11 is expressed in neural precursors throughout the neuroepithelium and is also expressed in areas of the brain in which neurons undergo differentiation during later stages of neural development[29]. SOX11 was found to be overexpressed in fetal brain tissue and malignant gliomas[30]. Expression of SOX11 in malignant glioma may be the result of a dedifferentiation process during tumorigenesis, as SOX11 is normally down-regulated after maturation of the brain[30]. Since we observed medulloblastoma to be characterized by a high expression level of SOX11, our data may underline the embryonal origin of these tumors.

In contrast to SOX4 and SOX11, SOX9 mRNA and protein expression levels were up-regulated in ependymoma. SOX9 belongs to the subgroup of SOX E genes, which control different aspects of differentiation of astrocytes, oligodendrocytes and Schwann cells[31]. Outside the central nervous system, SOX9 is required for chondrogenesis and the development of the male gonad[32]. SOX9 is likely to be of importance in ependymomas, as, in concordance with our results, strong nuclear SOX9 expression has also been described in pediatric and adult high grade neuro-epithelial tumors[33]. Moreover, data from the study of Modena et al.[34] (supplementary table 3; http://pierotti.group.ifom-ieo-campus.it/suppl/epd.html) also confirm SOX9 overexpression in ependymoma, showing an approximately 6-fold higher SOX9 expression in ependymomas compared to other tissues. In the intestinal epithelium SOX9 was found to be expressed in a pattern characteristic of Wnt targets[35]. Overexpression of SOX9 in cultured colon carcinoma cells, resulted in decreased expression of the tumor suppressor gene CDX2, suggesting SOX9 to be a potential important contributor to cancer progression[35]. In contrast, SOX9 expression was significantly associated with more favourable outcome in ependymoma in our study. As SOX9 does not seem to result in potentiation of disease progression of ependymoma, as was suggested in colon carcinoma, larger prospective studies should determine the exact role of SOX9 as a prognostic factor in ependymoma.

The presence of radiological leptomeningeal metastases at diagnosis is an important adverse prognostic factor in medulloblastoma patients[36]. We found BCAT1 mRNA expression levels to be median 15-fold increased in medulloblastoma with radiological leptomeningeal metastases. BCAT1 is a cytosolic branched-chain amino acid aminotransferase, which has been reported to be involved in the control of the cell cycle by suppressing the G1 to S transition of normal cells[37]. BCAT1 is involved in various malignancies. The mouse homolog of BCAT1 was amplified and overexpressed in a teratocarcinoma cell line[38]. Retroviral transduction of fetal rat brain cells with SV40 large T antigen induced tumors with characteristic features of medulloblastoma which showed amplification of BCAT1[39, 40]. In colorectal adenocarcinomas, high BCAT1 expression was associated with a greater tendency to metastasize and a decreased disease free survival rate[41]. As BCAT1 was found to be a direct target for myc-activation in oncogenesis[37, 42], the overexpression of BCAT1 in malignancies might be a result of myc-activation. In our study BCAT1 mRNA expression was not significantly correlated with c-, N- or L-myc mRNA expression (data not shown), which suggests that other factors are responsible for the up-regulation of BCAT1 expression in medulloblastoma, as was also suggested for other neuronal tumors[43].

Evaluation of BCAT1 expression in the dataset of Thompson et al.[7] did not show a significant difference in expression between medulloblastoma with and those without evident metastasized disease (≥M2 stage). In our study, the correlation between BCAT1 expression and metastatic disease in medulloblastoma was not clear at protein level, as several non-metastatic medulloblastoma also showed strong BCAT1 immunoreactivity. The lack of correlation between mRNA and protein expression levels can be caused by the instability of mRNA or protein, high turn-over of protein or translational repression by microRNAs[44]. Moreover, the fact that the pattern of BCAT1 staining was mainly focal and not homogeneous (Figure 6H), might also explain why positive BCAT1 immunohistochemistry did not correlate with high BCAT1 mRNA expression. As it is shown that BCAT1 positivity can be very variable within the tumor, overall BCAT1 expression as detected by microarray analysis might thus be very dependent on which part of the tumor is analyzed. The focal pattern of staining might suggest the presence of a subset of BCAT1-positive tumor cells in some medulloblastoma that may have a higher tendency to metastasize. It would be interesting to specifically study BCAT1 expression in the cells already metastasized within the CNS. As these isolated cells were not available, we evaluated BCAT1 protein expression (Western blot) in the cerebrospinal fluid of several medulloblastoma patients with metastasized disease and a number of control patients. Interestingly, BCAT1 protein expression was very low in the cerebrospinal fluid of all control patients and high in the cerebrospinal fluid of the medulloblastoma patients (data not shown). Therefore, BCAT1 might still be an interesting new marker for metastasis for which more extensive studies should be performed. In addition, as BCAT1 can be inhibited by gabapentin[45], its use as therapeutic target should also be investigated.

Besides evaluating the differential expression of genes in medulloblastoma and ependymoma, we performed a cox regression analysis to determine which genes were predictive of survival in these tumors. Interestingly, several of these genes have already been shown to be of importance in the biology of malignancies and may well be new interesting therapeutic targets in pediatric brain tumors. In medulloblastoma, one of the genes associated with adverse outcome was CHEK1, a serine/threonine kinase implicated in the DNA damage checkpoint response and the replication checkpoint[46]. Inhibition of CHEK1 has been used to sensitize tumor cells to DNA anti-metabolite chemotherapeutic drugs[47]. As increasing CHEK1 expression resulted in worse overall survival of medulloblastoma, inhibition of CHEK1 expression might also result in higher chemosensitivity of these tumors and consequently higher survival rates.

HDAC2, a histone deacetylase negatively influencing prognosis in medulloblastoma in our study, is overexpressed in colorectal cancer and required to maintain the transformed phenotype of colon carcinoma cells[48]. In addition, HDAC2 was capable to regulate p53 activity by inhibiting p53-DNA binding[49].

Interestingly, ECT2, another poor prognostic gene in medulloblastoma in our study, was also found to be indicative of an unfavorable outcome in glioma[50].

A gene associated with more favorable prognosis in medulloblastoma was NEUROG1. NEUROG1 is a basis helix-loop-helix transcription factor that is important during neurogenesis and is suggested to be a marker for a subgroup of medulloblastoma deriving from progenitor cells of the cerebellar ventricular zone[51]. NEUROG1 may thus be interesting in the search for the cells of origin of medulloblastoma. In contrast to our data, Rostomily et al.[52] found a correlation between NEUROG1 expression and the presence of distant metastases in medulloblastoma. However, they only evaluated NEUROG1 expression in 3 medulloblastoma patients without distant metastases.

In conclusion, this study shows that gene expression profiling, using Affymetrix HGU133 plus 2.0 microarrays, is a tool to identify genes that are aberrantly expressed and of prognostic importance in pediatric brain tumors. SOX4 and SOX9, overexpressed in respectively medulloblastoma and ependymoma, were also of influence on outcome. Prospective studies involving larger number of patients will need to confirm the prognostic impact of the genes identified in our study and analysis of the functional characteristics of the selected genes should reveal the possibilities of using these genes as new tumor marker and therapeutic target in pediatric medulloblastoma and ependymoma.

REFERENCES

1. Bleyer WA. Epidemiologic impact of children with brain tumors. Childs Nerv Syst. 1999 15(11-12):758-763.
2. Kleihues P, Louis DN, Scheithauer BW, et al. The WHO classification of tumors of the nervous system. J Neuropathol Exp Neurol 2002;61(3):215-225; discussion 226-229.
3. Packer RJ. Brain tumors in children. Arch Neurol 1999;56(4):421-425.
4. MacDonald TJ, Rood BR, Santi MR, et al. Advances in the diagnosis, molecular genetics, and treatment of pediatric embryonal CNS tumors. Oncologist 2003;8(2):174-186.
5. Packer RJ. New insights into childhood ependymoma. Curr Neurol Neurosci Rep 2005;5(2):107-109.
6. Pomeroy SL, Tamayo P, Gaasenbeek M, et al. Prediction of central nervous system embryonal tumour outcome based on gene expression. Nature 2002;415(6870):436-442.
7. Thompson MC, Fuller C, Hogg TL, et al. Genomics identifies medulloblastoma subgroups that are enriched for specific genetic alterations. J Clin Oncol 2006;24(12):1924-1931.
8. Lukashova VZI, Kneitz S, Monoranu CM, et al. Ependymoma gene expression profiles associated with histological subtype, proliferation, and patient survival. Acta Neuropathol (Berl) 2007;113(3):325-337.
9. de Bont JM, den Boer ML, Kros JM, et al. Identification of novel biomarkers in pediatric primitive neuroectodermal tumors and ependymomas by proteome-wide analysis. J Neuropathol Exp Neurol 2007;66(6):505-516.
10. Stam RW, den Boer ML, Meijerink JP, et al. Differential mRNA expression of Ara-C-metabolizing enzymes explains Ara-C sensitivity in MLL gene-rearranged infant acute lymphoblastic leukemia. Blood 2003;101(4):1270-1276.
11. Huber W, Von Heydebreck A, Sultmann H, Poustka A, Vingron M. Variance stabilization applied to microarray data calibration and to the quantification of differential expression. Bioinformatics 2002;18(Suppl 1):S96-104.
12. Benjamini Y, Drai D, Elmer G, Kafkafi N, Golani I. Controlling the false discovery rate in behavior genetics research. Behav Brain Res 2001;125(1-2):279-284.
13. Robinson PN, Wollstein A, Bohme U, Beattie B. Ontologizing gene-expression microarray data: characterizing clusters with Gene Ontology. Bioinformatics 2004;20(6):979-981.
14. Westfall P, Young S. Resampling-Based Multiple testing. New York: Wiley, 1993.
15. Michiels EM, Oussoren E, Van Groenigen M, et al. Genes differentially expressed in medulloblastoma and fetal brain. Physiol Genomics 1999;1(2):83-91.
16. Wegner M. From head to toes: the multiple facets of Sox proteins. Nucleic Acids Res 1999;27(6):1409-1420.
17. Kamachi Y, Uchikawa M, Kondoh H. Pairing SOX off: with partners in the regulation of embryonic development. Trends Genet 2000;16(4):182-187.
18. Cheung M, Abu-Elmagd M, Clevers H, Scotting PJ. Roles of Sox4 in central nervous system development. Brain Res Mol Brain Res 2000;79(1-2):180-191.
19. Schilham MW, Oosterwegel MA, Moerer P, et al. Defects in cardiac outflow tract formation and pro-B-lymphocyte expansion in mice lacking Sox-4. Nature 1996;380(6576):711-714.
20. Aaboe M, Birkenkamp-Demtroder K, Wiuf C, et al. SOX4 expression in bladder carcinoma: clinical aspects and in vitro functional characterization. Cancer Res 2006;66(7):3434-3442.
21. Frierson HF, Jr., El-Naggar AK, Welsh JB, et al. Large scale molecular analysis identifies genes with altered expression in salivary adenoid cystic carcinoma. Am J Pathol 2002;161(4):1315-1323.
22. Liu P, Ramachandran S, Ali Seyed M, et al. Sex-determining region Y box 4 is a transforming oncogene in human prostate cancer cells. Cancer Res 2006;66(8):4011-4019.

23. Yokota N, Mainprize TG, Taylor MD, et al. Identification of differentially expressed and developmentally regulated genes in medulloblastoma using suppression subtraction hybridization. Oncogene 2004;23(19):3444-3453.
24. Lee CJ, Appleby VJ, Orme AT, Chan WI, Scotting PJ. Differential expression of SOX4 and SOX11 in medulloblastoma. J Neurooncol 2002;57(3):201-214.
25. Suzuki T, Shen H, Akagi K, et al. New genes involved in cancer identified by retroviral tagging. Nat Genet 2002;32(1):166-174.
26. Du Y, Spence SE, Jenkins NA, Copeland NG. Cooperating cancer-gene identification through oncogenic-retrovirus-induced insertional mutagenesis. Blood 2005;106(7):2498-2505.
27. Hur EH, Hur W, Choi JY, et al. Functional identification of the pro-apoptotic effector domain in human Sox4. Biochem Biophys Res Commun 2004;325(1):59-67.
28. Neben K, Korshunov A, Benner A, et al. Microarray-based screening for molecular markers in medulloblastoma revealed STK15 as independent predictor for survival. Cancer Res 2004;64(9):3103-3111.
29. Kuhlbrodt K, Herbarth B, Sock E, et al. Cooperative function of POU proteins and SOX proteins in glial cells. J Biol Chem 1998;273(26):16050-16057.
30. Weigle B, Ebner R, Temme A, et al. Highly specific overexpression of the transcription factor SOX11 in human malignant gliomas. Oncol Rep 2005;13(1):139-144.
31. Cheung M, Briscoe J. Neural crest development is regulated by the transcription factor Sox9. Development 2003;130(23):5681-5693.
32. Foster JW, Dominguez-Steglich MA, Guioli S, et al. Campomelic dysplasia and autosomal sex reversal caused by mutations in an SRY-related gene. Nature 1994;372(6506):525-530.
33. Kordes U, Hagel C. Expression of SOX9 and SOX10 in central neuroepithelial tumor. J Neurooncol 2006;80(2):151-155.
34. Modena P, Lualdi E, Facchinetti F, et al. Identification of tumor-specific molecular signatures in intracranial ependymoma and association with clinical characteristics. J Clin Oncol 2006;24(33):5223-5233.
35. Blache P, van de Wetering M, Duluc I, et al. SOX9 is an intestine crypt transcription factor, is regulated by the Wnt pathway, and represses the CDX2 and MUC2 genes. J Cell Biol 2004;166(1):37-47.
36. Zeltzer PM, Boyett JM, Finlay JL, et al. Metastasis stage, adjuvant treatment, and residual tumor are prognostic factors for medulloblastoma in children: conclusions from the Children's Cancer Group 921 randomized phase III study. J Clin Oncol 1999;17(3):832-845.
37. Schuldiner O, Eden A, Ben-Yosef T, et al. ECA39, a conserved gene regulated by c-Myc in mice, is involved in G1/S cell cycle regulation in yeast. Proc Natl Acad Sci U S A 1996;93(14):7143-7148.
38. Niwa O, Kumazaki T, Tsukiyama T, et al. A cDNA clone overexpressed and amplified in a mouse teratocarcinoma line. Nucleic Acids Res 1990;18(22):6709.
39. Eibl RH, Kleihues P, Jat PS, Wiestler OD. A model for primitive neuroectodermal tumors in transgenic neural transplants harboring the SV40 large T antigen. Am J Pathol 1994;144(3):556-564.
40. Weggen S, Preuss U, Pietsch T, et al. Identification of amplified genes from SV40 large T antigen-induced rat PNET cell lines by subtractive cDNA analysis and radiation hybrid mapping. Oncogene 2001;20(16):2023-2031.
41. Yoshikawa R, Yanagi H, Shen CS, et al. ECA39 is a novel distant metastasis-related biomarker in colorectal cancer. World J Gastroenterol 2006;12(36):5884-5889.
42. Ben-Yosef T, Eden A, Benvenisty N. Characterization of murine BCAT genes: Bcat1, a c-Myc target, and its homolog, Bcat2. Mamm Genome 1998;9(7):595-597.
43. Ben-Yosef T, Yanuka O, Halle D, Benvenisty N. Involvement of Myc targets in c-myc and N-myc induced human tumors. Oncogene 1998;17(2):165-171.
44. Bartel DP. MicroRNAs: genomics, biogenesis, mechanism, and function. Cell 2004;116(2):281-297.

45. Hutson SM, Berkich D, Drown P, et al. Role of branched-chain aminotransferase isoenzymes and gabapentin in neurotransmitter metabolism. J Neurochem 1998;71(2):863-874.
46. Bartek J, Lukas J. Chk1 and Chk2 kinases in checkpoint control and cancer. Cancer Cell 2003;3(5):421-429.
47. Xiao Z, Xue J, Sowin TJ, Zhang H. Differential roles of checkpoint kinase 1, checkpoint kinase 2, and mitogen-activated protein kinase-activated protein kinase 2 in mediating DNA damage-induced cell cycle arrest: implications for cancer therapy. Mol Cancer Ther 2006;5(8):1935-1943.
48. Zhu P, Martin E, Mengwasser J, et al. Induction of HDAC2 expression upon loss of APC in colorectal tumorigenesis. Cancer Cell 2004;5(5):455-463.
49. Harms KL, Chen X. Histone deacetylase 2 modulates p53 transcriptional activities through regulation of p53-DNA binding activity. Cancer Res 2007;67(7):3145-3152.
50. Sano M, Genkai N, Yajima N, et al. Expression level of ECT2 proto-oncogene correlates with prognosis in glioma patients. Oncol Rep 2006;16(5):1093-1098.
51. Salsano E, Croci L, Maderna E, et al. Expression of the neurogenic basic helix-loop-helix transcription factor NEUROG1 identifies a subgroup of medulloblastomas not expressing ATOH1. Neuro Oncol 2007;9(3):298-307.
52. Rostomily RC, Bermingham-McDonogh O, Berger MS, et al. Expression of neurogenic basic helix-loop-helix genes in primitive neuroectodermal tumors. Cancer Res 1997;57(16):3526-3531.

Chapter 4

Identification of Novel Biomarkers in Pediatric Primitive Neuroectodermal Tumors and Ependymomas by Proteome-Wide Analysis

Judith M. de Bont[1], Monique L. den Boer[1], Johan M. Kros[2], Monique M.C.J. Passier[1], Roel E. Reddingius[1], Peter A.E. Sillevis Smitt[3], Theo M. Luider[3], Rob Pieters[1]

[1]Erasmus MC – Sophia Children's Hospital - University Medical Center Rotterdam – Department of Pediatric Oncology and Hematology, The Netherlands;
[2]Erasmus MC – University Medical Center Rotterdam – Department of Pathology, The Netherlands;
[3]Erasmus MC – University Medical Center Rotterdam – Department of Neuro-oncology, The Netherlands

J Neuropathol Exp Neurol 2007; **66***(6): 505-516*

ABSTRACT

This study was aimed at identifying aberrantly expressed proteins in pediatric primitive neuroectodermal tumors (PNETs) and ependymomas. Tumor tissue of 29 PNET and 12 ependymoma patients was subjected to 2-dimensional difference gel electrophoresis. Gel analysis resulted in 79 protein spots being differentially expressed between PNETs and ependymomas ($p<0.01$, fold-change difference in expression > 2). Three proteins, stathmin, annexin A1 and calcyphosine, were chosen for validation by immunohistochemistry. Stathmin was expressed 2.6-fold higher in PNETs than in ependymomas and annexin A1 and calcyphosine were expressed 2.5- and 37.6-fold higher, respectively, in ependymomas. All PNETs showed strong staining for stathmin, and all ependymomas were strongly positive for annexin A1, whereas control tissues were negative. Calcyphosine immunoreactivity was observed in 59% of the ependymomas and was most profound in ependymomas tissue showing epithelial differentiation. mRNA expression levels of stathmin, annexin A1 and calcyphosine significantly correlated ($R_s=0.65$ ($p<0.0001$), $R_s=0.50$ ($p=0.001$) and $R_s=0.72$ ($p<0.0001$), respectively) with protein expression levels. In conclusion, using a proteome-wide approach, stathmin, annexin A1 and calcyphosine were successfully identified as tumor-specific proteins in pediatric PNETs and ependymomas. Ongoing studies are focused on characterizing the role of these proteins as tumor marker and potential drug targets in pediatric brain tumors.

INTRODUCTION

Primitive neuroectodermal tumors (PNETs) represent a large group of malignant brain tumors in children[1, 2]. Medulloblastomas are the most frequently occurring PNETs, arising in the infratentorial posterior fossa and having the tendency to metastasize within the CNS[3]. Treatment, including surgical resection, craniospinal irradiation and chemotherapy, results in a cure in ~60% of the affected children[4]. The much less common supratentorial PNETs seem to be histologically identical to medulloblastoma, but are biologically and genetically distinct and more aggressive[2, 5].

Ependymoma is the third most common CNS tumor in children[1, 6]. This neuroepithelial tumor is thought to arise from ependymal cells in the wall of the cerebral ventricles or the spinal canal and therefore most frequently occurs in the posterior fossa or spinal cord[6].

Most prognostic factors currently known in pediatric brain tumors are based on clinical and histological criteria, such as age, extent of tumor resection and histological grading. However, many genetic and biological alterations that could be used to further characterize these tumors and those that can be used as new targets for therapy are still unknown.

The aim of the present study was to identify aberrantly expressed proteins in pediatric PNETs and ependymomas. Two-dimensional (2D)-fluorescence difference gel electrophoresis (DIGE) is based on fluorescence prelabeling of protein mixtures before conventional 2D gel electrophoresis. It allows multiplexing of up to 3 separate protein samples on the same gel because of the covalent fluorescent labeling of proteins with CyDyes[7]. 2D-DIGE has successfully been used to identify potential protein biomarkers in various disease entities[8, 9]. Using this proteome-wide 2D-DIGE approach we identified abnormally expressed proteins in PNETs and ependymomas that may be used as tumor markers and potential therapeutic targets in pediatric brain tumors. The aberrant expression of these proteins was validated by immunohistochemistry and gene expression (mRNA) levels of the identified proteins were analyzed by microarray.

MATERIALS AND METHODS

Study population and samples

A total of 41 fresh frozen tumor samples from 27 newly diagnosed PNETs (22 medulloblastoma, 4 supratentorial PNETs and 1 ependymoblastoma), 2 PNETs (2 medulloblastoma) at relapse, 10 newly diagnosed ependymomas (4 cellulare ependymoma and 6 anaplastic ependymoma) and 2 ependymomas at relapse (1 cellulare ependymoma and 1 anaplastic ependymoma) were analyzed by 2D-DIGE. An atypical teratoid rhabdoid tumor sample was analyzed by 2D-DIGE, but was not included in the analyses. Mean age at the time of tumor sample collection was 6.1 years (range 0.19-14.96 years) for the PNET patients and 5.3

years (range 0.66-17.60 years) for the ependymoma patients. All samples were collected at the Erasmus MC – University Medical Center – Sophia Children's Hospital in Rotterdam, the Netherlands between 1990 and 2004. After surgery, tumor samples were immediately placed in liquid nitrogen and stored at -80°C until processing. Control cerebellar tissue was obtained post-mortem from 7 adult patients without a history of the presence of a brain tumor. Before protein and RNA extraction, 4 µm cryosections were prepared and hematoxylin-eosine (HE) stained to confirm tumor histology.

Paraffin-embedded tissue for immunohistochemistry validation of the identified protein markers was available for 18 of the 29 PNETs and for 10 of the 12 ependymomas studied with 2D-DIGE. Twelve other newly diagnosed PNETs and 12 ependymomas were also included in the validation experiments without prior 2D-DIGE analysis because no fresh frozen tumor tissue was present for these patients. There was sufficient fresh frozen tissue available to extract RNA for microarray analysis for 27 of the 29 PNETs and 11 of the 12 ependymomas that were analyzed by 2D-DIGE.

Protein Extraction

Frozen tissue samples were suspended in lysis buffer (30 mM Tris-HCl, 2 M thiourea, 7 M urea, 4% w/v CHAPS) and sonified at 4°C using a Branson Sonifier 250 (Branson Ultrasonics Corporation, Danbury, CT). Samples were left on ice for 15 minutes and centrifuged at 16060xg for 10 min at 4°C. Supernatants were removed and protein concentrations were determined in duplicate by the 2D Quant kit (Amersham Biosciences, Uppsala, Sweden).

Two-Dimensional Difference Gel Electrophoresis

In total, 21 gels were run, 12 with each containing a medulloblastoma and an ependymoma sample, 4 with each containing a medulloblastoma and a supratentorial PNET sample, 1 with a medulloblastoma and an atypical teratoid/rhabdoid tumor sample, 1 with a medulloblastoma and an ependymoblastoma sample and 3 with each containing two medulloblastoma samples. The atypical teratoid/rhabdoid tumor sample was analyzed by 2D-DIGE, but was not included in the analyses. As the amount of tumor tissue was limited, cerebellar tissue from 7 adult non-tumor patients was pooled and this tissue was loaded on each gel as an internal standard. Protein samples were covalently labeled with spectrally distinct, charge- and mass-matched fluorescent CyDyes, which are N-hydroxy succinimidyl ester derivatives of Cy2, Cy3 and Cy5. The internal standard was always labeled with Cy2 and tumor samples were randomly labeled with Cy3 or Cy5. A quantity of 50 µg of each protein sample was mixed with 400 pmol CyDye, vortexed, and incubated on ice for 30 minutes in the dark. The reaction was quenched by the addition of 1 µl of 10 mM lysine followed by incubation on ice for another 10 minutes. The Cy2, Cy3 and Cy5 labeled protein samples were mixed and adjusted to 240 µl with lysis buffer, followed by adding 240 µl rehydration buffer (8 M urea, 4% w/v CHAPS, 1% Pharmalytes pH 3-10 and 13 mM dithiothreitol) and 4.8 µl

of Pharmalytes pH 3-10. Immobiline DryStrip gels pH 4-7, 24 cm (Amersham Biosciences, Uppsala, Sweden) were rehydrated overnight in the dark in an Immobiline DryStrip reswelling tray (Amersham Biosciences, Uppsala, Sweden) in the protein sample – rehydration buffer mixture overlaid with DryStrip cover fluid (Amersham Biosciences, Uppsala, Sweden).

Isoelectric focusing was performed using a Multiphor II (Amersham Biosciences, Uppsala, Sweden) and carried out at 500 V for 1 hour, at 1500 V for 1 hour and at 3000 V for 20 hours at 20°C, 10 mA. Strips were equilibrated for 15 minutes in equilibration buffer (0.05 M Tris-HCl pH 8.8, 6M urea, 30% v/v glycerol, 1% sodium dodecylsulfate) containing 32.5 mM dithiothreitol, followed by 15 minutes in the same buffer containing 240 mM iodoacetamide. The equilibrated strips were loaded on 12.5% polyacrylamide gels poured between low fluorescent glass plates. Gels were run in the Ettan Dalt Six electrophoresis unit (Amersham Biosciences, Uppsala, Sweden) at 1 W /gel overnight at 10°C until the dye front migrated off the bottom of the gels.

Image acquisition and analysis

The gels were directly scanned between the glass plates at a resolution of 100 µm using a Typhoon 9410 imager (Amersham Biosciences, Uppsala, Sweden) at excitation wavelengths 488, 532 and 633 nm and emission wavelengths of 520, 580 and 670 nm specific for Cy2, Cy3 and Cy5, respectively. Before analysis, images were cropped to remove areas extraneous to the gel image using Image Quant 5.2 (Amersham Bioscences, Uppsala, Sweden).

Image analysis was performed using the DeCyder 5.0 software (Amersham Biosciences, Uppsala, Sweden). The ratio between protein abundance in tumor samples and the internal standard for corresponding spots was calculated using the DIA (Differential in-gel analysis) module. Using the DeCyder BVA (Biological Variance analysis) module, Cy2 internal standard images were matched and normalized to correct for gel-to-gel variation, followed by statistical analysis (Student's t-test) of the abundance ratios of protein spots between samples. The number of protein spots for each co-detection procedure was estimated on 2500 per gel.

Protein identification

Two separate preparative gels were run containing respectively, a pool of 9 PNET tissue samples and 6 ependymoma tissue samples to identify proteins from the protein spots in each of the subgroups analyzed. Each of the samples included in the pools were shown to contain the spots of interest on the 2D images. A quantity of 50 µg of protein was labeled with CyDye as described above and 1400 µg of unlabeled protein from the same sample was added for identification purposes. The gels were fixed and stained with Coomassie Phastgel Blue R (Amersham Biosciences, Uppsala, Sweden). Protein spots were manually excised, destained at 4°C by washing twice for one hour with 50 mM NH_4HCO_3-acetonitrile (1:1, v/v) followed by a double-distilled H_2O wash and another two washes with 50 mM NH_4HCO_3-acetonitrile (1:1, v/v). The gel pieces were shrunk in 100% acetonitrile for 5

minutes and subsequently air-dried. A quantity of 15 µl of 0.01 µg/µl trypsin gold (Promega Benelux, Leiden, the Netherlands) in 0.1 mM HCl and 45 mM NH_4HCO_3 was added and the gel pieces were incubated overnight at 37°C. Peptides were extracted by adding 50 µl of 0.5% formic acid solution in 30% acetronitril, followed by 2 minutes of sonication in an ultrasonic bath and incubation for 30 minutes at room temperature. After the extraction steps were repeated, the supernatants were pooled and dried in a SpeedVac. Peptides were resuspended in 10 µl of saturated α-cyano 4-hydroxycinnamic acid in 50 % acetonitrile- 0.1 % TFA, and 1.5 µl of peptide mixture was spotted on a matrix-assisted laser desorption ionization (MALDI) target plate (660/384 anchor chip with transponder plate; Bruker Daltonics GmbH, Bremen, Germany). MALDI-time of flight (TOF) and tandem mass spectrometry (MS/MS) was performed on an Ultraflex I MALDI TOF/TOF mass spectrometer (Bruker Daltonics GmbH, Bremen, Germany) in the positive ion reflectron mode. Multiple laser shots (>1000) were averaged to generate the mass spectra. External calibration was performed using the ProteoMass peptide MALDI-MS calibration mix (Sigma Aldrich, Zwijndrecht, the Netherlands) after every 4 measured spots. Peptide peak lists were generated in Flex Analysis 2.4 (Bruker Daltonics GmbH, Bremen, Germany). Trypsin autolytic peptides were used to internally calibrate each mass spectrum. Searches with MS and MS/MS data were performed using MASCOT software (www.matrixscience.com) using a mass tolerance for the monoisotopic peptide window of 50 ppm, a MS/MS tolerance of 0.5 Da and allowing 1 trypsin miscleavage and carbamidomethyl global modifications and methionine sulfoxide variable modifications. Matches were defined as having a significant MOWSE score (p-value<0.05) within MASCOT software.

Immunohistochemistry

Formalin-fixed, paraffin embedded tissue of PNETs, ependymomas, control cerebella, cortex, white matter, normal ependyma and plexus choroideus were sectioned at 4-µm thickness and stained with hematoxylin and eosin for histological examination. Sections were deparaffinized and rehydrated through a graded series of xylene-ethanol and incubated for 30 minutes in 3% hydrogen peroxide in PBS to inhibit endogenous peroxidases. Antigen retrieval was performed by boiling the slides for 15 minutes in 0.01 mol/L citric acid (pH 6.0). Three percent horse serum or 3% goat serum (Vector Laboratories, Burlingame, CA) in PBS was used as a protein block for, respectively, the monoclonal antibodies against calcyphosine (Abnova, Taipei City, Taiwan) and annexin A-I (BD Biosciences, Alphen aan den Rijn, The Netherlands) and the polyclonal antibody against stathmin (Cell Signaling, Danvers, MA). Tissue sections were incubated with the primary antibody (calcyphosine, 1:50 dilution in 1% horse serum; annexin A1, 1:400 dilution in 1% horse serum; stathmin, 1:100 dilution in 1% goat serum) at 4°C overnight. The sections were then incubated with biotinylated horse anti-mouse IgG (Vector Laboratories, Burlingame, USA) for the monoclonal antibodies and biotinylated goat anti-rabbit IgG (Vector Laboratories, Burlingame, USA) for the polyclonal

antibody at a dilution of 1:1000 in PBS for 1 hour at room temperature. This was followed by 1-hour incubation with avidin-biotin peroxidase complex (dilution 1:400; Vectastain ABC kit, Vector Laboratories, Burlingame, USA). Staining was performed using 0.5 mg/ml 3,3' diaminobenzidine and 0.03% (v/v) hydrogen peroxide in 30 mM imidazole-1 mM EDTA (pH 7.0). Tissue sections were slightly counterstained with hematoxylin, dehydrated and mounted. As negative control, the primary antibodies were omitted.

Microarray Analysis

Total RNA was isolated by homogenizing tissue samples in TRizol reagent (Invitrogen, Breda, the Netherlands) using a tissue homogenizer (B. Braun, Spangenberg, Germany). RNA was isolated according to the manufacturer's protocol with minor modifications[10]**.** RNA integrity was checked using the Agilent 2100 Bioanalyzer (Agilent, Santa Clara, CA). Production of biotinylated antisense cRNA and hybridization of the labeled cRNA to HGU 133 plus 2.0 GeneChip oligonucleotide microarrays (Affymetrix, Santa Clara, CA) was performed according to manufacturer's protocols. Expression data were analyzed using R version 2.2.1. Raw data were vsn normalized and groups were statistically compared using the Wilcoxon test.

RESULTS

Two-Dimensional-Fluorescence Difference Gel Electrophoresis Analysis

2D-DIGE was used to compare protein expression profiles of pediatric PNETs and pediatric ependymomas. Figure 1A shows an example of an overlay image of the protein expression profiles of a newly diagnosed ependymoma and a newly diagnosed PNET run on the same gel and labeled with Cy3 and Cy5, respectively. Figure 1B and C show the separate gel images of the newly diagnosed PNET and ependymoma from figure 1A. An average of 2360 protein spots were detected per gel. On average, 57% of these spots were matched across all 21 gels and used for statistical analysis. 79 spots were found to be statistically different between the 29 PNET and 12 ependymoma tissue samples using the criteria of $p < 0.01$ and > 2-fold difference (up or down) in protein expression.

Identification of Differentially Expressed Proteins

To identify proteins, 2 separate 2D-DIGE gels each containing 1450 µg of a pool of PNET tissue or ependymoma tissue were run and post stained with Coomassie blue. Seven of the 79 differentially expressed spots from the statistical analysis could be identified by (tandem) mass spectrometry. In total, 93 visible spots were cut from the 2 gels and analyzed by MS/MS, resulting in the identification of 70 other proteins that were not differentially expressed (Table 1).

Table 1. Proteins identified by (tandem) mass spectrometry in ependymoma (figure 1B) and PNET (Figure 1C) tissue.

[1] Student's t-test p-value for the comparison of protein expression levels of PNETs and ependymomas
[2] Fold change in protein expression between PNET and ependymoma tissue
[3] Wilcoxon t-test p-value for the comparison of mRNA expression levels of PNETs and ependymomas
[4] Fold change in mRNA expression between PNET and ependymoma tissue
[5] Spearman correlation coefficient (R_s) of the correlation between protein and mRNA expression
[6] p-value of Spearman correlation coefficient
Acc no. Accession number according Swiss-Prot
MS Mascot score
% C Sequence coverage
MW Molecular weight
NP Number of peptides sequenced
PNET Primitive neuroectodermal tumor
2D-DIGE 2-dimensional fluorescence difference gel electrophoresis

		2D-DIGE								Microarray			
Protein spot nr.	**Name**	**Acc No.**	**MS**	**% C**	**Predicted MW (Da)**	**pI**	**NP**	**p-value; t-test[1]**	**Fold change P/E[2]**	**Wilcoxon p-value[3]**	**Fold change P/E[4]**	**R_s protein – mRNA[5]**	**p-value R_s [6]**
1	**Stathmin 1 (Phosphoprotein p19)**	**P16949**	**123**	**43**	**17292**	**5.76**	**4**	**0.0014**	**2.64**	**$9.47x10^{-5}$**	**4.13**	**0.72**	**<0.0010**
2	**Nuclear transport factor 2**	**P61970**	**62**	**62**	**14640**	**5.10**	**2**	**0.00069**	**2.29**	**0.036**	**0.82**	**-0.0090**	**0.96**
3	SET translocation (myeloid leukemia associated)	Q01105	69	27	31114	4.09	6	0.027	2.22	0.049	1.53	0.031	0.85
4	**Stathmin 1 (Phosphoprotein p19)**	**P16949**	**108**	**49**	**17292**	**5.76**	**2**	**0.0015**	**2.18**	**$9.47x10^{-5}$**	**4.13**	**0.54**	**<0.0010**
5	NM23 – H1	P15531	143	86	17309	5.83	8	0.00022	1.95	0.0017	1.75	0.70	<0.0010
6	Tubulin beta	Q9H4B7	178	53	50240	4.75	1	0.26	1.75	0.0035	2.62	0.054	0.74
7	Ubiquitin conjugating enzyme E2N	P61088	124	77	17184	6.13	4	$3.20x10^{-5}$	1.72	0.071	1.34	0.47	0.0020

		2D-DIGE								Microarray			
Protein spot nr.	**Name**	**Acc No.**	**MS**	**% C**	**Predicted MW (Da)**	**pI**	**NP**	**p-value; t-test[1]**	**Fold change P/E[2]**	**Wilcoxon p-value[3]**	**Fold change P/E[4]**	**R_s protein – mRNA[5]**	**p-value R_s [6]**
8	Hepatoma-derived growth factor	P51858	158	45	26886	4.70	0	0.051	1.70	0.68	1.22	-0.16	0.35
9	Chromobox protein homolog 1	P83916	49	40	21519	4.85	0	0.0027	1.70	0.0028	2.53	-0.22	0.18
10	Stathmin 1 (Phosphoprotein p19)	P16949	61	33	17292	5.76	3	$2.00x10^{-5}$	1.69	$9.47x10^{-5}$	4.13	0.72	<0.0010
11	Phosphoglycerate mutase I	P18669	165	63	28769	6.75	6	0.039	1.68	0.97	1.02	-0.018	0.92
12	Beta-2 microglobulin	P61769	32	46	11592	6.46	3	0.27	1.63	0.36	0.98	0.12	0.48
13	Synuclein alpha	P37840	36	27	14451	4.67	2	0.55	1.58	0.46	1.05	0.27	0.097
	Myosin regulatory light chain 2	Q6IB42	48	30	19707	4.67	4	0.55	1.58	0.81	0.99	0.022	0.89
	H^+ - transporting two sector ATPase, beta chain precursor	P06576	173	66	56525	5.26	8	0.55	1.58	0.039	1.68	0.43	0.0060
14	Actin beta	P60709	121	58	40536	5.55	10	0.020	1.55	0.45	1.03	0.086	0.60
15	Hemoglobin beta chain	P68871	116	80	11496	6.17	5	0.054	1.54	0.64	1.00	-0.051	0.76
16	Peroxiredoxin 2	P32119	99	36	21918	5.67	5	0.097	1.54	0.24	1.16	0.33	0.040
17	Peroxiredoxin 2	P32119	77	37	21918	5.67	7	0.13	1.50	0.24	1.16	0.25	0.13
18	Calbindin 3	P29377	84	46	30160	4.70	7	0.57	1.48	0.90	0.98	0.059	0.72
19	Superoxide dismutase 1	P00441	71	59	16154	5.70	6	0.020	1.46	0.55	1.08	0.068	0.68
20	Transthyretin precursor	P02766	114	68	15991	5.52	7	0.011	1.45	0.019	1.40	0.43	0.0060
21	ATP synthase, H^+ transporting, mitochondrial F1 complex, beta subunit	P06576	74	47	18405	5.22	1	0.012	1.43	0.039	1.68	0.32	0.047
22	14-3-3 protein gamma	P61981	122	56	28325	4.80	1	0.00082	1.42	0.00030	2.35	0.47	0.0020

			2D-DIGE							Microarray			
Protein spot nr.	**Name**	**Acc No.**	**MS**	**% C**	**Predicted MW (Da)**	**pI**	**NP**	**p-value; t-test[1]**	**Fold change P/E[2]**	**Wilcoxon p-value[3]**	**Fold change P/E[4]**	**R_s protein – mRNA[5]**	**p-value R_s [6]**
	14-3-3 protein theta	P27348	131	45	28032	4.68	1	0.00082	1.42	0.030	1.57	0.38	0.018
23	14-3-3 protein gamma	P61981	132	54	28325	4.80	5	0.012	1.39	0.00030	2.35	0.47	0.0020
24	Peroxiredoxin 2	P32119	69	43	21918	5.67	5	0.28	1.33	0.24	1.16	0.20	0.24
25	ATP synthase, H^+ transporting, mitochondrial F1 complex, beta subunit	P06576	81	53	18405	5.22	6	0.15	1.32	0.039	1.68	0.16	0.32
26	Rho GDP dissociation inhibitor alpha	P52565	74	29	23250	5.02	8	0.082	1.28	0.85	0.93	0.0030	0.98
27	Superoxide dismutatase I	P00441	61	53	16154	5.70	7	0.20	1.28	0.55	1.08	-0.0010	1.00
28	Rho GDP dissociation inhibitor alpha	P52565	74	43	20571	6.73	8	0.21	1.27	0.85	0.93	0.094	0.57
29	Tropomyosin 3	P06753	124	38	27386	4.77	0	0.26	1.26	0.0051	1.48	-0.25	0.13
30	Fatty acid binding protein 5	Q01469	111	58	15295	6.54	0	0.045	1.25	0.36	1.64	0.13	0.43
31	Protein disulfide isomerase precursor	P07237	130	40	57480	4.76	1	0.20	1.25	0.37	0.55	-0.070	0.67
32	Inorganic pyrophosphatase	Q15181	155	65	33095	5.54	1	0.51	1.22	0.019	1.62	0.27	0.10
33	14-3-3 protein zeta	P63104	106	60	27899	4.73	6	0.079	1.21	0.014	1.69	0.034	0.84
34	Septin 2	Q15019	139	58	41689	6.15	10	0.38	1.21	0.55	1.02	-0.049	0.77
35	Endoplasmic reticulum lumenal protein 28	Q3YAI4	75	36	29032	6.77	2	0.13	1.19	0.025	1.50	0.11	0.49
	6-phosphogluconolactonase	O95336	80	44	27815	5.70	3	0.13	1.19	0.034	0.85	-0.052	0.75
36	Peroxiredoxin 3	P30048	49	38	28017	7.67	10	0.16	1.18	0.55	0.86	0.33	0.041
37	Reticulocalbin 1 precursor	Q15293	110	37	38866	4.86	2	0.60	1.17	0.027	0.44	0.14	0.41

		2D-DIGE								Microarray			
Protein spot nr.	**Name**	**Acc No.**	**MS**	**% C**	**Predicted MW (Da)**	**pI**	**NP**	**p-value; t-test[1]**	**Fold change P/E[2]**	**Wilcoxon p-value[3]**	**Fold change P/E[4]**	**R_s protein – mRNA[5]**	**p-value R_s [6]**
	Vimentin	P08670	83	39	35089	4.70	0	0.60	1.17	0.0019	0.09	0.18	0.27
38	Hemoglobin beta chain	P68871	103	84	15866	6.70	1	0.82	1.14	0.64	1.00	0.030	0.86
39	Fibrinogen beta chain precursor	P02675	159	60	36331	7.66	0	0.26	1.13	1.00	1.00	-0.031	0.85
	Fructose-bisphosphate aldolase C	P09972	51	44	39699	6.46	0	0.26	1.13	0.0069	0.16	0.027	0.87
40	Thioredoxin	P10599	69	62	12015	4.82	6	0.82	1.13	0.37	1.25	0.39	0.015
41	Ubiquitin carboxyl-terminal hydrolase isozyme L1	P09936	98	57	23840	5.43	7	0.33	1.11	0.99	1.01	0.28	0.084
42	Glutathione S-transferase, MU-2	P28161	119	57	23569	5.43	9	0.71	1.10	0.0028	0.46	-0.36	0.023
43	Tumor protein, translationally controlled	P13693	62	39	21626	5.34	2	0.91	1.09	0.57	0.90	0.099	0.55
44	Heat-shock 90 kD protein I	P07900	220	40	84889	4.94	2	0.57	1.09	0.30	0.80	0.0060	0.97
45	Apolipoprotein A-I	P02647	144	64	28061	5.27	2	0.72	1.09	0.29	0.94	0.0030	0.98
46	Apolipoprotein A-I	P02647	218	69	28061	5.27	0	0.21	1.08	0.29	0.94	0.11	0.51
47	DJ protein 1	Q99497	62	34	20063	6.33	5	0.70	1.07	0.22	0.83	-0.075	0.65
48	Glial fibrillary acidic protein	P14136	131	46	49907	5.42	2	0.65	1.07	5.48×10^{-5}	0.020	-0.24	0.14
49	Tropomodulin 2	Q9NZR1	61	28	34502	6.41	0	0.98	1.03	0.53	1.25	-0.086	0.60
50	Protein phosphatase I, regulatory subunit 1B	Q9UD71	87	87	23063	4.48	8	0.76	1.00	3.24×10^{-7}	0.01	-0.43	0.0060
51	Apolipoprotein A-I fragment	P02647	134	58	28944	5.45	0	0.85	0.99	0.29	0.94	-0.063	0.70
52	Serum albumin	P02768	223	48	67931	5.69	4	0.92	0.99	0.87	0.96	-0.18	0.28

		2D-DIGE							Microarray			
Protein spot nr.	**Name**	**Acc No.**	**MS**	**% C**	**Predicted MW (Da)**	**pI**	**NP**	**p-value; t-test[1]**	**Fold change P/E[2]**	**Wilcoxon p-value[3]**	**Fold change P/E[4]**	**R_s protein – mRNA[5]**	**p-value R_s [6]**
53	T complex protein I, subunit beta	P78371	193	48	57663	6.02	3	0.74	0.98	0.00074	1.43	-0.21	0.21
54	Proteasome subunt alpha 1	P25786	115	60	29864	6.15	4	0.87	0.97	0.025	1.48	0.27	0.10
55	DJ protein 1	Q99497	67	54	20063	6.33	5	0.72	0.95	0.22	0.83	0.070	0.67
56	Recoverin	P35243	43	27	23099	5.06	2	0.65	0.93	0.29	0.90	0.30	0.068
57	Tumor rejection antigen (Gp96)	P14625	239	37	92567	4.77	7	0.33	0.93	0.41	0.93	0.089	0.59
58	L-Lactate dehydrogenase B chain	P07195	98	42	36769	5.72	1	0.28	0.91	0.90	0.89	-0.0050	0.97
	Guanine nucleotide-binding protein, beta-2	P62879	64	44	38048	5.60	1	0.28	0.91	0.00074	0.44	0.24	0.14
59	Vimentin	P08670	154	53	53454	5.06	5	0.71	0.88	0.0019	0.09	0.26	0.11
60	Ubiquitin carboxyl-terminal hydrolase isozyme L1	P09936	141	73	23840	5.43	8	0.48	0.87	0.99	1.01	0.29	0.071
61	Alpha enolase	P06733	122	46	47350	6.99	4	0.21	0.82	0.95	1.00	0.23	0.17
62	Cytochrome C oxidase subunit Va	P20674	67	48	16923	6.30	5	0.44	0.81	0.071	1.09	-0.099	0.55
63	Alpha enolase	P06733	75	27	47350	6.99	1	0.20	0.81	0.95	1.00	0.27	0.094
64	Tubulin beta	Q9H4B7	195	54	50240	4.75	5	0.24	0.80	0.0035	2.62	-0.10	0.54
65	Heterogeneous nuclear ribonucleoprotein H1	P31943	81	44	49352	5.89	1	0.046	0.76	0.19	1.07	-0.12	0.48
66	Acyl CoA binding protein	P07108	54	53	9907	6.11	3	0.028	0.75	0.0024	0.36	0.72	<0.0010
67	SH3 binding glutamate rich protein	O75368	85	71	12766	5.22	7	0.11	0.75	$1.66x10^{-5}$	0.42	0.36	0.024

		2D-DIGE								Microarray			
Protein spot nr.	**Name**	**Acc No.**	**MS**	**% C**	**Predicted MW (Da)**	**pI**	**NP**	**p-value; t-test[1]**	**Fold change P/E[2]**	**Wilcoxon p-value[3]**	**Fold change P/E[4]**	**R_s protein – mRNA[5]**	**p-value R_s [6]**
68	14-3-3 protein epsilon	P62258	221	69	26658	4.76	10	0.0095	0.72	0.00019	0.41	0.42	0.0070
69	Heterogeneous nuclear ribonucleoprotein H1	P31943	81	44	49352	5.89	1	0.11	0.70	0.19	1.07	0.72	<0.0010
70	Laminin receptor 1	P08865	126	49	32875	4.38	6	0.084	0.70	0.43	1.11	-0.097	0.56
71	Fibrinogen beta chain precursor	P02675	162	60	36331	7.66	0	0.60	0.69	1.00	1.00	-0.28	0.083
	Fructose-bisphosphate aldolase C	P09972	90	44	39699	6.46	0	0.60	0.69	0.0069	0.16	-0.16	0.33
72	Heat-shock 70 kD protein 5	Q5IST7	154	32	72185	5.03	0	0.0025	0.69	0.00030	0.38	0.53	0.0010
73	Inorganic pyrophosphatase	Q15181	114	57	33095	5.54	9	0.11	0.68	0.019	1.62	0.064	0.70
74	Fatty acid binding protein 7	O15540	71	58	14862	5.41	3	0.11	0.68	0.34	0.90	0.16	0.34
75	SH3 binding glutamate rich protein	O75368	79	58	12766	5.22	4	0.17	0.68	$1.66x10^{-5}$	0.42	0.34	0.034
76	Retinol binding protein 1	P09455	112	79	16011	4.99	4	0.13	0.62	0.030	0.16	0.46	0.0030
77	Annexin A1	P04083	69	41	38787	6.64	1	0.045	0.60	$1.34x10^{-5}$	0.020	0.65	<0.0010
	Glyceraldehyde-3-phosphate dehydrogenase	P04406	43	31	36201	8.57	1	0.045	0.60	0.50	0.79	-0.078	0.64
78	Synuclein gamma	O76070	64	53	13323	4.89	7	0.23	0.59	0.78	0.96	-0.21	0.197
79	Villin 2	P15311	124	32	69313	5.94	6	0.0015	0.58	0.50	1.02	0.28	0.090
80	Heat shock protein 27	P04792	183	63	22826	5.98	7	0.017	0.57	0.00098	0.36	0.25	0.12
81	Glutathione S-transferase MU-2	P28161	184	73	25768	6.02	2	0.0023	0.54	0.0028	0.46	0.55	<0.0010
82	NADH2 dehydrogenase	P03891	177	65	30337	6.99	5	0.0048	0.53	0.68	1.02	0.081	0.623

		2D-DIGE							Microarray			
Protein spot nr.	**Name**	**Acc No.**	**MS**	**% C**	**Predicted MW (Da)**	**pI**	**NP**	**p-value; t-test[1]**	**Fold change P/E[2]**	**Wilcoxon p-value[3]**	**Fold change P/E[4]**	**R_s protein – mRNA[5]**	**p-value R_s [6]**
83	Peroxiredoxin 6	P30041	191	66	25002	6.02	7	0.0037	0.52	0.00056	0.61	0.52	0.0010
84	Annexin V	P08758	227	60	35971	4.94	9	$5.70x10^{-5}$	0.52	$2.04x10^{-5}$	0.31	0.77	<0.0010
85	Annexin V	P08758	267	69	35971	4.94	0	$3.60x10^{-5}$	0.52	$2.04x10^{-5}$	0.31	0.80	<0.0010
86	Galectin 1	P09382	44	42	15048	5.34	1	0.077	0.52	0.48	0.99	0.25	0.13
	Cytochrome C oxidase subunit Va	P20674	66	52	16923	6.30	2	0.077	0.52	0.071	1.09	-0.099	0.55
87	Dimethylarginine dimethylaminohydrolase 1	O94760	92	45	31313	5.53	0	0.0061	0.52	$3.24x10^{-7}$	0.15	0.64	<0.0010
88	Phosphoprotein enriched in astrocytes 15	Q15121	68	41	15088	4.93	9	0.0087	0.51	$7.48x10^{-8}$	0.15	0.50	0.0010
89	**Peroxiredoxin 6**	**P30041**	**156**	**24**	**25002**	**6.02**	**3**	**0.00020**	**0.50**	**0.00056**	**0.61**	**0.34**	**0.033**
90	**Retinol binding protein 1**	**P09455**	**110**	**39**	**16011**	**4.99**	**4**	**0.0054**	**0.42**	**0.030**	**0.16**	**0.60**	**<0.0010**
91	**Annexin A1**	**P04083**	**94**	**44**	**38787**	**6.64**	**3**	**0.00015**	**0.40**	**$1.34x10^{-5}$**	**0.020**	**0.65**	**<0.0010**
92	**Dihydropyrimidinase related protein 2**	**Q14194**	**305**	**63**	**62711**	**5.95**	**2**	**$3.00x10^{-5}$**	**0.26**	**$3.07x10^{-5}$**	**0.20**	**0.63**	**<0.0010**
93	**Calcyphosine**	**Q13938**	**122**	**54**	**18422**	**4.68**	**8**	**$9.90x10^{-7}$**	**0.027**	**0.00041**	**0.040**	**0.50**	**0.0010**

Stathmin (2.6-fold higher expressed in PNETs than in ependymomas) (Figure 2A) and annexin AI and calcyphosine (respectively, 2.5- and 37.6-fold higher expressed in ependymomas than in PNETs (Figure 2B and C) were chosen for validation by immunohistochemistry. We identified stathmin from 3 differentially expressed protein spots (Figure 1C; spots 1, 4 and 10). Protein spot 1 corresponds to the unphosphorylated form of stathmin, whereas protein spots 4 and 10 correspond to 2 phosphorylated isoforms of stathmin[11].

Validation of Identified Tumor Markers by Immunohistochemistry

Immunohistochemistry confirmed the overexpression of stathmin in PNETs and the overexpression of annexin A1 and calcyphosine in ependymomas. Tumor cells of both supratentorial

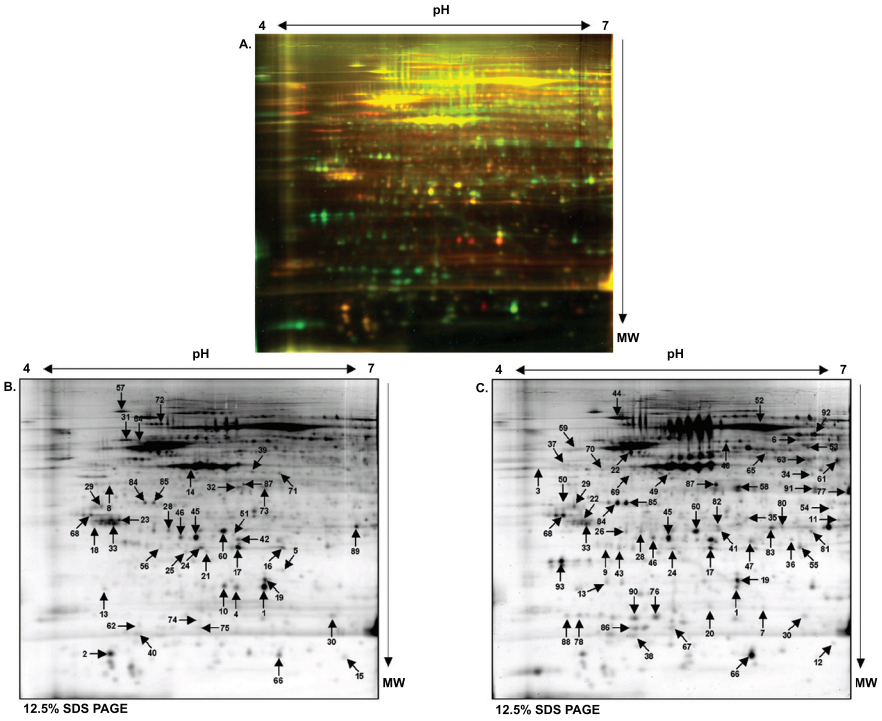

Figure 1. 2-dimensional (2D)-fluorescence difference gel electrophoresis gel images of ependymoma and PNET tissue.

Fifty micrograms of whole protein lysates of PNETs and ependymomas labeled with CyDyes were separated in the first dimension on pH 4-7 immobilized pH gradient strips and subsequently subjected to 12.5% sodium dodecyl sulfate-polyacrylamide gel electrophoresis(SDS-PAGE). (**A.**) A representative overlay image of ependymoma tissue labeled with Cy3 in green and PNET tissue labeled with Cy5 in red. (**B., C.**) Separate Cy3 (ependymoma) and Cy5 (PNET), respectively, 2D images. Proteins from the numbered spots were identified by mass spectrometry and correspond to the spot numbers in *Table 1*.

MW Molecular weight

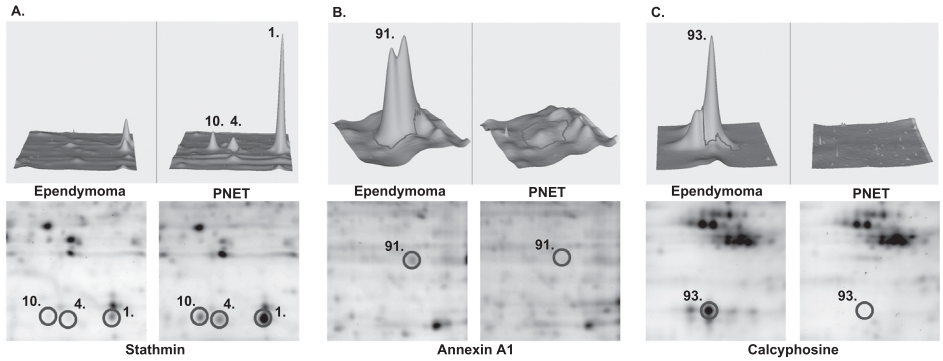

Figure 2. DeCyder output showing 3 of the identified differentially expressed proteins.
The selected spots, corresponding to stathmin, annexin A1 and calcyphosine are displayed as 3-dimensional images (top panel) and a partial view of the 2-dimensional gel (bottom panel). The unphosphorylated (spot 1) and phosphorylated (spot 4 and 10) isoforms of stathmin (**A.**) were overexpressed in primitive neuroectodermal tumor (PNET) tissue, whereas annexin A1 (spot 91) (**B.**) and calcyphosine (spot 93) (**C.**) were overexpressed in ependymomas.
Numbers correspond to the protein spot numbers in Table 1.

PNETs and medulloblastoma showed strong and diffuse cytoplasmic staining for stathmin (Figure 3A). In both cellular ependymoma and anaplastic ependymoma tumor cells only a weak cytoplasmic staining was observed, whereas endothelial cells were positively stained (Figure 3B). In cerebellum and cortex, weak cytoplasmic stathmin positivity was shown. Normal ependyma and plexus choroideus were negative for stathmin. As the stathmin antibody reacts with both the phosphorylated and unphosphorylated forms of stathmin, we could not determine the phosphorylation status of stathmin by immunohistochemistry.

All 17 ependymomas, both cellular ependymoma and anaplastic ependymoma, showed cytoplasmic and variable nuclear staining in tumor cells for annexin A1. Tumor cells of PNETs, except for 1 large cell medulloblastoma, were negative for annexin A1. In ependymomas, endothelial cells remained unstained, whereas in PNETs endothelial cells of blood vessels were positive for annexin A1 (Figure 3C and D). Endothelial cells in cerebellum, cortex, white matter and plexus choroideus were positive for annexin A1. Immunoreactivity of annexin A1 in normal ependymal cells was variable and weak compared to the strong staining observed in ependymoma.

Tumor tissue of 10 of 17 ependymomas (7 cellular ependymoma and 3 anaplastic ependymoma) showed strong cytoplasmic and nuclear positivity for calcyphosine (Figure 3E). Staining was most profound in ependymoma tissue with epithelial differentiation and did not correlate with histological grading. Ependymomas with predominantly glial differentiation, PNETs and control cerebellum, cortex, white matter and plexus choroideus did not show positivity for calcyphosine. Normal ependymal cells showed very weak calcyphosine positivity.

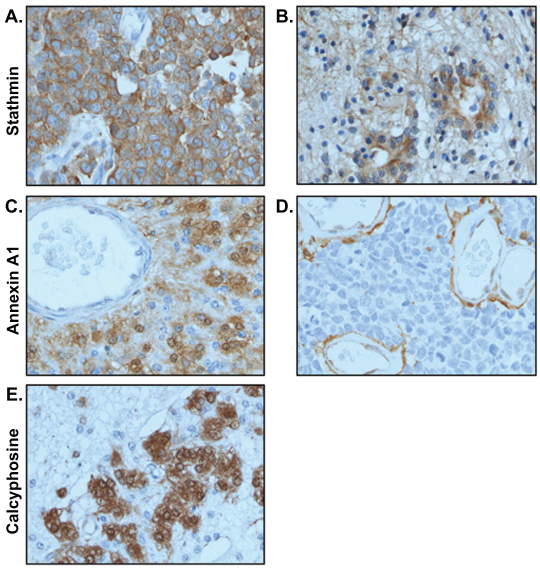

Figure 3. Immunohistochemistry of stathmin (A., B.), annexin A1 (C., D.) and calcyphosine (E.) on paraffin embedded primitive neuroectodermal (PNET) and ependymoma tissue.
Tumor cells of all PNETs showed strong diffuse cytoplasmic staining for stathmin (**A.**). In ependymoma tumor cells we observed weak cytoplasmic staining for stathmin, together with some positive staining of endothelial cells (**B.**). Tumor cells of all ependymomas showed cytoplasmic and variable nuclear staining for annexin A1. The endothelium of the tumor blood vessels remained negative (**C.**). PNET tumor cells did not show immunoreactivity for annexin A1. The endothelial cells of the tumor blood vessels stained positive for annexin A1 (**D.**). Ten of 17 ependymomas (7 ependymoma cellulare; 3 anaplastic ependymoma) showed strong tumor cell cytoplasmic and nuclear positivity for calcyphosine (**E.**). Staining was most profound in ependymoma tissue with epithelial differentiation. Ependymomas showing predominantly glial differentiation and PNETs and control cerebellum did not show positivity for calcyphosine (not shown).

Analysis of the Correlation Between mRNA and Protein Levels

mRNA expression levels of the identified proteins were analyzed by HGU133 plus 2.0 microarrays. Two hundred sixty-six probe sets on the Affymetrix HGU133 plus 2.0 arrays corresponded to the 77 identified proteins. Wilcoxon p-values for the comparison between PNETs and ependymomas of mRNA expression levels of the identified proteins are displayed in Table 1.

For 25 of the 77 identified proteins (32%) a statistically significant ($p<0.05$) correlation between mRNA and protein expression levels was observed (Table 1). For 6 of the 7 (86%) differentially expressed and identified proteins in PNET and ependymoma tissue, protein and mRNA levels were significantly correlated. For stathmin, annexin A1 and calcyphosine a positive correlation between mRNA expression levels and protein expression levels was found ($R_S=0.65$ ($p<0.0001$), $R_S=0.50$ ($p=0.001$) and $R_S=0.72$ ($p<0.0001$), respectively). In concordance with the protein expression levels, mRNA expression levels of stathmin,

annexin A1 and calcyphosine were significantly different between PNETs and ependymomas ($p=9.47x10^{-5}$ $p=1.34x10^{-5}$ and p=0.00041 respectively)(Figure 4). Calcyphosine mRNA levels were increased in the same ependymomas (~60%) as those that showed strong immunoreactivity for calcyphosine (Figure 4).

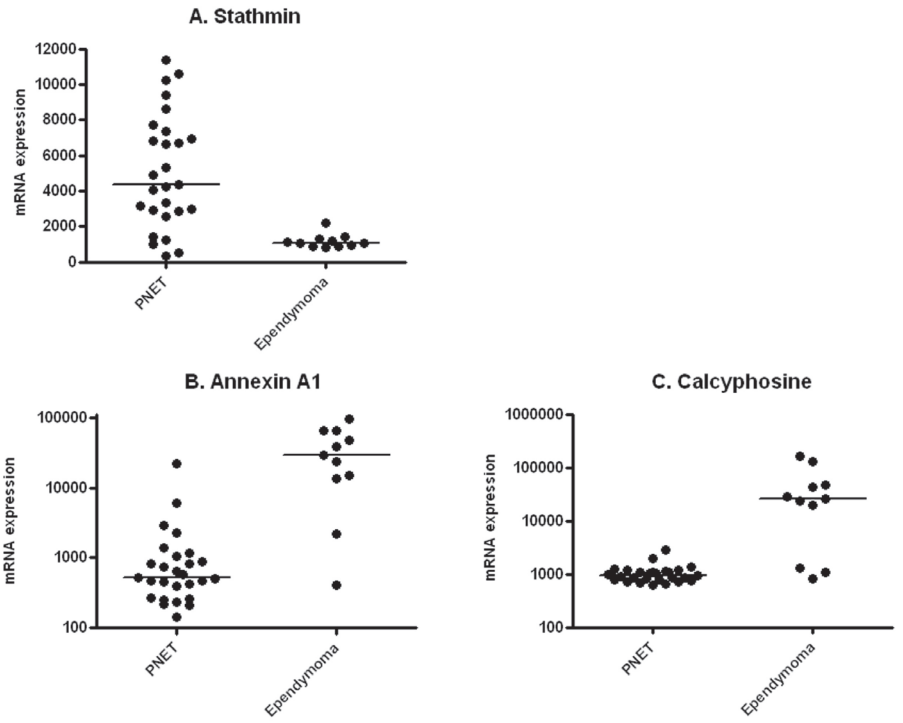

Figure 4. Representative mRNA expression levels of stathmin (200783_s_at STMN1) (A.), annexin A1 (201012_at ANXA1) (B.), calcyphosine (226424_at CAPS) (C.) in primitive neuroectodermal tumors (PNETs) and ependymomas obtained from Affymetrix HGU133 plus 2.0 microarrays.
Stathmin mRNA expression levels were significantly higher ($p=9.47x10^{-5}$) in PNET than in ependymoma tissue. Annexin A1 and calcyphosine mRNA expression levels were significantly increased in ependymomas compared to PNETs ($p=1.34x10^{-5}$ and p=0.00041, respectively, for annexin A1 anc calcyphosine). Other probesets present on the microarrays for these 3 proteins showed comparable expression patterns in the analyzed subgroups.
The lines represent the median value within each subgroup

DISCUSSION

In this study, protein expression profiles of PNETs and ependymomas were successfully compared using 2D-DIGE. Seventy-nine matched protein spots were found to be significantly different between PNET and ependymoma tissue. Seven of these spots proteins were

further characterized by MS/MS. The differential expression of stathmin, annexin A1 and calcyphosine was confirmed by immunohistochemistry at the protein level and by microarray analysis at the mRNA level.

For all identified proteins in our study, mRNA expression levels were analyzed by microarray. Interestingly, in only 32% of the identified proteins mRNA and protein expression levels were significantly correlated (Table 1). A lack of correlation between mRNA and protein expression levels in 68% of the proteins may be caused by the instability of mRNA or protein, high turn-over of protein, or translational repression by microRNAs[12].

Our study shows overexpression of stathmin in PNETs compared with ependymomas. Stathmin belongs to a family of phosphoproteins that is involved in microtubule dynamics. Phosphorylation of stathmin, e.g. during mitosis, impedes the depolymerization of microtubules and promotes their polymerization[13, 14]. The overexpression of both the unphosphorylated and the phosphorylated isoforms of stathmin in PNETs in our study might thus be indicative of a high mitotic rate in these tumors. External signals, such as growth factors[15], are known to promote the phosphorylation of stathmin.

Overexpression of stathmin has been reported in various types of malignancies[8, 16-22]. In several of these malignancies, (e.g. medulloblastoma[21]), a significant correlation between stathmin overexpression and prognostically unfavorable clinicopathologic parameters has been observed. Stathmin expression has been correlated to the sensitivity of cancer cells to cytostatic drugs that affect microtubule dynamics, such as taxanes and vinca alkaloids[23, 24]. A decrease in stathmin expression is thought to result in increased drug resistance to vinca alkaloids as the effects of the microtubule-destabilizing vinca alkaloids are counteracted. Stathmin expression might thus be an important feature to identify patients who are sensitive to vincristine and possibly other drugs like taxanes. Further research is ongoing to investigate the relationship between stathmin, drug sensitivity of PNETs and clinical outcome.

Protein expression levels of annexin A1 were high in ependymomas compared to those in PNETs. Annexin A1 belongs to a family of structurally related proteins that can bind negatively charged phospholipids in a Ca^{2+} dependent manner[25]. Annexin A1 is expressed in a wide range of normal organs and tissues, including neurons and ependymocytes[26-28]. Annexin A1 is involved in various biological processes such as the anti-inflammatory actions of glucocorticoids by inhibiting phospholipase A_2[29], the control of cell growth[30] and apoptosis[31]. Several malignant tumors of the central and peripheral nervous system (e.g. adult glioblastoma) have shown to be positive for annexin A1[28], which is in concordance with the high expression of annexin A1 in pediatric ependymomas in the present study. Immunohistochemistry of ependymomas in our study showed both cytoplasmic and nuclear annexin A1 staining. This may suggest a differentiation process as butyrate-induced differentiation of human colon adenocarcinoma not only induced annexin A1 expression, but also resulted in a subcellular redistribution of annexin A1 from the cytoplasm to perinuclear regions[32]. Annexin A1 is selectively overexpressed in the neovascular endothelium of multiple human solid tumors

and absent in the endothelium of normal tissues[33]. In our study we observed endothelial cells of ependymoma to be annexin A1 negative, whereas those in PNETs were positive, suggesting the expression of annexin A1 to be tissue/localization dependent. Tissue dependency may also explain why certain malignant tumors (e.g. breast[34], liver[35], stomach[36] and brain[28]) overexpress annexin A1, whereas others (e.g. prostate carcinoma[37], esophageal squamous cell carcinoma[38], nasopharyngeal carcinoma[39] and B cell lymphoma[40]) express low levels of annexin A1. Targeting annexin A1 with ^{125}I annexin A1 antibodies destroys solid tumors and results in improved animal survival with radioimmunotherapy[33], making it a potentially interesting therapeutic target.

A second protein marker that we found overexpressed in ependymomas is calcyphosine. Calcyphosine belongs to the calmodulin superfamily of calcium-binding proteins and is regulated by cyclic AMP through protein phosphorylation[41]. Interestingly, both annexin A1 and calcyphosine are calcium-binding proteins. However, there is no evidence thus far that annexin A1 and calcyphosine are involved in similar signal transduction pathways. Calcyphosine is detected in various cells of the central nervous system, such as ependymal cells and astrocytes[42]. In consistency with these findings, we observed variable immunoreactivity of normal ependymal cells for calcyphosine. However, this staining was far less intense than the positivity we observed in ependymomas. Interestingly, high calcyphosine protein and mRNA expression levels were detected in only 10 of the 17 ependymomas. Calcyphosine positivity was not related to histological grading or localization of the ependymomas, but was predominantly shown in tumors with epithelial differentiation. Calcyphosine may thus be a marker of a new subgroup of ependymomas.

CONCLUSION

In our study we successfully identified tumor biomarkers for pediatric PNETs and ependymomas using 2D-DIGE combined with MS/MS. Stathmin was significantly overexpressed in PNETs, whereas annexin A1 and calcyphosine were significantly overexpressed in ependymomas. Aberrant expression of these proteins was confirmed by immunohistochemistry. Protein expression levels of stathmin, annexin A1 and calcyphosine were significantly correlated with mRNA expression levels. Ongoing studies are focused on characterizing the biological importance of stathmin, annexin A1 and calcyphosine in the pathogenesis and biological behavior of pediatric PNETs and ependymomas.

REFERENCES

1. Kleihues P, Louis DN, Scheithauer BW, et al. The WHO classification of tumors of the nervous system. J Neuropathol Exp Neurol 2002;61(3):215-225; discussion 226-219.
2. MacDonald TJ, Rood BR, Santi MR, et al. Advances in the diagnosis, molecular genetics, and treatment of pediatric embryonal CNS tumors. Oncologist 2003;8(2):174-186.
3. Packer RJ. Brain tumors in children. Arch Neurol. 1999;56(4):421-425.
4. Kieran MW. Advances in pediatric neuro-oncology. Curr Opin Neurol. 2000;13(6):627-634.
5. Inda MM, Perot C, Guillaud-Bataille M, et al. Genetic heterogeneity in supratentorial and infratentorial primitive neuroectodermal tumours of the central nervous system. Histopathology 2005;47(6):631-637.
6. Merchant TE, Fouladi M. Ependymoma: new therapeutic approaches including radiation and chemotherapy. J Neurooncol. 2005;75(3):287-299.
7. Marouga R, David S, Hawkins E. The development of the DIGE system: 2D fluorescence difference gel analysis technology. Anal Bioanal Chem 2005;382(3):669-678.
8. Nakashima D, Uzawa K, Kasamatsu A, et al. Protein expression profiling identifies maspin and stathmin as potential biomarkers of adenoid cystic carcinoma of the salivary glands. Int J Cancer 2006;118(3):704-713.
9. Friedman DB, Hill S, Keller JW, et al. Proteome analysis of human colon cancer by two-dimensional difference gel electrophoresis and mass spectrometry. Proteomics 2004;4(3):793-811.
10. Stam RW, den Boer ML, Meijerink JP, et al. Differential mRNA expression of Ara-C-metabolizing enzymes explains Ara-C sensitivity in MLL gene-rearranged infant acute lymphoblastic leukemia. Blood 2003;101(4):1270-1276.
11. Beretta L, Dobransky T, Sobel A. Multiple phosphorylation of stathmin. Identification of four sites phosphorylated in intact cells and in vitro by cyclic AMP-dependent protein kinase and p34cdc2. J Biol Chem 1993;268(27):20076-20084.
12. Bartell DP. MicroRNAs: genomics, biogenesis, mechanism, and function. Cell 2004;116(2):281-297.
13. Curmi PA, Gavet O, Charbaut E, et al. Stathmin and its phosphoprotein family: general properties, biochemical and functional interaction with tubulin. Cell Struct Funct. 1999;24(5):345-357.
14. Melander Gradin H, Marklund U, Larsson N, Chatila TA, Gullberg M. Regulation of microtubule dynamics by Ca2+/calmodulin-dependent kinase IV/Gr-dependent phosphorylation of oncoprotein 18. Mol Cell Biol. 1997;17(6):3459-3467.
15. Doye V, Boutterin MC, Sobel A. Phosphorylation of stathmin and other proteins related to nerve growth factor-induced regulation of PC12 cells. J Biol Chem. 1990;265(20):11650-11655.
16. Brattsand G. Correlation of oncoprotein 18/stathmin expression in human breast cancer with established prognostic factors. Br J Cancer 2000;83(3):311-318.
17. Melhem R, Hailat N, Kuick R, Hanash SM. Quantitative analysis of Op18 phosphorylation in childhood acute leukemia. Leukemia 1997;11(10):1690-1695.
18. Friedrich B, Gronberg H, Landstrom M, Gullberg M, Bergh A. Differentiation-stage specific expression of oncoprotein 18 in human and rat prostatic adenocarcinoma. Prostate 1995;27(2):102-109.
19. Chen G, Wang H, Gharib TG, et al. Overexpression of oncoprotein 18 correlates with poor differentiation in lung adenocarcinomas. Mol Cell Proteomics 2003;2(2):107-116.
20. Kouzu Y, Uzawa K, Koike H, et al. Overexpression of stathmin in oral squamous-cell carcinoma: correlation with tumour progression and poor prognosis. Br J Cancer. 2006;94(5):717-723.
21. Neben K, Korshunov A, Benner A, et al. Microarray-based screening for molecular markers in medulloblastoma revealed STK15 as independent predictor for survival. Cancer Res 2004;64(9):3103-3111.
22. Takahashi M, Yang XJ, Lavery TT, et al. Gene expression profiling of favorable histology Wilms tumors and its correlation with clinical features. Cancer Res 2002;62(22):6598-6605.

23. Verrills NM, Liem NL, Liaw TY, et al. Proteomic analysis reveals a novel role for the actin cytoskeleton in vincristine resistant childhood leukemia--an in vivo study. Proteomics 2006;6(5):1681-1694.
24. Alli E, Bash-Babula J, Yang JM, Hait WN. Effect of stathmin on the sensitivity to antimicrotubule drugs in human breast cancer. Cancer Res 2002;62(23):6864-6869.
25. Gerke V, Moss SE. Annexins: from structure to function. Physiol Rev 2002;82(2):331-371.
26. Dreier R, Schmid KW, Gerke V, Riehemann K. Differential expression of annexins I, II and IV in human tissues: an immunohistochemical study. Histochem Cell Biol 1998;110(2):137-148.
27. Eberhard DA, Brown MD, VandenBerg SR. Alterations of annexin expression in pathological neuronal and glial reactions. Immunohistochemical localization of annexins I, II (p36 and p11 subunits), IV, and VI in the human hippocampus. Am J Pathol 1994;145(3):640-649.
28. Johnson MD, Kamso-Pratt J, Pepinsky RB, Whetsell WO, Jr. Lipocortin-1 immunoreactivity in central and peripheral nervous system glial tumors. Hum Pathol 1989;20(8):772-776.
29. Wallner BP, Mattaliano RJ, Hession C, et al. Cloning and expression of human lipocortin, a phospholipase A2 inhibitor with potential anti-inflammatory activity. Nature 1986;320(6057):77-81.
30. Croxtall JD, Flower RJ. Lipocortin 1 mediates dexamethasone-induced growth arrest of the A549 lung adenocarcinoma cell line. Proc Natl Acad Sci U S A 1992;89(8):3571-3575.
31. Solito E, de Coupade C, Canaider S, Goulding NJ, Perretti M. Transfection of annexin 1 in monocytic cells produces a high degree of spontaneous and stimulated apoptosis associated with caspase-3 activation. Br J Pharmacol 2001;133(2):217-228.
32. Guzman-Aranguez A, Olmo N, Turnay J, et al. Differentiation of human colon adenocarcinoma cells alters the expression and intracellular localization of annexins A1, A2, and A5. J Cell Biochem 2005;94(1):178-193.
33. Oh P, Li Y, Yu J, et al. Subtractive proteomic mapping of the endothelial surface in lung and solid tumours for tissue-specific therapy. Nature 2004;429(6992):629-635.
34. Ahn SH, Sawada H, Ro JY, Nicolson GL. Differential expression of annexin I in human mammary ductal epithelial cells in normal and benign and malignant breast tissues. Clin Exp Metastasis 1997;15(2):151-156.
35. Masaki T, Tokuda M, Ohnishi M, et al. Enhanced expression of the protein kinase substrate annexin in human hepatocellular carcinoma. Hepatology 1996;24(1):72-81.
36. Sinha P, Hutter G, Kottgen E, et al. Increased expression of annexin I and thioredoxin detected by two-dimensional gel electrophoresis of drug resistant human stomach cancer cells. J Biochem Biophys Methods 1998;37(3):105-116.
37. Kang JS, Calvo BF, Maygarden SJ, et al. Dysregulation of annexin I protein expression in high-grade prostatic intraepithelial neoplasia and prostate cancer. Clin Cancer Res 2002;8(1):117-123.
38. Xia SH, Hu LP, Hu H, et al. Three isoforms of annexin I are preferentially expressed in normal esophageal epithelia but down-regulated in esophageal squamous cell carcinomas. Oncogene 2002;21(43):6641-6648.
39. Rodrigo JP, Garcia-Pedrero JM, Fernandez MP, et al. Annexin A1 expression in nasopharyngeal carcinoma correlates with squamous differentiation. Am J Rhinol 2005;19(5):483-487.
40. Vishwanatha JK, Salazar E, Gopalakrishnan VK. Absence of annexin I expression in B-cell non-Hodgkin's lymphomas and cell lines. BMC Cancer 2004;4:8.
41. Kretsinger RH. Crystallographic studies of calmodulin and homologs. Ann N Y Acad Sci. 1980;356:14-19.
42. Halleux P, Schurmans S, Schiffman SN, et al. Calcium binding protein calcyphosine in dog central astrocytes and ependymal cells and in peripheral neurons. J Chem Neuroanat. 1998;15(4):239-250.

Chapter 5

Identification of Apolipoprotein A-II in Cerebrospinal Fluid of Pediatric Brain Tumor Patients by Protein Expression Profiling

Judith M. de Bont[1], Monique L. den Boer[1], Roel E. Reddingius[1], Jaap Jansen[2], Monique Passier[1], Ron H. N. van Schaik[3], Johan M. Kros[4], Peter A. E. Sillevis Smitt[5], Theo H. Luider[5], Rob Pieters[1]

[1]Erasmus MC – Sophia Children's Hospital - University Medical Center Rotterdam – Department of Pediatric Oncology and Hematology, The Netherlands
[2]Ciphergen Biosystems Inc, Fremont, United States
[3]Erasmus MC – University Medical Center Rotterdam – Department of Clinical Chemistry, The Netherlands
[4]Erasmus MC – University Medical Center Rotterdam – Department of Pathology, The Netherlands
[5]Erasmus MC – University Medical Center Rotterdam – Department of Neuro-oncology, The Netherlands

Clin Chem 2006; **52***(8): 1501-1509*

ABSTRACT

Background: Our aim was to detect differences in protein expression profiles of cerebrospinal fluid (CSF) from pediatric patients with and without brain tumors.

Methods: We used surface-enhanced laser desorption/ionization time-of-flight (SELDI-TOF) mass spectrometry and Q10 ProteinChip arrays to compare protein expression profiles of CSF from 32 pediatric brain tumor patients and 70 pediatric control patients. A protein with high discriminatory power was isolated and identified by subsequent anion-exchange and reversed-phase fractionation, gel electrophoresis, and mass spectrometry. Western blotting and immunohistochemistry confirmed the identity of the protein.

Results: Of the 247 detected protein peak clusters, 123 were differentially expressed between brain tumor and control patients with a false discovery rate of 1%. Double-loop classification analysis gave a mean prediction accuracy of 88% in discriminating brain tumor patients from control patients. From the 123 clusters, a highly overexpressed protein peak cluster in CSF from brain tumor patients was selected for further analysis and identified as apolipoprotein A-II. Apolipoprotein A-II expression in CSF was correlated with the CSF albumin concentration, suggesting that the overexpression of apolipoprotein A-II is related to a disrupted blood–brain barrier.

Conclusions: SELDI-TOF mass spectrometry can be successfully used to find differentially expressed proteins in CSF of pediatric brain tumor and control patients. Apolipoprotein A-II is highly overexpressed in CSF of pediatric brain tumor patients, which is most likely related to a disrupted blood–brain barrier. Ongoing studies are aimed at finding subtype specific proteins in larger groups of pediatric brain tumor patients.

INTRODUCTION

In contrast to hematological malignancies in childhood, knowledge of the basic biological characteristics of pediatric brain tumors is limited. Studies based on molecular analyses and gene expression profiling are now evolving and may provide possible clues about pathogenetic and prognostic factors in, for example, primitive neuroectodermal tumors[1]. Despite the power of genomic and transcriptomic technologies, a major shortcoming of these approaches is that gene expression does not always correlate with protein expression. Because proteins actually change the functional state of the cell, proteins are the most relevant markers of function. Early proteomic approaches used 2-dimensional gel electrophoresis followed by identification of differentially expressed proteins by mass spectrometry. Novel proteomic approaches aiming at identifying novel biomarkers for cancer diagnosis and staging are rapidly developing. Surface-enhanced laser desorption/ionization time-of-flight (SELDI-TOF) mass spectrometry is based on 2 techniques: chromatography and mass spectrometry[2]. Proteins from complex protein mixtures are retained on specific chromatographic surfaces and subsequently analyzed by a linear TOF mass spectrometer to detect differences in protein expression profiles between groups of patients. The SELDI approach has recently been used successfully to identify biomarkers in biological fluids in various malignancies[3-15].

It has been shown that disease-related proteins can be detected in cerebrospinal fluid (CSF) of patients with a primary brain tumor by 2-dimensional gel electrophoresis[16] and in Alzheimer patients by SELDI-TOF mass spectrometry[17]. The objective of this study was to determine whether protein expression profiles obtained by SELDI-TOF mass spectrometry of CSF can be used to distinguish pediatric brain tumor patients from control patients.

MATERIALS AND METHODS

Study population and samples

A total of 32 lumbar CSF samples from newly diagnosed and untreated pediatric brain tumor patients (17 males and 15 females; median age, 7.2 years) and 70 pediatric control patients (39 males and 31 females; median age, 8.5 years) were analyzed in this study. All CSF samples were collected at the Erasmus MC—University Medical Center— Sophia Children's Hospital in Rotterdam, The Netherlands under uniform and standardized conditions. The brain tumor group consisted of 16 patients with medulloblastoma and 16 brain tumor patients with other histological subtypes (high grade glioma n=7; atypical rhabdoid tumor n=2; pilocytic astrocytoma n=2; plexus carcinoma n=2; anaplastic ependymoma n=2; germ cell tumor n=1), which will be referred to as "other tumors".

The 70 lumbar control CSF samples were obtained from pediatric patients 1 year after the end of treatment for acute lymphoblastic leukemia (n=47), pediatric patients without a

malignancy (infection n=6; hematological disease n=4; autoimmune disease n=2, idiopathic intracranial hypertension n=1) and pediatric patients with a malignancy outside the central nervous system (Hodgkin's disease n=6; neuroblastoma n=4). Each patient or the patient's parents gave informed consent before enrollment.

Cytological analysis of the CSF samples showed malignant cells in 10 medulloblastoma CSF samples. CSF from patients with other tumors and from control patients did not show any cytological abnormalities.

Sample preparation

All CSF samples were immediately centrifuged at 250xg for 5 minutes to remove cellular debris, and cytospins were made to evaluate cytology. Supernatants were aliquoted and stored at -80°C until analysis. Only CSF samples without macroscopic blood contamination were included in the study.

Before SELDI protein profiling, the protein concentration of the CSF samples was determined by the bicinchoninic acid protein assay (Pierce).

SELDI protein profiling

Q10 ProteinChip® arrays (strong anion-exchange chromatographic surface; Ciphergen Biosystems Inc.) were equilibrated with 50 mmol/L Tris (pH 8.5) containing 1 mL/L Triton (binding buffer). Crude CSF samples, each containing 5 µg of protein, were loaded on the arrays in duplicate, together with binding buffer and incubated for 1 h at room temperature. Arrays were washed sequentially with 50 mmol/L Tris (pH 8.5) containing 1 mL/L Triton, 50 mmol/L Tris (pH 8.5), and deionized water. After the arrays were air-dried at room temperature, energy-absorbing matrix sinapinic acid in an aqueous solution containing 500 mL/L acetonitrile and 5 mL/L trifluoroacetic acid was added to each spot. Mass analysis of the bound proteins was performed with a PBS IIc instrument (Ciphergen Biosystems Inc.) in positive operating mode. Mass spectra were collected by the accumulation of 65 laser shots at a laser intensity of 175 and a detector sensitivity of 8. The highest mass to acquire was set at m/z 200 000 with an optimization range between m/z 2000 and 30 000. The instrument was calibrated by the use of Protein Calibration Standard I (Bruker Daltonics). Peak detection and clustering were performed with the ProteinChip Biomarker Wizard™ module embedded in the ProteinChip software, Ver. 3.1 (Ciphergen Biosystems Inc.).

All spectra were compiled, aligned to a common calibrant, and normalized to the total ion current. The Biomarker Wizard automatically detected peaks with a signal-to-noise ratio > 5. Subsequently, peaks were clustered by the use of a 0.3% mass window and a second-pass peak selection with a signal-to-noise ratio > 2. The part of the spectrum with m/z values < 2000 was not used for analysis because the signal for the energy-absorbing matrix generally interferes with peak detection in this area.

Statistical analysis

We used the nonparametric Mann–Whitney U-test implemented in the Biomarker Wizard software to statistically compare differences in intensity data for the various protein peak clusters after normalization between patients with brain tumors and control patients. We corrected for multiple testing errors by applying the false discovery rate (FDR) described by Benjamini and Hochberg[18]. We used a FDR of 1%, which means that 99% of the selected protein peaks are expected to be true positive and not found by chance. We used the 123 protein peak clusters differentially expressed between brain tumor and control patients to perform a double-loop classification analysis with Biomarker Patterns™ software (Ciphergen Biosystems Inc.). Biomarker Patterns software is a tool for tree-structured data analysis, in which classification and regression trees (CART) methodology[19] is implemented.

The data were randomly split into a training set (two thirds of the data; $n_{control}$=47, $n_{brain\ tumor}$=21) and a test set (one third of the data; $n_{control}$=23, $n_{brain\ tumor}$=11).

The training set was used to generate the optimal classification tree in the Biomarker Patterns Software by use of a 10-fold internal cross-validation procedure. The optimal classification tree was tested for accuracy by the test set. The prediction accuracy was calculated as the ratio of correctly classified brain tumor samples to the total number of brain tumor samples. Specificity was calculated as the ratio of correctly classified control samples to the total number of control samples. This procedure was repeated 3 times with randomly chosen training (two thirds of samples) and test (one third of samples) sets. Mean values of prediction accuracy and specificity of the 3 repeated classification analyses are reported.

Purification and identification of differentially expressed proteins

CSF samples were fractionated by use of Q ceramic HyperD® F columns (Ciphergen Biosystems Inc.), with 50 mmol/L Tris pH 9.0, pH 7.0, pH 5.0, pH 4.0, pH 3.0, and organic solvent washes. Subfractionation was done by use of reversed phase chromatography (RPC) beads (30 nm; Polymer Laboratories Ltd.) with increasing concentrations of acetonitrile in 1 mL/L trifluoroacetic acid. Fractions containing the protein peaks of interest [monitored on NP20 (normal-phase chromatographic surface) ProteinChip arrays] were subjected to nonreducing sodium dodecyl sulfate–polyacrylamide gel electrophoresis (SDS-PAGE) on 16% Tris-glycine gels. The gel was stained with Coomassie blue (Invitrogen), and gel bands were cut. After destaining in 500 mL/L acetonitrile–500 mL/L 50 mmol/L ammonium bicarbonate and dehydration in acetonitrile, bands were dried in a SpeedVac. Proteins were passively eluted out of the gel bands by rehydration in 450 mL/L formic acid–300 mL/L acetonitrile 100 mL/L isopropanol and sonication for 3.5 h at room temperature. The extracts containing the markers (tested on NP20 arrays) were dried in a SpeedVac, resuspended in 20 μg/L modified trypsin (Roche Applied Science) dissolved in 100 mmol/L ammonium bicarbonate–100 mL/L acetonitrile, and incubated for 4 h at 37°C. Peptide mass spectra obtained in the ProteinChip System Series 4000 instrument (Ciphergen Biosystems Inc.) were used for peptide mass

fingerprinting (ProFound database). Tandem mass spectrometry (MS/MS) of selected peptides was done with a Micromass Q-TOFII equipped with a PCI 1000 Protein- Chip Tandem MS Interface (Ciphergen Biosystems Inc.).

Western blot

CSF samples (9.7 µg of protein) were subjected to non-reducing 15% Tris-glycine SDS PAGE. After proteins were transferred to a nitrocellulose membrane at 140 V for 90 min at 4 °C in a wet transfer system (Bio-Rad) and blocked with block buffer [50 g/L nonfat milk in 0.01 mmol/L phosphate-buffered saline (pH 7.4) containing 2 mL/L Tween 20] for 30 minutes, the membrane was incubated overnight at 4°C with mouse monoclonal antibodies against apolipoprotein A-II (APO-A-II; Biodesign International) diluted (1:400) in blocking buffer. The membrane was washed with 2 mL/L Tween 20 in 0.01 mmol/L phosphate-buffered saline (pH 7.4) and incubated for 1 h at room temperature with anti-mouse IgG–horseradish peroxidase conjugate (DakoCytomation) diluted (1:500) in blocking buffer containing 20 mL/L pooled human serum. Detection solution (SuperSignal West Femto Maximum Sensitivity Substrate; Pierce) was prepared according to the manufacturer's instructions. Chemiluminescence was measured with the Syngene chemigenius.

CSF/blood albumin quotient

The albumin concentration was analyzed in paired CSF and EDTA-plasma samples from 22 brain tumor patients by an immunochemical albumin assay using the Image 800 system (Beckman Coulter). The CSF/blood albumin quotient (Q_{alb}) was calculated and used as an estimation of the integrity of the blood–brain barrier. In 20 CSF samples from control patients, the albumin concentration was determined by the same assay. As no paired plasma samples for these control patients were available, we determined the plasma albumin concentration reference range with this assay in a separate set of 27 healthy pediatric control patients (median, 32.3 g/L; range, 11.3–41.4 g/L). The Q_{alb} in the control patients was then calculated by use of the median plasma albumin concentration from the separate control set.

Immunohistochemistry

We sectioned formalin-fixed, paraffin-embedded tissues from the medulloblastoma, ependymoma, high-grade glioma, control cerebellum, and prostate carcinoma into 4-µm thick sections and stained them with hematoxylin and eosin for histological examination. Prostate carcinoma tissue sections showed specific staining after incubation with the primary antibodies and were used as positive control [also described by Malik et al.[6]]. Tissue sections incubated with only the secondary antibody were used as negative controls. Sections were deparaffinized and rehydrated through a graded xylene–ethanol series. Antigen retrieval, achieved by boiling the slides for 5 min in 0.01 mol/L citric acid (pH 6.0), was followed by a 30-min incubation in 30 mL/L hydrogen peroxide in 0.01 mmol/L phosphate-buffered saline

(pH 7.4) to inhibit endogenous peroxidases. We then added 30 mL/L goat serum or 30 mL/L horse serum (Vector Laboratories) as a protein block for the monoclonal and polyclonal antibodies, respectively. Tissue sections were incubated with either a monoclonal (1:2000; Biodesign International) or a polyclonal (1:2000; Rockland Immunochemicals) anti-APO A-II antibody overnight at 4 °C. The sections were then incubated for 1h at room temperature with 1:1000 dilutions of biotinylated goat anti-mouse IgG for the monoclonal antibody and biotinylated horse anti-rabbit IgG (Vector Laboratories) for the polyclonal antibody. Incubation with the secondary antibody was followed by a 1h incubation with avidin-biotin peroxidase complex (1:400 dilution; Vectastain ABC Kit; Vector Laboratories). Staining was performed with a solution containing 0.5 g/L 3,3 -diaminobenzidine and 0.3 mL/L hydrogen peroxide in 30 mmol/L imidazole/1 mmol/L EDTA (pH 7.0). Tissue sections were slightly counterstained with hematoxylin, dehydrated, and mounted.

RESULTS

Reproducibility

The CV for the protein peak intensities obtained by SELDI-TOF mass spectrometry was determined on 12 protein peak clusters present in both a brain tumor and a control sample, which were measured in 8 independent experiments. The CV of the peak intensities for the 12 peak clusters ranged from 6% to 24% and did not differ statistically between the brain tumor and control CSF sample.

SELDI mass spectrometry

Mass spectrometric analysis of the proteins from the CSF of brain tumor and control patients that were bound to the affinity tags of the Q10 ProteinChip arrays (Ciphergen Biosystems Inc.) revealed 247 protein peak clusters between m/z 2000 and 200000. When we used an FDR of 1%, 123 protein peak clusters were significantly different between brain tumor and control patients. These protein peak clusters were used in a double-loop classification analysis. The most accurate classification models had a mean prediction accuracy of 88% (range, 82%–100%) and a mean specificity of 88% (range, 78%–96%) in discriminating CSF of brain tumor patients from CSF of control patients.

None of the 247 detected protein peak clusters was differentially expressed between the different histological brain tumor subtypes or between medulloblastoma patients with and without CSF cytological abnormalities.

Identification of protein markers

From the 123 differentially expressed protein peak clusters, we selected a protein peak cluster at M_r 17000, consisting of a *m/z* 17 248 and a *m/z* 17 369 protein peak, that was

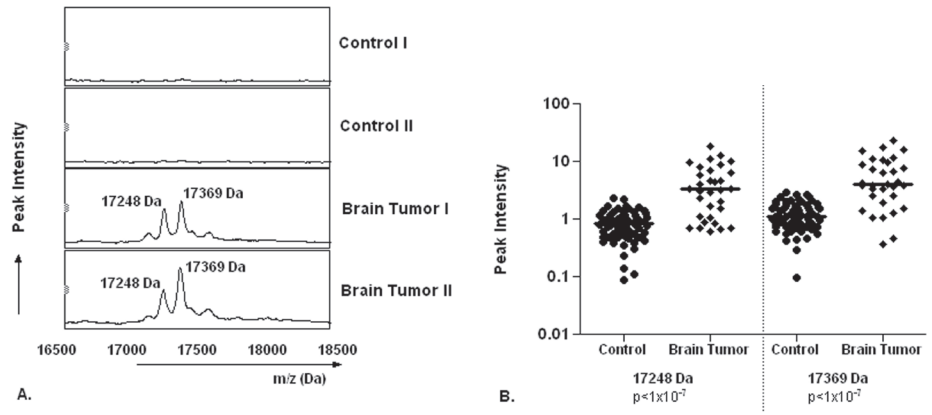

Figure 1. Differential expression of the Mr 17000 protein peak cluster in CSF of brain tumor and control patients.

A. Representative SELDI expression profiles of control and brain tumor CSF samples, showing significantly higher expression of a protein cluster at *m/z* 17000 in CSF of brain tumor patients compared to control patients.

B. Scatter plots of relative intensities of the *m/z* 17248 and *m/z* 17369 protein peaks (see panel A) as detected by SELDI-TOF analysis of 70 control and 32 brain tumor CSF samples.

The *lines* represent the median value within each subgroup.

highly abundant in brain tumor patients but virtually absent in control patients (Figure 1). To identify this protein cluster, we subjected CSF from a brain tumor patient sequentially to 3 fractionation methods. On anion-exchange Q ceramic HyperD F columns, the *m/z* 17000 protein cluster eluted in the pH 5.0 and pH 4.0 fractions (Figure 2A). When the pooled pH 4.0 and pH 5.0 fractions were further fractionated by use of RPC beads, the *m/z* 17000 peaks eluted in the 500 mL/L acetonitrile wash fraction (Figure 2B), which was subsequently subjected to non-reducing SDS-PAGE on 16% Tris-glycine gels (Figure 2C). Nine gel bands were cut from the gel (Figure 2C) and processed for passive elution, which revealed that the *m/z* 17000 protein cluster was present in gel band 7 (Figure 2D).

Subsequent peptide mass fingerprinting (ProFound) after tryptic digestion of the passive elution from band 7 gave a significant hit (Z=2.39) for APO A-II (sequence coverage: 88%). MS/MS analysis of 3 peptide peaks in the peptide mass spectrum (Figure 2E, peaks indicated by *) confirmed the identification of APO A-II [also see supplementary information I-III for MS/MS data on the 3 peptide peaks (http:// www.clinchem.org/content/vol52/issue8/)].

Western blot analysis revealed staining of 2 protein bands at approximately M_r 17 000 and M_r 34 000 by anti-APO A-II antibody. These proteins were abundantly present in CSF of brain tumor patients compared to control cases (Figure 3). This confirmed the identification and differential expression of APO A-II in CSF of control and brain tumor patients.

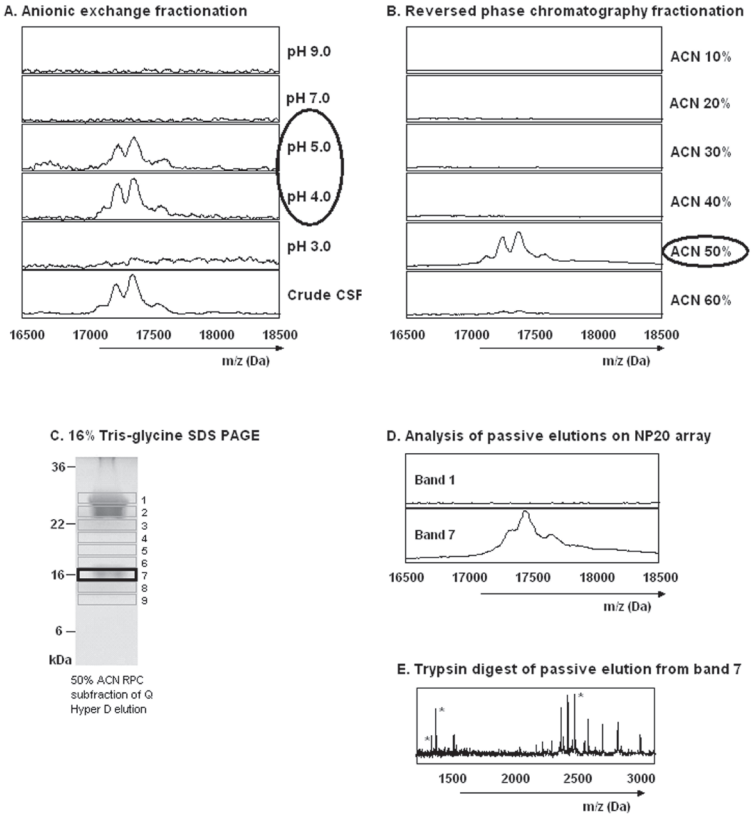

Figure 2. Purification and identification of the *m/z* 17 000 protein peak cluster.

A. CSF was subjected to anion-exchange fractionation on Q Hyper D F columns, and eluted protein fractions were tested on NP20 ProteinChips for the presence of the M_r 17000 protein cluster. The protein peak cluster at *m/z* 17000 eluted in the pH 4.0 and pH 5.0 fractions.

B. The pH 4.0 and 5.0 fractions were pooled and subfractionated by use of RPC beads.

C. The 50% acetonitrile RPC (ACN 50% in B) subfraction, which contained the *m/z* 17000 protein cluster, was run on a 16% Tris-glycine SDS-PAGE gel, which was stained with colloidal Coomassie blue.

D. Check of the passive elution of gel bands 1–9 on NP20 arrays showed that the *m/z* 17000 protein cluster was present in gel band 7. To illustrate the differences between the analyzed gel bands, the passive elution from band 1 is also displayed.

E. Peptide mass fingerprinting of the trypsin-digested protein extract from band 7 identified the *m/z* 17000 protein cluster as APO A-II. MS/MS analysis of the peptide peaks indicated with * (*m/z* 1156, 1199, and 2513) confirmed the identification of the *m/z* 17000 cluster as APO A-II [also see supplementary information I-III for MS/MS data of the 3 peptide peaks (http:// www.clinchem.org/content/vol52/issue8/)].

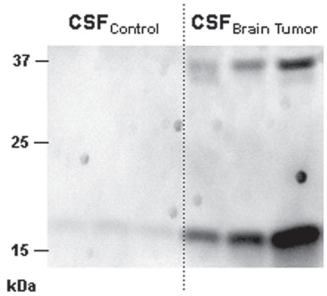

Figure 3. Differential expression of APO A-II in CSF from control and brain tumor patients.
Western blot analysis of CSF from control and brain tumor patients showed differential staining by anti-APO A-II antibody of a protein band at approximately the same mass as the band from which APO A-II was identified by MS/MS (Figure 2), confirming the identity of APO A-II.

Disrupted blood-brain barrier

The observed increase in APO A-II in CSF of brain tumor patients might be the result of protein leakage from the blood to the CSF attributable to a disrupted blood–brain barrier. To test this hypothesis, we measured the albumin concentration in CSF from brain tumor patients and control patients as well as the blood albumin concentration in brain tumor patients to calculate the CSF/blood albumin ratio (Q_{alb}), which serves as a good estimate of the integrity of the blood–brain barrier[20].

The median albumin concentration in CSF of brain tumor patients was significantly higher than that in CSF of control patients (0.19 and 0.10 g/L, respectively; p=0.0001). The median Q_{alb} in brain tumor and control patients were $8.61x10^{-3}$ and $3.04x10^{-3}$ ($p < 0.0001$), respectively (Figure 4), which suggests a disrupted blood–brain barrier in brain tumor patients,

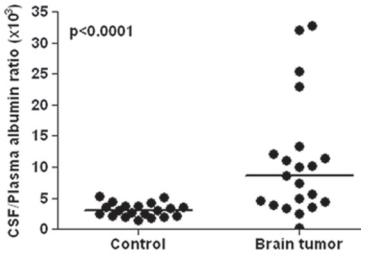

Figure 4. CSF/Blood albumin ratio in control and brain tumor patients.
The CSF/blood albumin ratio was calculated in control and brain tumor patients as representation of the integrity of the blood brain barrier. The CSF/blood albumin ratio was significantly higher in brain tumor patients than in control patients, suggesting a disruption of the blood–brain barrier in the brain tumor patients.
The *lines* represent the median value within each subgroup.

based on the reference Q_{alb} values in children (upper limit for patients under 15 years, $5.0x10^{-3}$)[21-23]. The albumin concentration in CSF was significantly ($p < 0.0001$) correlated with the peak intensities of the 2 protein peaks in the *m/z* 17000 APO A-II protein cluster in our SELDI experiments (Figure 5). These data indicate that a disrupted blood–brain barrier might explain the increased APO A-II concentration in CSF of brain tumor patients.

Immunohistochemistry did not show specific cellular APO A-II staining in pediatric brain tumor (see supplementary information IV (http:// www.clinchem.org/content/vol52/issue8/)) or healthy cerebellum tissue sections.

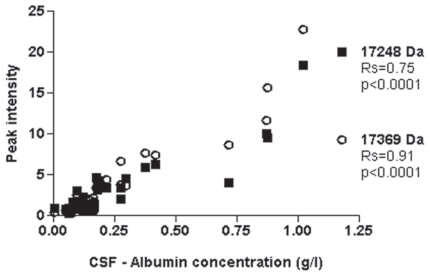

Figure 5. Correlation between CSF albumin concentration and relative intensity of *m/z* 17000 protein peak cluster in protein expression profiles.
The CSF albumin concentration was significantly correlated with the peak intensity of both proteins in the M_r 17000 protein cluster observed in the protein expression profiles.
m/z 17248 peak (Spearman correlation coefficient = 0.75; $p < 0.0001$)
m/z 17369 peak (Spearman correlation coefficient = 0.91; $p < 0.0001$).

DISCUSSION

SELDI ProteinChip technology has been used successfully to compare protein expression profiles in body fluids in various malignancies[3-15]. We analyzed SELDI protein expression profiles of CSF from pediatric brain tumor and control patients and observed 123 protein peak clusters that were differentially expressed with an FDR of 1%. Double-loop classification analysis gave a mean prediction accuracy of 88% and a mean specificity of 88% in discriminating brain tumor patients from control patients.

Probably because of the relatively small number of each brain tumor subtype in our study, we were not able to differentiate between different brain tumor subtypes based on the protein expression profiles of CSF. However, our analysis did identify a protein marker in CSF, which is common to all brain tumors. A protein cluster at *m/z* 17000 that was highly discriminative between tumor and control patients was identified as APO A-II by purification and subsequent peptide mass fingerprinting and MS/MS. Western blotting confirmed the identification and differential expression of APO A-II in CSF from brain tumor and control patients.

In most mammals, APO A-II is present in a monomeric form, whereas in humans, APO A-II also exists as a dimer of 2 identical chains, cross-linked by a single disulfide bond at cysteine-6 at the amino terminus of the protein[24, 25] . Because the monomeric form of APO A-II is M_r 8700, the M_r 17000 form identified in our study most likely represents the dimeric form of APO A-II. The masses of the 2 protein peaks (*m/z* 17 248 and 17 369) in the M_r 17000 protein peak cluster in our SELDI spectra were in concordance with previously described masses of isoforms of APO A-II[25, 26]. Multiple isoforms of APO A-II have been described in humans[25, 27-29] and are the result of posttranslational modifications, such as oxidization or truncation of the C-terminal glutamine residue[25-28].

APO A-II is the second most abundant human HDL apolipoprotein and is synthesized predominantly in the liver[30]. Despite the high abundance of APO A-II, little is known about its biological functions. APO A-II is thought to influence the metabolism of HDL and glucose[31-33]. Genetic variations in APO A-II appear to be involved in senile amyloidogenesis in mice and humans[30, 34, 35], and APO A-II has recently been linked to malignancies. In contrast to the increased APO A-II concentrations in CSF from brain tumor patients in our study, a study in mice indicated a decrease in serum APO A-II in mice that had received injections of a B-cell lymphoma[36]. A study in prostatic disease indicated that a monomeric isoform of APO A-II (M_r 8900) is specifically overexpressed in serum of patients with prostate cancer[6].

Our data suggest that the overexpression of APO A-II in CSF from brain tumor patients might have resulted from protein leakage from the blood through a disrupted blood–brain barrier. APO E and APO A-I are the major apolipoproteins in CSF, being present in HDL. Whereas evidence exists that, for example, APO E can be produced by astrocytes and microglia in the central nervous system[37], no data are available that indicate APO A-II production in the central nervous system. In patients with neuroborreliosis, CSF APO A-II concentrations were correlated with albumin concentrations regardless of cytology[38]. Because an increased Q_{alb} is indicative of a loss of integrity of the blood–brain barrier, increased APO A-II together with increased CSF albumin might reflect a disrupted blood–brain barrier. The significant difference in CSF albumin concentration between brain tumor patients and control patients, the increased Q_{alb} in brain tumor patients, and the significant correlation between the CSF albumin concentration and the intensity of the APO A-II peak in our SELDI experiments may indicate that a disrupted blood–brain barrier indeed might be the source of the increased APO A-II in CSF of brain tumor patients. Because none of the CSF samples in our study had macroscopic blood contamination, we excluded a traumatic lumbar puncture as the cause of the increased APO A-II in CSF. Additional evidence that the relative abundance of APO A-II in CSF may be attributable to a disrupted blood–brain barrier is our finding of the presence of the *m/z* 17000 APO A-II cluster in the protein expression profiles of 2 control patients with infected ventriculo-peritoneal drains, in whom ventricular instead of lumbar CSF was analyzed (data not shown).

Malik et al.[6] suggested that APO A-II is a potentially specific marker for prostatic disease. Several other apolipoproteins, such as APO D, E, and J, have also been linked to proliferation and cell growth in various malignancies[39-43], which may suggest that apolipoproteins, including APO A-II, are more general cancer markers, possibly being involved in the regulation of proliferation and growth of tumor cells. However, we observed no specific cellular APO A-II staining in our brain tumor tissue sections. This observation further strengthens the assumption that the increased APO A-II in the CSF of brain tumor patients might be related to a secondary phenomenon, such as a disrupted blood–brain barrier.

CONCLUSION

In conclusion, our study indicates that SELDI-TOF mass spectrometry can be successfully used to detect proteins that are differentially expressed in CSF of pediatric patients with and without brain tumors. Of the 123 differentially expressed protein peak clusters, we identified a highly overexpressed M_r 17000 peak cluster in CSF from brain tumor patients as APO A-II. The overexpression of APO A-II in CSF from brain tumor patients was correlated with an increased albumin concentration in CSF, which suggests a relationship with a disrupted blood–brain barrier. Ongoing studies are aimed at detecting subtype-specific proteins in larger groups of pediatric brain tumor patients.

ACKNOWLEDGEMENTS

We acknowledge Vladimir Podust, PhD, and Nathan Harris (Ciphergen Biosystems Inc.) for excellent suggestions regarding the protein purification procedure and providing us with the MS/MS data.

REFERENCES

1. Pomeroy S, L., Tamayo P, Gaasenbeek M, et al. Prediction of central nervous system embryonal tumour outcome based on gene expression. Nature 2002;415:436-442.
2. Tang N, Tornatore P, Weinberger SR. Current developments in SELDI affinity technology. Mass Spectrom Rev 2004;23(1):34-44.
3. Wright Jr. GL, Cazares LH, Leung S-M, et al. Proteinchip surface enhanced laser desorption/ionization (SELDI) mass spectrometry: a novel protein biochip technology for detection of prostate cancer biomarkers in complex protein mixtures. Prostate Cancer and Prostatic Diseases 2000;2:264-276.
4. Lehrer S, Roboz J, Ding H, et al. Putative protein markers in the sera of men with prostatic neoplasms. BJU Int 2003;92(3):223-225.
5. Gretzer MB, Chan DW, van Rootselaar CL, et al. Proteomic analysis of dunning prostate cancer cell lines with variable metastatic potential using SELDI-TOF. Prostate 2004;60(4):325-331.
6. Malik G, Ward MD, Gupta SK, et al. Serum levels of an isoform of apolipoprotein A-II as a potential marker for prostate cancer. Clin Cancer Res 2005;11(3):1073-1085.
7. Wong YF, Cheung TH, Lo KW, et al. Protein profiling of cervical cancer by protein-biochips: proteomic scoring to discriminate cervical cancer from normal cervix. Cancer Lett 2004;211(2):227-234.
8. Petricoin EF, Ardekani AM, Hitt BA, et al. Use of proteomic patterns in serum to identify ovarian cancer. Lancet 2002;359:572-577.
9. Paweletz CP, Trock B, Pennanen M, et al. Proteomic patterns of nipple aspirate fluids obtained by SELDI-TOF: potential for new biomarkers to aid in the diagnosis of breast cancer. Dis Markers 2001;17(4):301-307.
10. Won Y, Song HJ, Kang TW, et al. Pattern analysis of serum proteome distinguishes renal cell carcinoma from other urologic diseases and healthy persons. Proteomics 2003;3(12):2310-2316.
11. Wadsworth JT, Somers KD, Stack BC, Jr., et al. Identification of patients with head and neck cancer using serum protein profiles. Arch Otolaryngol Head Neck Surg 2004;130(1):98-104.
12. Zhukov TA, Johanson RA, Cantor AB, Clark RA, Tockman MS. Discovery of distinct protein profiles specific for lung tumors and pre-malignant lung lesions by SELDI mass spectrometry. Lung Cancer 2003;40:267-279.
13. Wilson LL, Tran L, Morton DL, Hoon DS. Detection of differentially expressed proteins in early-stage melanoma patients using SELDI-TOF mass spectrometry. Ann N Y Acad Sci 2004;1022:317-322.
14. Koopmann J, Zhang Z, White N, et al. Serum diagnosis of pancreatic adenocarcinoma using surface-enhanced laser desorption and ionization mass spectrometry. Clin Cancer Res 2004;10:860-868.
15. Rosty C, Christa L, Kuzdzal S, et al. Identification of Hepatocarcinoma-Intestine-Pancreas/Pancreatitis-associated protein I as a biomarker for pancreatic ductal adenocarcinoma by protein biochip technology. Cancer Res 2002;62:1868-1875.
16. Zheng P, Luider TM, Pieters R, et al. Identification of tumor-related proteins by proteomic analysis of cerebrospinal fluid from patients with primary brain tumors. J Neuropathol Exp Neurol 2003;62:855-862.
17. Carrette O, Demalte I, Scherl A, et al. A panel of cerebrospinal fluid potential biomarkers for the diagnosis of Alzheimer's disease. Proteomics 2003;3(8):1486-1494.
18. Benjamini Y, Hochberg Y. Controlling the False Discovery Rate: a Practical and Powerful Approach to Multiple Testing. Journal of the Royal Statistical Society B 1995;57:289-300.
19. Breiman L, Friedman JH, Olshen RA, Stone CL. Classification and Regression Trees. Belmont (CA-USA): Wadsworth International Group, 1984.
20. Reiber H. External quality assessment in clinical neurochemistry: survey of analysis for cerebrospinal fluid (CSF) proteins based on CSF/serum quotients. Clin Chem 1995;41(2):256-263.
21. Reiber H, Otto M, Trendelenburg C, Wormek A. Reporting cerebrospinal fluid data: knowledge base and interpretation software. Clin Chem Lab Med 2001;39(4):324-332.

22. Brettschneider J, Claus A, Kassubek J, Tumani H. Isolated blood-cerebrospinal fluid barrier dysfunction: prevalence and associated diseases. J Neurol 2005.
23. Tibbling G, Link H, Ohman S. Principles of albumin and IgG analyses in neurological disorders. I. Establishment of reference values. Scand J Clin Lab Invest 1977;37(5):385-390.
24. Puppione DL, Fischer WH, Park M, et al. Sequence of horse (Equus caballus) apoA-II. Another example of a dimer forming apolipoprotein. Comp Biochem Physiol B Biochem Mol Biol 2004;Part B 138:213-220.
25. Deterding LJ, Cutalo JM, Khaledi M, Tomer KB. Separation and characterization of human high-density apolipoproteins using a nonaqueous modifier in capillary elctrophoresis-mass spectrometry. Electrophoresis 2002;23:2296-2305.
26. Bondarenko PV, Farwig ZN, McNeal CJ, Macfarlane RD. MALDI- and ESI-MS of the HDL apolipoproteins; new isoforms of APO A-I, II. International Journal of Mass Spectrometry 2002;219:671-680.
27. Schmitz G, Ilsemann K, Melnik B, Assmann G. Isoproteins of human apolipoprotein A-II: isolation and characterization. J Lipid Res 1983;24(8):1021-1029.
28. Lackner KJ, Edge SB, Gregg RE, Hoeg JM, Brewer HBJ. Isoforms of apolipoprotein A-II in human plasma and thoracic duct lymph. Identification of proapolipoprotein A-II and sialic acid-containing isoforms. J Biol Chem 1985;260:703-706.
29. Niederkofler EE, Tubbs KA, Kiernan UA, Nedelkov D, Nelson RW. Novel mass spectrometric immunoassays for the rapid structural characterization of plasma apolipoproteins. J Lipid Res 2003;44(3):630-639.
30. Martin-Campos JM, Escola-Gil JC, Ribas V, Blanco-Vaca F. Apolipoprotein A-II, genetic variation on chromosome 1q21-q24, and disease susceptibility. Curr Opin Lipidol 2004;15:247-253.
31. Tailleux A, Duriez P, Fruchart J-C, Clavey V. Apolipoprotein A-II, HDL metabolism and atherosclerosis. Atherosclerosis 2002;164:1-13.
32. Dayal B, Ertel NH. ProteinChip technology: a new and facile method for identification and measurement of high-density lipoproteins apoA-I and apoA-II and their glycosylated products in patients with diabetes and cardiovascular disease. J Proteome Res 2002;1(4):375-380.
33. Warden CH, Daluiski A, Bu X. Evidence for linkage of the apolipoprotein A-II locus to plasma apolipoprotein A-II and free fatty acid levels in mice and humans. Proc Natl Acad Sci U S A 1993;90:10886-10890.
34. Higuchi K, Kitagawa K, Naiki H. Polymorphism of apolipoprotein A-II (apoA-II) among inbred strains of mice: relationship between the molecular type of apoA-II and mouse senile amyloidosis. Biochem J 1991;279:427-433.
35. Yazaki M, Lieprieks JJ, Barats MS. Hereditary systemic amyloidosis associated with a new apolipoprotein AII stop codon mutation Stop 78 Arg. Kidney Int 2003;64:11-16.
36. Chertov O, Biragyn A, Kwak LW, et al. Organic solvent extraction of proteins and peptides from serum as an effective sample preparation for detection and identification of biomarkers by mass spectrometry. Proteomics 2004;4:1195-1203.
37. Boyles JK, Pitas RE, Wilson E, Mahley RW, Taylor JM. Apolipoprotein E associated with astrocytic glia of the central nervous system and with non-myelinating glia of the peripheral nervous system. J Clin Invest 1985;76:1501-1513.
38. Taborsky L, Adam P, Sobek O, et al. Levels of apolipoprotein A-II in cerebrospinal fluid in patients with neuroborreliosis are associated with lipophagocytosis. Folia Microbiol (Praha) 2003;48(6):849-855.
39. Niemi M, Häkkinen T, Karttunen TJ, et al. Apolipoprotein E and colon cancer; Expression in normal and malignant human intestine and effect on cultured human colonic adenocarcinoma cells. Eur J Intern Med 2002;13:37-43.

40. Hunter S, Young A, Olson J, et al. Differential expression between pilocytic and anaplastic astrocytomas: identification of apolipoprotein D as a marker for low-grade, non-infiltrating primary CNS neoplasms. J Neuropathol Exp Neurol 2002;61(3):275-281.
41. Trougakos IP, Lourda M, Agiostratidou G, Kletsas D, Gonos ES. Differential effects of clusterin/apolipoprotein J on cellular growth and survival. Free Radic Biol Med 2005;38(4):436-449.
42. Alvarez ML, Barbon JJ, Gonzalez LO, et al. Apolipoprotein D expression in retinoblastoma. Ophthalmic Res 2003;35(2):111-116.
43. Chen YC, Pohl G, Wang TL, et al. Apolipoprotein E is required for cell proliferation and survival in ovarian cancer. Cancer Res 2005;65(1):331-337.

Chapter 6

Increased Total-Tau Levels in Cerebrospinal Fluid of Pediatric Hydrocephalus and Brain Tumor Patients

Judith M. de Bont[1], Hugo Vanderstichele[2], Roel E. Reddingius[1], Rob Pieters[1], Stefaan W. van Gool[3]

[1]Erasmus MC – Sophia Children's Hospital - University Medical Center Rotterdam – Department of Pediatric Oncology and Hematology, The Netherlands
[2]Innogenetics – Gent; Belgium;
[3]University Hospital Gasthuisberg – Leuven – Department of Pediatric Oncology and Hematology, Belgium

Eur J Paediatr Neurol 2008; **12***(4): 334-341*

ABSTRACT

Total tau (t-Tau), hyperphosphorylated Tau (p-Tau$_{(181P)}$) and ß-amyloid$_{(1-42)}$ in cerebrospinal fluid (CSF) have shown to be markers of neuronal and axonal degeneration in various neurological and neurodegenerative diseases. The aim of this study was to evaluate the influence of the presence of a brain tumor and hydrocephalus on t-Tau, p-Tau$_{(181P)}$ and ß-amyloid$_{(1-42)}$ levels in CSF of pediatric patients.

t-Tau, p-Tau$_{(181P)}$ and ß-amyloid$_{(1-42)}$ levels were simultaneously quantified by xMAP®-technology in 22 lumbar and 15 ventricular CSF samples from newly diagnosed pediatric brain tumor patients and 39 lumbar and 12 ventricular CSF samples from pediatric patients without a brain tumor.

t-Tau, p-Tau$_{(181P)}$ and ß-amyloid$_{(1-42)}$ levels in both lumbar and ventricular CSF were not significantly correlated with age. t-Tau levels in lumbar CSF were elevated in brain tumor patients, being especially high in medulloblastoma patients. Lumbar CSF p-Tau$_{(181P)}$ levels were lower in brain tumor patients compared to normal controls. Ventricular levels of t-Tau, p-Tau$_{(181P)}$ and ß-amyloid$_{(1-42)}$ were not significantly different between the brain tumor patients and non-tumor patients, but t-Tau levels were significantly increased in patients with radiological signs of hydrocephalus. Two patients with an infected ventriculo-peritoneal drain also had high CSF t-Tau levels.

In conclusion, high t-Tau levels in CSF are found in pediatric patients with a brain tumor, patients with hydrocephalus and patients with a serious CNS infection, reflecting neuronal and axonal damage. Ongoing studies should determine whether these neurodegenerative markers in CSF can be used to monitor neuronal and axonal degeneration in these patients during therapy and long-term follow up.

INTRODUCTION

In several disorders, total Tau (t-Tau), hyperphosphorylated $Tau_{(181P)}$ ($p\text{-}Tau_{(181P)}$) and $\beta\text{-amyloid}_{(1\text{-}42)}$ levels in cerebrospinal fluid (CSF) are markers for neurodegeneration. Changes in CSF t-Tau levels and $\beta\text{-amyloid}_{(1\text{-}42)}$ levels were first thought to be specific for Alzheimer's disease[1-9]. However, CSF t-Tau, $p\text{-}Tau_{(181P)}$ and $\beta\text{-amyloid}_{(1\text{-}42)}$ levels were also demonstrated to be of importance in various other diseases, such as frontotemporal[10-13] and Lewy body[10, 14] dementia, multiple sclerosis[15-17], Creutzfeldt-Jakob disease[18-22], amytrophic lateral sclerosis[23], stroke[24], acute brain injury[25], neuro-AIDS[26], normal pressure hydrocephalus[27, 28] and in hematological malignancies[29, 30]. Highest levels of t-Tau were found in disorders with the most intense neuronal degeneration, such as Creutzfeldt Jakob disease[18], suggesting that t-Tau is an indicator of the extent of neuronal damage, but is not disease-specific.

Van Gool et al.[30] measured t-Tau in CSF of children receiving central nervous system (CNS) prophylaxis as part of their treatment for a hematological malignancy. They found elevated CSF t-Tau levels at diagnosis in about one third of the patients and very high levels of t-Tau in patients who had leukemic infiltration of the CNS at diagnosis. In the same study three patients with a medulloblastoma, one patient with a germinoma and one patient with a CNS metastasized retinoblastoma had markedly elevated CSF t-Tau levels, which might indicate CSF t-Tau to be a marker of disease-related neural disintegrity in patients having a malignancy involving the CNS.

We hypothesized that the presence of a brain tumor and hydrocephalus, frequently present in newly diagnosed pediatric brain tumor patients, give rise to marked axonal and neuronal damage. We therefore evaluated t-Tau, $p\text{-}Tau_{(181P)}$, $\beta\text{-amyloid}_{(1\text{-}42)}$ levels in lumbar and ventricular CSF of pediatric brain tumor patients and control patients with and without hydrocephalus.

PATIENTS AND METHODS

Patients

In this study 22 lumbar and 15 ventricular CSF samples from newly diagnosed pediatric brain tumor patients and 39 lumbar and 12 ventricular CSF samples from pediatric patients without a malignancy in the CNS were analyzed (Table 1). CSF samples were collected at the Erasmus MC – University Medical Center – Sophia Children's Hospital in Rotterdam, the Netherlands.

In brain tumor patients, lumbar CSF was obtained by performing a lumbar puncture approximately 15 days after tumor resection, before starting chemo- and/or radiotherapy. Control lumbar CSF was obtained from 39 pediatric patients who did not have a brain tumor (acute lymphoblastic leukemia 1 year after stop of treatment (and thus in continuous

Table 1. Patient characteristics, median levels of total Tau (t-Tau), hyperphosphorylated Tau (p-Tau$_{(181P)}$) and ß-Amyloid$_{(1-42)}$ in lumbar and ventricular CSF of brain tumor and non-tumor patients.

[a] medulloblastoma n=14; ATRT n=1; ependymoma n=4; pilocytic astrocytoma n=1; germ cell tumor n=1; glioblastoma n=1

[b] acute lymphoblastic leukemia 1 year after stop of treatment (and thus in continuous complete remission for more than 2.5 years) (n=17), infectious disease outside CNS n=6; hematological disease n=4; autoimmune disease n=2, Hodgkin's disease n=6, Neuroblastoma n=4

[c] medulloblastoma n=4; ATRT n=1; pilocytic astrocytoma n=3; craniopharyngeoma n=1; plexus papilloma n=1; anaplastic astrocytoma n=1 ; ependymoma n=1; germ cell tumor n=2 ; pontic glioma n=1

	Lumbar CSF		**Ventricular CSF**			
	Brain tumor[a]	**Control[b]**	**Brain tumor[c]**	**Non-tumor with radiological signs of hydrocephalus**	**Non-tumor without radiological signs of hydrocephalus**	**Non-tumor with infected ventriculo-peritoneal drain**
Number of patients	22	39	15	6	4	2
Median age (years)	7.6	9.6	10.6	1.3	2.0	0.5
(range)	*(1.4-17.4)*	*(0.5-17.7)*	*(0.8-17.8)*	*(0.3-10.4)*	*(0.3-12.1)*	*(0.49-0.51)*
Sex (male/female)	13/9	23/16	12/3	3/6	3/1	1/1
Median CSF protein concentration (mg/ml)	0.8	0.6	0.7	4.3	0.4	4.5
(range)	*(0.4-2.8)*	*(0.4-1.1)*	*(0.2-1.3)*	*(0.3-8.0)*	*(0.3-0.9)*	*(4.0-5.1)*
Median t-Tau (pg/ml)	387.9	55.3	1106	1037.8	195.5	1186.4
(range)	*(46.0-1419.0)*	*(10.4-148.8)*	*(442.8-1419.0)*	*(285.0-1419.0)*	*(22.0-312.8)*	*(1186.4)*
Median p-Tau$_{(181P)}$ (pg/ml)	13.9	40.4	167.4	175.6	40.8	166.4
(range)	*(8.4-43.9)*	*(19.5-85.7)*	*(10.3-200.9)*	*(54.6-282.8)*	*(31.8-168.7)*	*(50.1-282.8)*
Median β-Amyloid$_{(1-42)}$ (pg/ml)	124.1	170.4	48.3	61.4	45.3	150.3
(range)	*(42.5-248.3)*	*(15.7-263.3)*	*(32.6-152.8)*	*(43.4-118.0)*	*(44.0-162.8)*	*(91.8-208.9)*

complete remission for more than 2.5 years) (n=17), infectious disease outside the CNS n=6; benign hematological disease n=4; autoimmune disease n=2, Hodgkin's disease n=6, neuroblastoma n=4).

Ventricular CSF of brain tumor patients was obtained during the placement a ventriculo-peritoneal drain (n=7) or performing a third ventriculostomy (n=8) prior to tumor biopsy or tumor resection. Ventricular CSF in non-tumor control patients was obtained just prior to the placement or revision (n=11) a ventriculoperitoneal drain or performing a third ventriculostomy (n=1). Six of these patients underwent surgery because of radiological features of hydrocephalus. Four patients did not have abnormalities on radiological imaging and 2 patients with a history of hydrocephalus had an infected ventriculo-peritoneal drain. In these 2 patients no pre-operative radiological imaging was available.

At least 3 ml of CSF was collected in polypropylene tubes and immediately centrifuged at 250xg to remove cellular debris. Cytospins were made to evaluate cytology. Supernatant was aliquoted and stored at -80°C until analysis. Protein concentration of the CSF samples was determined by a BCA protein assay (Pierce, Rockford, USA). Each patient or patient's relatives gave informed consent prior to enrollment.

Measurement of neurodegenerative markers in CSF

All biochemical analyses for the detection of CSF-Tau, CSF-pTau, CSF- ß-amyloid$_{(1-42)}$ were performed using xMAP®-technology without knowledge of the clinical diagnosis. All samples were tested undiluted.

The principle of the xMAP®-technology and technical details of the microsphere-based INNO-BIA AlzBio3 (Characteristics of antibodies and calibrators, test procedure, etc.) have been described previously[31, 32]. The INNO-BIA AlzBio3 is designed for simultaneous quantification in undiluted lumbar CSF of t-Tau, p-Tau$_{(181P)}$, phosphorylated at threonine 181 (p-Tau$_{181P}$) and ß-amyloid$_{(1-42)}$ using spectrally specific fluorescent microspheres linked to monoclonal antibodies. In short, 75 µl of CSF was incubated overnight (in the dark) at room temperature with biotinylated detector antibody. After a wash step, 100 µl of phycoerythrine-labeled-Streptavidin (Caltag Laboratories, Burlingame, CA, USA) was added and incubated for 1 hour on a plate shaker. After a second wash step, 100 µl of phosphate-buffered saline was added to each well. Samples were analyzed on the Luminex 100 IS system (Luminex Corporation, Austin, USA). For each microsphere region, 100 beads were analyzed. The concentration of each parameter was calculated with reference to a calibrator curve by sigmoidal curve fitting.

Radiological imaging

In non-tumor control and brain tumor patients from whom ventricular CSF was collected, CT and/or MRI reports prior to the neurosurgical intervention were evaluated for the presence of hydrocephalus.

Statistical analysis

The non-parametric Mann-Whitney U-test was used for statistical comparison of ordinal and continuous variables between groups. For correlation analysis the Spearman's correlation coefficient was calculated. All the statistical analyses were performed with the Statistical Package of the Social Sciences (SPSS version 11.0).

RESULTS

Patient characteristics

Patient characteristics are described in table 1. Non-tumor patients were significantly (p=0.014) younger than brain tumor patients in the ventricular CSF group. t-Tau, p-Tau$_{(181P)}$ and ß-amyloid$_{(1-42)}$ levels in both the lumbar and ventricular CSF group were not significantly correlated to age (Figure 1). We did not observe significant correlations between t-Tau or p-Tau$_{(181P)}$ levels and the total protein concentration in ventricular and lumbar CSF. ß-amyloid$_{(1-42)}$ levels in lumbar CSF were also not correlated to the protein concentration, but for ß-amyloid$_{(1-42)}$ levels in ventricular CSF we observed an increase in ß-amyloid$_{(1-42)}$ with increasing total protein concentration (Spearmann correlation coefficient (R_s)=0.67; p<0.0010). As the total protein concentration did not seem to have a large influence on most of the measurements of neurodegenerative markers in both lumbar and ventricular CSF, we decided not to correct the levels of neurodegenerative markers in CSF for the total protein concentration.

Measurement of t-Tau, p-Tau$_{(181P)}$ and ß-amyloid$_{(1-42)}$

Lumbar CSF

t-Tau levels in lumbar CSF were significantly increased in both medulloblastoma and other brain tumor patients compared to control patients without a brain tumor (p<0.0010 and p=0.0020, respectively)(Table 1, Figure 2A). Regarding the different brain tumor subgroups, t-Tau levels were especially elevated in lumbar CSF of medulloblastoma patients (Figure 2A). There was no significant difference in t-Tau levels between medulloblastoma patients with metastatic (M1 stage = tumor cells in CSF, but no radiological leptomeningeal metastases or M2 stage = radiological leptomeningeal metastases) and without metastatic disease (M0 stage). p-Tau$_{(181P)}$ levels in lumbar CSF were significantly lower in brain tumor patients compared to control patients (p<0.0010)(Table 1, Figure 2B) and we observed a trend towards lower ß-amyloid$_{(1-42)}$ levels in brain tumor patients compared to control patients (Table 1, Figure 2C). We did not observe significant differences in p-Tau$_{(181P)}$ and ß-amyloid$_{(1-42)}$ levels between medulloblastoma patients and patients with another brain tumor subtype or between medulloblastoma disease stages. Unfortunately, reference values for lumbar CSF

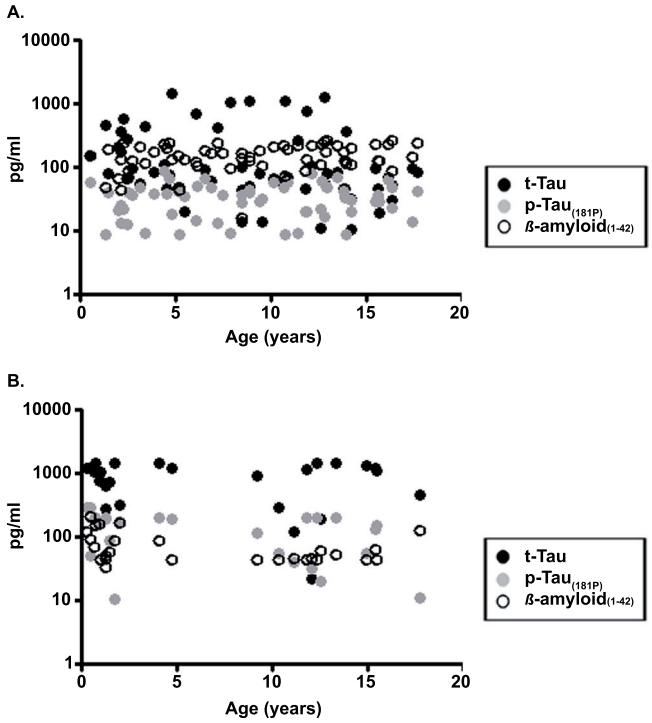

Figure 1. Absence of significant correlations between age and t-Tau, p-Tau$_{(181P)}$ and ß-amyloid$_{(1-42)}$ levels in lumbar (A.) and ventricular (B.) CSF.

t-Tau, p-Tau$_{(181P)}$ and ß-amyloid$_{(1-42)}$ levels are only available for results obtained by ELISA and not yet for results obtained by xMAP®-technology.

Ventricular CSF

Levels of t-Tau and p-Tau$_{(181P)}$ were significantly higher in ventricular CSF compared to lumbar CSF in brain tumor patients ($p<0.0010$ and $p=0.0010$, respectively), while ß-amyloid$_{(1-42)}$ levels were significantly lower in ventricular CSF compared to lumbar CSF ($p=0.0050$) (Table 1).

There are no well established reference values for t-Tau, p-Tau$_{(181P)}$ and ß-amyloid$_{(1-42)}$ in ventricular CSF. Regarding the few results[27] available for these markers in ventricular CSF, t-Tau levels of both brain tumor and non-tumor patients are increased in ventricular CSF. We did not observe significant differences in t-Tau, p-Tau$_{(181P)}$ and ß-amyloid$_{(1-42)}$ ventricular CSF levels between brain tumor and non-tumor patients.

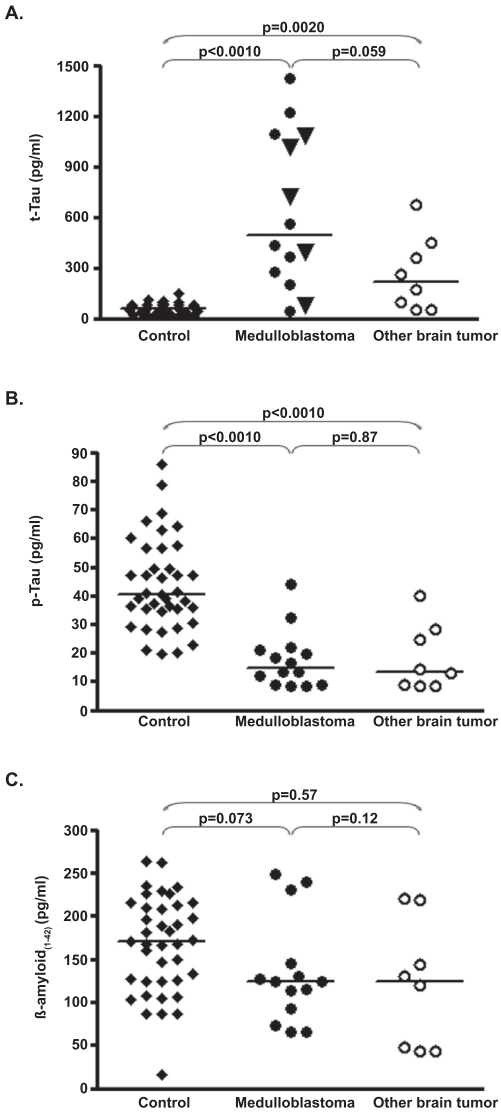

Figure 2. t-Tau (A.), p-Tau$_{(181P)}$ (B.) and ß-amyloid$_{(1-42)}$ (C.) levels in lumbar CSF of medulloblastoma patients and patients with other brain tumor subtypes.

Compared to control patients, t-Tau levels were significantly increased in lumbar CSF of brain tumor patients, especially in medulloblastoma patients. Patients with metastatic medulloblastoma did not have higher t-Tau levels than patients with a non-metastatic medulloblastoma (● metastatic medulloblastoma; ▼ non-metastatic medulloblastoma)(A.). p-Tau$_{(181P)}$ levels were significantly lower in brain tumor patients compared to control patients (B.) ß-amyloid$_{(1-42)}$ levels were decreased in the lumbar CSF of almost all brain tumor patients (C.). There was no difference in p-Tau$_{(181P)}$ and ß-amyloid$_{(1-42)}$ levels between medulloblastoma patients and patients with other brain tumor subtypes or between metastatic and non-metastatic medulloblastoma.

The line represents the median value within each group.

Hydrocephalus

The presence of hydrocephalus was only radiologically evaluated in patients in whom ventricular CSF was analyzed, as for these patients pre-operative radiological reports were available. All brain tumor patients, except one patient with a pilocytic astrocytoma, had high CSF t-Tau levels and showed hydrocephalus on CT and or MRI at the time of CSF sampling. As all brain tumor patients, except one, presented with hydrocephalus we could not evaluate separately the influence of hydrocephalus on the level of neurodegenerative markers in CSF in brain tumor patients. In 6 non-tumor control patients hydrocephalus was reported to be visible on the pre-operative scan. Four non-tumor patients did not have abnormalities on radiological imaging. We observed higher t-Tau levels in non-tumor patients with signs of hydrocephalus on radiological imaging before CSF sampling compared to patients without those abnormalities (Figure 3). Two non-tumor patients with a history of hydrocephalus underwent surgery because of an infected ventriculo-peritoneal drain. t-Tau levels were also very high in these patients. Unfortunately, pre-operative radiological reports were not available in these patients.

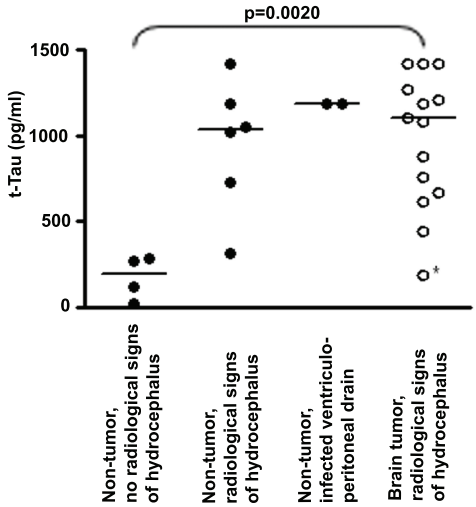

Figure 3. CSF t-Tau levels in ventricular cerebrospinal fluid of non-tumor control and brain tumor patients.

t-Tau levels were elevated in brain tumor and non-tumor control patients with radiological signs of hydrocephalus. Two patients undergoing surgery because of an infected ventriculo-peritoneal drain also showed markedly increased t-Tau levels. As all brain tumor patients, except one*, presented with hydrocephalus, we could not evaluate the influence of hydrocephalus on neurodegenerative markers in CSF in brain tumor patients.

The p-value (p=0.0020) refers to the comparison between non-tumor patients without radiological signs of hydrocephalus and brain tumor patients with hydrocephalus.

The line represents the median value within each group

Numbers of patients were too small to correlate the extent of hydrocephalus to levels of neurodegenerative markers in CSF.

DISCUSSION

This is the first study evaluating the neurodegenerative markers t-Tau, p-Tau$_{(181P)}$ and ß-amyloid$_{(1-42)}$ in the CSF of pediatric brain tumor and hydrocephalus patients.

We showed that t-Tau and p-Tau$_{(181P)}$ levels are higher and ß-amyloid$_{(1-42)}$ levels are lower in ventricular compared to lumbar CSF. This is in concordance with data from Reiber et al.[33] who showed that concentrations of brain derived proteins, such as t-Tau and p-Tau$_{(181P)}$ are higher in ventricular than in lumbar CSF. Concentrations of systemically derived proteins, such as ß-amyloid$_{(1-42)}$, are lower in ventricular CSF compared to lumbar CSF[33].

In concordance with Van Gool et al.[34] we did not observe significant correlations between age and the CSF levels of t-Tau, p-Tau$_{(181P)}$ and ß-amyloid$_{(1-42)}$. Lofberg et al.[35] showed that only in the first 3 months of life CSF proteins are significantly different from those CSF values during the entire life span. Although there have been conflicting results about the age variation of t-Tau and ß-amyloid$_{(1-42)}$ in adults[36, 37], CNS proteins in CSF only seem to increase slightly in healthy individuals above the age of 50[36, 37]. Therefore, reference values from adult studies might well have been applicable as the normal upper/lower limits for the pediatric patients in our study. However, reference values for lumbar CSF t-Tau, p-Tau$_{(181P)}$ and ß-amyloid$_{(1-42)}$ levels are only available for results obtained by ELISA. For the results obtained by xMAP® technology, as was used in our study, no reference values have been published. It has been shown that, in general, data obtained by ELISA and xMAP technology show a good correlation, however applying a correction factor, which is a constant factor over the whole concentration range and irrespective of disease groups, has not proven to be successful[38], making it difficult to directly compare our data to currently known reference values.

t-Tau protein is a microtubule-associated protein, predominantly localized in neuronal axons[39, 40]. Its physiological function is promoting the assembly and stabilization of the microtubular network in axons. After neuronal damage t-Tau is released into the extracellular space and CSF[16]. As a result, t-Tau in CSF may serve as a biochemical marker of neuronal and axonal damage. Compared to control patients, we observed increased t-Tau levels in the lumbar CSF of pediatric brain tumor patients (Figure 2A), indicating the presence of neuronal and axonal damage in these patients. t-Tau levels were especially high in medulloblastoma patients. The extent of neuronal and axonal damage was not related to disease stage in medulloblastoma, as patients presenting with metastatic (M1 or M2 stage) disease did not have higher CSF t-Tau levels than patients with localized disease (M0 stage).

In contrast to the differences in t-Tau levels in lumbar CSF, we did not observe significant differences in ventricular CSF t-Tau levels between brain tumor and non-tumor patients. This

could be explained by the fact that more than half of the non-tumor patients had radiological signs of hydrocephalus and hydrocephalus was associated with high t-Tau levels. t-Tau levels were significantly higher in the ventricular CSF of brain tumor patients and of non-tumor patients with hydrocephalic features on radiological images compared to non-tumor patients without hydrocephalus. It is difficult to interpret the t-Tau, p-$Tau_{(181P)}$ and ß-$amyloid_{(1-42)}$ profiles of ventricular CSF in patients, as there are no reference values for ventricular CSF in healthy individuals. In concordance with our results, Tisell et al.[27] also found increased levels of t-Tau in ventricular CSF of normal pressure hydrocephalus patients. Increased lumbar CSF t-Tau levels have also been reported in hydrocephalus patients[28]. It is known that in patients with hydrocephalus changes in the periventricular region, such as edema, demyelinaton and neuronal and axonal degeneration arise due to mechanical and ischemic effects[41-45]. t-Tau might thus be a good biochemical marker for the extent of neuronal and axonal damage in hydrocephalus patients.

Besides neuronal damage, a disrupted CSF outflow in obstructive hydrocephalus leading to decreased clearance and accumulation of brain-derived proteins might be another explanation for the increased ventricular CSF t-Tau levels in patients with signs of hydrocephalus in our study, as it was proposed that CSF flow rate is crucial for CSF protein concentrations[33]. However, t-Tau levels were not only markedly increased in the ventricular CSF, but also in the lumbar CSF of brain tumor patients in our study, contradicting this accumulation theory. In brain tumor patients it is not clear what exactly causes the high t-Tau levels in the ventricular CSF of brain tumor patients. Both local damage by tumor growth and the presence of hydrocephalus (all except one of the brain tumor patients had hydrocephalus at diagnosis) might have been of influence. As t-Tau levels are still increased in the lumbar CSF of brain tumor patients, in whom hydrocephalus was already resolved by placing a drain or (in)complete tumor resection, it is very likely that both tumor growth and hydrocephalus can contribute to neuronal and axonal damage and increased CSF t-Tau levels in brain tumor patients. Kudo et al.[28] showed that t-Tau levels were correlated to the severity of dementia, urinary incontinence and gait disturbance in normal pressure hydrocephalus. Due to the relatively small number of patients in our study we unfortunately were not able to correlate the t-Tau levels to the severity of hydrocephalus in brain tumor and non-tumor patients.

Two non-tumor patients with an infected ventriculo-peritoneal drain also showed relatively high CSF t-Tau levels in our study, suggesting that CNS infection might also give rise to marked neuronal and axonal damage and consequently increased levels of neurodegenerative markers. Increased t-Tau levels in pediatric patients with a serious CNS infection were also described by Rostasy et al.[46]. In their study, t-Tau levels were highest and far above upper reference limits in patients with various neurological inflammatory diseases, such as meningitis and encephalitis.

In Alzheimer's disease a combination of increased t-Tau and p-$Tau_{(181P)}$ levels is observed[47-50]. The Tau protein can become abnormally phosphorylated because of an imbalance of cellular

kinases and phosphatases. This hyperphosphorylated form twists into paired helical filaments that aggregate to form the neurofilbrillary tangle, for example found in Alzheimer's disease[40, 51-53]. In several other disease entities, such as stroke[24], Creutzfeldt Jakob disease[19], Lewy body dementia[54] patients a combined increase of t-Tau and p-Tau$_{(181P)}$ was not seen**.** In our study we observed significantly lower lumbar CSF p-Tau$_{(181P)}$ levels in brain tumor patients compared to controls in combination with increased t-Tau levels. Combining t-Tau and p-Tau$_{(181P)}$ profiles in CSF might thus be useful to discriminate between different disease entities. An isolated increase of t-Tau might reflect neuronal or axonal damage due to a more vascular related type of neurotoxicity, as is seen in acute stroke patients[24] and probably also in the patients in our study. Increased p-Tau$_{(181P)}$ levels might better reflect the formation of neurofibrillary tangles than being a marker for neuronal or axonal damage. The decreased p-Tau$_{(181P)}$ levels in the lumbar CSF of brain tumor patients is unclear, but it might be related to increased breakdown of the protein or increased activity of phosphatases.

We observed a trend toward decreased ß-amyloid$_{(1-42)}$ levels in the lumbar CSF of most brain tumor patients. It is unclear what causes the low ß-amyloid$_{(1-42)}$ levels in the lumbar CSF of brain tumor patients in our study. ß-amyloid$_{(1-42)}$ levels are frequently decreased in Alzheimer's disease, probably due to the accumulation of ß-amyloid$_{(1-42)}$ in senile plaques[52, 53]. Decreased ß-amyloid$_{(1-42)}$ levels were also described in Creutzfeldt Jakob patients, suggesting that a decrease in CSF ß-amyloid$_{(1-42)}$ is not only related to the formation of senile plaques, but can also occur in other pathological conditions. Schoonenboom et al.[55] investigated the effects of processing and storage conditions on ß-amyloid$_{(1-42)}$ concentrations in cerebrospinal fluid. It was shown that repeated freeze/thaw cycles and storage at 4, 18 and 37°C resulted in decreased ß-amyloid$_{(1-42)}$ results. As the CSF samples in our study were collected in polypropylene tubes, immediately stored at -80°C after centrifugation and repeated freeze/thaw cycles were avoided, it is unlikely that these factors have caused the relatively low ß-amyloid$_{(1-42)}$ levels in our study.

In conclusion, considering our study and previous ones, there is substantial overlap between different neurological disease entities regarding patterns of t-Tau, p-Tau$_{(181P)}$ and ß-amyloid$_{(1-42)}$ levels in CSF. High t-Tau levels in CSF seem to reflect neuronal and axonal damage in pediatric patients with a brain tumor, patients with hydrocephalus and also patients with a serious CNS infection. Studies involving larger number of patients are needed to further elucidate the clinical importance of t-Tau levels in CSF of pediatric brain tumor and hydrocephalus patients and the influence of the cause and severity of hydrocephalus. As was already done in patients treated for hematological malignancies[29, 30], longitudinal studies can provide information about neuronal and axonal degeneration caused by different treatment modalities, such as shunting operations in hydrocephalus patients and chemo- and radiotherapy in brain tumor patients. Furthermore, neuropsychological test should be included in these studies to investigate the presence of possible correlations between t-Tau,

p-Tau$_{(181P)}$ and ß-amyloid$_{(1-42)}$ levels in CSF and long-term neurological and neuropsychological impairments caused by the disease and consequent therapies.

ACKNOWLEDGEMENTS

We are grateful to Leentje Demeyer and Cindy Catry for their excellent technical assistance.

REFERENCES

1. Andreasen N, Minthon L, Clarberg A et al. Sensitivity, specificity, and stability of CSF-tau in AD in a community-based patient sample. Neurology. 1999;53:1488-1494
2. Andreasen N, Minthon L, Davidsson P et al. Evaluation of CSF-tau and CSF-Abeta42 as diagnostic markers for Alzheimer disease in clinical practice. Arch Neurol. 2001;58:373-379
3. Galasko D, Chang L, Motter R et al. High cerebrospinal fluid tau and low amyloid beta42 levels in the clinical diagnosis of Alzheimer disease and relation to apolipoprotein E genotype. Arch Neurol. 1998;55:937-945
4. Hulstaert F, Blennow K, Ivanoiu A et al. Improved discrimination of AD patients using beta-amyloid(1-42) and tau levels in CSF. Neurology. 1999;52:1555-1562
5. Shoji M, Matsubara E, Kanai M et al. Combination assay of CSF tau, A beta 1-40 and A beta 1-42(43) as a biochemical marker of Alzheimer's disease. J Neurol Sci. 1998;158:134-140
6. Motter R, Vigo-Pelfrey C, Kholodenko D et al. Reduction of beta-amyloid peptide42 in the cerebrospinal fluid of patients with Alzheimer's disease. Ann Neurol. 1995;38:643-648
7. Galasko D. Cerebrospinal fluid levels of A beta 42 and tau: potential markers of Alzheimer's disease. J Neural Transm Suppl. 1998;53:209-221
8. Kanai M, Matsubara E, Isoe K et al. Longitudinal study of cerebrospinal fluid levels of tau, A beta1-40, and A beta1-42(43) in Alzheimer's disease: a study in Japan. Ann Neurol. 1998;44:17-26
9. Tapiola T, Pirttila T, Mikkonen M et al. Three-year follow-up of cerebrospinal fluid tau, beta-amyloid 42 and 40 concentrations in Alzheimer's disease. Neurosci Lett. 2000;280:119-122
10. Arai H, Morikawa Y, Higuchi M et al. Cerebrospinal fluid tau levels in neurodegenerative diseases with distinct tau-related pathology. Biochem Biophys Res Commun. 1997;236:262-264
11. Green AJ, Harvey RJ, Thompson EJ, Rossor MN. Increased tau in the cerebrospinal fluid of patients with frontotemporal dementia and Alzheimer's disease. Neurosci Lett. 1999;259:133-135
12. Riemenschneider M, Wagenpfeil S, Diehl J et al. Tau and Abeta42 protein in CSF of patients with frontotemporal degeneration. Neurology. 2002;58:1622-1628
13. Fabre SF, Forsell C, Viitanen M et al. Clinic-based cases with frontotemporal dementia show increased cerebrospinal fluid tau and high apolipoprotein E epsilon4 frequency, but no tau gene mutations. Exp Neurol. 2001;168:413-418
14. Hampel H, Teipel SJ. Total and phosphorylated tau proteins: evaluation as core biomarker candidates in frontotemporal dementia. Dement Geriatr Cogn Disord. 2004;17:350-354
15. Bartosik-Psujek H, Archelos JJ. Tau protein and 14-3-3 are elevated in the cerebrospinal fluid of patients with multiple sclerosis and correlate with intrathecal synthesis of IgG. J Neurol. 2004;251:414-420
16. Bartosik-Psujek H, Stelmasiak Z. The CSF levels of total-tau and phosphotau in patients with relapsing-remitting multiple sclerosis. J Neural Transm. 2005
17. Brettschneider J, Maier M, Arda S et al. Tau protein level in cerebrospinal fluid is increased in patients with early multiple sclerosis. Mult Scler. 2005;11:261-265
18. Otto M, Wiltfang J, Tumani H et al. Elevated levels of tau-protein in cerebrospinal fluid of patients with Creutzfeldt-Jakob disease. Neurosci Lett. 1997;225:210-212
19. Buerger K, Otto M, Teipel SJ et al. Dissociation between CSF total tau and tau protein phosphorylated at threonine 231 in Creutzfeldt-Jakob disease. Neurobiol Aging. 2006;27:10-15
20. Cepek L, Steinacker P, Mollenhauer B et al. Follow-up investigations of tau protein and S-100B levels in cerebrospinal fluid of patients with Creutzfeldt-Jakob disease. Dement Geriatr Cogn Disord. 2005;19:376-382
21. Otto M, Esselmann H, Schulz-Shaeffer W et al. Decreased beta-amyloid1-42 in cerebrospinal fluid of patients with Creutzfeldt-Jakob disease. Neurology. 2000;54:1099-1102

22. Riemenschneider M, Wagenpfeil S, Vanderstichele H et al. Phospho-tau/total tau ratio in cerebrospinal fluid discriminates Creutzfeldt-Jakob disease from other dementias. Mol Psychiatry. 2003;8:343-347
23. Sjogren M, Davidsson P, Wallin A et al. Decreased CSF-beta-amyloid 42 in Alzheimer's disease and amyotrophic lateral sclerosis may reflect mismetabolism of beta-amyloid induced by disparate mechanisms. Dement Geriatr Cogn Disord. 2002;13:112-118
24. Hesse C, Rosengren L, Andreasen N et al. Transient increase in total tau but not phospho-tau in human cerebrospinal fluid after acute stroke. Neurosci Lett. 2001;297:187-190
25. Shiiya N, Kunihara T, Miyatake T et al. Tau protein in the cerebrospinal fluid is a marker of brain injury after aortic surgery. Ann Thorac Surg. 2004;77:2034-2038
26. Andersson L, Blennow K, Fuchs D et al. Increased cerebrospinal fluid protein tau concentration in neuro-AIDS. J Neurol Sci. 1999;171:92-96
27. Tisell M, Tullberg M, Mansson JE et al. Differences in cerebrospinal fluid dynamics do not affect the levels of biochemical markers in ventricular CSF from patients with aqueductal stenosis and idiopathic normal pressure hydrocephalus. Eur J Neurol. 2004;11:17-23
28. Kudo T, Mima T, Hashimoto R et al. Tau protein is a potential biological marker for normal pressure hydrocephalus. Psychiatry Clin Neurosci. 2000;54:199-202
29. Holownia A, Trofimiuk E, Krawczuk-Rybak M et al. Cerebrospinal fluid excitatory amino acids and tau protein in children with acute lymphoblastic leukemia treated according to the BFM protocol. Acta Haematol. 2004;112:222-224
30. Van Gool SW, Van Kerschaver E, Brock P et al. Disease- and treatment-related elevation of the neurodegenerative marker tau in children with hematological malignancies. Leukemia. 2000;14:2076-2084
31. Vanderstichele H, Demeyer L, De Roo K et al. Standardized multiparameter quantification of biomarkers for Alzheimer's disease in cerebrospinal fluid: Medimond S.r.l., 2005:183-189
32. Olsson A, Vanderstichele H, Andreasen N et al. Simultaneous measurement of beta-amyloid(1-42), total tau, and phosphorylated tau (Thr181) in cerebrospinal fluid by the xMAP technology. Clin Chem. 2005;51:336-345
33. Reiber H. Dynamics of brain-derived proteins in cerebrospinal fluid. Clin Chim Acta. 2001;310:173-186
34. Van Gool SW, De Meyer G, Van de Voorde A et al. Neurotoxicity marker profiles in the CSF are not age-dependent but show variation in children treated for acute lymphoblastic leukemia. Neurotoxicology. 2004;25:471-480
35. Lofberg H, Grubb AO, Sveger T, Olsson JE. The cerebrospinal fluid and plasma concentrations of gamma-trace and beta2-microglobulin at various ages and in neurological disorders. J Neurol. 1980;223:159-170
36. Burkhard PR, Fournier R, Mermillod B et al. Cerebrospinal fluid tau and Abeta42 concentrations in healthy subjects: delineation of reference intervals and their limitations. Clin Chem Lab Med. 2004;42:396-407
37. Sjogren M, Vanderstichele H, Agren H et al. Tau and Abeta42 in cerebrospinal fluid from healthy adults 21-93 years of age: establishment of reference values. Clin Chem. 2001;47:1776-1781
38. Reijn TS, Rikkert MO, van Geel WJ et al. Diagnostic accuracy of ELISA and xMAP technology for analysis of amyloid beta(42) and tau proteins. Clin Chem. 2007;53:859-865
39. Binder LI, Frankfurter A, Rebhun LI. The distribution of tau in the mammalian central nervous system. J Cell Biol. 1985;101:1371-1378
40. Spillantini MG, Goedert M. Tau protein pathology in neurodegenerative diseases. Trends Neurosci. 1998;21:428-433
41. Del Bigio MR. Neuropathological changes caused by hydrocephalus. Acta Neuropathol (Berl). 1993;85:573-585

42. Del Bigio MR. Cellular damage and prevention in childhood hydrocephalus. Brain Pathol. 2004;14:317-324
43. McAllister JP, 2nd, Chovan P. Neonatal hydrocephalus. Mechanisms and consequences. Neurosurg Clin N Am. 1998;9:73-93
44. Ding Y, McAllister JP, 2nd, Yao B et al. Axonal damage associated with enlargement of ventricles during hydrocephalus: a silver impregnation study. Neurol Res. 2001;23:581-587
45. Weller RO, Williams BN. Cerebral biopsy and assessment of brain damage in hydrocephalus. Arch Dis Child. 1975;50:763-768
46. Rostasy K, Withut E, Pohl D et al. Tau, phospho-tau, and S-100B in the cerebrospinal fluid of children with multiple sclerosis. J Child Neurol. 2005;20:822-825
47. Andreasen N, Vanmechelen E, Van de Voorde A et al. Cerebrospinal fluid tau protein as a biochemical marker for Alzheimer's disease: a community based follow up study. J Neurol Neurosurg Psychiatry. 1998;64:298-305
48. Ishiguro K, Ohno H, Arai H et al. Phosphorylated tau in human cerebrospinal fluid is a diagnostic marker for Alzheimer's disease. Neurosci Lett. 1999;270:91-94
49. Blennow K, Vanmechelen E, Hampel H. CSF total tau, Abeta42 and phosphorylated tau protein as biomarkers for Alzheimer's disease. Mol Neurobiol. 2001;24:87-97
50. Kohnken R, Buerger K, Zinkowski R et al. Detection of tau phosphorylated at threonine 231 in cerebrospinal fluid of Alzheimer's disease patients. Neurosci Lett. 2000;287:187-190
51. Goedert M. Tau protein and the neurofibrillary pathology of Alzheimer's disease. Trends Neurosci. 1993;16:460-465
52. Blennow K, Hampel H. CSF markers for incipient Alzheimer's disease. Lancet Neurol. 2003;2:605-613
53. Blennow K, Vanmechelen E. CSF markers for pathogenic processes in Alzheimer's disease: diagnostic implications and use in clinical neurochemistry. Brain Res Bull. 2003;61:235-242
54. Parnetti L, Lanari A, Amici S et al. CSF phosphorylated tau is a possible marker for discriminating Alzheimer's disease from dementia with Lewy bodies. Phospho-Tau International Study Group. Neurol Sci. 2001;22:77-78
55. Schoonenboom NS, Mulder C, Vanderstichele H et al. Effects of processing and storage conditions on amyloid beta (1-42) and tau concentrations in cerebrospinal fluid: implications for use in clinical practice. Clin Chem. 2005;51:189-195

Chapter 7

Various Components of the Insulin-like Growth Factor System in Tumor Tissue, Cerebrospinal Fluid and Peripheral Blood of Pediatric Medulloblastoma and Ependymoma Patients

Judith M. de Bont[1], Jaap van Doorn[2], Roel E. Reddingius[1], Gerard H.M. Graat[2], Monique M.C.J. Passier[1], Monique L. den Boer[1], Rob Pieters[1]

[1]Erasmus MC – Sophia Children's Hospital - University Medical Center Rotterdam – Department of Pediatric Oncology and Hematology, The Netherlands
[2]University Medical Center Utrecht – Dept. of Metabolic and Endocrine Diseases and Laboratory of Clinical Chemistry and Hematology, The Netherlands

Int J Cancer 2008; **123***(3):594-600*

ABSTRACT

The insulin-like growth factor (IGF) system plays an important role in neuronal development and may contribute to the development of brain tumors. In this study we studied mRNA expression levels of insulin-like growth factors (IGFs), insulin-like growth factor binding proteins (IGFBPs) and insulin-like growth factor receptors (IGFRs) in 27 pediatric medulloblastomas, 13 pediatric ependymomas and 5 control cerebella. Compared to normal cerebellum, mRNA levels of IGFBP-2 and IGFBP-3 were significantly increased in medulloblastomas and ependymomas. IGFBP-2 expression was indicative of poor prognosis in medulloblastomas, whereas IGFBP-3 mRNA levels were especially high in anaplastic ependymomas. IGFBP-5 and IGF-2 mRNA levels were significantly increased in ependymomas compared to control cerebellum. Protein expression levels of IGFs and IGFBPs were analyzed in the cerebrospinal fluid (CSF) of 16 medulloblastoma, 4 ependymoma and 23 control patients by radio-immuno assay to determine if they could be used as markers for residual disease after surgery. No aberrant CSF protein expression levels were found for ependymoma patients. In medulloblastoma patients, the IGFBP-3 protein levels were significantly higher than in ependymoma patients and controls. Moreover, enhanced levels of proteolytic fragments of IGFBP-3 were found in the CSF of medulloblastoma patients, being in concordance with a significantly increased IGFBP-3 proteolytic activity in the CSF of these patients. In conclusion, our data suggest that the IGF system is of importance in pediatric medulloblastomas and ependymomas. Larger studies should be conducted to validate the predictive values of the levels of intact IGFBP-3 and proteolytic fragments in CSF in the follow up of medulloblastomas.

INTRODUCTION

Medulloblastoma is one of the most common malignant pediatric central nervous system (CNS) tumors and accounts for approximately 20-25% of all malignant intra-cranial neoplasms in childhood[1]. It arises in the posterior fossa and has a tendency to metastasize within the CNS[2]. Ependymomas make up about 10% of childhood tumors of the CNS. They usually arise from the floor of the fourth ventricle, resulting in a tumor in the posterior fossa, but they can also occur in the spinal cord[2].

The insulin-like growth factor (IGF) system plays an important role in the regulation of the development and growth of the CNS[3], but also that of medulloblastoma and ependymoma[4-8]. This complex system consists of two mitogenic and anti-apoptotic peptides, IGF-1 and IGF-2, two IGF-receptors (IGF-1R and IGF-2R), six IGF binding proteins (IGFBP1-6), several IGFBP cell surface receptor proteins and IGFBP proteases[9]. IGF-1 is the most potent neurotrophic factor of the IGF family[3, 10]. In a previous study, we demonstrated the abundant expression of IGF-1 mRNA by medulloblastoma tumor cells[7]. Nine out of 14 tumors also showed variable but significant IGF-2 expression in a sub-population of Ki-M1P positive cells that were identified as microglia cells with a ramified morphology[7]. IGF-2 was overexpressed in medulloblastoma, predominantly the desmoplastic subtype, which is characterized by activated SHH signaling[11, 12]. IGF-2 overexpression was also observed in ependymomas[12]. Furthermore, a considerable part of medulloblastomas expresses the phosphorylated active form of the IGF-1R[5]. The presence of phosphorylated downstream intermediates also points to active IGF-1R signaling in these tumors. IGFBPs are involved in targeting and modulating IGF action. Various brain tumors, e.g. gliomas, astrocytomas and meningeomas are able to produce IGFBPs[13, 14].

In the present study we aimed at evaluating the importance of the IGF-system in pediatric medulloblastomas and ependymomas by comparing mRNA expression levels of IGFs, IGF-receptors (IGF-1R and IGF-2R) and various IGFBPs (i.e. IGFBP-2, IGFBP-3, IGFBP-4 and IGFBP-6) between medulloblastomas and ependymomas and normal cerebellum.

In both medulloblastoma and ependymoma patients, the extent of surgical resection is an important prognostic factor for survival, but surgery alone is often not sufficient to cure patients[15, 16]. Residual tumor cells may give rise local recurrence and especially in medulloblastomas they often spread into the cerebrospinal fluid (CSF). We hypothesized that these residual tumor cells still produce and secrete IGFs and IGFBPs, which may be detected in the cerebrospinal fluid. Indeed, increased levels of IGFBP-2 and IGFBP-3 in the cerebrospinal fluid (CSF) of patients with malignant brain tumors have been reported[17, 18]. Therefore, in addition to the analysis of the various components of the IGF-system in tumor tissue, we determined the levels of IGF-1, IGF-2, pro-IGF-2E[68-88], several IGFBPs and IGFBP-3 protease activity in the CSF of pediatric medulloblastoma and ependymoma patients after tumor resection, in order to determine if these proteins can serve as predictive markers for minimal residual disease.

PATIENTS AND METHODS

Patient samples

To study mRNA expression levels of the various components of the IGF system in tumor material of pediatric medulloblastoma and ependymoma patients, we used our previously described microarray dataset[19]. This dataset contains mRNA expression data of 40 fresh

Table 1. Protein levels of IGFBP-2, IGFBP-3, IGFBP-4, IGFBP-6, pro-IGF-IIE[68-88], IGF-1, IGF-2 and IGFBP-3 protease activity in the cerebrospinal fluid of control, medulloblastoma and ependymoma patients (A) and peripheral blood of medulloblastoma and ependymoma patients (B).

The displayed values are median concentrations of each parameter per subgroup. For measurements of protein levels of IGFs and IGFBPs in peripheral blood of medulloblastoma and ependymoma patients, standard deviation scores (SDS) are displayed.

* significantly different (p<0.05) from control

significantly different (p<0.05) between medulloblastoma and ependymoma

A.	Control (n=23)		Medulloblastoma (n=16)		Ependymoma (n=4)	
CSF	**median**	***range***	**median**	***range***	**median**	***range***
IGFBP-2 (ng/ml)	131.0	*76.5 ; 176.0*	163.3#	*64.8 ; 583.0*	86.5*#	*49.0 ; 118.0*
IGFBP-2 (ng/mg protein)	214.5	*123.5 ; 333.8*	204.4	*93.9 ; 474.0*	158.1*	*87.0 ; 200.0*
IGFBP-3 (ng/ml)	8.8	*3.4 ; 14.0*	27.6*#	*7.4 ; 27.6*	8.8#	*6.4 ; 13.8*
IGFBP-3 (ng/mg protein)	13.9	*5.2 ; 25.6*	38.1*#	*11.6 ; 88.8*	17.4#	*8.3 ; 26.0*
IGFBP-4 (ng/ml)	20.3	*10.9 ; 30.0*	33.4*	*10.4 ; 81.0*	16.7	*10.5 ; 25.4*
IGFBP-4 (ng/mg protein)	33.2	*16.0 ; 54.5*	39.1	*24.0 ; 165.3*	33.1	*15.3 ; 42.3*
IGFBP-6 (ng/ml)	61.0	*36.0 ; 118.0*	80.0*	*45.0 ; 271.0*	74.5	*29.0 ; 135.0*
IGFBP-6 (ng/mg protein)	96.8	*52.9 ; 214.5*	105.3	*53.4 ; 234.9*	131.8	*70.7 ; 181.1*
pro-IGF-II (ng/ml)	3.9	*1.6 ; 10.0*	5.1	*2.5 ; 9.6*	3.0	*2.2 ; 4.1*
pro-IGF-II (ng/mg protein)	6.5	*2.3 ; 18.2*	7.0	*2.8 ; 13.5*	6.0	*2.8 ; 7.7*
IGF-1 (ng/ml)	1.2	*0.9 ; 2.1*	1.5	*0.6 ; 4.6*	1.1	*0.5 ; 1.2*
IGF-1 (ng/mg protein)	2.0	*1.4 ; 3.5*	1.8	*1.3 ; 3.8*	1.7	*1.2 ; 2.2*
IGF-2 (ng/ml)	9.1	*6.1 ; 14.8*	9.5	*4.8 ; 29.6*	6.9	*5.2 ; 10.9*
IGF-2 (ng/mg protein)	15.6	*11.1 ; 24.3*	13.9	*6.1 ; 30.3*	14.0	*7.3 ; 18.2*
IGFBP3 protease activity	22.0	*15.0 ; 31.0*	38.0*#	*24.0 ; 55.0*	27.5#	*24.0 ; 38.0*
IGFBP3 protease activity (per mg protein)	38.3	*25.8 ; 59.6*	48.3*	*17.9 ; 97.7*	50.9	*37.7 ; 71.7*

B.	Medulloblastoma (n=15)		Ependymoma (n=4)	
Peripheral blood	**median**	***range***	**median**	***range***
IGFBP-2 (SDS)	0.4	*-3.7 ; 3.1*	-2.1	*-1.6 ; -2.8*
IGFBP-3 (SDS)	0.1	*-3.8 ; 1.4*	-0.1	*-0.1 ; -0.6*
IGFBP-4 (SDS)	-0.7	*-2.1 ; 0.8*	-1.1	*-0.6 ; -1.5*
IGFBP-6 (SDS)	-0.7	*-1.9 ; 0.4*	-1.4	*-2.4 ; -0.3*
pro-IGF-II (SDS)	0.07	*-1.4 ; 1.3*	-0.1	*-2.5 ; 0.1*
IGF-1 (SDS)	0.5	*-0.9 ; 2.6*	1.3	*-0.1 ; 2.5*
IGF-2 (SDS)	1	*-0.6 ; 2.0*	0.9	*-2.7 ; 1.6*

frozen tumor samples from 25 medulloblastomas at diagnosis (21 classic, 2 desmoplastic and 2 large cell/anaplastic medulloblastoma), 2 medulloblastomas at relapse (1 classic and 1 large cell/anaplastic medulloblastoma), 11 ependymomas at diagnosis (4 cellular ependymomas and 7 anaplastic ependymomas), 2 ependymomas at relapse (1 cellular and 1 anaplastic ependymoma) and 5 control cerebella. Since no cerebellum from previously healthy pediatric patients was available, we used cerebellum from adult patients who did not have a history of a malignancy of the central nervous system.

For 9 of the newly diagnosed medulloblastomas (7 classic, 1 desmoplastic and 1 large cell/anaplastic) 1 large cell/anaplastic medulloblastoma at relapse and 3 of the newly diagnosed ependymomas (1 cellular ependymoma, 2 anaplastic ependymomas) included in the microarray study, diagnostic lumbar CSF was available to assess the levels of IGF-1, IGF-2, pro-IGFIIE[68-88], which contains the first 21 amino acids of the E-domain, IGFBP-2, IGFBP-3, IGFBP-4, IGFBP-6 and IGFBP-3 protease activity (Table 1). These parameters were also determined in lumbar CSF from 6 additional patients with medulloblastomas (5 classic and 1 desmoplastic) and 1 patient with a cellular ependymoma from whom no fresh frozen material was available for microarray analysis.

CSF from was obtained from the medulloblastoma and ependymoma patients by performing a lumbar puncture approximately 2 weeks after tumor resection, before starting chemo- and/or radiotherapy. Control lumbar CSF samples (n=23) were obtained from age and gender matched patients previously treated for acute lymphoblastic leukemia, 1 year after ending cytostatic treatment (and thus being in complete remission for more than 2.5 years)(Table 1). At least 3 ml of CSF was collected in polypropylene tubes and immediately centrifuged at 250xg to remove cellular debris. Cytospins were made to evaluate cytology. Supernatant was collected and aliquots stored at -80°C until analysis. Simultaneously with the collection of the CSF samples, peripheral blood samples were obtained from 15 of the

16 medulloblastoma and the 4 ependymoma patients for the determination of the levels of IGFs, IGFBPs and the IGFBP-3 protease activity (serum). Unfortunately, no matched peripheral blood samples were available for the control patients. All CSF and blood samples were collected at the Erasmus MC – University Medical Center – Sophia Children's Hospital in Rotterdam, the Netherlands. Each patient or patient's parents gave informed consent prior to enrollment.

RNA extraction, labeling and hybridization and microarray analysis

Before RNA extraction, 4 µm cryosections were prepared and hematoxiline-eosine (HE) stained to confirm tumor histology. RNA from fresh frozen tumor tissue for gene expression profiling was prepared as described previously[19]. In brief, total RNA was isolated using TRizol reagent (Invitrogen, Breda, the Netherlands) according to the manufacturer's protocol with minor modifications[20] and the quality was checked using the Agilent 2100 Bioanalyzer (Agilent, Santa Clara, USA). Production of biotinylated antisense cRNA and hybridization of the labeled cRNA to Human Genome U133 plus 2.0 GeneChip oligonucleotide microarrays (Affymetrix, Santa Clara, USA) was performed according to manufacturer's protocols. All arrays included in the analysis had a 3′ to 5′ GAPDH ratio < 3.0.

Determination of IGF and IGFBP protein levels and IGFBP-3 proteolysis in CSF and peripheral blood

Protein contents of the CSF and peripheral blood were determined by a BCA protein assay (Pierce, Rockford, USA). Levels of IGF-1, total IGF-2, pro-IGF-IIE[68-88], IGFBP-1, -2, -3, -4, and -6 in CSF and plasma were all measured in duplicates in the Laboratory of Clinical Chemistry and Haematology (UMC Utrecht), by specific radio-immunoassays (RIAs) as described previously[21-26].

IGFBP-3 proteolysis in patient sera and CSF was assessed in duplicate as described by Koedam et al.[27]. In brief: either 2 µL of serum or 50µL of CSF, was mixed with 40,000 cpm ^{125}I- labeled E-coli derived (non-glycosylated) recombinant hIGFBP-3 in a total volume of 30 or 100 µL, respectively, 100 mM Tris-HCL buffer (pH 7.4) containing 0.5 mM $CaCl_2$ and 1% w/v Triton X-100. The mixture was incubated for 18 h at 37^{o}C and the reaction was stopped by the addition of 100µL SDS-sample buffer containing 10 % v/v 2-mercaptoethanol. The samples were subjected to SDS-PAGE. The intact ~35 kD recombinant hIGFBP-3 and its lower molecular weight proteolysis fragments were visualized and analyzed by the Molecular Imager System GS-363 of Bio-Rad (Veenendaal, the Netherlands). The extent of proteolysis in each lane was assessed by dividing the degradation products of IGFBP-3 by the total intensity of the signal in the lane, and expressed as a percentage. In addition, the results were compared with the amount of IGFBP-3 proteolytic activity in normal pooled serum of healthy individuals and third trimester pregnancy serum (which exhibits a high IGFBP-3 protease activity).

Western blotting

CSF samples (~9.7 µg of protein) were subjected to 10% Tris-glycine SDS PAGE. After transferring proteins to a nitrocellulose membrane at 140 V for 90 minutes at 4°C using a wet transfer system (Bio-Rad, Veenendaal, The Netherlands) and blocking with block buffer (5% nonfat milk in 0.2% tween-20 in PBS) for 30 minutes, the membrane was incubated overnight at 4°C with rabbit polyclonal anti-IGFBP-3 antibodies (Biodesign International, Saco, USA) diluted (1:400) in block buffer. The membrane was washed with 0.2% tween-20 in PBS and incubated for one hour at room temperature with anti-mouse IgG horseradish peroxidase conjugate (DakoCytomation, Glostrup, Denmark) diluted (1:500) in block buffer containing 2% pooled human serum. Detection solution (SuperSignal West Femto Maximum Sensitivity Substrate; Pierce, Rockford, USA) was prepared according to the manufacturer's instructions. Chemiluminescence was measured using the Syngene chemigenius (Syngene, Cambridge, United Kingdom).

Statistical analysis

Microarray expression data were analyzed using R version 2.4.0 as described earlier[19]. In short, raw data were normalized using the variance stabilization procedure (vsn)[28]. Gene expression levels of the IGF-1R, IGF-2R, IGF-1, IGF-2 and IGFBP-1-6 in medulloblastoma, ependymoma and control cerebellum tissue were statistically compared using the Wilcoxon test and corrected for multiple testing errors by applying the false discovery rate (FDR) described by Benjamini and Hochberg[29] (MULTTEST package). A FDR <5% was considered statistically significant, meaning that less than 5% of the significant genes are false positives.

The non-parametric Mann-Whitney U-test was used for statistical comparison of the concentrations of the various components of the IGF system in CSF between groups. For correlation analysis the non-parametric Spearman test was used. Levels of the IGFs and IGFBPs in plasma were expressed as SDS, using specific LMS reference curves based on the respective normative data which have been published previously[24-26].

A cox regression analysis was performed to investigate whether the levels of mRNA expression of the various parameters of the IGF-system in tumor tissue and those of protein in CSF were predictive for survival. For each parameter, a hazard ratio was calculated. An effect was considered statistically significant if p was ≤ 0.05. A hazard ratio <1 indicated a favorable influence on overall survival and a hazard ratio >1 indicated an unfavorable influence on overall survival. Overall survival was defined as time from diagnosis until death or last contact.

Statistical analyses of the data for CSF, peripheral blood and the survival analyses were performed with the Statistical Package of the Social Sciences (SPSS version 11.0).

RESULTS

Microarray gene expression analysis

Gene expression data were available for 27 medulloblastoma, 13 ependymoma and 5 control cerebellum samples. Twenty-nine probe sets present on the Affymetrix Human Genome U133 plus 2.0 arrays corresponded to components of the IGF-system, i.e. IGF-1R (n=7), IGF-2R (n=2), IGF-1 (n=4), IGF-2 (n=2), IGFBP-1 (n=2), IGFBP-2 (n=1), IGFBP-3 (n=2), IGFBP-4 (n=2), IGFBP-5 (n=6), and IGFBP-6 (n=1). Compared to normal cerebellum tissue, mRNA expression levels of IGFBP-2 and IGFBP-3 were significantly higher in both medulloblastomas and ependymomas (Figure 1). IGFBP-2 mRNA expression levels in ependymomas were significantly higher than those encountered for medulloblastomas (Figure 1). IGFBP-5 and IGF-2 mRNA levels were significantly higher in ependymomas compared to medulloblastomas and normal cerebellum (Figure 1). For the expression levels of the other parameters investigated, no significant differences were noted between normal cerebellum, medulloblastomas and ependymomas.

We did not observe significant differences in gene expression levels between the different histologically defined subtypes of medulloblastoma. IGFBP-3 expression levels were significantly higher in anaplastic ependymomas compared to cellular ependymomas (p=0.019). Six of the 27 medulloblastoma patients had radiological visible metastases in the central nervous system and IGFBP-3 mRNA levels were significantly higher in these patients compared to the patients without metastases (p=0.041). None of the ependymoma patients included in this study presented with metastasized disease.

The predictive impact of the gene expression levels of the components of the IGF system was tested by cox regression analysis. Higher IGFBP-2 mRNA expression levels were associated with unfavorable overall survival in medulloblastoma patients (p=0.037; hazard ratio 1.38). We also observed a trend towards less favorable prognosis with increasing IGF-1 expression levels in medulloblastoma patients (p-values for the two "_at probe sets" corresponding to IGF-1 were p=0.046 and 0.070, respectively, with a mean hazard ratio of 1.40). For ependymomas, none of the parameters of the IGF-system had significant impact on overall survival rates.

Concentrations of IGFs and IGFBPs in CSF and plasma

The concentrations of the IGFs, the various IGFBPs and the IGFBP-3 protease activity expressed per ml CSF are depicted in Table 1. IGFBP-1 levels in CSF were below detection limit of the assay (i.e. < 5 ng/mL). Levels of IGFBP-3 were significantly increased in the CSF of medulloblastoma patients compared to controls (p<0.0010) and ependymoma patients (p=0.016). Levels of IGFBP-4 and IGFBP-6 were significantly increased in medulloblastoma patients compared to controls (p=0.011 and p=0.010, respectively), but did not differ significantly (p>0.05) between ependymomas and controls nor between medulloblastoma and ependymoma.

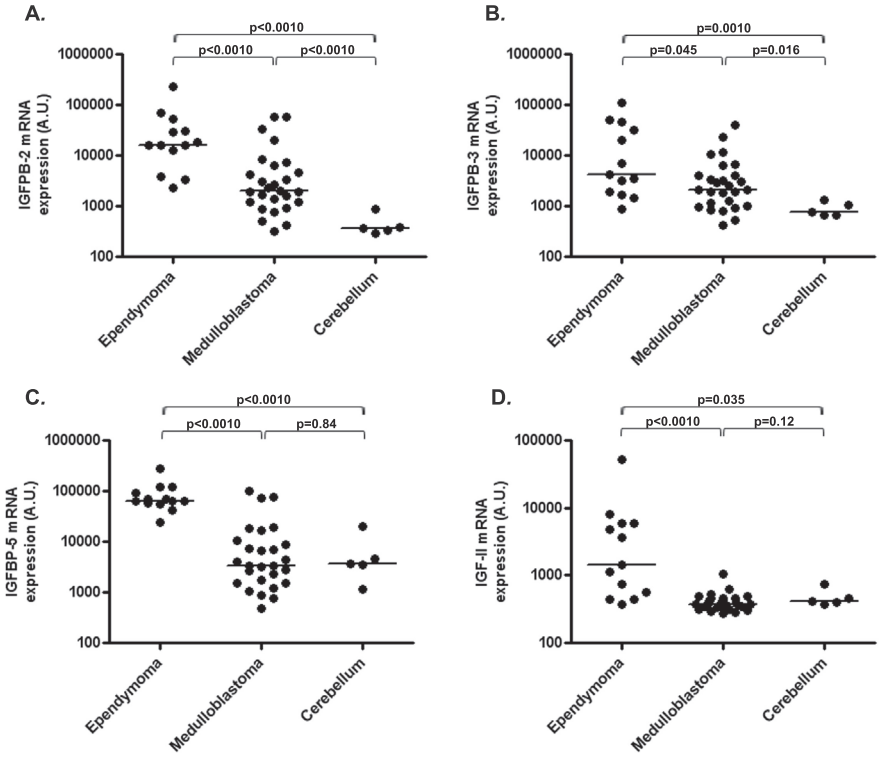

Figure 1. mRNA expression of IGFBP-2 (A.), IGFBP-3 (B.), IGFBP-5 (C.) and IGF-2 (D.) in ependymoma, medulloblastoma and cerebellum
mRNA expression levels were obtained by Affymetrix HGU133 plus 2.0 arrays.
A.U. = arbitrary units

Since the levels of the parameters of the IGF-system studied and the total protein contents of the various CSF samples were significantly correlated, data were also expressed per mg of protein (Table 1). IGFBP-3 levels, when expressed per mg of protein, were still significantly elevated in the CSF of patients with a medulloblastoma compared to those in CSF from control subjects and ependymoma patients. However, when CSF levels of IGFBP-2, IGFBP-4, IGFBP-6, pro-IGF-II[68-88] IGF-1 and IGF-2 were corrected for total protein contents, for all these parameters no significant differences were observed between controls, medulloblastoma or ependymoma patients.

CSF samples were obtained 2 weeks after tumor resection. Only 2 patients were in complete remission after surgery, having no residual tumor or metastatic disease at the post-operative images. We did not observe a significant difference in CSF protein levels of the IGFs and the IGFBPs between the patients in complete remission and those with residual tumor.

CSF protein expression levels of the measured members of the IGF system were not significantly different between the medulloblastoma subtypes or between patients with

and without malignant cells in their CSF. None of the ependymoma patients had detectable malignant cells in their CSF.

Both the uncorrected and protein-corrected CSF expression levels of the analyzed proteins were not significantly correlated with overall survival in medulloblastoma. Numbers of ependymoma patients were too small to evaluate the impact of protein expression on survival.

For the brain tumor patients, IGFs and IGFBPs were also quantified in plasma (Table 1). The concentrations of these parameters were not significantly different between patients with a medulloblastoma and those with an ependymoma. To make a comparison with normal reference values, standard deviation scores from the corresponding age and gender specific normative ranges were calculated for all variables studied. IGFBP-2 levels in plasma were decreased (<-2 SDS) in 3 ependymoma patients and 2 medulloblastoma patients, whereas 2 medulloblastoma patients exhibited increased (>2 SDS) values. Circulating levels of IGFBP3 were within the normal ranges (i.e. between –2 and 2 SDS) for all patients, except for 2 medulloblastoma patients, who showed decreased (<-2 SDS) IGFBP-3 levels. Two medulloblastoma and two ependymoma patients had increased plasma IGF-1 levels, whereas those of pro-IGF-IIE[68-88] were increased >2 SDS in an ependymoma patient. Plasma levels of IGF-2, IGFBP-4 and IGFBP-6 were within the normal range for all patients. For the various IGFs and IGFBPs studied no significant correlations existed between plasma values and the corresponding levels in CSF.

Western blot analysis of IGFBP-3 in CSF

IGFBP-3 was detectable by Western blotting of CSF and showed an increased expression of the intact IGFBP-3 protein (~43 kD) in medulloblastoma patients compared to control patients (Figure 2). Moreover, we observed overexpression of a proteolytic fragment of IGFBP-3 (~15 kD) in the CSF of medulloblastoma patients (Figure 2), which is in concordance with an increased IGFBP-3 proteolytic activity in CSF of medulloblastoma patients.

IGFBP-3 protease activity in CSF and serum

CSF from both controls and patients with medulloblastoma or ependymoma generated several proteolytic fragments of non-glycosylated rhIGFBP-3 that migrated on reduced SDS-PAGE at <10, 18, 22 and 25 kD with varying intensities. The band patterns were essentially similar as that observed for sera (data not shown). IGFBP-3 protease activity was significantly increased in the CSF of medulloblastoma patients compared to the activity encountered in the CSF of either controls ($p<0.0010$) or ependymoma patients ($p=0.046$) (Table 1). When expressed per mg of protein, IGFBP-3 protease activity still was significantly elevated ($p=0.027$) in medulloblastoma compared to control CSF, but the difference between CSF of medulloblastomas and ependymomas did not reach statistical significance.

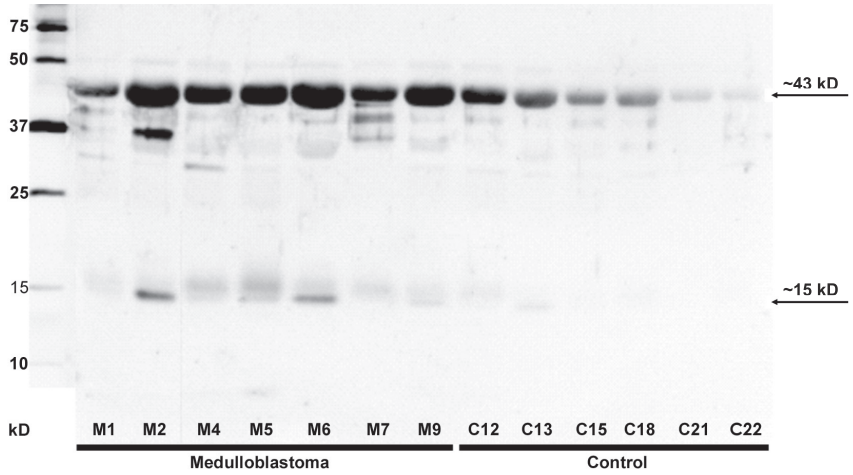

Figure 2. Western blot analysis of IGFBP-3
Figure 2 shows a representative picture of the IGFBP-3 Western blot analysis of CSF. The intact IGFBP-3 protein (~43 kD) and a proteolytic fragment of IGFBP3 (~15 kD) showed increased expression in the CSF of medulloblastoma patients compared to CSF of controls.

The extent of IGFBP-3 proteolysis as determined in several sera of patients with a medulloblastoma (n=10) or ependymoma (n=2) was similar to that observed for pooled normal human control serum (data not shown).

DISCUSSION

The IGF system is known to play an important role in the development of the CNS and is suggested to be involved in the pathogenesis of brain tumors[3, 9, 14]. This is the first study describing gene expression levels of the IGFs, IGFBPs and the IGF receptors in combination with the levels of these proteins in the CSF of pediatric medulloblastomas and ependymomas.

Overexpression of the IGF-1R has been described in several types of cancer[9] and the IGF-2R has been suggested to be a tumor suppressor, being mutated in a variety of malignancies[30]. However, in our study, mRNA levels of both IGF-1R and IGF-2R in the pediatric medulloblastoma and ependymoma tissue samples were not different from those found in normal cerebellum. It must be emphasized, however, that this finding does not exclude an increased activation of the IGF-1R, which is merely reflected by its phosphorylation status. Indeed, besides increased IGF-1R protein expression, Del Valle et al.[5] showed that 60% of the medulloblastomas expressed the phosphorylated form of the IGF-1R. The occurrence of active downstream signaling through the IGF-1R was confirmed by the observation that phosphorylated intermediates of the signaling cascade, such as Erk-1, Erk-2 and Akt/PKB could also be detected in these medulloblastomas.

IGF-2 is an important growth factor in the development of the CNS[3]. Aberrant IGF-2 expression and abnormal imprinting of the IGF-2 gene have been observed in various tumors, including several types of brain tumors[9]. IGF-2 is suggested to be a downstream target of Sonic hedgehog (SHH) signaling[31] and was overexpressed in desmoplastic medulloblastomas[11], in which SHH signaling is frequently activated. SHH and IGF-2 had a synergistic effect on the proliferation of cerebellar granule precursors and induced increased downstream target expression (Gli1 and Cyclin D1)[32, 33]. We did not observe increased expression of IGF-2 and the SHH downstream SHH targets Gli1 and cyclin D1 in the medulloblastomas in our study, but it must be emphasized that only 2 desmoplastic medulloblastomas were included in our study. The overexpression of IGF-2 in ependymoma cells as found in the present study and also demonstrated by others[12], would suggest a role for IGF-2 in the regulation of proliferation of this type of tumour. The production of relatively high amounts of IGF-2 by ependymoma tumor cells may promote tumor progression. mRNA levels of IGFBP-2 were increased in both medulloblastomas and ependymomas compared to normal cerebellum. Moreover, ependymomas exhibited increased levels of IGFBP-5. In glioblastoma, both IGFBP-2 and IGFBP-5 expression correlated with tumor grade[34, 35] and enhancement of tumor invasion[36, 37]. In concordance, we found IGFBP-2 expression to be indicative of poor overall survival in medulloblastoma patients. Fukushima et al.[36] showed that silencing of IGFBP-2 gene expression in glioblastoma cells resulted not only in decreased invasiveness, decreased saturation density of the cells in vitro and decreased tumorigenicity in nude mice, but also in reduced expression of CD24, a gene associated with tumor-progression. Interestingly, Boon et al[38] found CD24 to be significantly overexpressed in medulloblastoma compared to cerebellum. In our microarray dataset we also found significant overexpression of CD24 mRNA together with overexpression of IGFBP-2 in both medulloblastoma and ependymoma compared to control tissue (data not shown). However, a significant correlation between expression levels of CD24 and IGFBP-2 was not found, suggesting that a potential interaction between the two genes (as was observed in glioblastoma[36]), if any, must be more complex. IGFBP-5 exerts an anti-apoptotic effect, leading to enhanced cell survival[39], being important in the development of various malignancies[40-42]. Accordingly, the overexpression of IGFBP5 in ependymomas as observed in our study may play a role in prolonging the cell survival of these tumors. Decreasing IGFBP-5 gene expression, e.g. by treatment with antisense IGFBP-5 mRNA, as has been performed in prostate cancer models[41], could provide more information about the role of IGFBP-5 in pediatric ependymomas.

IGFBP-3 mRNA expression levels were increased in both medulloblastomas and ependymomas compared to normal cerebellum. IGFBP-3 possesses both pro-apoptotic and anti-apoptotic properties[43-45]. The contradictionary roles of IGFBP-3 may suggest that the function of IGFBP-3 is tissue-specific. As gene expression levels of IGFBP-3 were significantly higher in high-grade anaplastic ependymomas compared to low-grade cellular ependymo-

mas, this would suggest that the anti-apoptotic and proliferative effects predominate in ependymomas.

IGFBP-3 expression can be regulated by the tumor suppressor genes PTEN and p53[46, 47]. Regarding mRNA expression levels of the latter genes (data from our Affymetrix microarray analysis on medulloblastoma and ependymoma[19]) in the tumors included in our study, we found a significant correlation between p53 and IGFBP-3 mRNA expression (R_s=0.38; p=0.0050). PTEN mRNA expression levels did not correlate with IGFBP-3 mRNA expression, which may be explained by the fact that the activity of PTEN can also be regulated on the protein level by post-translational modifications, such as phosphorylation. IGFBP-3 promoter methylation has also been shown to be important in the regulation of IGFBP-3 expression[48].

In contrast to the increased mRNA expression levels of IGFBP-2 and IGFBP-3 in medulloblastomas and increased expression of IGFBP-2, IGFBP-3, IGF-2 and IGFBP-5 in ependymomas, we did not observe concordant aberrant protein levels in the CSF of these patients. The finding that the levels of the various components of the IGF-system in the CSF of ependymoma patients were comparable with those in the CSF of controls may be reflected by the fact that ependymoma tumor cells do not have a tendency to spread via the CSF. Thus, IGF-2, IGFBP-2 and IGFBP-5 may only exert their effects locally by inducing tumor growth via paracrine or autocrine mechanisms, thereby not reaching the CSF.

In contrast to ependymomas, medulloblastoma tumor cells are known for frequent spread via the cerebrospinal fluid[2]. However, despite the fact that medulloblastoma tumor cells show increased IGFBP-2 expression levels, we did not observe increased IGFBP-2 levels in the CSF of medulloblastoma patients. A lack of correlation between mRNA and protein expression levels can be caused by the instability of mRNA or protein or high turnover of protein. In contrast to our results, Müller et al.[18] observed elevated levels of IGFBP-2 in the CSF of brain tumor patients. As they did not consequently correct for the total protein content of CSF, it cannot be excluded that their observation may be explained by non-specific protein elevation, due to leakage through the blood brain barrier.

In contrast to IGFBP-2, increased IGFBP-3 mRNA expression levels in medulloblastoma tissue were accompanied by increased IGFBP-3 protein levels in the CSF of the majority of medulloblastoma patients. IGFBP-3 is only a minor component of the CSF of healthy subjects, but may be increased in pathological states such as CNS tumors (e.g. medulloblastoma)[17], and acute lymphoblastic leukemia[17, 49]. Levels of IGFBP-3 were normal in CSF from subjects suffering from meningitis, amyotrophic lateral sclerosis, or multiple sclerosis[17, 50, 51]. IGFBP-3 is thought to be predominantly synthesized in the liver and is the major IGFBP in the blood circulation[52]. Hence, the relatively high IGFBP-3 levels in the CSF of medulloblastoma patients could have been caused by the leakage of circulating IGFBP-3 through a disrupted blood brain barrier. Indeed, patients with a medulloblastoma often exhibit a disrupted blood brain barrier and we observed a significant correlation between IGFBP-3 levels and total CSF protein. However, IGFBP-3 levels in CSF from medulloblastoma patients remained elevated

after correction for total protein content. Moreover, plasma levels of IGFBP-3 were within the normal range for most patients and no significant correlation was found between the IGFBP-3 concentrations in the CSFs and the corresponding plasma samples. For all patients, the CSF samples were obtained routinely 2 weeks after tumor resection. Therefore, it cannot be entirely excluded that the increased IGFBP-3 levels in the CSF of medulloblastoma patients are the result of surgery-induced changes. However, both medulloblastomas and ependymomas were found at the same location, the posterior fossa, and surgical complete resection is essential in both tumors. Therefore, the surgical approach and procedure have been comparable in these patients. IGFBP-3 levels in the CSF of ependymoma patients were normal, and from these results we can deduce that CSF IGFBP-3 levels are not influenced by surgery or post-operative reactive changes. Because of the similarities in tumor location and surgical procedure between medulloblastomas and ependymomas, it can also be considered to be very unlikely that the IGFBP-3 levels in the CSF of medulloblastoma patients are influenced significantly by surgically induced changes.

All together, combined with our finding that IGFBP-3 mRNA expression levels were increased in medulloblastoma tumor tissue, especially metastasized medulloblastoma, these data suggest that the increased IGFBP-3 levels in the CSF of medulloblastoma patients are caused by IGFBP-3 production by residual medulloblastoma tumor cells. Unfortunately, the extent of tumor resection on CSF protein levels of IGFs and IGFBPs was difficult to evaluate in our study, as only 2 patients were in complete remission when the CSF was obtained. IGFBP-3 levels were also increased in the patients who were in radiological complete remission, which suggests the presence of residual tumor cells that were not visible with current radiological techniques.

Interestingly, not only the intact IGFBP-3 protein, but also the IGFBP-3 fragments were up-regulated in the CSF of medulloblastoma patients, which would be in agreement with the data on IGFBP-3 proteolysis. It may be that the tumor itself produces IGFBP-3 proteases resulting in an increased amount of IGFBP-3 fragments being able to influence its own growth, as the IGFBP-3 proteolytic fragments have shown to exert distinct biological functions[53, 54]. Moreover, the affinity of proteolyzed IGFBP-3 for the mitogenic IGFs is lower than that of intact IGFBP-3, which may result in increased availability of IGFs as growth factor for the tumor cells.

In conclusion, overexpression of IGFBP-2 and IGFBP-3 in both medulloblastomas and ependymomas and overexpression of IGFBP-5 and IGF-2 in the latter, suggests that the IGF system is important in the biology of these pediatric brain tumors. Protein CSF expression levels of these genes were not useful in ependymomas, but the increased IGFBP-3 levels and IGFBP-3 proteolytic activity in the CSF of medulloblastomas, suggests IGFBP-3 to be a potential marker of residual disease in medulloblastomas. Larger studies should be conducted to validate the predictive values of the levels of intact IGFBP-3 and the proteolytic fragments in CSF in the follow up of medulloblastomas.

REFERENCES

1. Kleihues P, Louis DN, Scheithauer BW, Rorke LB, Reifenberger G, Burger PC, Cavenee WK. The WHO classification of tumors of the nervous system. J Neuropathol Exp Neurol 2002;61:215-25; discussion 26-9.
2. Packer RJ. Brain tumors in children. Arch Neurol 1999;56:421-5.
3. Russo VC, Gluckman PD, Feldman EL, Werther GA. The insulin-like growth factor system and its pleiotropic functions in brain. Endocr Rev 2005;26:916-43.
4. Wang JY, Del Valle L, Gordon J, Rubini M, Romano G, Croul S, Peruzzi F, Khalili K, Reiss K. Activation of the IGF-1R system contributes to malignant growth of human and mouse medulloblastomas. Oncogene 2001;20:3857-68.
5. Del Valle L, Enam S, Lassak A, Wang JY, Croul S, Khalili K, Reiss K. Insulin-like growth factor I receptor activity in human medulloblastomas. Clin Cancer Res 2002;8:1822-30.
6. Ogino S, Kubo S, Abdul-Karim FW, Cohen ML. Comparative immunohistochemical study of insulin-like growth factor II and insulin-like growth factor receptor type 1 in pediatric brain tumors. Pediatr Dev Pathol 2001;4:23-31.
7. van Doorn J, Gilhuis HJ, Koster JG, Wesseling P, Reddingius RE, Gresnigt MG, Bloemen RJ, van Muijen GN, van Buul-Offers SC. Differential patterns of insulin-like growth factor-I and -II mRNA expression in medulloblastoma. Neuropathol Appl Neurobiol 2004;30:503-12.
8. Zumkeller W, Westphal M. The IGF/IGFBP system in CNS malignancy. Mol Pathol 2001;54:227-9.
9. Samani AA, Yakar S, LeRoith D, Brodt P. The role of the IGF system in cancer growth and metastasis: overview and recent insights. Endocr Rev 2007;28:20-47.
10. Bondy C, Werner H, Roberts CT, Jr., LeRoith D. Cellular pattern of type-I insulin-like growth factor receptor gene expression during maturation of the rat brain: comparison with insulin-like growth factors I and II. Neuroscience 1992;46:909-23.
11. Pomeroy SL, Tamayo P, Gaasenbeek M, Sturla LM, Angelo M, McLaughlin ME, Kim JY, Goumnerova LC, Black PM, Lau C, Allen JC, Zagzag D, et al. Prediction of central nervous system embryonal tumour outcome based on gene expression. Nature 2002;415:436-42.
12. Korshunov A, Neben K, Wrobel G, Tews B, Benner A, Hahn M, Golanov A, Lichter P. Gene expression patterns in ependymomas correlate with tumor location, grade, and patient age. Am J Pathol 2003;163:1721-7.
13. Unterman TG, Glick RP, Waites GT, Bell SC. Production of insulin-like growth factor-binding proteins by human central nervous system tumors. Cancer Res 1991;51:3030-6.
14. Zumkeller W. IGFs and IGF-binding proteins as diagnostic markers and biological modulators in brain tumors. Expert Rev Mol Diagn 2002;2:473-7.
15. Gilbertson RJ. Medulloblastoma: signalling a change in treatment. Lancet Oncol 2004;5:209-18.
16. Hargrave DR, Zacharoulis S. Pediatric CNS tumors: current treatment and future directions. Expert review of neurotherapeutics 2007;7:1029-42.
17. Muller HL, Oh Y, Gargosky SE, Lehrnbecher T, Hintz RL, Rosenfeld RG. Concentrations of insulin-like growth factor (IGF)-binding protein-3 (IGFBP-3), IGF, and IGFBP-3 protease activity in cerebrospinal fluid of children with leukemia, central nervous system tumor, or meningitis. J Clin Endocrinol Metab 1993;77:1113-9.
18. Muller HL, Oh Y, Lehrnbecher T, Blum WF, Rosenfeld RG. Insulin-like growth factor-binding protein-2 concentrations in cerebrospinal fluid and serum of children with malignant solid tumors or acute leukemia. J Clin Endocrinol Metab 1994;79:428-34.
19. de Bont JM, Kros JM, Passier MMCJ, Reddingius RE, Sillevis Smitt PAE, Luider TM, den Boer ML, Pieters R. Differential expression and prognostic significance of SOX genes in pediatric medulloblastoma and ependymoma identified by microarray analysis Neuro-oncology 2007;in press.
20. Stam RW, den Boer ML, Meijerink JP, Ebus ME, Peters GJ, Noordhuis P, Janka-Schaub GE, Armstrong SA, Korsmeyer SJ, Pieters R. Differential mRNA expression of Ara-C-metabolizing enzymes

explains Ara-C sensitivity in MLL gene-rearranged infant acute lymphoblastic leukemia. Blood 2003;101:1270-6.
21. Van Buul-Offers SC, Van Kleffens M, Koster JG, Lindenbergh-Kortleve DJ, Gresnigt MG, Drop SL, Hoogerbrugge CM, Bloemen RJ, Koedam JA, Van Neck JW. Human insulin-like growth factor (IGF) binding protein-1 inhibits IGF-1-stimulated body growth but stimulates growth of the kidney in snell dwarf mice. Endocrinology 2000;141:1493-9.
22. de Boer L, Hoogerbrugge CM, van Doorn J, van Buul-Offers SC, Karperien M, Wit JM. Plasma insulin-like growth factors (IGFs), IGF-Binding proteins (IGFBPs), acid-labile subunit (ALS) and IGFBP-3 proteolysis in individuals with clinical characteristics of Sotos syndrome. J Pediatr Endocrinol Metab 2004;17:615-27.
23. van Doorn J, Hoogerbrugge CM, Koster JG, Bloemen RJ, Hoekman K, Mudde AH, van Buul-Offers SC. Antibodies directed against the E region of pro-insulin-like growth factor-II used to evaluate non-islet cell tumor-induced hypoglycemia. Clinical chemistry 2002;48:1739-50.
24. Rikken B, van Doorn J, Ringeling A, Van den Brande JL, Massa G, Wit JM. Plasma levels of insulin-like growth factor (IGF)-I, IGF-2 and IGF-binding protein-3 in the evaluation of childhood growth hormone deficiency. Horm Res 1998;50:166-76.
25. Van Doorn J, Cornelissen AJ, Van Buul-Offers SC. Plasma levels of insulin-like growth factor binding protein-4 (IGFBP-4) under normal and pathological conditions. Clin Endocrinol (Oxf) 2001;54:655-64.
26. Van Doorn J, Ringeling AM, Shmueli SS, Kuijpers MC, Hokken-Koelega AC, van Buul-Offers SC, Jansen M. Circulating levels of human insulin-like growth factor binding protein-6 (IGFBP-6) in health and disease as determined by radioimmunoassay. Clin Endocrinol (Oxf) 1999;50:601-9.
27. Koedam JA, Hoogerbrugge CM, van Buul-Offers SC. Insulin-like growth factor-binding protein-3 protease activity in Snell normal and Pit-1 deficient dwarf mice. J Endocrinol 1998;157:295-303.
28. Huber W, Von Heydebreck A, Sultmann H, Poustka A, Vingron M. Variance stabilization applied to microarray data calibration and to the quantification of differential expression. Bioinformatics 2002;18:S96-104.
29. Benjamini Y, Hochberg Y. Controlling the False Discovery Rate: a Practical and Powerful Approach to Multiple Testing. Journal of the Royal Statistical Society B 1995;57:289-300.
30. Hebert E. Mannose-6-phosphate/insulin-like growth factor II receptor expression and tumor development. Bioscience reports 2006;26:7-17.
31. Hahn H, Wojnowski L, Specht K, Kappler R, Calzada-Wack J, Potter D, Zimmer A, Muller U, Samson E, Quintanilla-Martinez L. Patched target Igf2 is indispensable for the formation of medulloblastoma and rhabdomyosarcoma. J Biol Chem 2000;275:28341-4.
32. Hartmann W, Koch A, Brune H, Waha A, Schuller U, Dani I, Denkhaus D, Langmann W, Bode U, Wiestler OD, Schilling K, Pietsch T. Insulin-like growth factor II is involved in the proliferation control of medulloblastoma and its cerebellar precursor cells. Am J Pathol 2005;166:1153-62.
33. Rao G, Pedone CA, Valle LD, Reiss K, Holland EC, Fults DW. Sonic hedgehog and insulin-like growth factor signaling synergize to induce medulloblastoma formation from nestin-expressing neural progenitors in mice. Oncogene 2004;23:6156-62.
34. Elmlinger MW, Deininger MH, Schuett BS, Meyermann R, Duffner F, Grote EH, Ranke MB. In vivo expression of insulin-like growth factor-binding protein-2 in human gliomas increases with the tumor grade. Endocrinology 2001;142:1652-8.
35. Wang H, Wang H, Zhang W, Fuller GN. Overexpression of IGFBP5, but not IGFBP3, correlates with the histologic grade of human diffuse glioma: a tissue microarray and immunohistochemical study. Technol Cancer Res Treat 2006;5:195-9.
36. Fukushima T, Tezuka T, Shimomura T, Nakano S, Kataoka H. Silencing of insulin-like growth factor binding protein-2 (IGFBP-2) in human glioblastoma cells reduces both invasiveness and expression of progression-associated gene CD24. J Biol Chem 2007.

37. Wang H, Wang H, Shen W, Huang H, Hu L, Ramdas L, Zhou YH, Liao WS, Fuller GN, Zhang W. Insulin-like growth factor binding protein 2 enhances glioblastoma invasion by activating invasion-enhancing genes. Cancer Res 2003;63:4315-21.
38. Boon K, Edwards JB, Siu IM, Olschner D, Eberhart CG, Marra MA, Strausberg RL, Riggins GJ. Comparison of medulloblastoma and normal neural transcriptomes identifies a restricted set of activated genes. Oncogene 2003;22:7687-94.
39. Beattie J, Allan GJ, Lochrie JD, Flint DJ. Insulin-like growth factor-binding protein-5 (IGFBP-5): a critical member of the IGF axis. Biochem J 2006;395:1-19.
40. Johnson SK, Dennis RA, Barone GW, Lamps LW, Haun RS. Differential expression of insulin-like growth factor binding protein-5 in pancreatic adenocarcinomas: identification using DNA microarray. Mol Carcinog 2006;45:814-27.
41. Miyake H, Pollak M, Gleave ME. Castration-induced up-regulation of insulin-like growth factor binding protein-5 potentiates insulin-like growth factor-I activity and accelerates progression to androgen independence in prostate cancer models. Cancer Res 2000;60:3058-64.
42. Nordqvist AC, Mathiesen T. Expression of IGF-2, IGFBP-2, -5, and -6 in meningiomas with different brain invasiveness. J Neurooncol 2002;57:19-26.
43. Baxter RC. Signalling pathways involved in antiproliferative effects of IGFBP-3: a review. Mol Pathol 2001;54:145-8.
44. Ricort JM, Binoux M. Insulin-like growth factor binding protein-3 stimulates phosphatidylinositol 3-kinase in MCF-7 breast carcinoma cells. Biochem Biophys Res Commun 2004;314:1044-9.
45. Xi Y, Nakajima G, Hamil T, Fodstad O, Riker A, Ju J. Association of insulin-like growth factor binding protein-3 expression with melanoma progression. Mol Cancer Ther 2006;5:3078-84.
46. Buckbinder L, Talbott R, Velasco-Miguel S, Takenaka I, Faha B, Seizinger BR, Kley N. Induction of the growth inhibitor IGF-binding protein 3 by p53. Nature 1995;377:646-9.
47. Yi HK, Kim SY, Hwang PH, Kim CY, Yang DH, Oh Y, Lee DY. Impact of PTEN on the expression of insulin-like growth factors (IGFs) and IGF-binding proteins in human gastric adenocarcinoma cells. Biochem Biophys Res Commun 2005;330:760-7.
48. Chang YS, Wang L, Liu D, Mao L, Hong WK, Khuri FR, Lee HY. Correlation between insulin-like growth factor-binding protein-3 promoter methylation and prognosis of patients with stage I non-small cell lung cancer. Clin Cancer Res 2002;8:3669-75.
49. How HK, Yeoh A, Quah TC, Oh Y, Rosenfeld RG, Lee KO. Insulin-like growth factor binding proteins (IGFBPs) and IGFBP-related protein 1-levels in cerebrospinal fluid of children with acute lymphoblastic leukemia. J Clin Endocrinol Metab 1999;84:1283-7.
50. Pirttila T, Vanhatalo S, Turpeinen U, Riikonen R. Cerebrospinal fluid insulin-like growth factor-1, insulin growth factor binding protein-2 or nitric oxide are not increased in MS or ALS. Acta Neurol Scand 2004;109:337-41.
51. Wilczak N, Schaaf M, Bredewold R, Streefland C, Teelken A, De Keyser J. Insulin-like growth factor system in serum and cerebrospinal fluid in patients with multiple sclerosis. Neurosci Lett 1998;257:168-70.
52. Holly J, Perks C. The role of insulin-like growth factor binding proteins. Neuroendocrinology 2006;83:154-60.
53. Lalou C, Lassarre C, Binoux M. A proteolytic fragment of insulin-like growth factor (IGF) binding protein-3 that fails to bind IGFs inhibits the mitogenic effects of IGF-1 and insulin. Endocrinology 1996;137:3206-12.
54. Angelloz-Nicoud P, Lalou C, Binoux M. Prostate carcinoma (PC-3) cell proliferation is stimulated by the 22-25-kDa proteolytic fragment (1-160) and inhibited by the 16-kDa fragment (1-95) of recombinant human insulin-like growth factor binding protein-3. Growth Horm IGF Res 1998;8:71-5.

Chapter 8

Low Frequency of p53 Mutations and Differential Expression of p53 Regulatory Genes in Pediatric Medulloblastoma and Ependymoma

Judith M. de Bont[1], Pim J. French[2], Johan M. Kros[3], Monique M.C.J. Passier[1], Max van Noesel[1], Peter A.E. Sillevis Smitt[2], Monique L. den Boer[1], Rob Pieters[1]

[1]Erasmus MC – Sophia Children's Hospital - University Medical Center Rotterdam – Department of Pediatric Oncology and Hematology, The Netherlands;
[2]Erasmus MC – University Medical Center Rotterdam – Department of Neurology, The Netherlands;
[3]Erasmus MC – University Medical Center Rotterdam – Department of Pathology, The Netherlands

Submitted

ABSTRACT

In this study we screened for the presence of mutations in exons 5-9 of p53 in 32 pediatric medulloblastomas and 14 ependymomas and evaluated mRNA expression levels of genes involved in the p53 pathway. Two missense mutations were identified in the 32 medulloblastoma patients (6%), both not previously identified in medulloblastomas. A P151S mutation was found in both the primary and relapse tissue of a metastasized large cell/anaplastic medulloblastoma. Secondly, an Y163C mutation was identified in a classic medulloblastoma in a 5-month old child, who was concomitantly diagnosed with a rhabdoid tumor of the kidney. Although the family history of this patient showed a high incidence of malignancies at young age, the presence of a p53 germline mutation was excluded. No p53 mutations were found in ependymomas. Analysis of expression levels of p53 target genes in medulloblastomas revealed overexpression (FDR<1%) of cyclins and CDKs involved in the regulation of cell cycle checkpoints, which might suggest p53 inactivation as these genes are inhibited by functional p53. In addition, differential expression levels of genes known to regulate p53 activity, e.g. CHEK1/2, MDM2, PAX5 and PPM1D, were only likely to cause p53 inactivation in a small number of patients. Therefore, these results suggest that the p53 pathway is important in a minority of pediatric medulloblastomas and ependymomas.

INTRODUCTION

p53 is one of the most important tumor suppressor genes, which controls the cellular response to stress and DNA damage[1, 2]. Germline p53 mutations predispose to early-onset cancers and can result in hereditary cancer syndromes, such as Li-Fraumeni syndrome. These patients have an increased risk to develop a.o. medulloblastoma[1-3], one of the most frequent pediatric brain tumor[4, 5]. p53 germline mutations in ependymomas, another common brain tumor subtype in children, have also been described[6-10]. Both brain tumor subtypes frequently arise in the posterior fossa, but ependymomas can also be found along the spinal cord, arising within or adjacent to the ependymal lining of the ventricular system and spinal central canal[7].

Besides the importance in hereditary cancers, the p53 pathway is also dysfunctional in more than 50% of all sporadic human cancers[11]. Because loss of heterozygosity of the short arm of chromosome 17 is one of the most common abnormalities in medulloblastomas, p53, localized on chromosome 17p13, was suggested to be an important tumor suppressor gene in medulloblastomas[12, 13]. Although inactivation of p53 has been shown to facilitate medulloblastoma development in mice[14, 15] and medulloblastoma show positivity for p53 indicating a dysfunctional protein[16], p53 mutations are rare[12, 13, 17-19]. In order to characterize the functionality of the p53 pathway in pediatric medulloblastomas and ependymomas, we set out to screen for p53 mutations and analyzed the mRNA expression levels of genes involved in the p53 pathway.

MATERIAL AND METHODS

Study population and material

Tumor tissue from 46 pediatric brain tumors was analyzed for the presence of mutations in exons 5-9 of the p53 gene. Patient characteristics are displayed in Table 1. All material was collected at the Erasmus MC – Sophia Children's Hospital – University Medical Center, the Netherlands between 1990 and 2004. After surgery, fresh material was immediately placed in liquid nitrogen and stored at -80°C until processing. Before DNA extraction, 4 µm cryosections were prepared and hematoxiline-eosine (HE) stained to confirm histology. For one of the recurrent medulloblastoma patients and a concurrently diagnosed rhabdoid tumor in one of the patients, we used DNA isolated from paraffin embedded tissue to determine p53 status in the primary/concurrent tumor. Normal cerebellar tissue was obtained post-mortem from 7 adult patients without the history of a brain tumor and used as normal control.

Table 1. Patient characteristics

This table shows the patient characteristics of the patients included in the study.

*For 1 medulloblastoma patient tumor tissue from both the primary as from the recurrent tumor was screened for the presence of mutations

Characteristics	N
Sex	
Male	30
Female	16
Median age, years (range)	5.0 (0.2-15.6)
Histological subtype	
Medulloblastoma	**32**
Primary	31
Recurrent	2*
Cellular ependymoma	**7**
Primary	6
Recurrent	1
Anaplastic ependymoma	**7**
Primary	7
Recurrent	-

DNA isolation

Fresh frozen tissue samples were homogenized in TRizol reagent (Invitrogen, Breda, the Netherlands) using a tissue homogenizer (B. Braun, Spangenberg, Germany). Subsequently, DNA was isolated according to the manufacturer's protocol with minor modifications[20]. DNA samples were purified by Proteinase K (1 mg/ml) digestion (1 hour at 56°C) and precipitated in 0.5 mol/L NaCl, 60 µg glycogen and 2.5 volumes of 70% ethanol. We then further purified samples using an additional phenol extraction and chloroform extraction, followed by precipitation in 0.3 mol/L NaAc and 2 volumes of ethanol 70% and a wash using 70% ethanol. DNA was subsequently dissolved in TE buffer (10mM Tris, 1mM EDTA).

DNA was isolated from paraffin embedded tissue by placing four 5 µm sections in 200 µl of 20 mg/ml Proteinase K in Prot K active buffer (100 mM Tris, 10 mM NaCl, 5 mM EDTA, 1% SDS, pH 9.0) overnight at 56°C. DNA was purified by phenol/chloroform extraction and precipitated and dissolved as outlined above.

PCR amplification

We amplified exon 5-9 of the p53 gene in 4 separate polymerase chain reactions (PCR). We focused on exons 5-9, because most mutations (>90%) thus far identified are present within these exons (http://www. -p53.iarc.fr[21]). Primers for each of the reactions were designed in intron sequences flanking the exons of the p53 gene (Table 2). Each PCR reaction included 1x PCR buffer II (Applied Biosystems, Foster City, CA, USA), 2 mmol/L $MgCl_2$, 200 nmol/L of deoxynucleotide triphosphates (10 µmol/µL, Amersham Biosciences, Uppsala, Sweden), 1.25 units of AmpliTaq Gold (5 units/µL, Applied Biosystems, Foster City, CA, USA), 100 ng of genomic DNA and 300 nmol/L of the forward and reverse primer in a final volume

Table 2. Primers for exon 5-9 of p53

By the use of the displayed primer pairs exon 5-9 of p53 were amplified by polymerase chain reaction (PCR) in 3 separate PCR reactions.

*For the confirmation of the identified mutations in exon 5 on DNA isolated from paraffin embedded material (primary tumor from patient 1 and rhabdoid kidney tumor from patient 103) another primer pair, with a smaller product of 211 base pairs, was designed.

			PCR protocol	
Exon	**Primers 5'-3'**	**Product size (base pairs)**	**Touchdown**	**Annealing temperature**
5-6		453	10 cycli 60-55°C	30 cycli 55°C
Forward	CTGTTCACTTGTGCCCTGAC			
Reverse	CTCCCAGAGACCCCAGTTG			
7		217	10 cycli 58-53°C	30 cycli 55°C
Forward	ACAGGTCTCCCCAAGGC			
Reverse	AGCAGAGGCTGGGGCAC			
8-9		395	-	35 cycli 55°C
Forward	GCCTCTTGCTTCTCTTTTCC			
Reverse	GGCATTTTGAGTGTTAGACTGG			
5*		211	10 cycli 65-60°C	30 cycli 60°C
Forward	TGCCCTCAACAAGATGTTT			
Reverse	CCAGCCCTGTCGTCTCT			
5-6		453	10 cycli 60-55°C	30 cycli 55°C
Forward	CTGTTCACTTGTGCCCTGAC			
Reverse	CTCCCAGAGACCCCAGTTG			

of 50 µl. PCR cycling was performed on a 2720 Thermal Cycler (Applied Biosystems, Foster City, CA, USA). For exon 5-6, 5* and 7 a touchdown PCR protocol was used consisting of the following steps: DNA denaturing and Amplitaq Gold (Applied Biosystems, Foster City, CA, USA) activation for 5 minutes at 95°C, 10 cycle touchdown of annealing temperature with 30 seconds at 95°C, 1 minute annealing at 60-55°C (exon 5-6), 58-53°C (exon 7) or 65-60°C (exon 5*), and 1 minute at 72°C. Touchdown was followed by 30 cycles of 95°C for 30 seconds, 1 minute 55°C (exon 5-6 and 7) or 60°C (exon 5*) and 72°C for 1 minute and finished by a final extension step at 72°C for 10 minutes (Table 2). PCR conditions for exons 8-9 were 5 minutes at 95°C, 35 cycles of 95°C for 30 seconds, 1 minute 55°C and 72°C for 1 minute and a final extension step at 72°C (Table 2).

Sequencing

PCR products were purified using Multiscreen $PCR_{\mu 96}$ clean up filter plates (Millipore, Billerica, MA, USA) according to the manufacturer's protocol. The BigDye Terminator V1.1 cycle sequencing kit (Applied Biosystems, Foster City, CA, USA) was used according to the manufacturer's instructions, in combination with the primers used in the PCR reactions as sequencing primers. Reactions were run on an ABI 3100 Genetic Analyzer (Applied Biosys-

tems, Foster City, CA, USA). Sequences were analyzed using BioEdit software v4.8.10 (Tom Hall, Ibis Biosciences, Carlsbad, USA).

All mutations were confirmed in an independent RT-PCR reaction.

Pathway analysis

To analyze gene expression levels of genes regulating p53 activity or those being targeted by p53, we used our previously described microarray data[22]. Using the KEGG pathway database (http://www.genome.ad.jp/kegg/pathway.html) we identified 70 genes that were involved in the regulation and downstream signaling of the p53 signaling pathway. These 70 genes corresponded to 217 probe sets on the Affymetrix HGU 133 plus 2.0 microarrays, which were used for analysis in R (version 2.5.1). Raw data of all HGU133 plus 2.0 probe sets (54675) were normalized using the variance stabilization procedure (vsn)[23]. Expression levels of the 217 selected probe sets in medulloblastoma, ependymoma and cerebellum were statistically compared using the Wilcoxon test and corrected for multiple testing errors by applying the false discovery rate (FDR) as described by Benjamini and Hochberg[24] (MULTTEST package). A FDR <1% was considered statistically significant, meaning that less than 1% of the significant genes are false positives.

RESULTS

Mutational analysis

We have screened for mutations in exon 5-9 of p53 in 32 medulloblastomas and 14 ependymomas. We identified 2 homozygous missense mutations in the group of medulloblastomas. No mutations were identified in the ependymomas.

None of the 2 mutations identified in the medulloblastoma patients has previously been described in this tumor subtype. The first mutation was found in the recurrent tumor of a patient who had initially presented with a metastasized large cell/anaplastic medulloblastoma at the age of 12 years and who experienced a relapse in the left parietal lobe 2 years after diagnosis. The mutation was 451C>T resulting in P151S (Figure 1). DNA sequencing of the primary tumor of this patient revealed that this mutation was already present at diagnosis (Figure 1). The patient died of progressive medulloblastoma disease.

The second mutation was identified in the tumor of a 5-month old boy that presented with a classic medulloblastoma. The mutation was 488A>G, resulting in an amino acid substitution Y163C. Concomitantly with the medulloblastoma, a rhabdoid tumor of the kidney was found. Because of the presence of multiple tumors and the young age of the patient, it was decided not to start curative treatment. Sequence analysis of p53 of the renal tumor did not reveal the p53 mutation, which excludes the possibility of a germline mutation in this patient.

Table 3. Differentially expressed probesets (FDR<0.01) corresponding to genes involved in the p53 signaling pathway

Medulloblastoma vs Cerebellum					Ependymoma vs Cerebellum				
Gene	Probe ids	p-value	FDR	ratio MED-CB	Gene	Probe ids	p-value	FDR	ratio EP-CB
CCNB1	228729_at	0.000	0.003	3.61	**CCNG2**	228081_at	0.000	0.006	0.15
CCND2	200953_s_at	0.000	0.003	42.76	**CDC2**	203213_at	0.000	0.006	10.96
CDC2	203213_at	0.000	0.003	20.41	**CDC2**	210559_s_at	0.000	0.006	2.71
CDC2	210559_s_at	0.000	0.003	5.86	**FAS**	215719_x_at	0.000	0.006	1.97
PTEN2	242622_x_at	0.000	0.003	0.61	**PPM1D**	230330_at	0.000	0.006	0.39
RRM2	201890_at	0.000	0.003	19.45	**RRM2**	201890_at	0.000	0.006	4.40
RRM2	209773_s_at	0.000	0.003	6.05	**RRM2**	209773_s_at	0.000	0.006	3.38
CCND2	200951_s_at	0.000	0.004	4.99	**TP53**	201746_at	0.000	0.006	2.86
CCNB2	202705_at	0.000	0.005	7.59	**TP53I3**	210609_s_at	0.000	0.006	2.98
CCNE2	211814_s_at	0.000	0.005	1.51	**ATM**	1553387_at	0.000	0.007	0.71
CDC2	203214_x_at	0.000	0.005	3.01	**CCNG2**	202769_at	0.000	0.007	0.16
CDK6	224847_at	0.000	0.005	15.48	**CDK2**	204252_at	0.000	0.007	2.31
CDK6	224848_at	0.000	0.005	12.11	**FAS**	216252_x_at	0.000	0.007	1.57
GADD45G	204121_at	0.000	0.005	3.40	**SESN3**	235683_at	0.000	0.007	1.91
PTEN1	240964_at	0.000	0.005	1.28					
RFWD2	1552617_a_at	0.000	0.005	2.34					
CDK2	211804_s_at	0.000	0.006	1.43					
CHEK1	205394_at	0.000	0.006	3.04					
TP53I3	210609_s_at	0.000	0.006	2.33					
CCNG2	228081_at	0.001	0.007	0.38					
CHEK1	205393_s_at	0.001	0.007	3.07					
CDK2	204252_at	0.001	0.009	2.48					
CDK6	235287_at	0.001	0.009	1.73					

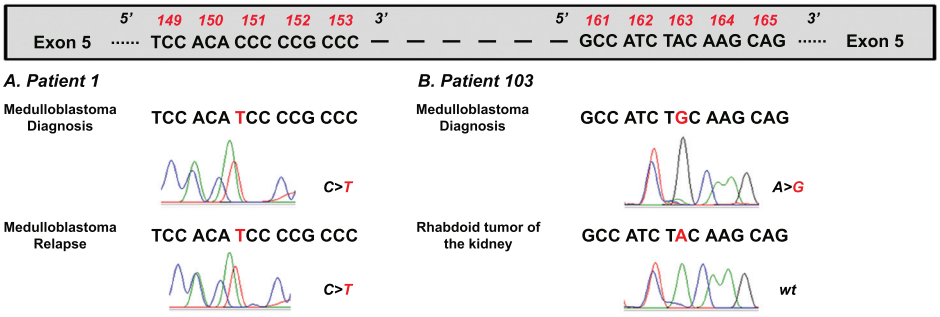

Figure 1. Mutations identified in exon 5 of p53 in 2 medulloblastoma patients
In two medulloblastoma patients we identified mutations in respectively residue 151 (A.) and 163 (B.) of exon 5. In patient 1 (A.) the C>T missense mutation was initially found in the relapse sample. Screening the DNA isolated from the paraffin embedded material from the diagnostic tumor showed that the same C>T mutation in residue 151 was present. In patient 103 (B.) a A>G missense mutation was identified in the tumor tissue of the medulloblastoma, but not in the concomitantly diagnosed rhabdoid renal tumor of the same patient.

p53 pathway analysis

The expression of 70 individual genes (217 probe sets) involved in the p53 pathway was analyzed in medulloblastoma, ependymoma and control cerebellum. Compared to normal cerebellum, 14 genes (23 probe sets) were differentially expressed (FDR<1%) in medulloblastoma. In ependymoma, 10 genes (14 probe sets) were differentially expressed (FDR<1%) compared to normal cerebellum (Table 3).

p53 target genes

Compared to normal cerebellum, medulloblastomas predominantly showed increased expression of genes important in the regulation of 2 cell cycle checkpoints (G1/S and G2/M), e.g. cyclin B1, cyclin D2, cyclin E2, CDC2, CDK2 and CDK6 (Table 3, Figure 2). In the 2 medulloblastomas with p53 mutations cyclin D1 expression levels were 4-11-fold higher (p=0.02) compared to the medulloblastomas without p53 mutations (Figure 3). In contrast, cyclin D2 overexpression was not detected in the patients with a p53 mutation (Figure 3).

In contrast to the abnormal expression of multiple genes in 2 tightly linked branches of p53-signaling in medulloblastoma, our results indicate that in ependymomas, differential expression of individual genes was found in 4 different branches of downstream p53 signaling (Figure 2).

p53 regulatory genes

The overexpression of the genes involved in cell cycle checkpoints might result from p53 inactivation, as p53 normally inhibits the expression of these genes via p21, 14-3-3 and GADD45 (Figure 2). However, as the incidence of p53 mutations was very low, another

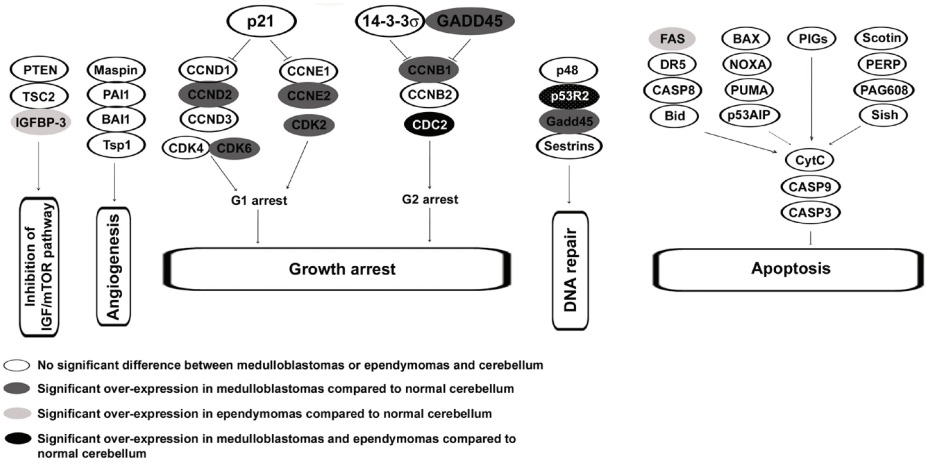

Figure 2. Expression profile of p53 target genes in medulloblastoma and ependymoma patients

This figure shows a schematic representation of the downstream p53 pathway according to the KEGG database. Gene expression levels of the genes involved in this pathway were analyzed in medulloblastoma and ependymoma and compared to normal cerebellar tissue. Genes significantly over- or under-expressed at 1% FDR are indicated by the differently colored circles.

mechanism for p53 inactivation might play a role. Therefore, we specifically analyzed gene expression levels of genes that are known to regulate p53 activity in the ependymomas and medulloblastomas without p53 mutations: MDM2, PAX5, PPM1D and CCNG2, which are able to inactivate p53 and $p14^{ARF}$, ATM, CHEK1 and 2, which are known to activate p53[6, 25, 26]. The expression of the p53 inhibiting genes PPM1D and CCNG2 was significantly decreased (~2.5- and ~6-fold change, respectively; $p<0.001$ for both, Table 3) in ependymomas compared to normal cerebellum and medulloblastomas. CHEK1 was significantly overexpressed in medulloblastomas compared to normal cerebellum (fold-change~3; $p<0.001$, Table 3). The expression of MDM2, PAX5, $p14^{ARF}$, ATM and CHEK2 was not significantly different between medulloblastoma or ependymoma and normal cerebellum (Table 3). Although no significance was reached for the whole group of medulloblastomas, we observed a more than 2-fold overexpression (range 2.1-137.2) of PAX5 in 12 medulloblastoma patients and a more than 2-fold overexpression (range 2.1-9.8) of PPM1D in 9 patients compared to median expression levels of these genes in cerebellum.

DISCUSSION

Overall, inactivation of p53 by mutation is one of the most common genetic alterations in human cancer. In medulloblastoma, p53 was also suggested to be an important tumor suppressor

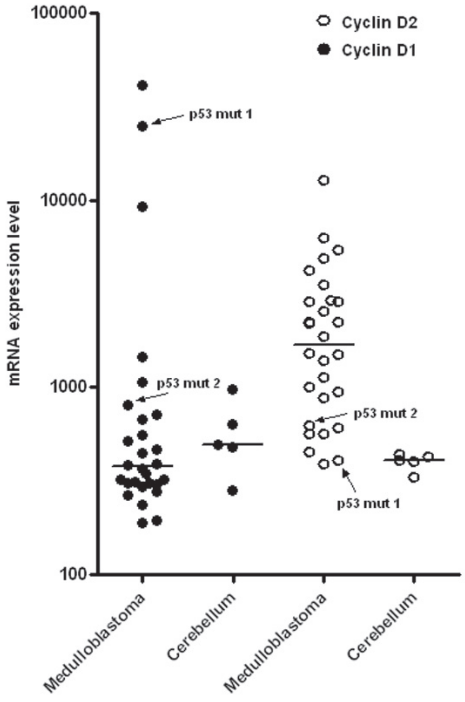

Figure 3. Cyclin D2 expression levels in medulloblastomas.
Cyclin D1 expression levels were found to be higher in the 2 medulloblastomas with p53 mutations. In contrast, cyclin D2 expression levels were relatively lower in the patients with the p53 mutated medulloblastomas (p53 mut 1 and mut 2).

gene, since loss of 17p is one of the most frequent cytogenetic abnormalities. In this study we determined the frequency and identity of mutations in the hotspot area of mutations (exon 5-9) of p53 in pediatric medulloblastoma and ependymoma. We only found p53 mutations in 2/32 medulloblastoma (6%) and 0/14 ependymomas, which confirms the low incidence of p53 mutations in pediatric brain tumors shown in earlier studies (Table 4)[12, 13, 17, 18].

Interestingly, the 2 identified missense mutations in p53 in the medulloblastoma patients in our study have not been previously described in medulloblastomas. The 451C>T mutation identified in patient 1 in our study results in the replacement of a large proline residue for a smaller serine residue. This residue is located in one of the hotspot mutational regions and plays a role in stabilizing the structure of the short loops at the end of the β sheet skeleton, opposite the DNA binding surface[27]. Mutation in this residue is expected to result in extension of the preceding α helix by one residue leading to decreased stability of the p53 protein[28, 29]. Interestingly, this mutation has also been identified as a de novo germline mutation in a young girl with multiple tumors, respectively an adrenal cortical carcinoma at 7 months of age, a fibrosarcoma at 3 years of age and a rhabdomyosarcoma at the age of 5[30].

Table 4. p53 mutations in pediatric medulloblastomas and ependymomas.

Medulloblastoma			Ependymoma		
Somatic mutations					
No. of mutations	**Type of mutation**	**Ref**	**No. of mutations**	**Type of mutation**	**Ref**
1/9 (11%)	Glu285Val	12	0/14 (0%)	_	17
0/12 (0%)	_	13	0/24 (0%)	_	18
0/4 (0%)	_	17	0/15 (0%)	_	44
2/19 (11%)	His193Pro	44	0/8 (0%)	_	45
	Del1 codon 213		0/1 (0%)	_	46
0/3 (0%)	_	45	0/2 (0%)	_	47
1/14 (7%)	Del1 codon 164	48	1/26 (3.8%)	Pro89Leu	39
2/20 (10%)	Cys247Tyr	49	1/5 (20%)	?	50
	Arg248Gln		1/18 (5.6%)	?	51
2/35 (6%)	Cys247Tyr	52	0/11 (0%)	_	53
	Arg248Gln		0/8 (0%)	_	54
1/3 (33%)	Arg175His	47	0/7 (0%)	_	55
3/29 (10.3%)	Arg196Stop	32	0/14 (0%)	_	Present study
	Thr230Ile				
	Del bp13068-13105				
1/51 (2%)	Arg248Trp	34			
2/22 (9.1%)	?	56			
0/10 (0%)	_	55			
2/32 (6.3%)	Pro151Ser	Present study			
	Tyr163Cys				
Germline mutations					
	Arg273His	57		Asn235Ser	10
	Arg248Gln	58		Thr125Thr	8
	Del1 codon 241	59		Met237Ile	9
	Codon 213 STOP	60		Cys242Tyr	6
	Del1 codon 257	61			
	Arg248Gln	62			
	Arg248Trp	62			
	I6-intron	63			
	I6-intron	64			
	Arg273Cys	9			
Intron4/exon5; addition G in splice acceptor site		8			

The Y163C mutation, also located in the β sheet skeleton of p53[27] is one of the infrequent mutations in which p53 is predominantly localized in the cytoplasm instead of the nucleus[31]. As this type of mutation shows little interference with nuclear wild-type p53, the effects of the mutation may be limited. However, in both our patients with p53 mutations no wild type p53 was found, which excluded the presence of functional p53 and might suggest loss of 17p. Unfortunately we do not have cytogenetic data of these patients.

The mutation in residue 163 was found in a classic medulloblastoma. This patient was diagnosed with multiple tumors. In addition, malignancies were frequently observed in his family and hence the presence of a p53 germline mutation was suggested. The mutation in residue 163 has been identified as a germline mutation twice before (p53 database; http://www.-p53.iarc.fr) in a patient with a brain tumor (histology not documented) and in an osteosarcoma patient. Since no mutation was present in the concomitantly diagnosed rhabdoid tumor of the kidney of our patient, a hereditary p53-linked syndrome was excluded.

Despite the low incidence of p53 mutations in the pediatric medulloblastomas and ependymomas, accumulation of defective p53 protein is observed in up to 40% of medulloblastoma[16, 32] and p53 inactivation facilitates medulloblastoma development in mouse models[14, 15]. In our study, the expression of several downstream target genes of p53, e.g. cyclins and CDKs, was up-regulated, especially in medulloblastomas (Figure 2). Without inhibition by p53 (e.g. by mutations in p53), these genes stimulate progression through the cell cycle. Amplification and/or overexpression of cyclins and CDKs have been described previously in medulloblastoma. Cdk6 is amplified in ~30% of medulloblastoma and both cyclin D1 and cdk6 expression are associated with poor prognosis in these tumors[33, 34]. As p53 mutations were rare in medulloblastomas, other ways of p53 inactivation might be suggested to cause this downstream activation. Increased expression of MDM2, PAX5, PPM1D and CCNG2 and decreased expression of $p14^{ARF}$, ATM and CHEK1 and 2 may for example also lead to p53 inactivation. However, our data indicate that these genes are mostly not differentially expressed in the hypothesized direction. E.g. the expression of PPM1D and CCNG2, both able to phosphorylate and activate MDM2, was decreased in the ependymomas and CHEK1 was overexpressed in medulloblastomas. These expression levels would rather indicate an activation of p53 instead of p53 inactivation. PAX5 and PPM1D have been suggested to play a role in medulloblastomas[34-36]. PPM1D was predominantly amplified and overexpressed in medulloblastoma with 17q gain and isochromosome 17q. Overexpression of PAX5 and PPM1D (>2-fold) was only found in a small subset of patients, but as data from previous studies have been predominantly based on protein expression of these genes, data are not easily comparable. Although overexpression of MDM2 protein was correlated with short survival in adult medulloblastomas, MDM2 amplification was of no importance in pediatric medulloblastomas and ependymomas. The lack of increased MDM2 mRNA expression in our study is in correspondence with these data[12, 32, 37].

Regarding the fact that both p53 mutations and p53 inactivation by differential expression of p53 regulatory genes appear infrequent in pediatric medulloblastomas and ependymomas, the observed downstream overexpression of p53 target genes is presumably caused by other mechanisms. Activated SHH and Wnt signaling, which is observed frequently in medulloblastomas[38-40], can also result in the downstream expression of cyclins and CDKs. Cyclin D1 is for example an important target gene of multiple signaling pathways, e.g. p53, sonic hedgehog (SHH) and Wnt signaling. In addition, loss of CDK inhibitory proteins, such

as Ink4C, which is found in a significant proportion of medulloblastomas, may also result in increased abundance of CDKs[15, 41].

In conclusion, despite the fact that p53 mutations may predispose to and facilitate pediatric brain tumor development, the low incidence of p53 mutations and differential expression of p53 regulatory genes suggests that p53 inactivation is important in a minority of pediatric medulloblastomas and ependymomas.

REFERENCES

1. Biegel JA. Cytogenetics and molecular genetics of childhood brain tumors. Neuro Oncol 1999;1(2):139-151.
2. Bondy M, Wiencke J, Wrensch M, Kyritsis AP. Genetics of primary brain tumors: a review. J Neurooncol 1994;18(1):69-81.
3. Taylor MD, Mainprize TG, Rutka JT. Molecular insight into medulloblastoma and central nervous system primitive neuroectodermal tumor biology from hereditary syndromes: a review. Neurosurgery 2000;47(4):888-901.
4. Packer RJ. Brain tumors in children. Arch Neurol 1999;56(4):421-425.
5. MacDonald TJ, Rood BR, Santi MR, et al. Advances in the diagnosis, molecular genetics, and treatment of pediatric embryonal CNS tumors. Oncologist 2003;8(2):174-186.
6. Metzger AK, Sheffield VC, Duyk G, et al. Identification of a germ-line mutation in the p53 gene in a patient with an intracranial ependymoma. Proc Natl Acad Sci U S A 1991;88(17):7825-7829.
7. Packer RJ. New insights into childhood ependymoma. Curr Neurol Neurosci Rep 2005;5(2):107-109.
8. Chompret A, Brugieres L, Ronsin M, et al. P53 germline mutations in childhood cancers and cancer risk for carrier individuals. Br J Cancer 2000;82(12):1932-1937.
9. Bougeard G, Limacher JM, Martin C, et al. Detection of 11 germline inactivating TP53 mutations and absence of TP63 and HCHK2 mutations in 17 French families with Li-Fraumeni or Li-Fraumeni-like syndrome. J Med Genet 2001;38(4):253-257.
10. Huusko P, Castren K, Launonen V, et al. Germ-line TP53 mutations in Finnish cancer families exhibiting features of the Li-Fraumeni syndrome and negative for BRCA1 and BRCA2. Cancer Genet Cytogenet 1999;112(1):9-14.
11. Hanahan D, Weinberg RA. The hallmarks of cancer. Cell 2000;100(1):57-70.
12. Adesina AM, Nalbantoglu J, Cavenee WK. p53 gene mutation and mdm2 gene amplification are uncommon in medulloblastoma. Cancer Res 1994;54(21):5649-5651.
13. Saylors RL, 3rd, Sidransky D, Friedman HS, et al. Infrequent p53 gene mutations in medulloblastomas. Cancer Res 1991;51(17):4721-4723.
14. Lee Y, McKinnon PJ. DNA ligase IV suppresses medulloblastoma formation. Cancer Res 2002;62(22):6395-6399.
15. Uziel T, Zindy F, Xie S, et al. The tumor suppressors Ink4c and p53 collaborate independently with Patched to suppress medulloblastoma formation. Genes Dev 2005;19(22):2656-2667.
16. Woodburn RT, Azzarelli B, Montebello JF, Goss IE. Intense p53 staining is a valuable prognostic indicator for poor prognosis in medulloblastoma/central nervous system primitive neuroectodermal tumors. J Neurooncol 2001;52(1):57-62.
17. Nozaki M, Tada M, Matsumoto R, et al. Rare occurrence of inactivating p53 gene mutations in primary non-astrocytic tumors of the central nervous system: reappraisal by yeast functional assay. Acta Neuropathol (Berl) 1998;95(3):291-296.
18. Gaspar N, Grill J, Geoerger B, et al. p53 Pathway dysfunction in primary childhood ependymomas. Pediatr Blood Cancer 2006;46(5):604-613.
19. Fink KL, Rushing EJ, Schold SC, Jr., Nisen PD. Infrequency of p53 gene mutations in ependymomas. J Neurooncol 1996;27(2):111-115.
20. Stam RW, den Boer ML, Meijerink JP, et al. Differential mRNA expression of Ara-C-metabolizing enzymes explains Ara-C sensitivity in MLL gene-rearranged infant acute lymphoblastic leukemia. Blood 2003;101(4):1270-1276.
21. Petitjean A, Mathe E, Kato S, et al. Impact of mutant p53 functional properties on TP53 mutation patterns and tumor phenotype: lessons from recent developments in the IARC TP53 database. Hum Mutat 2007;28(6):622-629.

22. de Bont JM, Kros JM, Passier MMCJ, et al. Differential expression and prognostic significance of SOX genes in pediatric medulloblastoma and ependymoma identified by microarray analysis Neuro-Oncology 2008;in press.
23. Huber W, Von Heydebreck A, Sultmann H, Poustka A, Vingron M. Variance stabilization applied to microarray data calibration and to the quantification of differential expression. Bioinformatics 2002;18(Suppl 1):S96-104.
24. Benjamini Y, Drai D, Elmer G, Kafkafi N, Golani I. Controlling the false discovery rate in behavior genetics research. Behav Brain Res 2001;125(1-2):279-284.
25. Lu X, Ma O, Nguyen TA, et al. The Wip1 Phosphatase acts as a gatekeeper in the p53-Mdm2 autoregulatory loop. Cancer Cell 2007;12(4):342-354.
26. Stuart ET, Haffner R, Oren M, Gruss P. Loss of p53 function through PAX-mediated transcriptional repression. Embo J 1995;14(22):5638-5645.
27. Cho Y, Gorina S, Jeffrey PD, Pavletich NP. Crystal structure of a p53 tumor suppressor-DNA complex: understanding tumorigenic mutations. Science 1994;265(5170):346-355.
28. Wright JD, Lim C. A fast method for predicting amino acid mutations that lead to unfolding. Protein Eng 2001;14(7):479-486.
29. Brandt-Rauf PW, Monaco R, Pincus MR. Conformational effects of environmentally induced, cancer-related mutations in the p53 protein. Proc Natl Acad Sci U S A 1994;91(20):9262-9266.
30. Gutierrez MI, Bhatia KG, Barreiro C, et al. A de novo p53 germline mutation affecting codon 151 in a six year old child with multiple tumors. Hum Mol Genet 1994;3(12):2247-2248.
31. Dearth LR, Qian H, Wang T, et al. Inactive full-length p53 mutants lacking dominant wild-type p53 inhibition highlight loss of heterozygosity as an important aspect of p53 status in human cancers. Carcinogenesis 2007;28(2):289-298.
32. Frank AJ, Hernan R, Hollander A, et al. The TP53-ARF tumor suppressor pathway is frequently disrupted in large/cell anaplastic medulloblastoma. Brain Res Mol Brain Res 2004;121(1-2):137-140.
33. Eberhart CG, Kepner JL, Goldthwaite PT, et al. Histopathologic grading of medulloblastomas: a Pediatric Oncology Group study. Cancer 2002;94(2):552-560.
34. Giordana MT, Duo D, Gasverde S, et al. MDM2 overexpression is associated with short survival in adults with medulloblastoma. Neuro Oncol 2002;4(2):115-122.
35. Neben K, Korshunov A, Benner A, et al. Microarray-based screening for molecular markers in medulloblastoma revealed STK15 as independent predictor for survival. Cancer Res 2004;64(9):3103-3111.
36. Mendrzyk F, Radlwimmer B, Joos S, et al. Genomic and protein expression profiling identifies CDK6 as novel independent prognostic marker in medulloblastoma. J Clin Oncol 2005;23(34):8853-8862.
37. Kozmik Z, Sure U, Ruedi D, Busslinger M, Aguzzi A. Deregulated expression of PAX5 in medulloblastoma. Proc Natl Acad Sci U S A 1995;92(12):5709-5713.
38. Castellino RC, De Bortoli M, Lu X, et al. Medulloblastomas overexpress the p53-inactivating oncogene WIP1/PPM1D. J Neurooncol 2008;86(3):245-256.
39. Tong CY, Ng HK, Pang JC, et al. Molecular genetic analysis of non-astrocytic gliomas. Histopathology 1999;34(4):331-341.
40. Koch A, Waha A, Tonn JC, et al. Somatic mutations of WNT/wingless signaling pathway components in primitive neuroectodermal tumors. Int J Cancer 2001;93(3):445-449.
41. Thompson MC, Fuller C, Hogg TL, et al. Genomics identifies medulloblastoma subgroups that are enriched for specific genetic alterations. J Clin Oncol 2006;24(12):1924-1931.
42. Marino S. Medulloblastoma: developmental mechanisms out of control. Trends Mol Med 2005;11(1):17-22.
43. Sherr CJ, Roberts JM. CDK inhibitors: positive and negative regulators of G1-phase progression. Genes Dev 1999;13(12):1501-1512.
44. Ohgaki H, Eibl RH, Wiestler OD, et al. p53 mutations in nonastrocytic human brain tumors. Cancer Res 1991;51(22):6202-6205.

45. Wu JK, Ye Z, Darras BT. Frequency of p53 tumor suppressor gene mutations in human primary brain tumors. Neurosurgery 1993;33(5):824-830; discussion 830-821.
46. Urioste M, Martinez-Ramirez A, Cigudosa JC, et al. Complex cytogenetic abnormalities including telomeric associations and MEN1 mutation in a pediatric ependymoma. Cancer Genet Cytogenet 2002;138(2):107-110.
47. Kato H, Kato S, Kumabe T, et al. Functional evaluation of p53 and PTEN gene mutations in gliomas. Clin Cancer Res 2000;6(10):3937-3943.
48. Raffel C, Thomas GA, Tishler DM, Lassoff S, Allen JC. Absence of p53 mutations in childhood central nervous system primitive neuroectodermal tumors. Neurosurgery 1993;33(2):301-305; discussion 305-306.
49. Cogen PH, Daneshvar L, Metzger AK, et al. Involvement of multiple chromosome 17p loci in medulloblastoma tumorigenesis. Am J Hum Genet 1992;50(3):584-589.
50. Tominaga T, Kayama T, Kumabe T, Sonoda Y, Yoshimoto T. Anaplastic ependymomas: clinical features and tumour suppressor gene p53 analysis. Acta Neurochir (Wien) 1995;135(3-4):163-170.
51. von Haken MS, White EC, Daneshvar-Shyesther L, et al. Molecular genetic analysis of chromosome arm 17p and chromosome arm 22q DNA sequences in sporadic pediatric ependymomas. Genes Chromosomes Cancer 1996;17(1):37-44.
52. Burnett ME, White EC, Sih S, von Haken MS, Cogen PH. Chromosome arm 17p deletion analysis reveals molecular genetic heterogeneity in supratentorial and infratentorial primitive neuroectodermal tumors of the central nervous system. Cancer Genet Cytogenet 1997;97(1):25-31.
53. Hsieh LL, Hsia CF, Wang LY, Chen CJ, Ho YS. p53 gene mutations in brain tumors in Taiwan. Cancer Lett 1994;78(1-3):25-32.
54. Felix CA, Slavc I, Dunn M, et al. p53 gene mutations in pediatric brain tumors. Med Pediatr Oncol 1995;25(6):431-436.
55. Jin W, Xu X, Yang T, Hua Z. p53 mutation - EGFR gene amplification and loss of heterozygosity on chromosome 10 - 17p in human gliomas. Chin Med J (Eng) 2000;113(7):662-666.
56. Badiali M, Iolascon A, Loda M, et al. p53 gene mutations in medulloblastoma. Immunohistochemistry, gel shift analysis, and sequencing. Diagn Mol Pathol 1993;2(1):23-28.
57. Kovar H, Auinger A, Jug G, Muller T, Pillwein K. p53 mosaicism with an exon 8 germline mutation in the founder of a cancer-prone pedigree. Oncogene 1992;7(11):2169-2173.
58. Giunta C, Youil R, Venter D, et al. Rapid diagnosis of germline p53 mutation using the enzyme mismatch cleavage method. Diagn Mol Pathol 1996;5(4):265-270.
59. Orellana C, Martinez F, Hernandez-Marti M, et al. A novel TP53 germ-line mutation identified in a girl with a primitive neuroectodermal tumor and her father. Cancer Genet Cytogenet 1998;105(2):103-108.
60. Reifenberger J, Janssen G, Weber RG, et al. Primitive neuroectodermal tumors of the cerebral hemispheres in two siblings with TP53 germline mutation. J Neuropathol Exp Neurol 1998;57(2):179-187.
61. Mazoyer S, Lalle P, Moyret-Lalle C, et al. Two germ-line mutations affecting the same nucleotide at codon 257 of p53 gene, a rare site for mutations. Oncogene 1994;9(4):1237-1239.
62. Birch JM, Hartley AL, Tricker KJ, et al. Prevalence and diversity of constitutional mutations in the p53 gene among 21 Li-Fraumeni families. Cancer Res 1994;54(5):1298-1304.
63. Avigad S, Barel D, Blau O, et al. A novel germ line p53 mutation in intron 6 in diverse childhood malignancies. Oncogene 1997;14(13):1541-1545.
64. Barel D, Avigad S, Mor C, et al. A novel germ-line mutation in the noncoding region of the p53 gene in a Li-Fraumeni family. Cancer Genet Cytogenet 1998;103(1):1-6.

Chapter 9

Summary and General Discussion

Survival rates of pediatric brain tumor patients have significantly improved over the years due to developments in diagnostic techniques, neurosurgery, chemotherapy, radiotherapy and supportive care. However, brain tumors are still an important cause of cancer-related deaths in children. The current prediction of the prognosis is still highly dependent on clinical characteristics such as the age of the patient, tumor type, stage and localization. Therefore, increased knowledge about the genetic and biological features of these tumors may point to new rationales needed to optimize the diagnosis and treatment of these patients.

In **chapter 2** an overview is given of the currently known genetic and biological events in medulloblastomas and ependymomas. Initially, knowledge was obtained by studying the genetic defects causing hereditary syndromes predisposing to the development of a brain tumor[1-3]. More recently, data have become available about the cells of origin of these tumors and about the possible existence of brain tumor stem cells[4, 5]. Newly developed array-based techniques for studying gene expression, copy number aberrations and epigenetic events have led to the identification of other potentially important biological abnormalities in pediatric medulloblastomas and ependymomas. It has become clear that the deregulation of signaling pathways essential in brain development, e.g. SHH, Wnt and Notch, plays an important role in the pathogenesis and biological behavior of especially medulloblastomas[6].

In this thesis we aimed at finding additional new markers in pediatric brain tumor patients, which might facilitate diagnosis, improve the risk stratification or serve as new therapeutic targets in order to improve the outcome of these patients.

Gene expression profiling

Gene expression profiling using microarrays allows a relatively fast way of screening the expression of a large number of genes. It is a useful tool for the classification of subgroups and for risk stratification of brain tumor patients[7-17]. In embryonal CNS tumors, aberrant gene expression levels of genes involved in signaling pathways important in brain development (e.g. SHH, Wnt, Notch) are correlated to functional abnormalities in these pathways[16, 18-20]. Gene expression profiling led to the important finding that ependymomas from different locations of the CNS correlate with those of the corresponding normal tissue[5]. In **chapter 3** we analyzed gene-expression profiles of pediatric medulloblastomas, ependymomas and normal cerebellum using Affymetrix HGU133 plus 2.0 microarrays. For each subgroup we identified a set of differentially expressed genes. Amongst the most discriminative genes for medulloblastomas and ependymomas are several members of the SOX transcription factor family. SOX genes are transcription factors which are important in embryogenesis[21-24]. This may point to a role of deregulated developmental pathways in the pathogenesis of pediatric brain tumors. We showed that SOX4 and SOX11 are highly overexpressed in medulloblastomas, whereas the expression of SOX9 is significantly increased in ependymomas. This finding was confirmed by other techniques[25, 26]. SOX4 and 11 belong to subgroup C of the SOX gene family, which play a role in normal embryonic development of a.o. the heart, CNS, lungs and thymus[21, 22, 27,

[28]. SOX4 is one of the most frequently targeted genes by retroviral insertional mutagenesis[29, 30] and has both anti- and pro-apoptotic effects[31, 32]. The balance between anti- and pro-apoptotic signals induced by SOX4 expression might thus be tissue-specific and dependent on external signals such as growth factors. SOX9 belongs to the subgroup of SOX E genes, which control the differentiation of astrocytes, oligodendrocytes and Schwann cells[23]. In the intestinal epithelium SOX9 is expressed in a pattern characteristic of Wnt targets[33], which suggests a role for Wnt signaling in ependymomas with high level SOX9 expression.

In addition to the analysis of genes specific for each subgroup of tumors, we studied the influence of gene expression on clinical outcome. High expression of SOX4 and SOX9 are predictive for better outcome in respectively medulloblastomas and ependymomas. To be used as predictive factor in a clinical setting, these results need to be validated in an independent cohort. In addition, we found elevated BCAT1 mRNA expression levels to be correlated to the presence of leptomeningeal metastases in medulloblastoma. BCAT1 is a cytosolic branched-chain amino acid aminotransferase, which is involved in the control of the cell cycle by suppressing the G1 to S transition[34]. Although BCAT1 was not associated with metastatic medulloblastoma disease in other studies[16], its expression is increased in e.g. progressive colorectal carcinomas[35]. The correlation of BCAT1 overexpression and the presence of metastasized disease in medulloblastomas as found in our study, may be mediated by c-myc, which targets BCAT1[36]. c-myc is amplified in approximately 5-10% of medulloblastomas and is associated with a poor prognosis[37-39]. Regarding the focal staining that we observed for BCAT1, it might be that BCAT1 is specific for medulloblastoma cells that have the potency or tendency to metastasize. As BCAT1 can be inhibited by gabapentin[40], its use as a therapeutic target should be investigated.

Protein expression profiling

Differential gene expression does not always lead to a detectable change in protein expression and for some markers the differential expression at protein level is not accompanied by a change at RNA level. Therefore, and because protein levels actually determine the state and function of the cell, it is essential to screen and validate tumor markers at the protein level. Proteomic research can be complicated, as many techniques require relatively large amounts of protein. In addition, antibodies can only be used to study known proteins and results of these studies are highly dependent on the availability and specificity of the antibody. In **chapter 4** we used a new proteome-wide screening approach, two-dimensional difference gel electrophoresis (2D-DIGE), in combination with mass spectrometry (MS), to study the expression of known and unknown proteins in medulloblastomas, primitive neuroectodermal tumors (PNETs) and ependymomas. The advantage of 2D-DIGE compared to conventional 2D electrophoresis, which was for example previously used to analyzed protein expression profiles of medulloblastoma cell lines[41], is the use of fluorescent labeling of proteins, which increases the sensitivity and the presence of an internal standard that allows correction for

gel-to-gel variation[42]. Seventy-nine differentially expressed protein spots were detected by 2D-DIGE and subsequently identified by tandem mass spectrometry. Of these, stathmin was highly overexpressed in medulloblastomas and PNETs compared to normal cerebellum. This overexpression is of interest since stathmin belongs to a family of phosphoproteins involved in microtubule dynamics. Phosphorylation of stathmin, e.g. during mitosis, impairs the depolymerization of microtubules and promotes their polymerization[43, 44]. The high expression of stathmin may thus be indicative for a high mitotic rate in medulloblastomas and PNETs. Interestingly, stathmin expression may influence the sensitivity of tumor cells to vinca-alkaloids and taxanes[45]. A decrease in stathmin expression is thought to result in increased resistance to vinca-alkaloids as the effects of the microtubule-destabilizing vinca-alkaloids are counteracted. Stathmin expression levels might therefore point to patients who are sensitive to vinca-alkaloids and taxanes.

Two proteins that were found at high levels in ependymomas by 2D-DIGE/MS are annexin A1 and calcyphosine, which are both calcium-binding proteins. Little is known about the role of these proteins in tumor cells. These might play a role in the prevention of apoptosis as they may bind the excess of calcium which normally causes apoptosis[46]. Annexin A1 is an interesting potential therapeutic target as treatment with ^{125}I annexin A1 antibodies destroys solid tumors resulting in improved animal survival[47]. Overexpression of calcyphosine was predominantly observed in ependymomas with epithelial differentiation, which might be used as a marker for a new subgroup of ependymomas. The differential protein expression of the stathmin, annexin A1 and calcyphosine was confirmed by immunohistochemistry.

Proteomic techniques are also useful for the identification of disease-related markers in the cerebrospinal fluid (CSF) of brain tumor patients. CSF, which surrounds the brain, may contain proteins excreted by tissues induced by the presence of a tumor or secreted by the tumor cells itself.

In **chapter 5** we studied protein expression profiles of CSF of 32 pediatric brain tumor patients and 70 pediatric control patients. Q10 anionic exchange protein chip arrays and SELDI-TOF mass spectrometry were used, which combines extraction of proteins by chromatography and identification by mass spectrometry. One hundred twenty three differentially expressed protein peak clusters were found that discriminated brain tumor patients from control patients with a prediction accuracy of 88%. Apolipoprotein A-II (APO A-II), overexpressed in the CSF of brain tumor patients, was one of the most discriminative proteins. A recent study suggests that APO A-II might be used as a marker for prostate cancer[48]. However, CSF APO A-II levels were correlated to CSF albumin levels in our study and therefore a disrupted blood brain barrier most likely causes the overexpression of APO A-II in the CSF of brain tumor patients. In addition, the absence of specific cellular APO A-II staining in any of the brain tumor subtypes further indicates that tumor cells do not produce APO A-II. This also suggests that the high levels of APO A-II are caused by secondary changes related to the presence of a tumor such as a disrupted blood brain barrier.

Pediatric brain tumor patients frequently present with hydrocephalus. An aberrant protein expression profile in hydrocephalus patients is caused by a change in CSF flow rate, and subsequent aberrant CSF protein concentrations[49]. In addition, the presence of edema, demyelinisation and neurodegeneration also change protein constitution as a result of mechanical and ischemic effects[50-52]. Total tau (t-Tau), hyperphosphorylated Tau (p-$Tau_{(181P)}$) and ß-$amyloid_{(1-42)}$ levels in CSF are markers of neuronal and axonal degeneration. In **chapter 6** we evaluated the influence of the presence of a brain tumor and hydrocephalus on the levels of these neurodegenerative markers in the CSF of pediatric patients. In concordance with other studies, we showed that t-Tau levels in the CSF of brain tumor patients, especially medulloblastoma patients, and in hydrocephalus patients and patients with a serious infection of the central nervous system are increased, reflecting severe neuronal damage[53, 54]. As it is known that many pediatric brain tumor patients suffer from long-term neurological side-effects, the neurodegenerative markers present in CSF may be used in longitudinal studies to provide information about the extent of neuronal and axonal degeneration caused by different treatment modalities, such as surgery, chemo- and radiotherapy. The inclusion of neuropsychological tests in these studies may be used to investigate the presence of possible correlations between t-Tau, p-$Tau_{(181P)}$ and ß-$amyloid_{(1-42)}$ levels in CSF and long-term neurological and neuropsychological impairments caused by the disease and therapies.

In **chapter 7** we studied gene expression levels of members of the insulin growth factor (IGF) system and the corresponding protein expression levels in the CSF of medulloblastoma, ependymoma and control patients. We focused on the IGF system, as it is important in the development of normal brain and brain-tissue derived tumors. The importance of the IGF system in medulloblastomas has previously been shown by the detection of the phosphorylated form of the IGF-1R and its downstream targets in the majority of medulloblastomas[55, 56]. We described the overexpression of IGFBP-2 and IGFBP-3 in both medulloblastomas and ependymomas and the overexpression of IGFBP-5 and IGF-2 in ependymomas. Overexpression of IGF-2 in ependymomas was also found in other studies[12] and suggests the involvement of the IGF signaling pathway in ependymomas. However, overexpression of this gene may also indicate the role for active SHH signaling in ependymomas as IGF-2 is a downstream target of SHH[57]. Interestingly, medulloblastoma tumor growth can be reduced by inhibition of the IGF-1R signaling pathway[58], suggesting that this pathway is an interesting therapeutic target. As this inhibition is augmented by constitutive GSK3β phosphorylation[59], the combined inhibition of the IGF-1R and dephosphorylation of GSK3β might be an effective treatment option for medulloblastoma.

In addition to the gene expression analysis of the IGF system, we studied levels of the corresponding proteins in the CSF, as the identification of more specific tumor markers in the CSF might be useful at diagnosis or to detect minimal residual disease after surgery or early relapse. In contrast to the differential mRNA expression of several members of the IGF system, only IGFBP-3 was found to be a possible candidate CSF marker in medulloblastoma, as total

IGFBP-3, proteolytic fragments of IGFBP-3 and IGFBP-3 proteolytic activity were significantly increased. IGFBP-3 may therefore be a marker for residual disease, potentially useful in the follow up of medulloblastoma patients. As IGFBP-3 may control the amount of free IGF-1 and IGF-2 being able to bind to the IGF-1R, it is an important regulator of IGF pathway activation. Because of the fact that IGFBP-3 proteolytic fragments have decreased affinity for IGF-ligands, the increased proteolysis in the CSF of medulloblastoma patients might result in higher levels of functional ligand and consequently IGF-1R activation. Proteolytic fragments of IGFBP-3 have also been shown to possess IGF-independent tissue-specific pro-apoptotic or anti-apoptotic properties[60-62].

Despite increased IGFBP-2, IGFBP-3, IGFBP-5 and IGF-2 mRNA expression levels in ependymoma cells, protein levels of these genes in CSF were normal in ependymoma patients. The absence of increased protein levels in the CSF of ependymoma patients might be explained by the fact that ependymomas usually do not spread via the CSF. Furthermore, these proteins may also exert their effects locally by paracrine or autocrine mechanisms, thereby not reaching the CSF.

In **chapter 8** we evaluated another signaling pathway involved in many malignancies, which involves the p53 tumor suppressor gene[63]. We screened for inactivating p53 mutations in pediatric medulloblastomas and ependymomas and used the gene expression data from chapter 3 to study the expression levels of genes regulating p53 activation and p53 target genes. In concordance with previous studies[64-67], p53 inactivating mutations were rare in medulloblastomas and ependymomas. In 2 medulloblastoma patients we identified missense mutations in p53 that have not been previously described in embryonal CNS tumors. No p53 mutations were found in ependymoma patients. Despite the low incidence of inactivating p53 mutations, a significant overexpression of cyclins and CDKs was observed in medulloblastomas versus normal tissue, which might indicate a dysfunctional p53 pathway as the expression of these genes is inhibited by normal p53. However, the low incidence of p53 mutations and normal expression levels of upstream p53 regulatory genes implies that the p53 signaling pathway is important in a minority of pediatric medulloblastomas and ependymomas.

CONCLUSION AND FUTURE PERSPECTIVES

In conclusion, this thesis shows that both genomic and proteomic techniques may be successfully used to increase the knowledge about genetic and biological characteristics of brain tumor patients. The functional characteristics of the identified differentially expressed genes and proteins needs to be further studied in order to evaluate their importance as tumor marker, prognostic marker and drug target in pediatric brain tumors. Modulating SOX expression by RNAi, as was already successfully shown for SOX4 in prostate cancer

[31], may provide more information about the functional role of the overexpression of the SOX genes in pediatric medulloblastoma and ependymoma. Stathmin overexpression in medulloblastoma warrants further investigation, as stathmin expression might be an important feature to identify patients who are sensitive to vinca-alkaloids and taxanes due to its role in microtubule dynamics. Activated signaling pathways in medulloblastoma and ependymoma, such as IGF-signaling, might be used as new therapeutic targets in order to improve outcome. The identification of disease markers in the CSF of brain tumor patients provides additional possibilities for follow-up of patients in addition to conventional techniques, such as radiological imaging. APO A-II as new marker for a disrupted blood brain barrier might be of use in studies investigating the delivery of drugs to the central nervous system. The expression of neurodegenerative markers in CSF, such as t-Tau, might predict long-term neurological complications, which should be explored in studies combining CSF measurements and neurological and neuro-psychological follow up. The use of IGFBP-3 as a marker of minimal residual disease or early relapse in medulloblastoma patients should also be validated in longitudinal follow up studies.

Few of the currently known brain tumor markers have consistently been found to have prognostic value in pediatric brain tumors, which may be due to the wide range of subgroups based on e.g. histology and localization, which results in relatively small series of patients. In addition, different treatment strategies also complicate the comparison of patient groups between different institutions. Cooperation between institutions in order to achieve larger study populations is therefore warranted. Further progress in the characterization of pediatric brain tumors may be accomplished by improvements in the sensitivity and resolution of the currently available techniques. Combining different genomic and proteomic methods will provide valuable information, which is for example illustrated by the combination of array CGH and gene expression profiling data, leading to the identification of the involved genes in recurrent copy number aberrations[68-70]. In addition, the development of new techniques, such as exon array and microRNA screening, may provide new information about alternative splicing events and posttranscriptional control of gene expression important in the pathogenesis of pediatric brain tumors.

REFERENCES

1. Biegel JA. Cytogenetics and molecular genetics of childhood brain tumors. Neuro Oncol 1999;1(2):139-151.
2. Collins VP. Brain tumours: classification and genes. J Neurol Neurosurg Psychiatry 2004;75 Suppl 2:ii2-11.
3. Taylor MD, Mainprize TG, Rutka JT. Molecular insight into medulloblastoma and central nervous system primitive neuroectodermal tumor biology from hereditary syndromes: a review. Neurosurgery 2000;47(4):888-901.
4. Nicolis SK. Cancer stem cells and "stemness" genes in neuro-oncology. Neurobiol Dis 2007;25(2):217-229.
5. Taylor MD, Poppleton H, Fuller C, et al. Radial glia cells are candidate stem cells of ependymoma. Cancer Cell 2005;8(4):323-335.
6. Fogarty MP, Kessler JD, Wechsler-Reya RJ. Morphing into cancer: the role of developmental signaling pathways in brain tumor formation. J Neurobiol 2005;64(4):458-475.
7. Pusztai L. Chips to bedside: incorporation of microarray data into clinical practice. Clin Cancer Res 2006;12(24):7209-7214.
8. Pomeroy SL, Tamayo P, Gaasenbeek M, et al. Prediction of central nervous system embryonal tumour outcome based on gene expression. Nature 2002;415(6870):436-442.
9. Mischel PS, Cloughesy TF, Nelson SF. DNA-microarray analysis of brain cancer: molecular classification for therapy. Nat Rev Neurosci 2004;5(10):782-792.
10. Chopra A, Brown KM, Rood BR, Packer RJ, MacDonald TJ. The use of gene expression analysis to gain insights into signaling mechanisms of metastatic medulloblastoma. Pediatr Neurosurg 2003;39(2):68-74.
11. Fernandez-Teijeiro A, Betensky RA, Sturla LM, et al. Combining gene expression profiles and clinical parameters for risk stratification in medulloblastomas. J Clin Oncol 2004;22(6):994-998.
12. Korshunov A, Neben K, Wrobel G, et al. Gene expression patterns in ependymomas correlate with tumor location, grade, and patient age. Am J Pathol 2003;163(5):1721-1727.
13. Neben K, Korshunov A, Benner A, et al. Microarray-based screening for molecular markers in medulloblastoma revealed STK15 as independent predictor for survival. Cancer Res 2004;64(9):3103-3111.
14. Lukashova-v Zangen I, Kneitz S, Monoranu CM, et al. Ependymoma gene expression profiles associated with histological subtype, proliferation, and patient survival. Acta Neuropathol 2007;113(3):325-337.
15. Sowar K, Straessle J, Donson AM, Handler M, Foreman NK. Predicting which children are at risk for ependymoma relapse. J Neurooncol 2006;78(1):41-46.
16. Thompson MC, Fuller C, Hogg TL, et al. Genomics identifies medulloblastoma subgroups that are enriched for specific genetic alterations. J Clin Oncol 2006;24(12):1924-1931.
17. MacDonald TJ, Brown KM, LaFleur B, et al. Expression profiling of medulloblastoma: PDGFRA and the RAS/MAPK pathway as therapeutic targets for metastatic disease. Nat Genet 2001;29(2):143-152.
18. Lee Y, Miller HL, Jensen P, et al. A molecular fingerprint for medulloblastoma. Cancer Res 2003;63(17):5428-5437.
19. Lee Y, McKinnon PJ. DNA ligase IV suppresses medulloblastoma formation. Cancer Res 2002;62(22):6395-6399.
20. Oliver TG, Grasfeder LL, Carroll AL, et al. Transcriptional profiling of the Sonic hedgehog response: a critical role for N-myc in proliferation of neuronal precursors. Proc Natl Acad Sci U S A 2003;100(12):7331-7336.
21. Kamachi Y, Uchikawa M, Kondoh H. Pairing SOX off: with partners in the regulation of embryonic development. Trends Genet 2000;16(4):182-187.

22. Kuhlbrodt K, Herbarth B, Sock E, et al. Cooperative function of POU proteins and SOX proteins in glial cells. J Biol Chem 1998;273(26):16050-16057.
23. Cheung M, Briscoe J. Neural crest development is regulated by the transcription factor Sox9. Development 2003;130(23):5681-5693.
24. Foster JW, Dominguez-Steglich MA, Guioli S, et al. Campomelic dysplasia and autosomal sex reversal caused by mutations in an SRY-related gene. Nature 1994;372(6506):525-530.
25. Yokota N, Mainprize TG, Taylor MD, et al. Identification of differentially expressed and developmentally regulated genes in medulloblastoma using suppression subtraction hybridization. Oncogene 2004;23(19):3444-3453.
26. Lee CJ, Appleby VJ, Orme AT, Chan WI, Scotting PJ. Differential expression of SOX4 and SOX11 in medulloblastoma. J Neurooncol 2002;57(3):201-214.
27. Cheung M, Abu-Elmagd M, Clevers H, Scotting PJ. Roles of Sox4 in central nervous system development. Brain Res Mol Brain Res 2000;79(1-2):180-191.
28. Schilham MW, Oosterwegel MA, Moerer P, et al. Defects in cardiac outflow tract formation and pro-B-lymphocyte expansion in mice lacking Sox-4. Nature 1996;380(6576):711-714.
29. Suzuki T, Shen H, Akagi K, et al. New genes involved in cancer identified by retroviral tagging. Nat Genet 2002;32(1):166-174.
30. Du Y, Spence SE, Jenkins NA, Copeland NG. Cooperating cancer-gene identification through oncogenic-retrovirus-induced insertional mutagenesis. Blood 2005;106(7):2498-2505.
31. Liu P, Ramachandran S, Ali Seyed M, et al. Sex-determining region Y box 4 is a transforming oncogene in human prostate cancer cells. Cancer Res 2006;66(8):4011-4019.
32. Hur EH, Hur W, Choi JY, et al. Functional identification of the pro-apoptotic effector domain in human Sox4. Biochem Biophys Res Commun 2004;325(1):59-67.
33. Blache P, van de Wetering M, Duluc I, et al. SOX9 is an intestine crypt transcription factor, is regulated by the Wnt pathway, and represses the CDX2 and MUC2 genes. J Cell Biol 2004;166(1):37-47.
34. Schuldiner O, Eden A, Ben-Yosef T, et al. ECA39, a conserved gene regulated by c-Myc in mice, is involved in G1/S cell cycle regulation in yeast. Proc Natl Acad Sci U S A 1996;93(14):7143-7148.
35. Yoshikawa R, Yanagi H, Shen CS, et al. ECA39 is a novel distant metastasis-related biomarker in colorectal cancer. World J Gastroenterol 2006;12(36):5884-5889.
36. Ben-Yosef T, Eden A, Benvenisty N. Characterization of murine BCAT genes: Bcat1, a c-Myc target, and its homolog, Bcat2. Mamm Genome 1998;9(7):595-597.
37. Grotzer MA, Hogarty MD, Janss AJ, et al. MYC messenger RNA expression predicts survival outcome in childhood primitive neuroectodermal tumor/medulloblastoma. Clin Cancer Res 2001;7(8):2425-2433.
38. Herms J, Neidt I, Luscher B, et al. C-MYC expression in medulloblastoma and its prognostic value. Int J Cancer 2000;89(5):395-402.
39. Stearns D, Chaudhry A, Abel TW, et al. c-myc overexpression causes anaplasia in medulloblastoma. Cancer Res 2006;66(2):673-681.
40. Hutson SM, Berkich D, Drown P, et al. Role of branched-chain aminotransferase isoenzymes and gabapentin in neurotransmitter metabolism. J Neurochem 1998;71(2):863-874.
41. Peyrl A, Krapfenbauer K, Slavc I, et al. Protein profiles of medulloblastoma cell lines DAOY and D283: identification of tumor-related proteins and principles. Proteomics 2003;3(9):1781-1800.
42. Marouga R, David S, Hawkins E. The development of the DIGE system: 2D fluorescence difference gel analysis technology. Anal Bioanal Chem 2005;382(3):669-678.
43. Curmi PA, Gavet O, Charbaut E, et al. Stathmin and its phosphoprotein family: general properties, biochemical and functional interaction with tubulin. Cell Struct Funct 1999;24(5):345-357.
44. Melander Gradin H, Marklund U, Larsson N, Chatila TA, Gullberg M. Regulation of microtubule dynamics by Ca2+/calmodulin-dependent kinase IV/Gr-dependent phosphorylation of oncoprotein 18. Mol Cell Biol 1997;17(6):3459-3467.

45. Alli E, Bash-Babula J, Yang JM, Hait WN. Effect of stathmin on the sensitivity to antimicrotubule drugs in human breast cancer. Cancer Res 2002;62(23):6864-6869.
46. Orrenius S, Zhivotovsky B, Nicotera P. Regulation of cell death: the calcium-apoptosis link. Nat Rev Mol Cell Biol 2003;4(7):552-565.
47. Oh P, Li Y, Yu J, et al. Subtractive proteomic mapping of the endothelial surface in lung and solid tumours for tissue-specific therapy. Nature 2004;429(6992):629-635.
48. Malik G, Ward MD, Gupta SK, et al. Serum levels of an isoform of apolipoprotein A-II as a potential marker for prostate cancer. Clin Cancer Res 2005;11(3):1073-1085.
49. Reiber H. Dynamics of brain-derived proteins in cerebrospinal fluid. Clin Chim Acta 2001;310(2):173-186.
50. Del Bigio MR. Cellular damage and prevention in childhood hydrocephalus. Brain Pathol 2004;14(3):317-324.
51. Weller RO, Williams BN. Cerebral biopsy and assessment of brain damage in hydrocephalus. Arch Dis Child 1975;50(10):763-768.
52. Ding Y, McAllister JP, 2nd, Yao B, Yan N, Canady AI. Axonal damage associated with enlargement of ventricles during hydrocephalus: a silver impregnation study. Neurol Res 2001;23(6):581-587.
53. Tisell M, Tullberg M, Mansson JE, et al. Differences in cerebrospinal fluid dynamics do not affect the levels of biochemical markers in ventricular CSF from patients with aqueductal stenosis and idiopathic normal pressure hydrocephalus. Eur J Neurol 2004;11(1):17-23.
54. Van Gool SW, Van Kerschaver E, Brock P, et al. Disease- and treatment-related elevation of the neurodegenerative marker tau in children with hematological malignancies. Leukemia 2000;14(12):2076-2084.
55. Del Valle L, Enam S, Lassak A, et al. Insulin-like growth factor I receptor activity in human medulloblastomas. Clin Cancer Res 2002;8(6):1822-1830.
56. Del Valle L, Wang JY, Lassak A, et al. Insulin-like growth factor I receptor signaling system in JC virus T antigen-induced primitive neuroectodermal tumors--medulloblastomas. J Neurovirol 2002;8 Suppl 2:138-147.
57. Hahn H, Wojnowski L, Specht K, et al. Patched target Igf2 is indispensable for the formation of medulloblastoma and rhabdomyosarcoma. J Biol Chem 2000;275(37):28341-28344.
58. Wang JY, Del Valle L, Gordon J, et al. Activation of the IGF-1R system contributes to malignant growth of human and mouse medulloblastomas. Oncogene 2001;20(29):3857-3868.
59. Urbanska K, Trojanek J, Del Valle L, et al. Inhibition of IGF-1 receptor in anchorage-independence attenuates GSK-3beta constitutive phosphorylation and compromises growth and survival of medulloblastoma cell lines. Oncogene 2007;26(16):2308-2317.
60. Baxter RC. Signalling pathways involved in antiproliferative effects of IGFBP-3: a review. Mol Pathol 2001;54(3):145-148.
61. Ricort JM, Binoux M. Insulin-like growth factor binding protein-3 stimulates phosphatidylinositol 3-kinase in MCF-7 breast carcinoma cells. Biochem Biophys Res Commun 2004;314(4):1044-1049.
62. Xi Y, Nakajima G, Hamil T, et al. Association of insulin-like growth factor binding protein-3 expression with melanoma progression. Mol Cancer Ther 2006;5(12):3078-3084.
63. Hanahan D, Weinberg RA. The hallmarks of cancer. Cell 2000;100(1):57-70.
64. Adesina AM, Nalbantoglu J, Cavenee WK. p53 gene mutation and mdm2 gene amplification are uncommon in medulloblastoma. Cancer Res 1994;54(21):5649-5651.
65. Nozaki M, Tada M, Matsumoto R, et al. Rare occurrence of inactivating p53 gene mutations in primary non-astrocytic tumors of the central nervous system: reappraisal by yeast functional assay. Acta Neuropathol 1998;95(3):291-296.
66. Saylors RL, 3rd, Sidransky D, Friedman HS, et al. Infrequent p53 gene mutations in medulloblastomas. Cancer Res 1991;51(17):4721-4723.

67. Fink KL, Rushing EJ, Schold SC, Jr., Nisen PD. Infrequency of p53 gene mutations in ependymomas. J Neurooncol 1996;27(2):111-115.
68. Lo KC, Rossi MR, Burkhardt T, Pomeroy SL, Cowell JK. Overlay analysis of the oligonucleotide array gene expression profiles and copy number abnormalities as determined by array comparative genomic hybridization in medulloblastomas. Genes Chromosomes Cancer 2007;46(1):53-66.
69. Modena P, Lualdi E, Facchinetti F, et al. Identification of tumor-specific molecular signatures in intracranial ependymoma and association with clinical characteristics. J Clin Oncol 2006;24(33):5223-5233.
70. Lo KC, Rossi MR, Eberhart CG, Cowell JK. Genome wide copy number abnormalities in pediatric medulloblastomas as assessed by array comparative genome hybridization. Brain Pathol 2007;17(3):282-296.

Chapter 10

Nederlandse Samenvatting

HERSENTUMOREN BIJ KINDEREN

Tumoren van het centrale zenuwstelsel zijn na acute lymfatische leukemie de meest voorkomende vorm van kanker bij kinderen. Jaarlijks wordt bij ongeveer 2-2,5 per 100.000 kinderen een hersentumor vastgesteld. De gemiddelde leeftijd bij diagnose van de ziekte is 6 jaar. Hersentumoren bij kinderen verschillen van hersentumoren bij volwassenen in lokalisatie, histologisch subtype en respons op behandeling (Tabel 1). Hersentumoren bij kinderen zijn voornamelijk gelokaliseerd in de achterste schedelgroeve, terwijl hersentumoren bij volwassenen voornamelijk ontstaan in de cerebrale hemisferen. De meeste hersentumoren die bij kinderen worden gezien, zoals de primitieve neuro-ectodermale tumoren, komen slechts zelden voor bij volwassenen. De klinische symptomen van een hersentumor worden bepaald door de plaats en grootte van de tumor. Veelal berusten de klachten op een verhoogde intracraniële druk (hoofdpijn, braken, gedragsveranderingen) en lokale symptomen die

Tabel 1. Overzicht van hersentumoren bij kinderen naar histologisch subtype en lokalisatie.
*Percentage van het totaal aantal hersentumoren

Lokalisatie en histologisch subtype	Percentage*
Infratentorieel	
Primitieve neuroectodermale tumor	5
Medulloblastoom	20
Laag-gradig astrocytoom, cerebellum	12-18
Ependymoom	4-8
Maligne glioom, hersenstam	3-9
Laag-gradig astrocytoom, hersenstam	3-6
Overig	2-5
Supratentorieel	
Laag-gradig astrocytoom	8-20
Maligne glioom	6-12
Ependymoom	2-5
Gemengd glioom	1-5
Gangliogliоom	1-5
Oligodendroglioom	1-2
Plexus choroideus tumor	1-2
Primitieve neuroectodermale tumor	1-2
Meningeoom	0.5-2
Overig	1-3
Centraal gelegen supratentorieel	
Suprasellar craniopharyngioom	6-9
Glioom in chiasma-hypothalamus	4-8
Germinoom	1-2
Hypofyseadenoom	0.5-2.5
Regio pinealis	
Glioom	1-2
Germinoom	0.5-2
Pinealoom	0.5-2

samenhangen met functiestoornissen ter plaatse van de tumor door verplaatsing of beschadiging van het normale hersenweefsel. De behandeling van hersentumoren bestaat veelal uit een combinatie van chirurgie, radiotherapie en chemotherapie, maar is afhankelijk van het type tumor, de lokalisatie en de leeftijd van de patiënt. Ruwweg geneest 60% van de kinderen met een hersentumor.

Veel voorkomende hersentumoren bij kinderen

Astrocytomen zijn tumoren die bij kinderen voorkomen, met name het graad I pilocytair astrocytoom. Dit zijn weinig agressieve tumoren en de prognose is goed wanneer de tumoren volledig chirurgisch verwijderd kunnen worden. Deze tumoren kunnen overal in de hersenen voorkomen, maar worden met name gezien rond de kleine hersenen en de oogzenuw. In tegenstelling tot volwassen zijn graad III en IV astrocytomen zeldzaam bij kinderen. Ongeveer 10% van alle hersentumoren bij kinderen zijn ponsgliomen die door het gebrek aan behandelingsmogelijkheden geassocieerd zijn met een zeer slechte prognose.

Het medulloblastoom is een kwaadaardige tumor die zich altijd in het gebied van de kleine hersenen bevindt. Het medulloblastoom is een tumor die hoort tot de groep van z.g. embryonale tumoren van het centraal zenuwstelsel. De tumor zaait dikwijls uit binnen het centrale zenuwstelsel. Jonge kinderen en patiënten met uitzaaiingen hebben een slechte prognose. Door de lokalisatie van de tumor treedt vaak hydrocefalus op, een belemmering van de afvoer van het hersenvocht door het samendrukken van de vierde hersenkamer. Jonge leeftijd, de aanwezigheid van uitzaaiingen en incomplete chirurgische resectie zijn ongunstige prognostische factoren. Met de huidige therapie, die bestaat uit chirurgie, radiotherapie en chemotherapie, overleeft 60-80% van de laag-risico patiënten, terwijl slechts 25% van de hoog-risico patiënten genezen kunnen worden.

Ependymomen ontstaan uit cellen die de bekleding vormen van de hersenholten, de ependymcellen. Deze tumoren worden vaak in de 4e ventrikel in de achterste schedelgroeve of in het spinale kanaal gezien. De overleving van het ependymoom bij kinderen is over het algemeen slechter dan bij volwassenen. De meest belangrijke prognostische factor bij ependymomen is de mate van chirurgische resectie. Bij patiënten waarbij de tumor volledig verwijderd kan worden, overleeft 50-70%, terwijl maximaal 30% van de patiënten overleeft wanneer geen complete resectie mogelijk is. Naast chirurgie vormt radiotherapie een belangrijk onderdeel van de behandeling van ependymomen. Chemotherapie lijkt vooralsnog niet bij te dragen aan de verbetering van de overleving.

Andere hersentumor subtypes, zoals plexustumoren, kiemceltumoren en craniofaryngeomen zijn relatief zeldzaam bij kinderen.

ONDERZOEK NAAR GENETISCHE EN BIOLOGISCHE FACTOREN

De overlevingskansen van kinderen met een hersentumor zijn de laatste jaren sterk toegenomen. Helaas vormen hersentumoren echter nog steeds de belangrijkste doodsoorzaak bij kinderen met kanker. Daarnaast treden bij deze kinderen vaak ernstige neurologische en neuropsychologische bijwerkingen op waardoor de kwaliteit van leven van deze kinderen aanzienlijk wordt verminderd. De prognose van kinderen met een hersentumor is nog steeds voornamelijk afhankelijk van een aantal klinische kenmerken, zoals de leeftijd van de patiënt, het histologische type en de lokalisatie van de tumor. Om de behandeling van deze patiënten te verbeteren is het van belang om meer te weten te komen over de genetische en biologische kenmerken van deze tumoren die kunnen helpen bij het stellen van de diagnose, kunnen worden gebruikt voor een verbeterde risicoclassificatie, of als target voor een nieuw te ontwikkelen behandeling. Verschillende technieken op genomisch en eiwitniveau zijn de laatste jaren ontwikkeld om deze karakteristieken te identificeren.

In **hoofdstuk 2** wordt een overzicht gegeven van de genetische en biologische afwijkingen die op dit moment bekend zijn in medulloblastomen en ependymomen bij kinderen. De eerste kennis over deze tumoren werd verkregen door de bestudering van de genetische afwijkingen bij erfelijke syndromen waarbij een verhoogd risico bestaat op de ontwikkeling van hersentumoren. De laatste tijd is echter meer bekend geworden over de cellulaire origine van deze tumoren en over het mogelijke bestaan van hersentumor stamcellen. Met name in medulloblastomen is het duidelijk geworden dat signaaltransductie paden betrokken bij de normale hersenontwikkeling, zoals SHH, Wnt and Notch, verstoord zijn in hersentumoren. Een afwijkende expressie van de betrokken genen, bijvoorbeeld veroorzaakt door mutaties, amplificaties of epigenetische veranderingen, wordt frequent gevonden in deze tumoren. Nieuw ontwikkelde array technieken voor het bestuderen van de expressie van genen en chromosomale en epigenetische afwijkingen hebben ook geleid tot de identificatie van mogelijk belangrijke biologische afwijkingen in medulloblastomen en ependymomen.

Genexpressie in tumorcellen

In **hoofdstuk 3** beschrijven we een genoom-brede screening van genexpressie profielen van medulloblastomen, ependymomen en normaal cerebellum. Voor elke subgroep zijn genen geïdentificeerd die differentieel tot expressie komen. Verschillende leden van de SOX transcriptiefactor familie werden geïdentificeerd als discriminatieve genen in medulloblastomen en ependymomen. mRNA en eiwit expressieniveaus van SOX4 en SOX11 waren sterk verhoogd in medulloblastomen en in ependymomen gold dit voor SOX9. Naast de analyse van genen specifiek voor elke subgroep tumoren, werd ook een analyse verricht naar de genen waarvan de expressie geassocieerd is met de prognose. In medulloblastomen en ependymomen correleerden respectievelijk 35 en 13 genen met de behandelingsresultaten op lange termijn. Daarnaast bleek ook de expressie van SOX4 en SOX9 te correleren met een

betere prognose in deze patiënten. De mRNA expressie van BCAT1 bleek gecorreleerd met de aanwezigheid van leptomeningeale metastasen in medulloblastomen, maar dit kon op eiwitniveau niet bevestigd worden.

Eiwitexpressie in tumorcellen

Aangezien mRNA en eiwitexpressieniveaus niet altijd met elkaar overeenkomen en eiwitten de uiteindelijke functie van het gen in de cel vervullen, is het belangrijk ook de eiwitexpressie te bestuderen. In **hoofdstuk 4** hebben we een eiwitexpressie screening methode toegepast waarbij 2-dimensionale differentiële gel electroforese (2D-DIGE) werd gecombineerd met massaspectrometrie om de expressie van bekende en nieuwe eiwitten in medulloblastomen, primitieve neuro-ectodermale tumoren (PNET) en ependymomen te bestuderen. In totaal werden 79 eiwitten geïdentificeerd die differentieel tot expressie kwamen in deze tumoren. Stathmine kwam verhoogd tot expressie in medulloblastomen en PNETs en annexine A1 en calcyphosine toonden overexpressie in ependymomen in vergelijking tot normaal cerebellum. De afwijkende expressie van deze eiwitten werd bevestigd door middel van immunohistochemie en genexpressie studies bevestigden ook een afwijkende expressie op mRNA niveau. De overexpressie van calcyphosine werd specifiek waargenomen in ependymomen die gekenmerkt werden door epitheliale differentiatie, mogelijk wijzend op de identificatie van een nieuwe subgroep van ependymomen.

Eiwitexpressie in het hersenvocht

Naast de analyse van gen- en eiwitexpressieprofielen van tumorcellen, werd de eiwitexpressie van het hersenvocht van hersentumorpatiënten bestudeerd om nieuwe hersentumormarkers te identificeren die door de tumorcellen worden uitgescheiden of die geïnduceerd worden door de aanwezigheid van een tumor. In **hoofdstuk 5** werden met behulp van eiwitarrays en massaspectrometrie de eiwitexpressieprofielen bestudeerd van het hersenvocht van 32 hersentumorpatiënten en 70 controle patiënten. Er werden 123 eiwitclusters geïdentificeerd die differentieel tot expressie kwamen in het hersenvocht van hersentumorpatiënten ten opzichte van controle patiënten. Met behulp van deze eiwitclusters konden hersentumorpatiënten van controle patiënten worden onderscheiden met een nauwkeurigheid van 88%. Een eiwitcluster met een grootte van 17 kDa dat tot overexpressie kwam in het hersenvocht van hersentumorpatiënten, werd geselecteerd voor verdere analyse en geïdentificeerd als apolipoprotein A-II. We toonden aan dat de overexpressie van dit eiwit meest waarschijnlijk het gevolg is van een verstoorde bloedhersenbarrière, aangezien de expressie van apolipoprotein A-II in hersenvocht correleerde met de expressie van het bloed-eiwit albumine en specifieke apolipoprotein A-II aankleuring in de tumorcellen ontbrak.

Expressie van neurodegeneratieve eiwitten in het hersenvocht

In **hoofdstuk 6** werden ook eiwitmarkers in het hersenvocht van hersentumorpatiënten bestudeerd. In verscheidene neurologische en neurodegeneratieve ziekten zijn totaal Tau (t-Tau), gefosforyleerd Tau (p-$Tau_{(181P)}$) en β-$amyloid_{(1-42)}$ in het hersenvocht geïdentificeerd als markers voor neuronale en axonale degeneratie. We hebben de relatie bestudeerd tussen de aanwezigheid van een hersentumor en hydrocefalus en de expressie van deze neurodegeneratieve markers in het hersenvocht van kinderen met een hersentumor. De expressie van t-Tau bleek sterk verhoogd in het hersenvocht van hersentumorpatiënten, met name in medulloblastoom patiënten, patiënten met hydrocefalus en patiënten met een ernstige infectie van het centraal zenuwstelsel. Dit wijst op ernstige neuronale en axonale schade. Aangezien hersentumorpatiënten op lange termijn vaak veel neurologische bijwerkingen hebben, kunnen deze markers mogelijk gebruikt worden om deze neurologische en neuropsychologische bijwerkingen tijdens de therapie en follow-up te vervolgen.

Afwijkende signaaltransductiepaden in tumorcellen en hersenvocht

In **hoofdstuk 7** hebben wij naast de genexpressieanalyse van genen betrokken bij het IGF transductiesysteem de eiwitexpressie van deze genen in het hersenvocht van hersentumorpatiënten bestudeerd. Het IGF transductiesysteem is betrokken bij de normale ontwikkeling van de hersenen. De mRNA expressie van IGFBP-2 en IGFBP-3 bleek sterk verhoogd in medulloblastomen en ependymomen. Tevens kwamen IGFBP-5 en IGF-2 sterk tot overexpressie in ependymomen. Deze resultaten laten zien dat het IGF transductiesysteem ook afwijkend is in medulloblastomen en ependymomen bij kinderen. In het hersenvocht van ependymoompatiënten was de eiwitexpressie van de bestudeerde IGFs en IGFBPs normaal, maar er werd een verhoogde eiwitexpressie van IGFBP-3 en een verhoogde IGFBP-3 proteolytische activiteit waargenomen in het hersenvocht van medulloblastoompatiënten na resectie van de tumor. IGFBP-3 is dus mogelijk een marker voor minimale restziekte in medulloblastomen en zou nuttig kunnen zijn in de follow-up van deze patiënten.

In **hoofdstuk 8** bestudeerden we een ander signaaltransductiesysteem in medulloblastomen en ependymomen waarbij het p53 tumorsuppressorgen betrokken is en dat afwijkend is in een groot aantal tumoren. Naast het bepalen van de aanwezigheid van p53 mutaties hebben we de genexpressie data uit **hoofdstuk 3** gebruikt om de genexpressie van de genen te analyseren die de activiteit van p53 regelen of waarvan de activiteit door p53 wordt beïnvloed. p53 mutaties waren zeldzaam in de medulloblastomen en ependymomen bij kinderen. In 2 medulloblastoompatiënten identificeerden we missense mutaties in p53 die niet eerder in deze tumoren gevonden zijn. Er werden geen p53 mutaties in ependymomen waargenomen. Ondanks de lage incidentie van p53 mutaties, bleken verscheidene p53 target genen differentieel tot expressie te komen. In medulloblastomen was de expressie van cyclines en cycline afhankelijke kinases sterk verhoogd, wat zou kunnen wijzen op p53 inactivatie aangezien de expressie van deze genen wordt geremd door functioneel p53. Echter, de lage

incidentie van mutaties in p53 en de afwezigheid van afwijkende expressie van genen die de activiteit van p53 beïnvloeden, maken het onwaarschijnlijk dat het p53 transductiepad een belangrijke rol speelt in medulloblastomen en ependymomen bij kinderen.

CONCLUSIE EN TOEKOMSTPERSPECTIEVEN

Om de prognose van kinderen met een hersentumor te verbeteren is meer kennis nodig over de biologische kenmerken van deze tumoren. In dit proefschrift hebben we verschillende technieken op genomisch en eiwitniveau gebruikt om nieuwe biologische markers te identificeren in de tumorcellen en het hersenvocht van hersentumorpatiënten. Een nadere analyse van de functionele kenmerken van de genen en eiwitten die in deze tumoren differentieel tot expressie komen is noodzakelijk om het belang als tumor marker, prognostische marker of nieuw target voor nieuw te ontwikkelen behandelingen te bepalen.

De rol van de overexpressie van SOX genen in medulloblastomen en ependymomen kan bijvoorbeeld onderzocht worden door de expressie van deze genen in tumorcellen te beïnvloeden met RNA-interference. De overexpressie van stathmine lijkt interessant, omdat stathmine een rol speelt in de organisatie van de microtubuli en dus een mogelijke marker is voor de gevoeligheid voor chemotherapeutica die de organisatie van microtubuli beïnvloeden, zoals de vinca-alkaloïden en de taxanen. Geactiveerde signaaltransductiepaden, zoals het IGF-transductiepad, kunnen gebruikt worden als target voor nieuwe therapieën die mogelijk de prognose van patiënten kunnen verbeteren. Tenslotte kunnen eiwitten met een afwijkende expressie in het hersenvocht van hersentumoren patiënten gebruikt worden bij diagnose of in de follow-up. APO A-II is een nieuwe marker voor het opsporen van een verstoorde bloed-hersenbarrière, neurodegeneratieve markers, zoals t-Tau, kunnen worden gebruikt voor het opsporen en vervolgen van neurologische en neuropsychologische complicaties op lange termijn en meer tumorspecifieke markers, zoals IGFBP-3, zouden nuttig kunnen zijn bij het opsporen van minimale restziekte of een recidief.

Voor toekomstige studies is het essentieel dat verschillende centra samenwerken om grotere patiëntgroepen te verzamelen, waardoor de prognostische invloed van de afwijkende expressie van genen en eiwitten met grotere betrouwbaarheid kan worden bepaald. Tevens zullen de verbeterde gevoeligheid en resolutie van onderzoekstechnieken, het combineren van verschillende technieken en de ontwikkeling van nieuwe technieken, zoals bijvoorbeeld de exon en microRNA arrays, bijdragen aan een verbetering van de biologische kennis over hersentumoren bij kinderen.

About the Author

Curriculum Vitae

Judith Maria de Bont werd geboren op 14 april 1979 te Leiden. Na het behalen van haar VWO-diploma (cum laude) aan het Markland College in Oudenbosch in 1997, startte zij met de studie geneeskunde aan de Erasmus Universiteit in Rotterdam.

In 2001 sloot zij haar doctoraalfase af (cum laude) met een afstudeeronderzoek naar non-Hodgkinlymfomen bij allochtone en autochtone kinderen op de afdeling Kinderoncologie en -hematologie in het Erasmus MC - Sophia in Rotterdam onder begeleiding van Dr. K. Hählen. Na het behalen van haar artsexamen (cum laude) in 2003 startte zij op deze afdeling als arts-onderzoeker een promotieonderzoek dat resulteerde in het tot stand komen van dit proefschrift. Onder begeleiding van Prof. Dr. R. Pieters, Dr. M.L. Den Boer en Dr. R.E. Reddingius verrichtte zij onderzoek naar biologische kenmerken aan hersentumoren bij kinderen. Tijdens haar co-schappen en de eerste twee jaar van het promotieonderzoek werkte zij tevens als SKION datamanager hematologische maligniteiten bij de afdeling Kinderoncologie en -hematologie in het Erasmus MC – Sophia in Rotterdam.

In februari 2008 is zij gestart met haar opleiding tot neuroloog in het Erasmus MC te Rotterdam (opleider: Prof. Dr. P.A.E. Sillevis Smitt)

List of Publications

de Bont JM, Pieters R.
Management of hyperuricemia with rasburicase - review.
Nucleosides Nucleotides Nucleic Acids 2004; **23**(8-9): 1431-1440
de Bont JM, Holt B, Dekker AW, van der Does-van den Berg A, Sonneveld P, Pieters R.
Significant difference in outcome for adolescents with acute lymphoblastic leukemia treated on pediatric vs adult protocols in the Netherlands.
Leukemia. 2004 **18**(12): 2032-2035
van Zutven LJ, van Drunen E, **de Bont JM**, Wattel MM, Den Boer ML, Pieters R, Hagemeijer A, Slater RM, Beverloo HB.
CDKN2 deletions have no prognostic value in childhood precursor-B acute lymphoblastic leukaemia.
Leukemia 2005; **19**(7): 1281-1284
de Bont JM, van der Holt B, Dekker AW, van der Does-van den Berg A, Sonneveld P, Pieters R.
Adolescents with acute lymphatic leukaemia achieve significantly better results when treated following Dutch paediatric oncology protocols than with adult protocols
Ned Tijdschr Geneeskd 2005; **149**(8): 400-406
de Bont JM, den Boer ML, Reddingius RE, Jansen J, Passier M, van Schaik RH, Kros JM, Sillevis Smitt PA, Luider TH, Pieters R.
Identification of apolipoprotein A-II in cerebrospinal fluid of pediatric brain tumor patients by protein expression profiling.
Clin Chem 2006; **52**(8): 1501-1509
de Bont JM, den Boer ML, Kros JM, Passier MM, Reddingius RE, Smitt PA, Luider TM, Pieters R.
Identification of novel biomarkers in pediatric primitive neuroectodermal tumors and ependymomas by proteome-wide analysis.
J Neuropathol Exp Neurol 2007; **66**(6): 505-516
de Bont JM, Vanderstichele H, Reddingius RE, Pieters R, van Gool SW.
Increased total-Tau levels in cerebrospinal fluid of pediatric hydrocephalus and brain tumor patients.
Eur J Paediatr Neurol 2008; **12**(4): 334-341
de Bont JM, van Doorn J, Reddingius RE, Graat GH, Passier MM, den Boer ML, Pieters R.
Various components of the insulin-like growth factor system in tumor tissue, cerebrospinal fluid and peripheral blood of pediatric medulloblastoma and ependymoma patients.
Int J Cancer 2008; **123**(3):594-600
de Bont JM, den Boer ML, Kros JM, Passier MMCJ, Reddingius RE, Smitt PA, Luider TM, Pieters R.
Differential expression and prognostic significance of SOX genes in pediatric medulloblastoma and ependymoma identified by microarray analysis.
Neuro-Oncology 2008; Jun 24 [Epub ahead of print]
de Bont JM, Packer RJ, Michiels EM, den Boer ML, Pieters R.
Biological background of pediatric medulloblastoma and ependymoma - A review from a translational research perspective.
Neuro-Oncology 2008; accepted for publication
de Bont JM, French PJ, Kros JM, Passier MMCJ, van Noesel M, Sillevis Smitt PAE, den Boer ML, Pieters R.
Low frequency of p53 mutations and differential expression of p53 regulatory genes in pediatric medulloblastoma and ependymoma
Submitted for publication

Dankwoord

Het is klaar! Het schrijven van dit dankwoord, het laatste, maar tevens meest gelezen deel van het proefschrift, voelt dan ook een beetje als afscheid nemen. Reden te meer om de talloze herinneringen aan deze intensieve periode vast te leggen en iedereen die heeft bijgedragen aan het tot stand komen van dit proefschrift te bedanken.

Prof. Dr. R. Pieters, beste Rob, de besprekingen met jou waren essentieel voor het vasthouden van de rode draad. Zeker wat betreft schrijfstijl heb ik een hoop van je geleerd, schrappen in mijn vaak veel te uitgebreide teksten is echt een kunst geworden!

Dr. M.L. Den Boer, beste Monique, bedankt voor het mogelijk maken van de studies in dit proefschrift. Zowel het hersentumor- als het proteomics onderzoek was voor ons allebei een nieuwe uitdaging. We hebben er samen veel van geleerd en hopelijk vormt dit een goede basis voor succesvol vervolgonderzoek!

Dr. R.E. Reddingius, beste Roel, hoewel onderzoek doen helaas niet echt jouw ding bleek te zijn, wil ik je bedanken voor je inzet bij het opstarten van de liquorstudies en daaruit voortgekomen samenwerkingsprojecten.

Prof. Dr. Sillevis Smitt, beste Peter, tot mijn eigen verbazing koos ik uiteindelijk voor de neurologie met het uiteindelijke doel dit te combineren met mijn net zo`n grote interesse in de kindergeneeskunde. Bedankt voor je vertrouwen!

Dr. T. Luider, beste Theo, je wijdde me in in de wereld van de proteomics. Ik wil jou, en alle anderen van het massaspectrometrie lab, zoals Lennard, Halima en Peter, bedanken voor alle hulp en uitleg aan deze onwetende dokter!

Prof. Dr. J.M. Kros, beste Max, heel wat uren heb ik doorgebracht achter de microscoop op je kamer, om weer eens een hele serie coupes te beoordelen. Ik weet dat je liever gezien had dat het onderzoek wat meer de diepte in was gegaan, maar ik ben nog niet klaar met onderzoeken want, zoals je weet, dit is pas het begin!

Prof. Dr. S. Van Gool, beste Stefaan, onze samenwerking omtrent de lumbale vochtjes begon bij toeval tijdens een bijeenkomst over temozolomide. Inmiddels is de studie succesvol afgerond, maar ik hoop dat we in de toekomst nog vaker projecten samen kunnen starten!

Dr. H. Vanderstichele, beste Hugo, via Stefaan van Gool kwamen we in contact en was de samenwerking naar de neurodegeneratieve eiwitten in liquor snel geregeld. Bedankt voor al je hulp, de liquorbepalingen, het meedenken en -schrijven bij het manuscript!

Dr. J. Van Doorn, beste Jaap, het onderzoek naar het IGF systeem bij hersentumoren bij kinderen was niet gemakkelijk, zonder je hulp was het zeker niet gelukt! Bedankt voor je tijd voor overleg in Utrecht of Rotterdam, je uitgebreide inzet bij het schrijven van het manuscript en je altijd zeer snelle reacties, met name bij het afronden van de studie!

Dr. J. Jansen, beste Jaap, hoe kan ik je bedanken voor je tomeloze energie en inzet bij de identificatie van de eiwitten uit de SELDI studie, in één woord super! Ik hoop dat je inmiddels weer een leuke werkplek hebt gevonden!

Dr. R. van Schaik, beste Ron, bedankt voor je hulp bij de analyse naar de verstoorde bloed-hersenbarrière bij hersentumorpatiënten. Geweldig dat die bepalingen allemaal op korte termijn konden plaatsvinden!

Dr. French, beste Pim, ik heb erg veel geleerd van jullie wetenschappelijke neuro-oncologische kennis. Bedankt voor de hulp bij de p53 studie en de recent opgestarte exon-array studie, ben benieuwd naar de uitkomst!

Dr. R. Packer, thank you for your help and advise with the medulloblastoma and ependymoma review. Thank you very much for the offer for a neuro-oncology fellowship in your hospital, I will surely keep it in mind!

Ruim 7 jaar op de afdeling kinderoncologie en hematologie....heel wat herinneringen om bij stil te staan. Allereerst Inekee en Eline, 4 jaar lang waren we kamergenootjes, lief en leed hebben we gedeeld en ik mis jullie nog dagelijks! Maar gelukkig zullen onze film- en eetuitjes met Barbara en Rolinda blijven bestaan, lang leve Bridget Jones! Barbara, bedankt voor al je promotieadviezen en gezelligheid! Wanneer we het allebei wat rustiger hebben, moeten we toch echt weer eens wat vaker afspreken!

De kinderoncologen, Dr. K. Hählen, Dr. F. Hakvoort, Dr. I. Appel, Dr. A. Beishuizen, Dr. M. Zwaan, Dr. M. Van den Heuvel-Eibrink, Dr. M. Van Noesel, Dr. Michiels, Dr. De Vries, met ieder van jullie heb ik in meer of mindere mate te maken gehad tijdens het onderzoek. Dr. Hählen, bij u ontstond de interesse in kinderoncologisch onderzoek tijdens mijn 4e jaars afstudeerstage. Max, dank voor het mede mogelijk maken van de p53 studie! Erna, je kwam in het laatste stukje van mijn onderzoek de groep versterken. Veel hebben we nog niet samen kunnen doen, maar in ieder geval al veel dank voor je input bij het review!

Verder natuurlijk alle mensen van de kinderoncologiepoli en het specieel hematologisch lab, in het bijzonder Mieke, Rolinda, Carla en Henk, bedankt voor alle hulp, uitleg en gezelligheid! En niet te vergeten Jacqueline en Jeanine, wat zou de afdeling zijn zonder jullie…. bedankt voor alle hulp en geregel!

Na 2 jaar onderzoek vanuit het Sophia, verplaatste mijn werkplek zich naar het lab kindergeneeskunde voor het echte laboratoriumwerk. Ook hier heb ik heel wat mensen te bedanken die me een heleboel hebben geleerd, maar ook veel gezelligheid hebben gebracht.

Monique, bedankt voor alles, niet alleen voor je ondersteuning in het lab met de arrays, cellijnen, immunohistochemie, maar ook voor alle chocolade en kletsmomenten als het weer even lastig was! Helaas ontbreekt de tijd me nu om gezellig brownies te gaan eten beneden of elitair te gaan lunchen (Ronald bedankt!), maar ik ben blij dat je mijn paranimf wil zijn op deze grote dag! Heel veel geluk met je nieuwe baan, we zullen elkaar zeker niet uit het oog verliezen!

Onno, PPP, jou moet ik toch zeker noemen in dit dankwoord, zonder jou had stelling 11 nooit bestaan! Je maakte maar erg kort deel uit van ons clubje, maar jouw gezelligheid en natuurlijk getrommel zal ik nooit vergeten! Veel succes in Utrecht!

Mirjam, jij kwam Onno vervangen, samen hebben we nog heel wat 2D ellende doorstaan, hopelijk levert de toekomst wat meer proteomics geluk!

Theo H., jouw ervaring en kennis op het gebied van 2D electroforese en massaspectrometrie hebben me enorm geholpen toen ik begon in het eiwitonderzoek; altijd kon ik bij je terecht, bedankt daarvoor!

Jules, heel wat uren hebben we gekletst over vanalles en nog wat, bedankt voor je oppeppende lunches bij onze favoriete broodjeszaak aan het water! Het zat recent niet mee met je gezondheid, maar ik hoop dat je vanaf nu weer op volle kracht verder kunt. Ik heb bewondering voor je wetenschappelijke inzet en prestaties!

Esther, allebei inwoners van Capelle en al jaren m`n vaste buurvrouw op de kamer, bedankt voor al je hulp, alle vragen kon ik op je afvuren en altijd wist je wel een antwoord of oplossing richting het antwoord!

Ronald, als er iemand is die ik moet bedanken voor de gezelligheid op de kamer ben jij het wel, cabaret, Acda en de Munnick, het maakte niet uit! Bedankt voor je hulp en meedenken bij het onderzoek, ook al was proteomics niet jouw favoriete onderdeel!

Alle andere AIO`s en post-docs, Brian, Dominique, Pieter, Martine (zet hem op volgende week!), Irene, Iris, Diane, Jill, Marjon, Marjolein, Trudy, Linda, succes met jullie onderzoek! De analisten, Mathilde, Pauline, Susan, Jessica, Wilco, Pieter, allemaal hebben jullie me wel met iets geholpen, dank daarvoor! Verder iedereen bedankt voor de supertijd op het lab, de labdagen, uitjes, etc! Speciale dank aan Dickie, Ingrid, Janneke, Anita en Maria voor de hulp op het histolab en Ingrid L voor gewoonweg alles wat je voor het lab KG doet!

Myrthe, vanaf de Eurekaweek waren we aan elkaar overgeleverd, bedankt voor alle gezellige theateruitjes (die houden we erin!), SPSS puzzelmomenten, lunches, salsabelevenissen, co-schappentijd in Zeeland (wanneer was het ook alweer nationale rampendag?), etc! Geweldig dat je mijn paranimf wil zijn! Frank, jij natuurlijk ook bedankt voor stelling 11, geweldig!

Ruud, wat hebben we een lol gehad op de dansvloer, eerst weer latin dansen, later salsa, hopelijk kunnen we het binnenkort weer oppakken!

Pepijn, Patricia, Gordon, Cecile, Oscar, Carleine, Roel, Cindy en de kleintjes, het Maastrichtse vriendenclubje, wat heerlijk waren die middagen op het terras in Maastricht, voor mij nog steeds het ultieme vakantiegevoel! Jullie zijn echt goede vrienden geworden!

Ouders van Joris, Emile en Tineke, bedankt voor het gastvrije onderdak bij onze tripjes naar het zuiden! Bram en Bregje, gelukkig voor Joris ook een beetje gezellige zuidelijkheid in de Randstad!

Lieve papa en mama, zonder jullie onvoorwaardelijke steun weet ik niet hoe ik het zo ver had kunnen brengen. De telefoonrekeningen zijn dikwijls boven verwachting geweest, maar

ik had de gesprekken echt niet kunnen of willen missen! Hopelijk kan ik nog eens zoveel terugdoen als dat jullie voor mij hebben gedaan!

Lieve Joris, door jou ken ik de heerlijkheden van het Limburgse leven. Je hebt altijd gezegd, als we dit boekje overleven, dan kunnen we alles aan… het boekje is nu af, dus kom maar op met de rest van ons leven!